THE ROLE OF JAZ PROTEINS IN THE REGULATION OF PLANT GROWTH-DEFENSE TRADEOFFS

By

Qiang Guo

A DISSERTATION

Submitted to
Michigan State University
in partial fulfillment of requirements
for the degree of

Plant Biology - Doctor of Philosophy

2018

ABSTRACT

THE ROLE OF JAZ PROTEINS IN THE REGULATION OF PLANT GROWTH-DEFENSE TRADEOFFS

By

Qiang Guo

As sessile organisms, plants constantly experience challenges from the surrounding environment. In response to these biotic stresses, plants invest a prominent portion of their metabolic capacity in the production of defense-associated compounds and physical structures. However, expression of defense traits is often associated with growth restriction and ultimately reduces reproductive output. Although this growth-defense antagonism has a profound impact on plant biology and agricultural practice, the mechanisms that regulate tradeoffs between growth and defense are poorly understood. The plant hormone jasmonate (JA) plays a dual role in enhancing immune responses and inhibiting growth. The JA signaling cascade is switched on when the bioactive form of the hormone is recognized by the COI1-JAZ co-receptor complex, which leads to the degradation of JAZ repressors via the SCF^{COI1}-26S proteasome pathway and subsequent relief of JA-responsive transcription factors (TFs). In this dissertation research, I first show that JAZ proteins promote growth and reproductive fitness in the model plant *Arabidopsis thaliana* by suppressing metabolic pathways for defense. Characterization of a *jaz* decuple (*jazD*) mutant defective in 10 *JAZ* genes revealed that hyperactivation of JA signaling significantly increased resource allocation to defense pathways, thereby improving plant resistance to insect herbivores and necrotrophic pathogens. The elevated defense of *jazD* was linked to carbon starvation, curtailed seed production and, under extreme conditions, lethality. Secondly, I show that the allocation costs associated with heightened JA responses in *jazD* was largely dependent on the bHLH-type TFs MYC2, MYC3 and MYC4, and that MYC2/3/4 played overlapping and

conserved roles in metabolic reprogramming in *jazD*. Characterization of *jazD myc* mutants further showed that the JAZ-MYC transcriptional module controls the production of endoplasmic reticulum (ER)-derived structures called ER bodies, which are implicated in plant immunity. Finally, the *jazD* mutant was employed as a parental line in a genetic suppressor screen aimed at identification of novel mutations that uncouple growth-defense antagonism. Characterization of these *suppressor of jazD* (*sjd*) mutants revealed that JA signaling interacts with the red light signaling pathway to influence growth-defense balance. One *sjd* mutant (*sjd56*) not affected in red light signaling was also shown to partially uncouple growth-defense antagonism in *jazD.* Taken together, results from this dissertation provide evidence that growth-defense tradeoffs at low to moderate levels of defense are controlled by hardwired transcriptional networks, whereas high levels of defense inhibit growth through metabolic competition (allocation costs) between primary and secondary metabolism. Consistent with this view, JAZ proteins promote growth and reproductive fitness by preventing the negative effects of an unrestrained immune responses. The findings described in this dissertation may benefit the development of crop plants that are optimized for both growth and defense.

ACKNOWLEDGEMENTS

There are many people to whom I want to express my thanks during my PhD career in Michigan State University. Research described in this dissertation could not be completed without the help from many wonderful people.

My deepest gratitude goes to my advisor Dr. Gregg A. Howe, who has provided me with fantastic mentoring. I will always remember how Gregg spent time discussing research progress with me every Friday afternoon and helped me to resolve difficulties I met. Gregg's patience, enthusiasm and integrity profoundly influence me. I appreciate all the time, ideas and support I received from Gregg.

I am very fortunate to have a group of supportive and passionate committee members to guide me throughout my PhD studies. I would like to express my gratitude to Dr. Christoph Benning, Dr. Sheng Yang He, Dr. Jianping Hu, and Dr. Thomas Sharkey for their constructive suggestions and comments. Committee meetings and comprehensive exams with them have been enjoyable, and helped me gain insights into plant biology.

The Howe lab has been a family to me since I joined in 2014. Thanks to Ian Major, who has taught me a number of lab techniques and who was always available when I was stuck with research or life problems. The knowledge and research ethics I learned from him will be with me wherever I go. Koichi Sugimoto has been a good friend to me and has given me much technical assistance. I am sure he will enjoy the food and research in his hometown. My research would not have been possible without the contributions from Yuki Yoshida, who constructed many of the higher-order *jaz* mutants described in the dissertation. His dedication to research has inspired me. Marcelo Campos was my supervisor when I did my rotation. It was fun to work with him.

His smile and optimism left a deep impression on me. Yani Chen and Kyaw Aung gave me many tips on performing molecular experiments. I would like to thank them for “adopting” me during the trip to St. Louis for the 2017 ICAR conference. Nathan Havko has helped me with pathogen infection assays, and I am sure that he will come up with some exciting stories in the future. Leah Johnson, Caitlin Thireault, and Brian St. Aubin are talented graduate students I met in Howe lab. A significant portion of work described in Chapter Four was performed by Jinling Zhai, who was a visiting scholar from Hainan University in China. I also appreciate the efforts from my undergrads, including George Kapali, Alison Page, and Sam Heiler, who made many contributions to my project. Also thanks to Changxian Yang, Michael Das, and Julia Tu, who brought me with many joyful moments in the lab.

The PRL, Plant Biology Department, and MSU plant science community have provided me with a friendly environment to grow. None of my work would be possible without the company of my friends and colleagues in MSU.

My special thanks go to the PRL, DOE, and Plant Biology Department for continuous support of my studies at Michigan State University.

Finally, I would like to say thanks to my fiancée Jing Yang, who has been by my side no matter what happens. I deeply appreciate her love, understanding and support. I am grateful to my parents and sister for their love and encouragement.

TABLE OF CONTENTS

LIST OF TABLES

LIST OF FIGURES

CHAPTER ONE - LITERATURE REVIEW: RESOLUTION OF GROWTH-DEFENSE CONFLICT: MECHANISTIC INSIGHTS FROM JASMONATE SIGNALING

Part of work presented in this chapter has been published:

Guo, Q., Major, I.T., and Howe, G.A. (2018). Resolution of growth-defense conflict: mechanistic insights from jasmonate signaling. Current Opinion in Plant Biology **44**, 72-81.

Abstract

Induced plant resistance depends on the production of specialized metabolites that repel attack by biotic aggressors and is often associated with reduced growth of vegetative tissues. Despite progress in understanding the signal transduction networks that control growth-defense tradeoffs, much remains to be learned about how growth rate is coordinated with changes in metabolism during growth-to-defense transitions. Here, we highlight recent advances in jasmonate (JA) research to suggest how a major branch of plant immunity is dynamically regulated to calibrate growth-defense balance with shifts in carbon availability. We review evidence that diminished growth, as an integral facet of induced resistance, may optimize the temporal and spatial expression of defense compounds without compromising other critical roles of central metabolism. New insights into the evolution of JA signaling further suggest that opposing selective pressures associated with too much or too little defense may have shaped the emergence of a modular JA pathway that integrates primary and specialized metabolism through the control of repressor-transcription factor complexes. A better understanding of the mechanistic basis of growth-defense balance has important implications for boosting plant productivity, including insights into how these tradeoffs may be uncoupled for agricultural improvement.

Introduction

Plant growth rate and reproductive output are intimately linked to the availability of photoassimilated carbon and other vital resources obtained from the environment. These same resources, however, are also used to produce defense compounds and physical structures that protect tissues from destruction by herbivores and pathogens. The notion that plant growth and immunity are antagonistically linked stems from the observation that elevated defense is commonly associated with growth inhibition and, of agricultural relevance, reduced yield. Given the importance of these traits for plant fitness in diverse environments, it is generally assumed that plants have evolved strategies to balance growth and reproductive output with the need for defense (Herms and Mattson, 1992; Heil and Baldwin, 2002; Stamp, 2003; Zust and Agrawal, 2017). A mechanistic appreciation of how growth and immunity intersect has important implications for understanding not only the diversity of defense strategies employed across the plant kingdom, but also for improving sustainable crop production.

Significant progress has been made in understanding the molecular mechanisms of crosstalk between growth and immune signaling networks (Belkhadirl et al., 2014; Huot et al., 2014; Lozano-Duran and Zipfel, 2015; Havko et al., 2016). While it is now clear that gene regulatory networks exert major control over growth-defense balance, a better understanding of the inherent conflicts between these major physiological tasks is needed to accurately predict genotype-by-environment interactions that give rise to tradeoffs (Chae et al., 2016; Zust and Agrawal, 2017). Hormone-based defense systems in which broad-spectrum resistance is conferred by induced expression of specialized defense proteins and metabolites, with associated growth suppression, provide attractive experimental systems in which to address the underlying mechanisms of growth-defense tradeoffs (Havko et al., 2016).

Here we discuss growth-defense conflict from a mechanistic and metabolic perspective. We use the JA signaling pathway to highlight how reprogramming of the interface between primary and specialized metabolism may be linked to changes in carbon availability and re-calibration of growth rate. We also propose a framework for understanding the modular architecture of the JA signaling pathway in the context of opposing selective pressures associated with too much or too little defense, and how this signaling system integrates primary and specialized metabolism through control of repressor-transcription factor complexes. Finally, we consider how recent mechanistic insights into crosstalk between growth and immune signaling networks provide opportunities to uncouple growth-defense tradeoffs for agricultural benefit.

Biosynthesis and metabolism of JA

JA was first isolated from the essential oil of jasmine flowers in the form of methyl-JA (MeJA) (Demole et al., 1962). Since its identification, tremendous advances in JA research have been made to understand its function in regulating various physiological processes, especially its dual roles in inhibiting growth and promoting defense. The biosynthetic pathway of JA was characterized by many forward and reverse genetic screens (Wasternack, 2015). Biosynthesis of JA takes place in the chloroplast, peroxisome and cytosol (Howe, 2018). The first step of JA production is the release of α-linolenic acid (18:3) by the action of plastidic lipases, one of which is DEFECTIVE IN ANTHER DEHISCENCE 1 (DAD1) expressed in stamen filaments (Figure 1.1) (Ishiguro et al., 2001). Recently, Wang *et al.* showed that overexpression of two additional lipase genes *PLASTID LIPASE 2* (*PLIP2*) and *PLASTID LIPASE 3* (*PLIP3*) gives rise to the accumulation of JA and its derivatives in Arabidopsis leaves (Wang et al., 2018), suggesting that these two lipases also contribute to the accumulation of JA. Consistent with this hypothesis, the

restricted growth of *PLIP2-OX* and *PLIP3-OX* plants resembles the phenotype of mutants in which the JA pathway is constitutively activated, and blocking of JA perception in these *PLIP-OX* lines restores their growth phenotype (Wang et al., 2018). Once released from membrane lipids, α-linolenic acid is converted by 13-lipoxygenases (13-LOXs) to 13-hydroxyperoxylinolenic acid (13-HPOT) (Figure 1.1) (Bell et al., 1995; Bannenberg et al., 2009; Chauvin et al., 2013). In Arabidopsis, 13-LOXs are encoded by the *LOX2*, *LOX3*, *LOX4* and *LOX6* genes (Bannenberg et al., 2009; Chauvin et al., 2013; Chauvin et al., 2016). 13-HPOT is further metabolized to 12-oxo-phytodienoic acid (OPDA) in the chloroplast by the sequential action of ALLENE OXIDE SYNTHASE (AOS) (Song and Brash, 1991) and ALLENE OXIDE CYCLASE (AOC) (Figure 1.1) (Ziegler et al., 2000).

OPDA is transported from chloroplast to peroxisome, most likely by a process involving the peroxisomal ATP-BINDING CASSETTE (ABC) transporter COMATOSE (CTS, also known as PXA1) (Figure 1.1) (Theodoulou et al., 2005). Within the peroxisome, OPDA is metabolized to 3-oxo-2(2' (Z)-pentenyl)-cyclopentane-1-octanoic acid (OPC-8:0) by OPDA REDUCTASE 3 (OPR3) (Stintzi and Browse, 2000) and then ligated to CoA by OPC-8:0 CoA LIGASE (OPCL) to produce OPC 8:0-CoA (Figure 1.1) (Schneider et al., 2005). OPC 8:0-CoA then goes through three cycles of β-oxidation to complete the production of JA (Figure 1.1) (Vick and Zimmerman, 1984; Li et al., 2005; Schilmiller et al., 2007). A recent study by Chini *et al.* revealed that an OPR3-independent pathway for JA biosynthesis exists in plants (Chini et al., 2018). They found that a mutant (*opr3-3*) defective in OPR3 is still resistant to insect herbivores and necrotrophic pathogens, and is able to activate the COI1-dependent JA signaling pathway under stressed conditions (Chini et al., 2018). This work also showed that, in the absence of

OPR3, OPDA can be converted to 4,5-didehydro-JA (ddh-JA) and that this compound can be reduced to JA by the enzyme OPDA REDUCTASE 2 (OPR2) (Figure 1.1) (Chini et al., 2018).

Following its export from the peroxisome, JA is metabolized to a myriad of metabolites in the cytoplasm. For example, JA can be conjugated to isoleucine (Ile) by JASMONATE RESISTANT 1 (JAR1) to form JA-Ile, which is the major bioactive form of the hormone (Figure 1.1) (Staswick et al., 2002; Thines et al., 2007; Katsir et al., 2008; Fonseca et al., 2009). Metabolism of JA may also inactivate this hormone. Recent studies found that four paralogous 2-oxoglutarate/Fe(II)-dependent (2-OGD) oxygenases, named JASMONATE-INDUCED OXYGENASE (JOX) or JASMONIC ACID OXIDASE (JAO), hydroxylate JA to form 12-OH-JA in Arabidopsis (Figure 1.1) (Caarls et al., 2017; Smirnova et al., 2017). Mutation of four *JOX* genes in Arabidopsis led to overaccumulation of JA, and as a consequence, this quadruple mutant showed elevated resistance to the necrotrophic fungus *Botrytis cinerea* and the caterpillar *Mamestra brassicae* (Caarls et al., 2017). Genetic complementation of the quadruple mutant with individual JOX genes reduced the level of JA, indicating that all four JOXs contribute to the inactivation of the precursor form of JA-Ile (Caarls et al., 2017).

JA signaling

Perception of JA-Ile requires the F-box protein CORONATINE INSENSITIVE 1 (COI1), which is a component of the SCF (Skp/Cullin/F-box) E3-type ubiquitin ligase (Xie et al., 1998). The *coi1* mutant was isolated in a screen for ethylmethanesulfonate (EMS)-mutagenized plants that were insensitive to coronatine, which is a molecular mimic of JA-Ile (Feys et al., 1994). Many phenotypes observed in *coi1*, including short anther filaments and male sterility, resemble phenotypes of mutants defective in JA biosynthesis (McConn and Browse, 1996). Likewise, a

screen for tomato mutants that are insensitive to MeJA identified the mutant *jasmonate insensitive 1* (*jai1*), which is defective in the tomato ortholog of Arabidopsis COI1 (Li et al., 2004). Given the fact that F-box proteins provide specificity to the SCF ligase complex by recognizing particular targets for ubiquitination and degradation via the 26S proteasome, identification of COI1 as a F-box protein suggested that protein degradation is a key step in the JA signaling cascade (Xie et al., 1998).

A decade after the discovery of COI1, JASMONATE ZIM-DOMAIN (JAZ) proteins were identified as the targets of this F-box protein (Chini et al., 2007; Thines et al., 2007; Yan et al., 2007). JAZ proteins belong to the TIFY protein family, which possesses a conserved TIFY motif within the ZIM domain (named for a zinc-finger protein expressed in the inflorescence meristem) (Vanholme et al., 2007; Bai et al., 2011). The main feature that distinguishes JAZ from other TIFY proteins is the 27-amino-acid Jas motif located near the C terminus (Howe et al., 2018). When cellular JA levels are low, the Jas motif interacts with the JAZ-interacting domain (JID) at the N terminus of the basic helix-loop-helix (bHLH) MYC transcription factors (TFs) (Zhang et al., 2015), which are the most intensively studied JA-responsive TFs. Structural, biochemical and *in planta* analyses indicate that JAZ proteins impose transcriptional repression by competitively impeding the binding of MEDIATOR 25 (MED25), which bridges TFs and RNA polymerase II to promote gene expression (Kazan and Manners, 2013; Zhang et al., 2015). JAZ proteins also attenuate TF activity by recruiting TOPLESS (TPL) proteins that suppress gene expression via epigenetic modification (Ke et al., 2015). TPL is recruited to JAZ either directly via an EAR motif (Shyu et al., 2012) or indirectly through the NOVEL INTERACTOR OF JAZ (NINJA) adaptor protein (Pauwels et al., 2010).

The accumulation of JA-Ile above a threshold concentration activates JA-mediated signal transduction. JA-Ile is perceived by a receptor complex consisting of the F-box protein COI1, JAZ repressors, as well as an inositol pentakisphosphate that interacts with both COI1 and JAZs (Sheard et al., 2010). The three-dimensional structure of the receptor complex shows that JA-Ile is recognized by an open pocket in COI1, which is docked in the α-helix formed by a bipartite degron sequence within the Jas motif of JAZ proteins (Sheard et al., 2010). In addition to the α-helix, this degron also consists of a loop region to trap the hormone to its binding pocket (Sheard et al., 2010). Recruitment of JAZ proteins to COI1 triggers polyubiquitination and subsequent degradation of JAZ by the 26S proteasome (Chini et al., 2007; Thines et al., 2007), resulting in the activation of TFs that drive JA-responsive genes. Recent studies have shown that JA-induced degradation of JAZ repressors is facilitated by the direct interaction between COI1 and MED25, which brings COI1 to the transcriptional start sites of MYC2 target genes (An et al., 2017). Furthermore, MED25 recruits HISTONE ACETYLTRANSFERASE 1 (HAC1), which promotes gene expression by acetylating histone (H) 3 lysine (K) 9 (H3K9) (An et al., 2017). Besides JAZ proteins, JA-Ile promotes the destruction of another repressor of the JA signaling, namely JASMONATE-ASSOCIATED VQ MOTIF GENE 1 (JAV1) (Hu et al., 2013). Despite the fact that JAV1 is degraded by the 26S proteasome upon JA-Ile elicitation, this protein does not directly interact with COI1 (Hu et al., 2013). However, JA-Ile-induced degradation of JAV1 is still dependent on COI1, as MeJA treatment of *coi1* mutant does not spur JAV1 destruction (Hu et al., 2013). It is conceivable that COI1 may activate the production an unidentified E3 ligase that recognizes JAV1 for degradation by the 26S proteasome (Hu et al., 2013).

Redundancy and specificity of JAZ proteins

The 13 *JAZ* genes (*JAZ1-13*) in Arabidopsis are classified into five phylogenetic groups (Group I-V) (Thireault et al., 2015; Howe et al., 2018). Most mutants harboring loss-of-function insertional alleles in single *JAZ* genes do not show strong JA-induced phenotypes, suggesting that JAZ proteins are functionally redundant (Chini et al., 2007; Thines et al., 2007; Thireault et al., 2015). One exception is *jaz10*, which displays increased sensitivity to exogenous JA (Demianski et al., 2012). A JAZ10 alternative splice variant called JAZ10.4 lacks the Jas motif, however, it retains the ability to repress JA responses and is highly resistant to JA-induced degradation (Chung and Howe, 2009). Thus, mutants defective in *JAZ10* exhibit hypersensitivity to JA likely because they lose the ability to produce splice variants that are stabilized against degradation. Compared to *jaz* single mutants, the responsiveness of a *jaz* quintuple (*jazQ*) mutant deficient in five *JAZ* genes (*JAZ1/3/4/9/10*) to JA application is enhanced (Campos et al., 2016). This mutant also shows other JA-associated phenotypes, including overaccumulation of anthocyanin and increased defense responses (Campos et al., 2016). However, these phenotypes are mild compared to JA-elicited phenotypes (Campos et al., 2016), indicating that the remaining JAZs are still functional in *jazQ*.

Despite apparent redundancy among *JAZ* genes, recent studies demonstrate that some JAZ proteins possess specific functions. Functional specialization among gene family members may be achieved through expression in particular tissues or cell types. For instance, JAZ2 is strongly expressed in stomatal guard cells and inhibits stomatal opening by constraining the activity of MYC TFs, which directly regulate the expression of three homologous NAC family TFs to modulate stomata aperture (Zheng et al., 2012; Gimenez-Ibanez et al., 2017). This COI1-JAZ2-MYC-NAC module can be hijacked by *Pseudomonas syringae* bacteria to facilitate

pathogen infection (Gimenez-Ibanez et al., 2017). Another mechanism to achieve functional specificity among JAZ family members is through differential JAZ binding to specific TFs. For example, only JAZ3 interacts with the YABBY (YAB) family transcription factor FILAMENTOUS FLOWER (FIL)/YAB1, which regulates disease resistance and the production of anthocyanin and chlorophyll (Boter et al., 2015).

The bHLH MYC transcription factors

The best characterized JAZ-interacting TFs are the subgroup IIIe bHLH proteins MYC2, MYC3, MYC4 and MYC5 (Fernandez-Calvo et al., 2011; Major et al., 2017). Mutants defective in MYC2, MYC3 or MYC4 display reduced resistance to insect herbivores (Lorenzo et al., 2004; Fernandez-Calvo et al., 2011; Chico et al., 2014; Major et al., 2017). It has been shown that MYC TFs promote the production of a myriad of defense compounds that are derived from terpenoid, alkaloid, phenylpropanoid and amino acid biosynthetic pathways (Goossens et al., 2017). For example, MYC2, MYC3 and MYC4 are involved in the production of glucosinolates (Schweizer et al., 2013), which are major anti-insect secondary metabolites in the Brassicaceae family. A *myc2 myc3 myc4* triple mutant is almost completely devoid of glucosinolates and, as a consequence, is susceptible to insect attack (Schweizer et al., 2013). Molecular and biochemical analyses showed that MYC TFs physically interact with MYB TFs (i.e. MYB28/29/34/51/76/122) to synergistically control the expression of glucosinolate biosynthetic genes (Schweizer et al., 2013).

In addition to governing the expression of defense traits, MYC TFs execute other JA-mediated physiological tasks. For example, MYC2 reduces the activity of the root meristem by inhibiting the expression of *PLETHORA 1* (*PLT1*) and *PLETHORA 2* (*PLT2*), which mediate

auxin-induced regulation of stem cell niche maintenance (Chen et al., 2011a). MYC TFs also affect biomass accumulation. A mutant lacking MYC2, MYC3 and MYC4 displayed increased shoot growth in comparison with WT (Major et al., 2017). Reproductive processes are also influenced by MYC TFs. MYC2, MYC3, MYC4 and MYC5 interact with MYB TFs MYB21 and MYB24 to cooperatively modulate stamen development (Qi et al., 2015). The *myc2 myc3 myc4 myc5* quadruple mutant exhibits defects in stamen development and reduced seed yield (Qi et al., 2015).

JA signaling reshapes the metabolic interface between growth and defense

Induced plant defense is associated with the production of a vast array of specialized metabolites (SMs) that mediate plant interactions with associated biota. Biosynthetic pathways for the major classes of SMs, including phenylpropanoids, polyketides, terpenoids, and nitrogen-containing compounds, are often regulated in an inducible fashion by JA (De Geyter et al., 2012; Zhou and Memelink, 2016). Because SMs are derived from one or more primary metabolites, induced production of SMs must be coordinated with corresponding changes in appropriate sectors of primary metabolism (D'Auria and Gershenzon, 2005; Aharoni and Galili, 2011). Pathways that highlight some of the major interconnections between specialized and primary metabolism in Arabidopsis are depicted in Figure 1.2. For example, cinnamates generated by the phenylpropanoid pathway are precursors for monolignols and lignin production, as well as diverse phenylpropanoid and polyketide products. Large pools of proteinogenic amino acids are required for the biosynthesis of numerous defensive proteins that can accumulate to high levels in JA-elicited tissues. Similarly, various amino acid precursors such as indole provide building blocks for nitrogen-containing SMs, including glucosinolates. As the largest and most diverse

group of plant metabolites, terpenoids are produced from isoprene units and include primary metabolites (e.g., carotenoids) as well as a myriad of specialized mono-, sesqui-, di-, and triterpenes. Other plant species produce distinct groups of SMs that are also derived from intermediates of primary metabolism; examples include the synthesis of phenolic glycosides from cinnamate, stilbenes from cinnamate and malonyl-CoA, cyanogenic glycosides from tryptophan, benzoxazinoids from indole, and complex alkaloids from amino acids, polyamines, and purines.

The reported effects of biotic stress on primary metabolism often vary depending on the experimental system under study (Schwachtje and Baldwin, 2008; Zhou et al., 2015; Papazian et al., 2016). Nevertheless, increasing evidence indicates that changes in primary metabolism may serve to save time and energy during the transition from growth to defense. A notable example is the effect of biotic challenge on photosynthetic metabolism. The commonly observed repressive effect of biotic stress on photosynthesis gene expression may reflect a strategy to reprogram the cell's biosynthetic machinery without actual losses in photosynthetic efficiency; photosynthetic robustness in the face of genetic and environmental perturbations would ensure a continuous supply of carbon skeletons for the rapid production of defense proteins and metabolites (Schwachtje and Baldwin, 2008; Luo et al., 2009; Bilgin et al., 2010; Attaran et al., 2014; Zhou et al., 2015; Havko et al., 2016). Similarly, turnover of photosynthesis-related transcripts and proteins may increase the pool of resources needed to fuel induced defense responses (Attaran et al., 2014) and also increase the availability of ribosomes for translation of defense-related mRNAs. Optimization of ribosome capacity during the onset of defense responses may thus serve to mitigate the high cost of protein synthesis in relation to growth (Ishihara et al., 2017; Xu et al., 2017).

Changes to primary metabolism elicited by JA also include reductions in sugar and starch content that is associated with increased biosynthesis of SMs, suggesting depletion of resources to produce SMs (Machado et al., 2013). Direct evidence for the diversion of resources to SMs was obtained by N flux studies in *N. attenuata*, which showed that assimilated N was directed to N-rich SMs (e.g., phenolamides) instead of soluble proteins (Ullmann-Zeunert et al., 2013). Ancillary pools of primary metabolites are also affected by specialized metabolism and can dramatically alter nutrient distribution. Glucosinolate production, for instance, can influence plant sulfur content via demand for activated sulfate (Falk et al., 2007; Mugford et al., 2009).

The production of SMs is tightly regulated by transcription factors, some of which also appear to coordinate upstream pathways of primary metabolism (Aharoni and Galili, 2011). For example, MYB8 directs phenolamide biosynthesis and, perhaps indirectly, protein pool sizes in *N. attenuata* (Ullmann-Zeunert et al., 2013). MYB34 and MYB51, which are principal regulators of indole glucosinolate biosynthesis, directly regulate expression of genes involved in tryptophan biosynthesis and sulfate metabolism, revealing coordinated regulation of primary metabolic pathways with specialized metabolism (Celenza et al., 2005; Gigolashvili et al., 2007; Yatusevich et al., 2010). Metabolic costs of SM production include not only precursors and cofactors required for biosynthesis, but also costs associated with transport, maintenance, and storage (Gershenzon, 1994; Bekaert et al., 2012; Nour-Eldin et al., 2012; Havko et al., 2016). Flux balance analysis of glucosinolate production in Arabidopsis, for example, indicates that photosynthetic output would need to increase by 15% to account for metabolic processes associated with the production of these compounds (Bekaert et al., 2012). Overall, the changes to primary and specialized metabolism observed during growth to defense transitions are likely coordinated to support the energy and resource demands of SM production without sacrificing

other key roles of primary metabolism. Given the costs of chemical defense and the direct linkages between primary and specialized metabolism, it is perhaps not surprising that SM production is often associated with reduced growth.

The raison d'être of growth inhibition

Two general hypotheses have been proposed to explain why plant growth is inhibited upon induced expression of defense responses. One common interpretation invokes a resource-based cost (also referred to as allocation costs) in which increased allocation of one or more resources to defense necessarily restricts resources that could otherwise be used for growth, reproductive development, or other physiological tasks (Heil and Baldwin, 2002; Havko et al., 2016; Zust and Agrawal, 2017). This hypothesis could apply to any limiting biochemical resource that is shared by primary and specialized metabolism, including amino acids and photoassimilated carbon skeletons (Figure 1.2). The resource-based tradeoff model is challenging to test because of the difficulty in defining (and therefore measuring) metabolic costs of specific defense compounds, and likely oversimplifies a highly complex relationship that is shaped by strategies to offset the costs of defense (Neilson et al., 2013; Havko et al., 2016; Kliebenstein, 2016; Karasov et al., 2017; Zust and Agrawal, 2017). That plants can be manipulated to grow and defend well at the same time (e.g., Campos et al., 2016) further indicates that growth-defense antagonism is not simply determined by resource limitation but rather is controlled at the transcriptional level by hard-wired regulatory circuits.

Nevertheless, it is evident that high-level production of SMs, which is commonly observed in plants, must reduce the pool of resources that is used to support other physiological processes. It is possible that resource-based tradeoffs are difficult to detect because they occur in

a context-dependent manner, for example being manifested during specific stages of ontogeny or only when the flux of primary metabolites into defense pathways exceeds a certain (likely high) threshold (Zust and Agrawal, 2017). As discussed below, multi-tiered mechanisms to powerfully repress the expression of chemical defenses may serve to prevent deleterious effects of carbon depletion or metabolic imbalance during the growth to defense transition, which if true would make resource-based tradeoffs difficult to detect in wild-type plants grown under most laboratory conditions.

A second general hypothesis to explain the antagonistic relationship between induced resistance and growth is that growth restriction is an adaptive response mediated by hardwired interactions between growth and immune signaling networks. This regulatory view of growth-defense tradeoffs is analogous to strategies used by microorganisms to cope with nutrient scarcity (Matin, 1991; De Virgilio, 2012). Among the key features of many microbial responses to nutrient starvation are: i) mechanisms to sense nutrient scarcity prior to complete depletion of the resource; ii) turnover and recycling of cellular components, including protein degradation in response to amino acid starvation; iii) transcriptional activation of genes encoding protective compounds to help ensure survival during the quiescent state; and iv) the onset of general resistance to stresses other than nutrient limitation. Analogous to these microbial strategies, the emerging view in plants is that growth inhibition is often not a direct consequence of depleting a critical nutrient but rather is a highly programmed response that prepares the organism for harsh environmental conditions, from which robust growth can resume when conditions improve (Campos et al., 2016; Kliebenstein, 2016; Karasov et al., 2017; Machado et al., 2017; Zust and Agrawal, 2017).

The notion that immune-triggered growth inhibition is a strategy to avoid starvation of essential metabolic intermediates is generally consistent with the acclimatory response hypothesis, which provides an explanation for how plant growth rate is adjusted in response to diurnal changes in carbon supply and demand (Smith and Stitt, 2007). In extending this hypothesis to induced chemical defense, it is conceivable that rapid flux of carbon intermediates into defense pathways may have effects similar to those observed in plants subjected to extended night or other conditions associated with carbon starvation. Specifically, it is envisioned that nutrient-sensing systems detect carbon limitation or energy imbalances to recalibrate (i.e., reduce) growth to the new level of available carbon, thus protecting against the deleterious effects of growth arrest upon exhaustion of assimilated carbon (Smith and Stitt, 2007). Empirical support for this idea comes from studies showing that JA elicitation depletes sucrose and starch content in several plant species (Babst et al., 2005; Hanik et al., 2010; Machado et al., 2015; Machado et al., 2017). There is also increasing evidence to link JA to various energy sensing systems, including the target of rapamycin (TOR) and sucrose non-fermenting kinase 1 (SnRK1) pathways, that influence growth-defense balance (Schwachtje et al., 2006; Liu et al., 2017; Song et al., 2017; De Vleesschauwer et al., 2018). That slow growth is a common phenotype among plant mutants affected in metabolism raises the additional possibility that metabolic imbalance during the growth-defense transition, rather than chemical defense production *per se*, is a general cue for growth attenuation.

Mechanisms of growth antagonism by JA

The signal transduction networks that control growth-defense conflict are highly complex in their ability to integrate extracellular cues with the action of various growth and defense hormones.

The function of JA in both promoting defense and inhibiting growth provides a focal point for understanding how a well-defined signal within this larger network contributes to growth-defense balance at a mechanistic level. Indeed, there is increasing evidence that the core JA pathway is hub for integrating diverse developmental and stress-related cues that collectively serve to optimize plant fitness in changing environments (Howe et al., 2018). A compelling example of this comes from studies showing that defense responses are directly influenced by changes in the activity of phytochrome B during the shade avoidance response (Moreno et al., 2009; Chico et al., 2014). That JA inhibits growth of both dicot and monocot species suggests that the mechanisms responsible for linking hormone action to the control of cell division are conserved (Yan et al., 2007; Zhang and Turner, 2008; Yang et al., 2012; Noir et al., 2013; Havko et al., 2016; Hibara et al., 2016). Time course studies in Arabidopsis indicate the rapid defense activation and restriction of shoot growth in response to JA are tightly coupled processes that occur in the absence of reductions in photosynthetic efficiency (Attaran et al., 2014). Genetic analyses further show that MYC transcription factors negatively regulate leaf growth, whereas JAZ proteins, as repressors of MYCs, promote growth (Campos et al., 2016; Major et al., 2017). These studies support a model in which elevated levels of bioactive JA-L-isoleucine (JA-Ile) lead to JAZ degradation and de-repression of MYC transcription factors, which in turn exert opposing effects on growth and defense.

The JAZ-MYC transcriptional module may restrict leaf growth and biomass accretion by one or more of several mechanisms (Figure 1.3A). According to the acclimatory response hypothesis (Smith and Stitt, 2007), activation of defense metabolism by MYC and perhaps other JAZ-interacting transcription factors could generate a metabolic signal that tunes growth rate downward to match the new metabolic state in which fewer resources are available for growth.

JA-inducible transcription factors such as MYC may also attenuate leaf growth through negative regulation of genes involved in cell cycle control (Noir et al., 2013; Attaran et al., 2014; Gasperini et al., 2015; Major et al., 2017). This could involve the synergistic interaction of JA with other phytohormones such as ethylene, which signals through ERF (ETHYLENE RESPONSE FACTORS) transcription factors to control cell division (Dubois et al., 2018). A function for MYCs as negative regulators of leaf growth is analogous to the role of the JAZ-MYC module in inhibiting the activity of PLETHORA transcription factors that promote auxin-dependent control of cell proliferation in the root meristem (Chen et al., 2011b; Gasperini et al., 2015; Major et al., 2017).

A third hypothesis is that JA-mediated growth-defense tradeoffs are controlled by antagonistic crosstalk between the JA-Ile and gibberellin (GA) signaling pathways (Navarro et al., 2008) (Figure 1.3A). The DELLA repressors of GA signaling have been implicated in wound- and JA-mediated growth inhibition of Arabidopsis roots (Hou et al., 2010) and hypocotyls (Yang et al., 2012), but as yet there is little evidence for this in leaves (Zhang and Turner, 2008). These findings suggest that different mechanisms of growth antagonism may operate in different tissues or that different members of the DELLA family exert differential effects on growth-defense antagonism, perhaps through specific DELLA-JAZ interactions. Studies with *N. attenuata* provide evidence that JA-mediated carbohydrate depletion and shoot growth inhibition occur independently of the production of JA-Ile-regulated defense compounds, arguing against a resource tradeoff model in this experimental system (Machado et al., 2017). Based on the analysis of plants treated with exogenous JA and GA, it was proposed that JA indirectly represses shoot growth by antagonizing the GA pathway, perhaps through down regulation of photosynthesis (Machado et al., 2017). These collective studies indicate that,

despite detailed insight into how JA-Ile perception in the nucleus is coupled to defense gene expression (Howe et al., 2018), a satisfactory explanation of how this hormone inhibits growth is far from complete.

Modularity in JA signaling: conflict between too little and too much defense

Theories to explain variable patterns of plant defense often invoke the existence of strategies to offset the costs of immunity (Heil and Baldwin, 2002; Neilson et al., 2013; Karasov et al., 2017; Zust and Agrawal, 2017). A recurring theme among these strategies, which encompass all forms of induced defense, is exquisite control over the spatial and temporal expression pattern of defense genes and the physiological traits they specify. The regulatory mechanisms that dictate these patterns of defense may provide a window into evolutionary trajectories that shaped the emergence of extant defense systems (Yang et al., 2012; Hibara et al., 2016; Major et al., 2017). As an example, we present a speculative model of how selective pressures imposed by too little or too much defense may have shaped the modular architecture of JA-Ile signaling in higher plants (Figure 1.4).

A striking feature of the JA branch of immunity is the prevalence of molecular components involved in transcriptional repression of defense gene expression (Campos et al., 2014; Howe et al., 2018). These mechanisms operate at multiple temporal and spatial scales, and include: i) metabolic depletion of JA-Ile (Koo and Howe, 2012; Heitz et al., 2016); ii) increased stability of JAZ repressors through alternative splicing and variation in degron efficiency (Chung et al., 2010; Shyu et al., 2012; Thireault et al., 2015); iii) structurally distinct MYC-interaction domains within JAZ repressors (Moreno et al., 2013; Zhang et al., 2017); iv) competitive inhibition of MYC binding to promoters of target genes (Nakata et al., 2013; Song et al., 2013;

Fonseca et al., 2014); v) age-dependent termination of JA signaling (Mao et al., 2017); and vi) and other negative feedback loops (Zhou et al., 2016) (Figure 1.4). Why are JA-based defense responses subject to so many levels of negative regulation? The answer to this question likely lies in the observation that sustained de-repression of JA-Ile signaling, for example from continuous exposure to exogenous precursors (e.g., methyl-JA) of JA-Ile, results in growth arrest, extreme senescence-like symptoms, and lethality (Ueda and Kato, 1980; Zhang and Xing, 2008; Campos et al., 2016). This and other examples of the deleterious effects of autoimmunity (Chae et al., 2016) suggest that, under some conditions, the advantages of switching off defense outweigh the advantages of switching it on.

The dual role of JAZ proteins in both JA-Ile perception and repression of transcription factor activity raises the question of which of these two functions first emerged during evolution of the pathway (Howe et al., 2018). Although it is generally assumed that JA signaling evolved as a strategy to activate defense in response to danger signals (Howe and Jander, 2008; Koo and Howe, 2009; Thaler et al., 2012), it is possible that JAZ repressors originated in response to selective pressures to mitigate the metabolic costs of constitutive (i.e., costly) defenses prior to the emergence of JA-Ile and its coreceptor COI1 (Figure 1.4). In support of this hypothesis, a wealth of genetic and biochemical data suggest that JAZ degradation is the main, if not exclusive, function of COI1 and JA-Ile in vascular plants (Howe et al., 2018). There is also recent evidence to indicate that COI1, as well as the capacity to synthesize JA-Ile, arose in early land plants (Bowman et al., 2017; Pratiwi et al., 2017; Howe et al., 2018). Future studies of JA signaling in the basal plant lineages promises to provide important insights into the evolutionary origins of this major branch immunity and its role in regulating growth-defense balance. As mentioned above, it will be particularly informative to determine whether ancestral JAZ repressors evolved

before or after the emergence of COI1 and the capacity to synthesize the COI1-associated ligand (Figure 1.4).

Summary and future perspectives: conflict resolution through phenotypic optimization

An increased understanding of growth-defense tradeoffs is expected to inform research aimed producing plants in which metabolic resources are optimally allocated to growth and defense, thereby enhancing productivity in a given environment (Figure 1.3B). The Pareto front concept has proven useful for analyzing the optimal allocation of resources to physiological tasks that trade off with each other in nature (Shoval et al., 2012). Given that the best plant phenotype for growth is usually a poor phenotype for defense (and vice versa), additional research is needed to determine how the relevant metabolic and signal transduction networks can be rewired to uncouple, or at least minimize, tradeoffs to produce plants that exhibit robust growth and defense at the same time. Genetic suppressor screens offer one approach to achieve this goal. Campos et al (Campos et al., 2016) started with a *jaz* quintuple mutant (*jazQ*) of Arabidopsis that lacks five JAZ repressors and, as a consequence, exhibits heightened defense against insect attack and accompanying growth restriction. A suppressor screen revealed that loss of the red light receptor phytochrome B (phyB) in the *jazQ* background reverts the low biomass phenotype without compromising resistance to chewing insects. Uncoupling of growth-defense tradeoffs in *jazQ phyB* plants was attributed in part to simultaneous activation of the MYC and PIF transcription factor modules, which in wild-type plants antagonize one another in part through direct interaction between JAZ and DELLA proteins (Hou et al., 2010; Yang et al., 2012) (Figure 1.3A). Remarkably, the unique combination of *jazQ phyB* results in a plant that is phenotypically superior to wild-type plants in terms of anti-insect defense in the absence of a growth penalty, at

least under ideal laboratory growth conditions (Figure 1.3C) (Shoval et al., 2012; Chae et al., 2016; Zust and Agrawal, 2017). Although these findings suggest that rational redesign of the underlying regulatory networks may be used to optimize growth-defense balance, it will ultimately be important to determine how such genetic changes influence plant fitness in diverse environmental conditions (Zust and Agrawal, 2017).

There is additional evidence that constitutive activation or priming of JA-mediated defenses can be achieved with minimum effects on growth (Chen et al., 2006; Smirnova et al., 2017). One striking example comes from work showing that downregulation of the Arabidopsis JAV1 repressor results in increased resistance to both necrotrophic fungi and insect herbivores without affecting growth (Hu et al., 2013). In addition to genetic modifications, it may also be possible to use chemical approaches to break the antagonistic link between growth and defense. For example, application of a synthetic macrolactone analog of JA-Ile was sufficient to induce JA-regulated defense responses in *N. attenuata* without obvious diminution of growth or fitness (Jimenez-Aleman et al., 2017). Although the molecular basis of this effect remains to be determined, it is possible that JA-Ile macrolactones work through specific COI1-JAZ coreceptor subtypes to promote defense at a level that does not restrict growth.

Finally, we note that strategies to optimize growth-defense tradeoffs extend beyond JA and include other components of growth and immune signaling networks. Plant breeders have long been engaged in efforts to reduce growth and yield penalties that accompany resistance (*R*) gene-mediated crop protection against pathogens and pests (Brown, 2002; Chae et al., 2016; Karasov et al., 2017; Ning et al., 2017). Recent molecular studies in rice provide compelling examples of how broad-spectrum resistance to *Magnaporthe oryzae*, the causal agent of rice blast disease, can occur in the absence of significant growth or yield penalties (Deng et al., 2017;

Li et al., 2017). These and other (Xu et al., 2017) recent studies highlight the utility of fine-tuning the expression of defense pathways as a strategy to maximize resistance while minimizing negative pleiotrophic effects on growth and yield.

APPENDIX

Figures

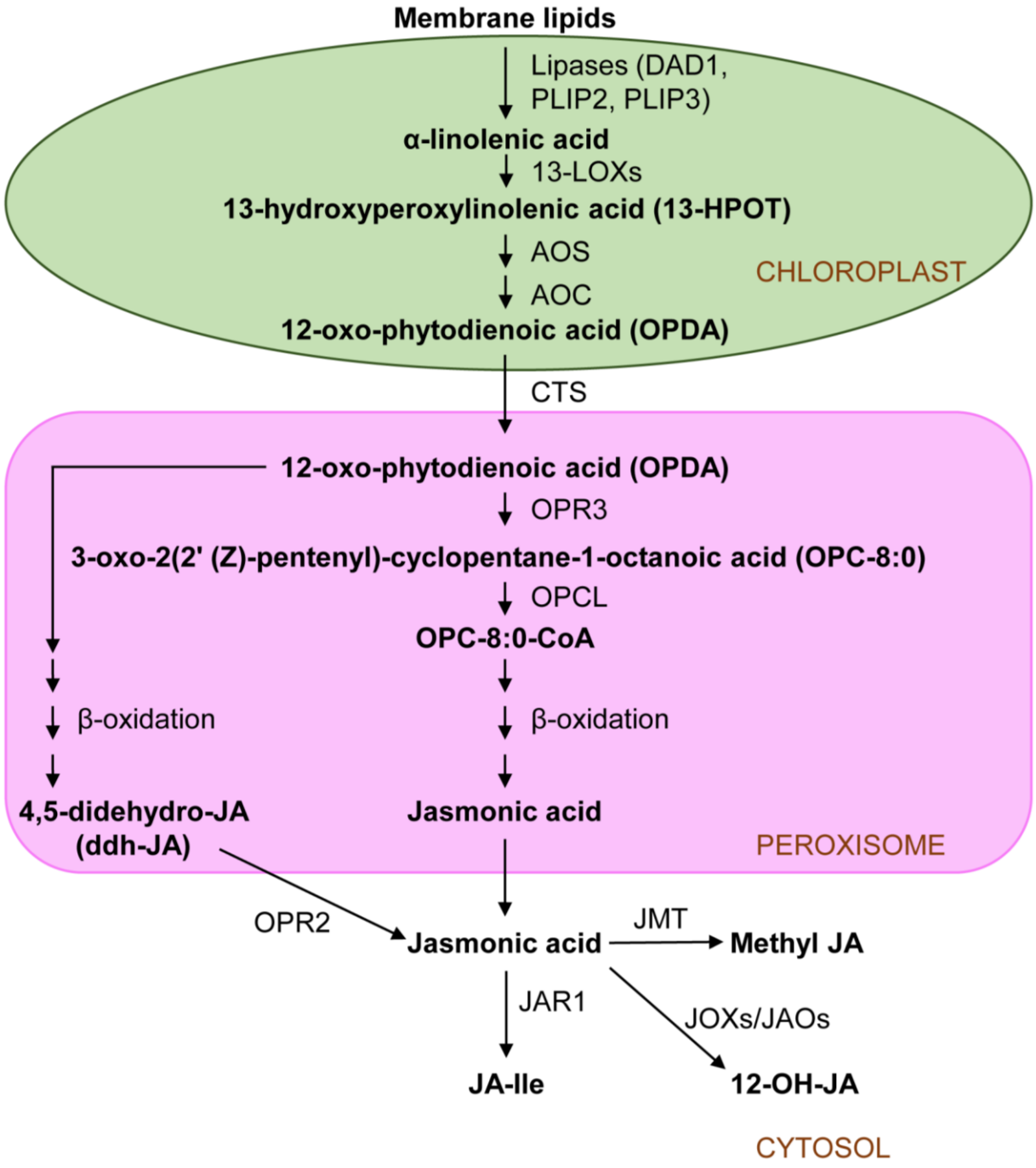

Figure 1.1. Biosynthesis and metabolism of JA in Arabidopsis.

JA biosynthesis involves two organelles: chloroplast and peroxisome. Intermediate products are highlighted in bold. Abbreviations: DAD1: DEFECTIVE IN ANTHER DEHISCENCE 1; PLIP2: PLASTID LIPASE 2; PLIP3: PLASTID LIPASE 3; 13-LOXs: 13-LIPOXYGENASEs; AOS: ALLENE OXIDE SYNTHASE; AOC: ALLENE OXIDE CYCLASE; CTS: COMATOSE;

Figure 1.1. (cont'd) OPR3: OPDA REDUCTASE 3; OPCL: OPC-8:0 COA LIGASE; OPR2: OPDA REDUCTASE 2; JAR1: JASMONATE RESISTANT 1; JOX: JASMONATE-INDUCED OXYGENASES; JAO: JASMONIC ACID OXIDASES; JMT: JA CARBOXYL METHYLTRANSFERASE.

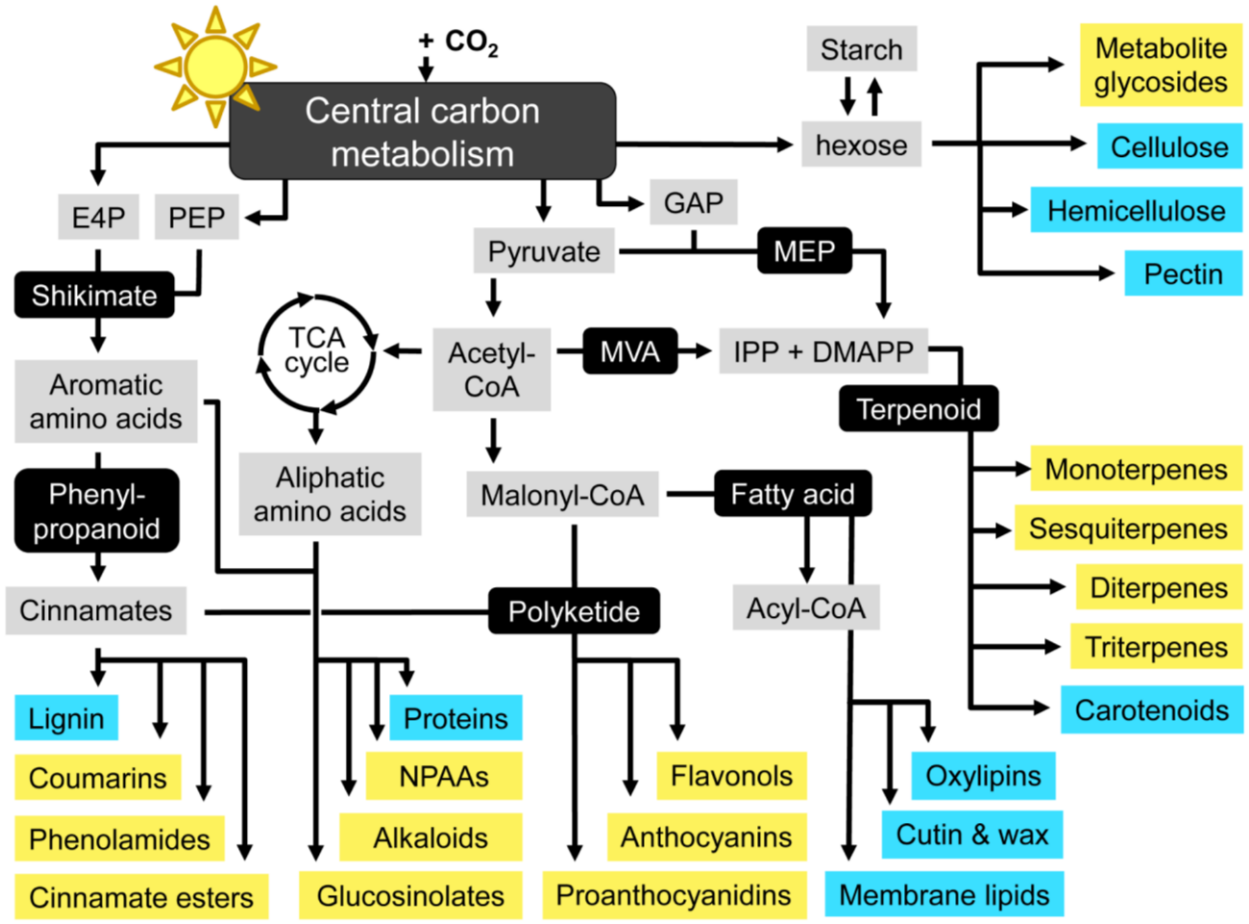

Figure 1.2. Connectivity between primary and specialized metabolism.

Core metabolites (grey) in primary carbon metabolism (Calvin-Benson cycle, pentose phosphate pathway, glycolysis) are precursors for a variety of metabolic pathways (black boxes) that produce diverse primary (blue) and specialized (yellow) metabolites. Metabolic intermediates that are shared by primary and specialized metabolism illustrate potential for resource-based tradeoffs via competition between pathways. Defense-associated compounds in Arabidopsis include coumarins (e.g., scopoletin), cinnamate esters (e.g., sinapoyl malate), phenolamides (e.g., coumaroylagmatine), non-protein amino acids (NPAAs; e.g., Nδ-acetylornithine), alkaloids (e.g., camalexin), glucosinolates (e.g., 4-methylthiobutyl-glucosinolate), flavonols (e.g., kaempferol glycosides), anthocyanins (e.g., cyanidin glycosides), proanthocyanidins (e.g., epicatechin polymers), monoterpenes (e.g., (*E*)-β-ocimene), sesquiterpenes (e.g., (*E*)-β-caryophyllene), diterpenes (e.g., rhizathalene), and triterpenes (e.g., thalianol). Not shown is the derivation of the polyamine moiety of phenolamides from aliphatic amino acids. Glycosylation (upper right) of metabolites, including coumarins, cinnamate esters, glucosinolates, flavonoids and terpenoids, serves multiple roles in defense. Whereas most alkaloids are derived from amino acids, some are generated from other precursors such as purines, terpenes, and polyketides. E4P, erythrose-4-phosphate; PEP, phosphoenolpyruvate, GAP, glyceraldehyde 3-phosphate; TCA, tricarboxylic

Figure 1.2. (cont'd) acid; MVA, mevalonate; MEP, methylerythritol 4-phosphate; IPP, isopentenyl pyrophosphate; DMAPP, dimethylallyl pyrophosphate.

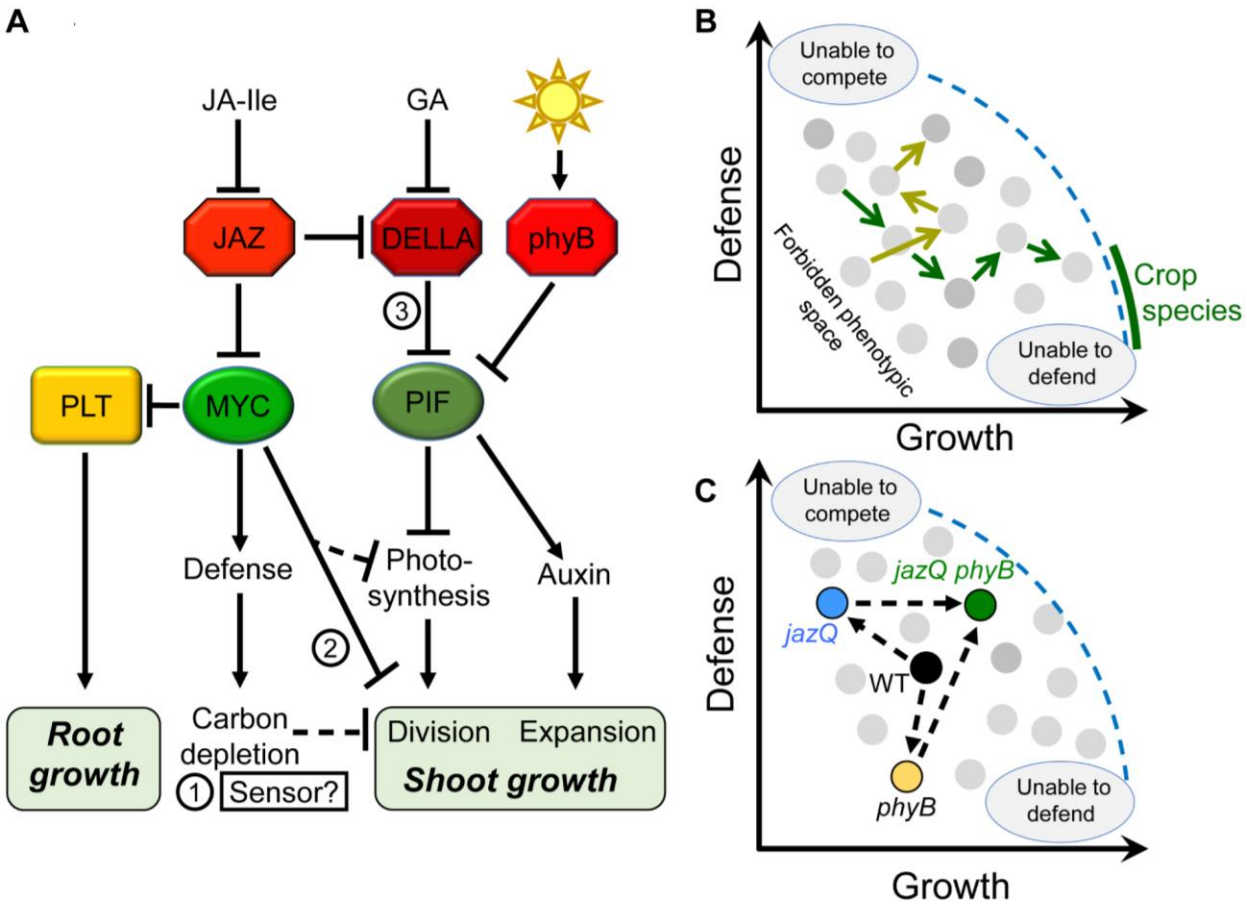

Figure 1.3. Signaling networks and phenotypic space associated with growth-defense conflict.

(A) Possible mechanisms to explain how JA restricts leaf growth. (1) JA-induced defense responses reduce carbon availability by diverting resources to the production of secondary metabolites. Altered carbon status may be detected by energy-sensing systems to reduce growth rate to a level that matches carbon availability. (2) MYC transcription factors inhibit growth independently of JA-induced defense responses. In roots, for example, MYC2 decreases the activity of the root meristem by repressing the expression of AP2-domain PLETHORA (PLT) transcription factors. In leaves, MYCs repress the expression of photosynthesis genes and may also constrain growth through unidentified regulators that repress cell division or cell expansion. (3) Crosstalk between JA-Ile and GA signaling pathways modulates growth responses. JAZ degradation releases DELLA proteins, which negatively regulate PIF transcription factors to inhibit cell expansion-type growth. PIF transcription factors inhibit chlorophyll biosynthesis and stimulate auxin production as part of the shade avoidance growth response. Points of positive and negative regulation are indicated by arrows and perpendicular lines, respectively. Dashed lines denote connections for which there is little direct evidence.
(B) Hypothetical relationship between growth and defense among individuals (grey circles) within a population. The dashed blue line denotes the so-called Pareto front (Shoval et al., 2012), which represents the most efficient allocations of resources to growth and defense within the physiological limits of the plant. Arrows denote evolutionary trajectories that give rise to

Figure 1.3. (cont'd) preferred genotypes that are closest to the Pareto front. Yellow arrows exemplify the hypothetical trajectory of a genotype having strong defense but less ability to compete in a given environment. Green arrows exemplify a hypothetical breeding selection for crop species having elevated growth (or yield) but less ability to defend; such tradeoffs are typically offset through the use of pesticides.
(C) Illustration of phenotypic space in which growth-defense balance can be optimized by genetic manipulation of the JA-Ile and phytochrome B (phyB) signaling pathways. Circles denote individuals within a population that exhibit various allocations to growth and defensed in a given environment. In Arabidopsis, *phyB* (yellow) and *jazQ* (blue) mutations favor rapid cell extension-type growth (i.e., shade avoidance) and defense, respectively. *jazQ phyB* (green) "double" mutants perform both tasks well at the same time and may even outperform wild-type (WT) plants under certain growth conditions (Campos et al., 2016). Dashed arrows denote how the indicated mutations shift allocations between growth and defense.

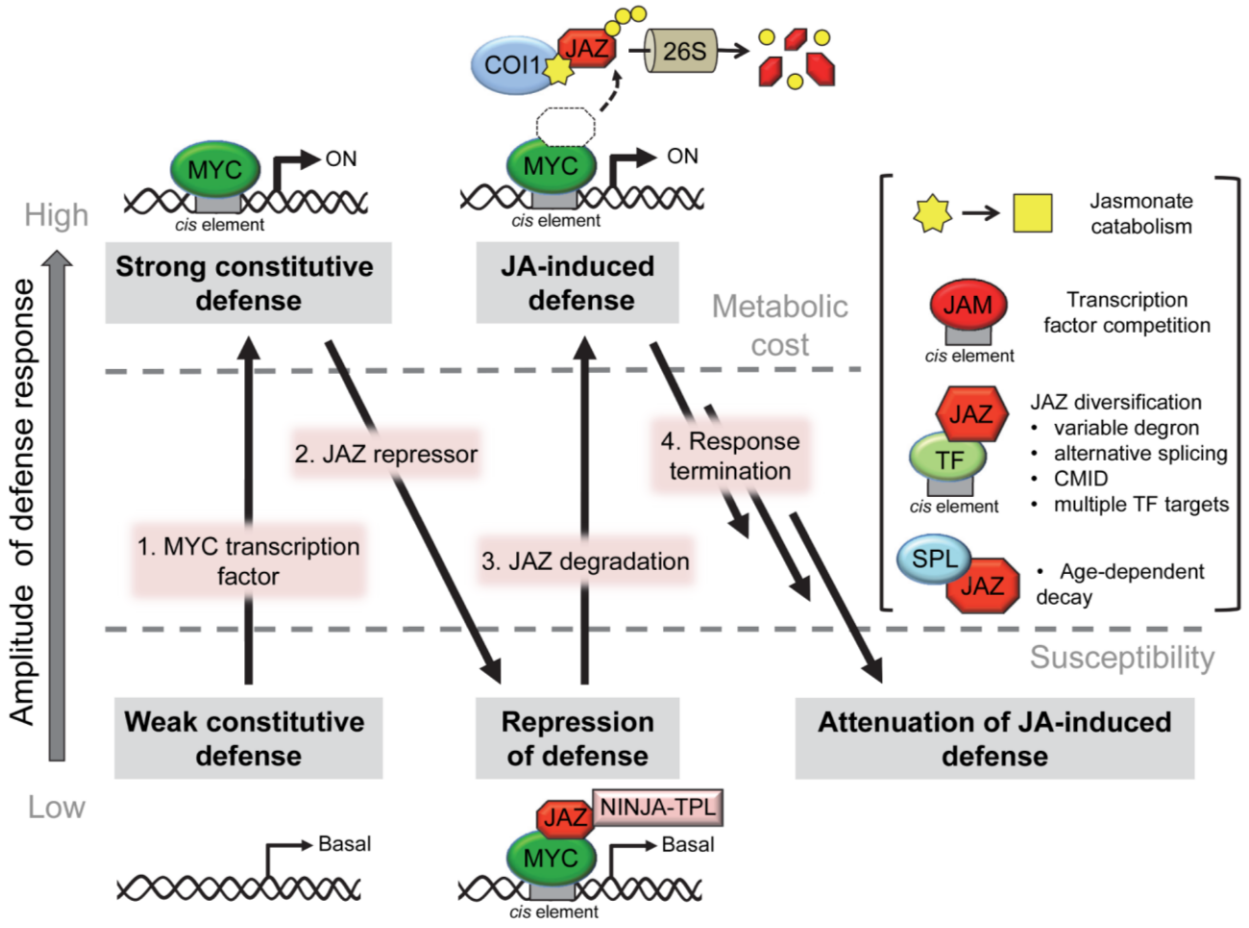

Figure 1.4. Speculative model of an evolutionary trajectory for JA-inducible defense.

The model proposes that JA-inducible defense evolved stepwise in response to selective pressure imposed by too little (e.g., susceptibility to biotic attackers) or too much (e.g., metabolic costs) defense. Initially, constitutive expression of neofunctionalized defense proteins or secondary metabolites derived from primary metabolism provided a low level of protection against plant consumers. Promoter mutations and recruitment of transcription factors (e.g., MYC2, green ovals) served to increase defense expression and plant fitness in environments where biotic aggressors were prevalent. In some conditions, the metabolic cost of heightened defense outweighed its benefit in a given environment (e.g., low frequency of biotic attack). In second step, selective pressure to reduce defense expression led to the recruitment of JAZ repressors (red octagon), perhaps from an ancestral TIFY protein, and associated NINJA-TOPLESS (TPL) co-repressors (pink rectangle). JAZ-mediated repression of MYC activity curtails the metabolic costs of high defense and, depending on the nature of the JAZ-MYC interaction, may promote growth at the expense of resistance in environments where biotic pressure was high or unpredictable. In a third major step, a JA-triggered ubiquitin-proteasome system emerged as a mechanism to degrade JAZ repressors and relieve repression on transcription factors. The F-box protein COI1 (blue oval) interacts with JAZ in the presence of JA-Ile (yellow star) to promote ubiquitination (yellow circles) and subsequent degradation of JAZ by the 26S proteasome. De-repression of defense gene expression in this manner could, under certain selective conditions,

Figure 1.4. (cont'd) incur other metabolic costs, including reduced carbon availability. In step 4 of this model, multiple mechanisms emerged to temporally and spatially restrain JA-regulated defense responses. Response termination includes catabolism of bioactive JA (yellow star to square), multiple mechanisms to increase the repressive activity of JAZ (red octagon), competitive inhibition by JAM transcription factors (red oval), and age-dependent decay of JA signaling. Dashed grey lines represent thresholds at which excessive metabolic costs and susceptibility to biotic aggressors impose selective pressure. CMID, cryptic MYC interaction domain.

REFERENCES

REFERENCES

Aharoni, A., and Galili, G. (2011). Metabolic engineering of the plant primary-secondary metabolism interface. Curr Opin Biotech **22,** 239-244.

An, C., Li, L., Zhai, Q., You, Y., Deng, L., Wu, F., Chen, R., Jiang, H., Wang, H., Chen, Q., and Li, C. (2017). Mediator subunit MED25 links the jasmonate receptor to transcriptionally active chromatin. Proceedings of the National Academy of Sciences of the United States of America **114,** E8930-E8939.

Attaran, E., Major, I.T., Cruz, J.A., Rosa, B.A., Koo, A.J.K., Chen, J., Kramer, D.M., He, S.Y., and Howe, G.A. (2014). Temporal Dynamics of Growth and Photosynthesis Suppression in Response to Jasmonate Signaling. Plant Physiol **165,** 1302-1314.

Babst, B.A., Ferrieri, R.A., Gray, D.W., Lerdau, M., Schlyer, D.J., Schueller, M., Thorpe, M.R., and Orians, C.M. (2005). Jasmonic acid induces rapid changes in carbon transport and partitioning in Populus. New Phytol **167,** 63-72.

Bai, Y.H., Meng, Y.J., Huang, D.L., Qi, Y.H., and Chen, M. (2011). Origin and evolutionary analysis of the plant-specific TIFY transcription factor family. Genomics **98,** 128-136.

Bannenberg, G., Martinez, M., Hamberg, M., and Castresana, C. (2009). Diversity of the Enzymatic Activity in the Lipoxygenase Gene Family of Arabidopsis thaliana. Lipids **44,** 85-95.

Bekaert, M., Edger, P.P., Hudson, C.M., Pires, J.C., and Conant, G.C. (2012). Metabolic and evolutionary costs of herbivory defense: systems biology of glucosinolate synthesis. New Phytol **196,** 596-605.

Belkhadirl, Y., Yang, L., Hetzel, J., Dangl, J.L., and Chory, J. (2014). The growth-defense pivot: crisis management in plants mediated by LRR-RK surface receptors. Trends Biochem Sci **39,** 447-456.

Bell, E., Creelman, R.A., and Mullet, J.E. (1995). A chloroplast lipoxygenase is required for wound-induced jasmonic acid accumulation in Arabidopsis. Proceedings of the National Academy of Sciences of the United States of America **92,** 8675-8679.

Bilgin, D.D., Zavala, J.A., Zhu, J., Clough, S.J., Ort, D.R., and DeLucia, E.H. (2010). Biotic stress globally downregulates photosynthesis genes. Plant Cell Environ **33,** 1597-1613.

Boter, M., Golz, J.F., Gimenez-Ibanez, S., Fernandez-Barbero, G., Franco-Zorrilla, J.M., and Solano, R. (2015). FILAMENTOUS FLOWER Is a Direct Target of JAZ3 and Modulates Responses to Jasmonate. Plant Cell **27,** 3160-3174.

Bowman, J.L., Kohchi, T., Yamato, K.T., Jenkins, J., Shu, S.Q., Ishizaki, K., Yamaoka, S., Nishihama, R., Nakamura, Y., Berger, F., Adam, C., Aki, S.S., Althoff, F., Araki, T.,

Arteaga-Vazquez, M.A., Balasubrmanian, S., Barry, K., Bauer, D., Boehm, C.R., Briginshaw, L., Caballero-Perez, J., Catarino, B., Chen, F., Chiyoda, S., Chovatia, M., Davies, K.M., Delmans, M., Demura, T., Dierschke, T., Dolan, L., Dorantes-Acosta, A.E., Eklund, D.M., Florent, S.N., Flores-Sandoval, E., Fujiyama, A., Fukuzawa, H., Galik, B., Grimanelli, D., Grimwood, J., Grossniklaus, U., Hamada, T., Haseloff, J., Hetherington, A.J., Higo, A., Hirakawa, Y., Hundley, H.N., Ikeda, Y., Inoue, K., Inoue, S.I., Ishida, S., Jia, Q.D., Kakita, M., Kanazawa, T., Kawai, Y., Kawashima, T., Kennedy, M., Kinose, K., Kinoshita, T., Kohara, Y., Koide, E., Komatsu, K., Kopischke, S., Kubo, M., Kyozuka, J., Lagercrantz, U., Lin, S.S., Lindquist, E., Lipzen, A.M., Lu, C.W., De Luna, E., Martienssen, R.A., Minamino, N., Mizutani, M., Mizutani, M., Mochizuki, N., Monte, I., Mosher, R., Nagasaki, H., Nakagami, H., Naramoto, S., Nishitani, K., Ohtani, M., Okamoto, T., Okumura, M., Phillips, J., Pollak, B., Reinders, A., Rovekamp, M., Sano, R., Sawa, S., Schmid, M.W., Shirakawa, M., Solano, R., Spunde, A., Suetsugu, N., Sugano, S., Sugiyama, A., Sun, R., Suzuki, Y., Takenaka, M., Takezawa, D., Tomogane, H., Tsuzuki, M., Ueda, T., Umeda, M., Ward, J.M., Watanabe, Y., Yazaki, K., Yokoyama, R., Yoshitake, Y., Yotsui, I., Zachgo, S., and Schmutz, J. (2017). Insights into Land Plant Evolution Garnered from the Marchantia polymorpha Genome. Cell **171,** 287-304.

Brown, J.K.M. (2002). Yield penalties of disease resistance in crops. Current Opinion in Plant Biology **5,** 339-344.

Caarls, L., Elberse, J., Awwanah, M., Ludwig, N.R., de Vries, M., Zeilmaker, T., Van Wees, S.C.M., Schuurink, R.C., and Van den Ackerveken, G. (2017). Arabidopsis JASMONATE-INDUCED OXYGENASES down-regulate plant immunity by hydroxylation and inactivation of the hormone jasmonic acid. Proceedings of the National Academy of Sciences of the United States of America **114,** 6388-6393.

Campos, M.L., Kang, J.H., and Howe, G.A. (2014). Jasmonate-Triggered Plant Immunity. J Chem Ecol **40,** 657-675.

Campos, M.L., Yoshida, Y., Major, I.T., de Oliveira Ferreira, D., Weraduwage, S.M., Froehlich, J.E., Johnson, B.F., Kramer, D.M., Jander, G., Sharkey, T.D., and Howe, G.A. (2016). Rewiring of jasmonate and phytochrome B signalling uncouples plant growth-defense tradeoffs. Nature communications **7,** 12570.

Celenza, J.L., Quiel, J.A., Smolen, G.A., Merrikh, H., Silvestro, A.R., Normanly, J., and Bender, J. (2005). The Arabidopsis ATR1 Myb transcription factor controls indolic glucosinolate homeostasis. Plant Physiol **137,** 253-262.

Chae, E., Tran, D.T.N., and Weigel, D. (2016). Cooperation and Conflict in the Plant Immune System. Plos Pathogens **12,** e1005452.

Chauvin, A., Caldelari, D., Wolfender, J.L., and Farmer, E.E. (2013). Four 13-lipoxygenases contribute to rapid jasmonate synthesis in wounded Arabidopsis thaliana leaves: a role for lipoxygenase 6 in responses to long-distance wound signals. New Phytol **197,** 566-575.

Chauvin, A., Lenglet, A., Wolfender, J.L., and Farmer, E.E. (2016). Paired Hierarchical Organization of 13-Lipoxygenases in Arabidopsis. Plants (Basel) **5,** 16.

Chen, H., Jones, A.D., and Howe, G.A. (2006). Constitutive activation of the jasmonate signaling pathway enhances the production of secondary metabolites in tomato. Febs Lett **580,** 2540-2546.

Chen, Q., Sun, J.Q., Zhai, Q.Z., Zhou, W.K., Qi, L.L., Xu, L., Wang, B., Chen, R., Jiang, H.L., Qi, J., Li, X.G., Palme, K., and Li, C.Y. (2011a). The Basic Helix-Loop-Helix Transcription Factor MYC2 Directly Represses PLETHORA Expression during Jasmonate-Mediated Modulation of the Root Stem Cell Niche in Arabidopsis. Plant Cell **23,** 3335-3352.

Chen, Q., Sun, J., Zhai, Q., Zhou, W., Qi, L., Xu, L., Wang, B., Chen, R., Jiang, H., Qi, J., Li, X., Palme, K., and Li, C. (2011b). The basic helix-loop-helix transcription factor MYC2 directly represses PLETHORA expression during jasmonate-mediated modulation of the root stem cell niche in Arabidopsis. Plant Cell **23,** 3335-3352.

Chico, J.M., Fernandez-Barbero, G., Chini, A., Fernandez-Calvo, P., Diez-Diaz, M., and Solano, R. (2014). Repression of Jasmonate-Dependent Defenses by Shade Involves Differential Regulation of Protein Stability of MYC Transcription Factors and Their JAZ Repressors in Arabidopsis. Plant Cell **26,** 1967-1980.

Chini, A., Fonseca, S., Fernandez, G., Adie, B., Chico, J.M., Lorenzo, O., Garcia-Casado, G., Lopez-Vidriero, I., Lozano, F.M., Ponce, M.R., Micol, J.L., and Solano, R. (2007). The JAZ family of repressors is the missing link in jasmonate signalling. Nature **448,** 666-671.

Chini, A., Monte, I., Zamarreno, A.M., Hamberg, M., Lassueur, S., Reymond, P., Weiss, S., Stintzi, A., Schaller, A., Porzel, A., Garcia-Mina, J.M., and Solano, R. (2018). An OPR3-independent pathway uses 4,5-didehydrojasmonate for jasmonate synthesis. Nat Chem Biol **14,** 171-178.

Chung, H.S., and Howe, G.A. (2009). A critical role for the TIFY motif in repression of jasmonate signaling by a stabilized splice variant of the JASMONATE ZIM-domain protein JAZ10 in Arabidopsis. Plant Cell **21,** 131-145.

Chung, H.S., Cooke, T.F., Depew, C.L., Patel, L.C., Ogawa, N., Kobayashi, Y., and Howe, G.A. (2010). Alternative splicing expands the repertoire of dominant JAZ repressors of jasmonate signaling. Plant J **63,** 613-622.

D'Auria, J.C., and Gershenzon, J. (2005). The secondary metabolism of Arabidopsis thaliana: growing like a weed. Current Opinion in Plant Biology **8,** 308-316.

De Geyter, N., Gholami, A., Goormachtig, S., and Goossens, A. (2012). Transcriptional machineries in jasmonate-elicited plant secondary metabolism. Trends Plant Sci **17,** 349-359.

De Virgilio, C. (2012). The essence of yeast quiescence. Fems Microbiol Rev **36,** 306-339.

De Vleesschauwer, D., Filipe, O., Hoffman, G., Seifi, H.S., Haeck, A., Canlas, P., Van Bockhaven, J., De Waele, E., Demeestere, K., Ronald, P., and Hofte, M. (2018). Target of rapamycin signaling orchestrates growth-defense trade-offs in plants. New Phytol **217,** 305-319.

Demianski, A.J., Chung, K.M., and Kunkel, B.N. (2012). Analysis of Arabidopsis JAZ gene expression during Pseudomonas syringae pathogenesis. Mol Plant Pathol **13,** 46-57.

Demole, E., Lederer, E., and Mercier, D. (1962). Isolement Et Determination De La Structure Du Jasmonate De Methyle, Constituant Odorant Caracteristique De Lessence De Jasmin. Helv Chim Acta **45,** 675-685.

Deng, Y., Zhai, K., Xie, Z., Yang, D., Zhu, X., Liu, J., Wang, X., Qin, P., Yang, Y., Zhang, G., Li, Q., Zhang, J., Wu, S., Milazzo, J., Mao, B., Wang, E., Xie, H., Tharreau, D., and He, Z. (2017). Epigenetic regulation of antagonistic receptors confers rice blast resistance with yield balance. Science **355,** 962-965.

Dubois, M., Van den Broeck, L., and Inze, D. (2018). The Pivotal Role of Ethylene in Plant Growth. Trends Plant Sci **23,** 311-323.

Falk, K.L., Tokuhisa, J.G., and Gershenzon, J. (2007). The effect of sulfur nutrition on plant glucosinolate content: Physiology and molecular mechanisms. Plant Biology **9,** 573-581.

Fernandez-Calvo, P., Chini, A., Fernandez-Barbero, G., Chico, J.M., Gimenez-Ibanez, S., Geerinck, J., Eeckhout, D., Schweizer, F., Godoy, M., Franco-Zorrilla, J.M., Pauwels, L., Witters, E., Puga, M.I., Paz-Ares, J., Goossens, A., Reymond, P., De Jaeger, G., and Solano, R. (2011). The Arabidopsis bHLH Transcription Factors MYC3 and MYC4 Are Targets of JAZ Repressors and Act Additively with MYC2 in the Activation of Jasmonate Responses. Plant Cell **23,** 701-715.

Feys, B.J.F., Benedetti, C.E., Penfold, C.N., and Turner, J.G. (1994). Arabidopsis Mutants Selected for Resistance to the Phytotoxin Coronatine Are Male-Sterile, Insensitive to Methyl Jasmonate, and Resistant to a Bacterial Pathogen. Plant Cell **6,** 751-759.

Fonseca, S., Chini, A., Hamberg, M., Adie, B., Porzel, A., Kramell, R., Miersch, O., Wasternack, C., and Solano, R. (2009). (+)-7-iso-Jasmonoyl-L-isoleucine is the endogenous bioactive jasmonate. Nat Chem Biol **5,** 344-350.

Fonseca, S., Fernandez-Calvo, P., Fernandez, G.M., Diez-Diaz, M., Gimenez-Ibanez, S., Lopez-Vidriero, I., Godoy, M., Fernandez-Barbero, G., Van Leene, J., De Jaeger, G., Franco-Zorrilla, J.M., and Solano, R. (2014). bHLH003, bHLH013 and bHLH017 are new targets of JAZ repressors negatively regulating JA responses. Plos One **9,** e86182.

Gasperini, D., Chetelat, A., Acosta, I.F., Goossens, J., Pauwels, L., Goossens, A., Dreos, R., Alfonso, E., and Farmer, E.E. (2015). Multilayered Organization of Jasmonate Signalling in the Regulation of Root Growth. Plos Genet **11,** e1005300.

Gershenzon, J. (1994). Metabolic costs of terpenoid accumulation in higher plants. J Chem Ecol **20,** 1281-1328.

Gigolashvili, T., Berger, B., Mock, H.P., Muller, C., Weisshaar, B., and Fluegge, U.I. (2007). The transcription factor HIG1/MYB51 regulates indolic glucosinolate biosynthesis in Arabidopsis thaliana. Plant J **50,** 886-901.

Gimenez-Ibanez, S., Boter, M., Ortigosa, A., Garcia-Casado, G., Chini, A., Lewsey, M.G., Ecker, J.R., Ntoukakis, V., and Solano, R. (2017). JAZ2 controls stomata dynamics during bacterial invasion. New Phytol **213,** 1378-1392.

Goossens, J., Mertens, J., and Goossens, A. (2017). Role and functioning of bHLH transcription factors in jasmonate signalling. Journal of experimental botany **68,** 1333-1347.

Hanik, N., Gomez, S., Best, M., Schueller, M., Orians, C.M., and Ferrieri, R.A. (2010). Partitioning of New Carbon as C-11 in Nicotiana tabacum Reveals Insight into Methyl Jasmonate Induced Changes in Metabolism. J Chem Ecol **36,** 1058-1067.

Havko, N.E., Major, I.T., Jewell, J.B., Attaran, E., Browse, J., and Howe, G.A. (2016). Control of Carbon Assimilation and Partitioning by Jasmonate: An Accounting of Growth-Defense Tradeoffs. Plants (Basel) **5,** E7.

Heil, M., and Baldwin, I.T. (2002). Fitness costs of induced resistance: emerging experimental support for a slippery concept. Trends Plant Sci **7,** 61-67.

Heitz, T., Smirnova, E., Widemann, E., Aubert, Y., Pinot, F., and Menard, R. (2016). The Rise and Fall of Jasmonate Biological Activities. Subcell Biochem **86,** 405-426.

Herms, D.A., and Mattson, W.J. (1992). The Dilemma of Plants - to Grow or Defend. Q Rev Biol **67,** 283-335.

Hibara, K., Isono, M., Mimura, M., Sentoku, N., Kojima, M., Sakakibara, H., Kitomi, Y., Yoshikawa, T., Itoh, J., and Nagato, Y. (2016). Jasmonate regulates juvenile-to-adult phase transition in rice. Development **143,** 3407-3416.

Hou, X.L., Lee, L.Y.C., Xia, K.F., Yen, Y.Y., and Yu, H. (2010). DELLAs Modulate Jasmonate Signaling via Competitive Binding to JAZs. Dev Cell **19,** 884-894.

Howe, G.A. (2018). Metabolic end run to jasmonate. Nat Chem Biol **14,** 109-110.

Howe, G.A., and Jander, G. (2008). Plant immunity to insect herbivores. Annual Review of Plant Biology **59,** 41-66.

Howe, G.A., Major, I.T., and Koo, A.J. (2018). Modularity in Jasmonate Signaling for Multistress Resilience. Annual Review of Plant Biology, **69,** 387-415.

Hu, P., Zhou, W., Cheng, Z.W., Fan, M., Wang, L., and Xie, D.X. (2013). JAV1 Controls Jasmonate-Regulated Plant Defense. Mol Cell **50,** 504-515.

Huot, B., Yao, J., Montgomery, B.L., and He, S.Y. (2014). Growth-defense tradeoffs in plants: a balancing act to optimize fitness. Mol Plant **7,** 1267-1287.

Ishiguro, S., Kawai-Oda, A., Ueda, J., Nishida, I., and Okada, K. (2001). The DEFECTIVE IN ANTHER DEHISCENCE1 gene encodes a novel phospholipase A1 catalyzing the initial step of jasmonic acid biosynthesis, which synchronizes pollen maturation, anther dehiscence, and flower opening in Arabidopsis. Plant Cell **13,** 2191-2209.

Ishihara, H., Moraes, T.A., Pyl, E.T., Schulze, W.X., Obata, T., Scheffel, A., Fernie, A.R., Sulpice, R., and Stitt, M. (2017). Growth rate correlates negatively with protein turnover in Arabidopsis accessions. Plant J **91,** 416-429.

Jimenez-Aleman, G.H., Machado, R.A.R., Baldwin, I.T., and Boland, W. (2017). JA-Ile-macrolactones uncouple growth and defense in wild tobacco. Org Biomol Chem **15,** 3391-3395.

Karasov, T.L., Chae, E., Herman, J.J., and Bergelson, J. (2017). Mechanisms to Mitigate the Trade-Off between Growth and Defense. Plant Cell **29,** 666-680.

Katsir, L., Schilmiller, A.L., Staswick, P.E., He, S.Y., and Howe, G.A. (2008). COI1 is a critical component of a receptor for jasmonate and the bacterial virulence factor coronatine. Proceedings of the National Academy of Sciences of the United States of America **105,** 7100-7105.

Kazan, K., and Manners, J.M. (2013). MYC2: The Master in Action. Molecular Plant **6,** 686-703.

Ke, J.Y., Ma, H.L., Gu, X., Thelen, A., Brunzelle, J.S., Li, J.Y., Xu, H.E., and Melcher, K. (2015). Structural basis for recognition of diverse transcriptional repressors by the TOPLESS family of corepressors. Sci Adv **1,** e1500107.

Kliebenstein, D.J. (2016). False idolatry of the mythical growth versus immunity tradeoff in molecular systems plant pathology. Physiol Mol Plant P **95,** 55-59.

Koo, A.J., and Howe, G.A. (2012). Catabolism and deactivation of the lipid-derived hormone jasmonoyl-isoleucine. Front Plant Sci **3,** 19.

Koo, A.J.K., and Howe, G.A. (2009). The wound hormone jasmonate. Phytochemistry **70,** 1571-1580.

Li, C., Schilmiller, A.L., Liu, G., Lee, G.I., Jayanty, S., Sageman, C., Vrebalov, J., Giovannoni, J.J., Yagi, K., Kobayashi, Y., and Howe, G.A. (2005). Role of beta-oxidation in jasmonate biosynthesis and systemic wound signaling in tomato. Plant Cell **17,** 971-986.

Li, L., Zhao, Y.F., McCaig, B.C., Wingerd, B.A., Wang, J.H., Whalon, M.E., Pichersky, E., and Howe, G.A. (2004). The tomato homolog of CORONATINE-INSENSITIVE1 is required for the maternal control of seed maturation, jasmonate-signaled defense responses, and glandular trichome development. Plant Cell **16,** 126-143.

Li, W.T., Zhu, Z.W., Chern, M.S., Yin, J.J., Yang, C., Ran, L., Cheng, M.P., He, M., Wang, K., Wang, J., Zhou, X.G., Zhu, X.B., Chen, Z.X., Wang, J.C., Zhao, W., Ma, B.T., Qin, P., Chen, W.L., Wang, Y.P., Liu, J.L., Wang, W.M., Wu, X.J., Li, P., Wang, J.R., Zhu, L.H., Li, S.G., and Chen, X.W. (2017). A Natural Allele of a Transcription Factor in Rice Confers Broad-Spectrum Blast Resistance. Cell **170,** 114-126.

Liu, X.J., An, X.H., Liu, X., Hu, D.G., Wang, X.F., You, C.X., and Hao, Y.J. (2017). MdSnRK1.1 interacts with MdJAZ18 to regulate sucrose-induced anthocyanin and proanthocyanidin accumulation in apple. Journal of experimental botany **68,** 2977-2990.

Lorenzo, O., Chico, J.M., Sanchez-Serrano, J.J., and Solano, R. (2004). Jasmonate-insensitive1 encodes a MYC transcription factor essential to discriminate between different jasmonate-regulated defense responses in Arabidopsis. Plant Cell **16,** 1938-1950.

Lozano-Duran, R., and Zipfel, C. (2015). Trade-off between growth and immunity: role of brassinosteroids. Trends Plant Sci **20,** 12-19.

Luo, R., Wei, H., Ye, L., Wang, K., Chen, F., Luo, L., Liu, L., Li, Y., Crabbe, M.J., Jin, L., Li, Y., and Zhong, Y. (2009). Photosynthetic metabolism of C3 plants shows highly cooperative regulation under changing environments: a systems biological analysis. Proceedings of the National Academy of Sciences of the United States of America **106,** 847-852.

Machado, R.A.R., Baldwin, I.T., and Erb, M. (2017). Herbivory-induced jasmonates constrain plant sugar accumulation and growth by antagonizing gibberellin signaling and not by promoting secondary metabolite production. New Phytol **215,** 803-812.

Machado, R.A.R., Arce, C.C.M., Ferrieri, A.P., Baldwin, I.T., and Erb, M. (2015). Jasmonate-dependent depletion of soluble sugars compromises plant resistance to Manduca sexta. New Phytol **207,** 91-105.

Machado, R.A.R., Ferrieri, A.P., Robert, C.A.M., Glauser, G., Kallenbach, M., Baldwin, I.T., and Erb, M. (2013). Leaf-herbivore attack reduces carbon reserves and regrowth from the roots via jasmonate and auxin signaling. New Phytol **200,** 1234-1246.

Major, I.T., Yoshida, Y., Campos, M.L., Kapali, G., Xin, X.F., Sugimoto, K., de Oliveira Ferreira, D., He, S.Y., and Howe, G.A. (2017). Regulation of growth-defense balance by the JASMONATE ZIM-DOMAIN (JAZ)-MYC transcriptional module. New Phytol **215,** 1533-1547.

Mao, Y.B., Liu, Y.Q., Chen, D.Y., Chen, F.Y., Fang, X., Hong, G.J., Wang, L.J., Wang, J.W., and Chen, X.Y. (2017). Jasmonate response decay and defense metabolite

accumulation contributes to age-regulated dynamics of plant insect resistance. Nature communications **8,** 13925.

Matin, A. (1991). The molecular basis of carbon-starvation-induced general resistance in Escherichia coli. Mol Microbiol **5,** 3-10.

McConn, M., and Browse, J. (1996). The Critical Requirement for Linolenic Acid Is Pollen Development, Not Photosynthesis, in an Arabidopsis Mutant. Plant Cell **8,** 403-416.

Moreno, J.E., Tao, Y., Chory, J., and Ballare, C.L. (2009). Ecological modulation of plant defense via phytochrome control of jasmonate sensitivity. Proceedings of the National Academy of Sciences of the United States of America **106,** 4935-4940.

Moreno, J.E., Shyu, C., Campos, M.L., Patel, L.C., Chung, H.S., Yao, J., He, S.Y., and Howe, G.A. (2013). Negative Feedback Control of Jasmonate Signaling by an Alternative Splice Variant of JAZ10. Plant Physiol **162,** 1006-1017.

Mugford, S.G., Yoshimoto, N., Reichelt, M., Wirtz, M., Hill, L., Mugford, S.T., Nakazato, Y., Noji, M., Takahashi, H., Kramell, R., Gigolashvili, T., Flugge, U.I., Wasternack, C., Gershenzon, J., Hell, R., Saito, K., and Kopriva, S. (2009). Disruption of Adenosine-5 '-Phosphosulfate Kinase in Arabidopsis Reduces Levels of Sulfated Secondary Metabolites. Plant Cell **21,** 910-927.

Nakata, M., Mitsuda, N., Herde, M., Koo, A.J.K., Moreno, J.E., Suzuki, K., Howe, G.A., and Ohme-Takagi, M. (2013). A bHLH-Type Transcription Factor, ABA-INDUCIBLE BHLH-TYPE TRANSCRIPTION FACTOR/JA-ASSOCIATED MYC2-LIKE1, Acts as a Repressor to Negatively Regulate Jasmonate Signaling in Arabidopsis. Plant Cell **25,** 1641-1656.

Navarro, L., Bari, R., Achard, P., Lison, P., Nemri, A., Harberd, N.P., and Jones, J.D.G. (2008). DELLAs control plant immune responses by modulating the balance and salicylic acid signaling. Curr Biol **18,** 650-655.

Neilson, E.H., Goodger, J.Q.D., Woodrow, I.E., and Moller, B.L. (2013). Plant chemical defense: at what cost? Trends Plant Sci **18,** 250-258.

Ning, Y., Liu, W., and Wang, G.L. (2017). Balancing Immunity and Yield in Crop Plants. Trends Plant Sci **22,** 1069-1079.

Noir, S., Bomer, M., Takahashi, N., Ishida, T., Tsui, T.L., Balbi, V., Shanahan, H., Sugimoto, K., and Devoto, A. (2013). Jasmonate Controls Leaf Growth by Repressing Cell Proliferation and the Onset of Endoreduplication while Maintaining a Potential Stand-By Mode. Plant Physiol **161,** 1930-1951.

Nour-Eldin, H.H., Andersen, T.G., Burow, M., Madsen, S.R., Jorgensen, M.E., Olsen, C.E., Dreyer, I., Hedrich, R., Geiger, D., and Halkier, B.A. (2012). NRT/PTR transporters are essential for translocation of glucosinolate defence compounds to seeds. Nature **488,** 531-534.

Papazian, S., Khaling, E., Bonnet, C., Lassueur, S., Reymond, P., Moritz, T., Blande, J.D., and Albrectsen, B.R. (2016). Central Metabolic Responses to Ozone and Herbivory Affect Photosynthesis and Stomatal Closure. Plant Physiol **172,** 2057-2078.

Pauwels, L., Barbero, G.F., Geerinck, J., Tilleman, S., Grunewald, W., Perez, A.C., Chico, J.M., Vanden Bossche, R., Sewell, J., Gil, E., Garcia-Casado, G., Witters, E., Inze, D., Long, J.A., De Jaeger, G., Solano, R., and Goossens, A. (2010). NINJA connects the co-repressor TOPLESS to jasmonate signalling. Nature **464,** 788-U169.

Pratiwi, P., Tanaka, G., Takahashi, T., Xie, X., Yoneyama, K., Matsuura, H., and Takahashi, K. (2017). Identification of Jasmonic Acid and Jasmonoyl-Isoleucine, and Characterization of AOS, AOC, OPR and JAR1 in the Model Lycophyte Selaginella moellendorffii. Plant & cell physiology **58,** 789-801.

Qi, T., Huang, H., Song, S., and Xie, D. (2015). Regulation of Jasmonate-Mediated Stamen Development and Seed Production by a bHLH-MYB Complex in Arabidopsis. Plant Cell **27,** 1620-1633.

Schilmiller, A.L., Koo, A.J.K., and Howe, G.A. (2007). Functional diversification of acyl-coenzyme A oxidases in jasmonic acid biosynthesis and action. Plant Physiol **143,** 812-824.

Schneider, K., Kienow, L., Schmelzer, E., Colby, T., Bartsch, M., Miersch, O., Wasternack, C., Kombrink, E., and Stuible, H.P. (2005). A new type of peroxisomal acyl-coenzyme A synthetase from Arabidopsis thaliana has the catalytic capacity to activate biosynthetic precursors of jasmonic acid. J Biol Chem **280,** 13962-13972.

Schwachtje, J., and Baldwin, I.T. (2008). Why does herbivore attack reconfigure primary metabolism? Plant Physiol **146,** 845-851.

Schwachtje, J., Minchin, P.E.H., Jahnke, S., van Dongen, J.T., Schittko, U., and Baldwin, I.T. (2006). SNF1-related kinases allow plants to tolerate herbivory by allocating carbon to roots. Proceedings of the National Academy of Sciences of the United States of America **103,** 12935-12940.

Schweizer, F., Fernandez-Calvo, P., Zander, M., Diez-Diaz, M., Fonseca, S., Glauser, G., Lewsey, M.G., Ecker, J.R., Solano, R., and Reymond, P. (2013). Arabidopsis Basic Helix-Loop-Helix Transcription Factors MYC2, MYC3, and MYC4 Regulate Glucosinolate Biosynthesis, Insect Performance, and Feeding Behavior. Plant Cell **25,** 3117-3132.

Sheard, L.B., Tan, X., Mao, H.B., Withers, J., Ben-Nissan, G., Hinds, T.R., Kobayashi, Y., Hsu, F.F., Sharon, M., Browse, J., He, S.Y., Rizo, J., Howe, G.A., and Zheng, N. (2010). Jasmonate perception by inositol-phosphate-potentiated COI1-JAZ co-receptor. Nature **468,** 400-U301.

Shoval, O., Sheftel, H., Shinar, G., Hart, Y., Ramote, O., Mayo, A., Dekel, E., Kavanagh, K., and Alon, U. (2012). Evolutionary Trade-Offs, Pareto Optimality, and the Geometry of Phenotype Space. Science **336,** 1157-1160.

Shyu, C., Figueroa, P., DePew, C.L., Cooke, T.F., Sheard, L.B., Moreno, J.E., Katsir, L., Zheng, N., Browse, J., and Howe, G.A. (2012). JAZ8 Lacks a Canonical Degron and Has an EAR Motif That Mediates Transcriptional Repression of Jasmonate Responses in Arabidopsis. Plant Cell **24,** 536-550.

Smirnova, E., Marquis, V., Poirier, L., Aubert, Y., Zumsteg, J., Menard, R., Miesch, L., and Heitz, T. (2017). Jasmonic Acid Oxidase 2 Hydroxylates Jasmonic Acid and Represses Basal Defense and Resistance Responses against Botrytis cinerea Infection. Mol Plant **10,** 1159-1173.

Smith, A.M., and Stitt, M. (2007). Coordination of carbon supply and plant growth. Plant Cell Environ **30,** 1126-1149.

Song, S.S., Qi, T.C., Fan, M., Zhang, X., Gao, H., Huang, H., Wu, D.W., Guo, H.W., and Xie, D.X. (2013). The bHLH Subgroup IIId Factors Negatively Regulate Jasmonate-Mediated Plant Defense and Development. Plos Genet **9,** e1003653.

Song, W.C., and Brash, A.R. (1991). Purification of an Allene Oxide Synthase and Identification of the Enzyme as a Cytochrome-P-450. Science **253,** 781-784.

Song, Y., Zhao, G., Zhang, X.Y., Li, L.X., Xiong, F.J., Zhuo, F.P., Zhang, C.J., Yang, Z.R., Datla, R., Ren, M.Z., and Li, F.G. (2017). The crosstalk between Target of Rapamycin (TOR) and Jasmonic Acid (JA) signaling existing in Arabidopsis and cotton. Sci Rep **7,** 45830.

Stamp, N. (2003). Out of the quagmire of plant defense hypotheses. Q Rev Biol **78,** 23-55.

Staswick, P.E., Tiryaki, I., and Rowe, M.L. (2002). Jasmonate response locus JAR1 and several related Arabidopsis genes encode enzymes of the firefly luciferase superfamily that show activity on jasmonic, salicylic, and indole-3-acetic acids in an assay for adenylation. Plant Cell **14,** 1405-1415.

Stintzi, A., and Browse, J. (2000). The Arabidopsis male-sterile mutant, opr3, lacks the 12-oxophytodienoic acid reductase required for jasmonate synthesis. Proceedings of the National Academy of Sciences of the United States of America **97,** 10625-10630.

Thaler, J.S., Humphrey, P.T., and Whiteman, N.K. (2012). Evolution of jasmonate and salicylate signal crosstalk. Trends Plant Sci **17,** 260-270.

Theodoulou, F.L., Job, K., Slocombe, S.P., Footitt, S., Holdsworth, M., Baker, A., Larson, T.R., and Graham, I.A. (2005). Jasmonoic acid levels are reduced in COMATOSE ATP-binding cassette transporter mutants. Implications for transport of jasmonate precursors into peroxisomes. Plant Physiol **137,** 835-840.

Thines, B., Katsir, L., Melotto, M., Niu, Y., Mandaokar, A., Liu, G., Nomura, K., He, S.Y., Howe, G.A., and Browse, J. (2007). JAZ repressor proteins are targets of the SCF(COI1) complex during jasmonate signalling. Nature **448,** 661-665.

Thireault, C., Shyu, C., Yoshida, Y., St Aubin, B., Campos, M.L., and Howe, G.A. (2015). Repression of jasmonate signaling by a non-TIFY JAZ protein in Arabidopsis. Plant J **82,** 669-679.

Ueda, J., and Kato, J. (1980). Isolation and Identification of a Senescence-Promoting Substance from Wormwood (Artemisia-Absinthium L). Plant Physiol **66,** 246-249.

Ullmann-Zeunert, L., Stanton, M.A., Wielsch, N., Bartram, S., Hummert, C., Svatos, A., Baldwin, I.T., and Groten, K. (2013). Quantification of growth-defense trade-offs in a common currency: nitrogen required for phenolamide biosynthesis is not derived from ribulose-1,5-bisphosphate carboxylase/oxygenase turnover. Plant J **75,** 417-429.

Vanholme, B., Grunewald, W., Bateman, A., Kohchi, T., and Gheysen, G. (2007). The tify family previously known as ZIM. Trends Plant Sci **12,** 239-244.

Vick, B.A., and Zimmerman, D.C. (1984). Biosynthesis of Jasmonic Acid by Several Plant-Species. Plant Physiol **75,** 458-461.

Wang, K., Guo, Q., Froehlich, J.E., Hersh, H.L., Zienkiewicz, A., Howe, G.A., and Benning, C. (2018). Two Abscisic Acid-Responsive Plastid Lipase Genes Involved in Jasmonic Acid Biosynthesis in Arabidopsis thaliana. Plant Cell **30,** 1006-1022.

Wasternack, C. (2015). How Jasmonates Earned their Laurels: Past and Present J Plant Growth Regul **34,** 761-794.

Xie, D.X., Feys, B.F., James, S., Nieto-Rostro, M., and Turner, J.G. (1998). COI1: An Arabidopsis gene required for jasmonate-regulated defense and fertility. Science **280,** 1091-1094.

Xu, G., Yuan, M., Ai, C., Liu, L., Zhuang, E., Karapetyan, S., Wang, S., and Dong, X. (2017). uORF-mediated translation allows engineered plant disease resistance without fitness costs. Nature **545,** 491-494.

Yan, Y.X., Stolz, S., Chetelat, A., Reymond, P., Pagni, M., Dubugnon, L., and Farmer, E.E. (2007). A downstream mediator in the growth repression limb of the jasmonate pathway. Plant Cell **19,** 2470-2483.

Yang, D.L., Yao, J., Mei, C.S., Tong, X.H., Zeng, L.J., Li, Q., Xiao, L.T., Sun, T.P., Li, J.G., Deng, X.W., Lee, C.M., Thomashow, M.F., Yang, Y.N., He, Z.H., and He, S.Y. (2012). Plant hormone jasmonate prioritizes defense over growth by interfering with gibberellin signaling cascade. Proceedings of the National Academy of Sciences of the United States of America **109,** E1192-E1200.

Yatusevich, R., Mugford, S.G., Matthewman, C., Gigolashvili, T., Frerigmann, H., Delaney, S., Koprivova, A., Flugge, U.I., and Kopriva, S. (2010). Genes of primary sulfate assimilation are part of the glucosinolate biosynthetic network in Arabidopsis thaliana. Plant J **62,** 1-11.

Zhang, F., Yao, J., Ke, J., Zhang, L., Lam, V.Q., Xin, X.F., Zhou, X.E., Chen, J., Brunzelle, J., Griffin, P.R., Zhou, M., Xu, H.E., Melcher, K., and He, S.Y. (2015). Structural basis of JAZ repression of MYC transcription factors in jasmonate signalling. Nature **525,** 269-273.

Zhang, L., Zhang, F., Melotto, M., Yao, J., and He, S.Y. (2017). Jasmonate signaling and manipulation by pathogens and insects. Journal of experimental botany **68,** 1371-1385.

Zhang, L.R., and Xing, D. (2008). Methyl jasmonate induces production of reactive oxygen species and alterations in mitochondrial dynamics that precede photosynthetic dysfunction and subsequent cell death. Plant and Cell Physiology **49,** 1092-1111.

Zhang, Y., and Turner, J.G. (2008). Wound-Induced Endogenous Jasmonates Stunt Plant Growth by Inhibiting Mitosis. Plos One **3,** e3699.

Zheng, X.Y., Spivey, N.W., Zeng, W.Q., Liu, P.P., Fu, Z.Q., Klessig, D.F., He, S.Y., and Dong, X.N. (2012). Coronatine Promotes Pseudomonas syringae Virulence in Plants by Activating a Signaling Cascade that Inhibits Salicylic Acid Accumulation. Cell Host Microbe **11,** 587-596.

Zhou, M., and Memelink, J. (2016). Jasmonate-responsive transcription factors regulating plant secondary metabolism. Biotechnol Adv **34,** 441-449.

Zhou, S.Q., Lou, Y.R., Tzin, V., and Jander, G. (2015). Alteration of Plant Primary Metabolism in Response to Insect Herbivory. Plant Physiol **169,** 1488-1498.

Zhou, W.W., Brochmoller, T., Ling, Z.H., Omdahl, A., Baldwin, I.T., and Xu, S.Q. (2016). Evolution of herbivore-induced early defense signaling was shaped by genome wide duplications in Nicotiana. Elife **5**.

Ziegler, J., Stenzel, I., Hause, B., Maucher, H., Hamberg, M., Grimm, R., Ganal, M., and Wasternack, C. (2000). Molecular cloning of allene oxide cyclase. The enzyme establishing the stereochemistry of octadecanoids and jasmonates. J Biol Chem **275,** 19132-19138.

Zust, T., and Agrawal, A.A. (2017). Trade-Offs Between Plant Growth and Defense Against Insect Herbivory: An Emerging Mechanistic Synthesis. Annual Review of Plant Biology **68,** 10.11-10.22.

CHAPTER TWO - JAZ REPRESSORS OF METABOLIC DEFENSE PROMOTE GROWTH AND REPRODUCTIVE FITNESS IN ARABIDOPSIS

Work presented in this chapter has been published:

Guo, Q., Yoshida, Y., Major, I.T., Wang, K., Sugimoto, K., Kapali, G., Havko, N.E., Benning, C., and Howe, G.A. (2018). JAZ repressors of metabolic defense promote growth and reproductive fitness in Arabidopsis. Proceedings of the National Academy of Sciences of the United States of America **115**, E10768-E10777.

Abstract

Plant immune responses mediated by the hormone jasmonoyl-L-isoleucine (JA-Ile) are metabolically costly and often linked to reduced growth. Although it is known that JA-Ile activates defense responses by triggering the degradation of JASMONATE ZIM DOMAIN (JAZ) transcriptional repressor proteins, expansion of the *JAZ* gene family in vascular plants has hampered efforts to understand how this hormone impacts growth and other physiological tasks over the course of ontogeny. Here, we combined mutations within the 13-member Arabidopsis *JAZ* gene family to investigate the effects of chronic JAZ deficiency on growth, defense, and reproductive output. A higher-order mutant (*jaz* decuple, *jazD*) defective in ten *JAZ* genes (*JAZ1-7*, *-9*, *-10*, and *-13*) exhibited robust resistance to insect herbivores and fungal pathogens, which was accompanied by slow vegetative growth and poor reproductive performance. Metabolic phenotypes of *jazD* discerned from global transcript and protein profiling were indicative of elevated carbon partitioning to amino acid-, protein-, and endoplasmic reticulum body-based defenses controlled by the JA-Ile and ethylene branches of immunity. Resource allocation to a strong defense sink in *jazD* leaves was associated with increased respiration and hallmarks of carbon starvation but no overt changes in photosynthetic rate. Depletion of the remaining JAZ repressors in *jazD* further exaggerated growth stunting, nearly abolished seed production and, under extreme conditions, caused spreading necrotic lesions and tissue death. Our results demonstrate that JAZ proteins promote growth and reproductive success at least in part by preventing catastrophic metabolic effects of an unrestrained immune response.

Introduction

As sessile organisms, plants continuously adjust their growth, development, and metabolism in response to environmental stress. Complex regulatory networks involving plant hormones play a central part in linking stress perception to transcriptional responses that permit acclimation to harsh environments (Pieterse et al., 2009; Santner et al., 2009). The lipid-derived hormone jasmonoyl-L-isoleucine (JA-Ile) and its metabolic precursors and derivatives, collectively known as jasmonates (JAs), perform a critical role in plant resilience to many environmental challenges (Wasternack and Hause, 2013; Howe et al., 2018). JAs are perhaps best known for orchestrating local and systemic immunity to organisms that exploit plants as a source of food and shelter (Campos et al., 2014). The hormone controls the expression of large sets of genes that specify a myriad of defense traits, including the biosynthesis of specialized metabolites that thwart attack by diverse organisms ranging from microbes to mammals (Howe and Jander, 2008; Wu and Baldwin, 2010; Chini et al., 2016). Interestingly, transcriptional responses triggered by JA-Ile also result in growth inhibition (Yan et al., 2007; Zhang and Turner, 2008; Attaran et al., 2014; Havko et al., 2016; Major et al., 2017; Bomer et al., 2018). The dual role of JA-Ile in promoting defense and restricting growth provides an attractive opportunity to better understand the antagonistic relationship between growth and immunity, with implications for improving crop productivity (Karasov et al., 2017; Zust and Agrawal, 2017). Many gaps remain, however, in understanding how defense hormones reconfigure metabolism within the constraints of available resources to achieve an optimal balance between immunity and other physiological tasks (Guo et al., 2018).

In cells containing low JA-Ile levels, JASMONATE ZIM-DOMAIN (JAZ) proteins bind directly to and repress the activity of various transcription factors (TFs) (Chini et al., 2007; Thines et al., 2007; Yan et al., 2007). The most thoroughly studied JAZ-interacting TFs are MYC2 and

its closely related paralogs (Fernandez-Calvo et al., 2011; Kazan and Manners, 2013; Figueroa and Browse, 2015; Qi et al., 2015). JAZ proteins repress MYC activity by providing a scaffold on which to recruit corepressors such as NINJA and TOPLESS (Pauwels et al., 2010; Shyu et al., 2012), as well as by impeding the association of the coactivator protein MED25 with the transcription initiation complex (Katsir et al., 2008; Zhang et al., 2015; An et al., 2017). In addition to recruiting transcriptional repression complexes to the promoters of JA-responsive genes, JAZ proteins participate in the primary JA-Ile perception event leading to ubiquitin-dependent JAZ degradation. When intracellular levels of JA-Ile rise above a threshold concentration, the hormone promotes binding of JAZ to the F-box protein CORONATINE INSENSITIVE 1 (COI1), which is a component of the E3 ubiquitin ligase complex SCF^{COI1} (Thines et al., 2007; Katsir et al., 2008; Yan et al., 2018). JAZ proteins tagged with polyubiquitin chains by SCF^{COI1} are destined for proteolytic destruction by the 26S proteasome, thereby relieving repression on MYC activity. Genetic epistasis analyses in Arabidopsis are consistent with biochemical and structural studies showing that COI1 and JA-Ile comprise a functional module dedicated to JAZ degradation, and that JAZ depletion is sufficient to derepress the expression of target genes controlled by MYC and other TFs (Major et al., 2017).

Positive regulators of the core JA-Ile signaling pathway in Arabidopsis, including MYC TFs and components (e.g., COI1) of the JAZ degradation machinery, have been thoroughly studied through characterization of the corresponding loss-of-function mutants (Browse, 2009). In contrast, an understanding of how JAZ proteins negatively regulate JA responses has been hindered by the multi-membered nature of *JAZ* gene families, which in Arabidopsis consists of 13 members (*JAZ1-13*) (Thireault et al., 2015; Chini et al., 2016; Howe et al., 2018). Although there is evidence that individual *JAZ* genes control JA responses in specific tissues and cell types

(Gimenez-Ibanez et al., 2017; Li et al., 2017), the absence of strong phenotypes in most *jaz* single mutants described to date suggests some degree of redundancy among *JAZ* family members (Thines et al., 2007; Campos et al., 2016; Chini et al., 2016; Gimenez-Ibanez et al., 2017). Analysis of Arabidopsis mutants defective in multiple *JAZ* genes supports this interpretation. For example, constitutive JA responses in a *jaz* quintuple (*jazQ*) mutant defective in *JAZ1/3/4/9/10* are relatively mild in comparison to the effects of exogenous JA treatment, and are fully suppressed by mutations that block JA-Ile biosynthesis or perception (Campos et al., 2016; Major et al., 2017). Indeed, treatment of plants with methyl-JA (MeJA) and other precursors of JA-Ile has been used extensively to study short-term responses (hours to days) to the hormone. This approach, however, is limited in its ability to target specific JAZ proteins or the tissues in which they are expressed. Multiple negative feedback circuits involving JA-Ile catabolism and JAZ repressors that are recalcitrant to JA-Ile-mediated degradation further mask the full range of responses to the hormone (reviewed in (Howe et al., 2018)). These considerations provide a rationale for using extreme higher-order *jaz* mutants to investigate the physiological, metabolic, and developmental consequences of derepressing JA responses over the course of ontogeny.

Here, we developed a series of higher-order *jaz* mutants with which to interrogate the effects of chronic overactivation of JA responses. Progressive mutation of *JAZ* genes was positively correlated with the strength of defense traits and inversely associated with growth and fertility. Detailed characterization of a *jaz* decuple (*jazD*) mutant defective in *JAZ1/2/3/4/5/6/7/9/10/13* revealed constitutive activation of both JA and ethylene responses, leading to resistance to caterpillar feeding and infection by a necrotrophic fungal pathogen. Metabolic phenotypes of *jazD* were indicative of elevated carbon and sulfur partitioning to chemical defense traits controlled by the MYC and ethylene response factor (ERF) branches of

immunity. The strong defense sink in *jazD* leaves was also associated with increased cellular respiration and carbon starvation, but not reductions in photosynthetic rate. Introduction of a *jaz8* mutation into the *jazD* background further exacerbated growth defects and nearly abolished seed production in the resulting *jaz* undecuple mutant. Similarly, elicitation of JA responses in the sensitized *jazD* background caused spreading necrotic lesions and tissue death. Collectively, our data indicate that JAZ proteins promote growth and reproductive success by attenuating the harmful metabolic effects of an unfettered JA response.

Results

Reduced growth and fertility of a *jaz* decuple mutant is associated with extreme sensitivity to jasmonate

We used insertion mutations to construct a series of higher-order *jaz* mutants with which to interrogate the biological consequences of chronic JAZ deficiency in Arabidopsis (Figure 2.1). The 13-member JAZ family in Arabidopsis is comprised of five phylogenetic groups (I-V) that are common to angiosperms (Figure 2.2A). The previously described *jazQ* mutant harbors mutations in the sole member (*JAZ10*) of group III, all three members of group V (*JAZ3/4/9*), and one member (*JAZ1*) of the largest group I clade. Building on the *jazQ* chassis, we used genetic crosses to introduce five additional mutations that target the remaining group I members (*JAZ2/5/6*) and two genes (*JAZ7/13*) within group IV (Figure 2.2). The resulting homozygous *jaz1/2/3/4/5/6/7/9/10/13* decuple mutant, referred to hereafter as *jazD*, thus targets all *JAZ*s except for *JAZ8* and the two group II genes (*JAZ11* and *JAZ12*).

Cultivation of plants in the absence of exogenous JA showed that whereas *jazQ* roots and leaves grow more slowly than wild-type (WT) Col-0, growth of *jazD* was even slower than *jazQ* (Figure 2.3A and 2.3B). Soil-grown *jazD* plants displayed less leaf area and shorter petioles than *jazQ*, and also accumulated more anthocyanins (Figure 2.3B mock and 2.5). Leaf biomass measurements taken over a 20-d time course confirmed that the relative growth rate (RGR) of *jazD* rosettes during this developmental stage was significantly less than WT (Figure 2.3C). That the RGR of *jazQ* was comparable to WT, despite the reduced biomass of *jazQ* rosettes at later times in development, may reflect growth changes occurring prior to the first time point of sampling (11 d after sowing) or the lack of statistical power needed to resolve small differences in RGR that are compounded over time into larger differences in rosette size. Although bulk protein, lipid, and cell

wall content of rosette leaves was similar between all three genotypes under our growth conditions, the ratio of leaf dry weight to fresh weight was increased in *jazD* relative to WT and *jazQ* (Figure 2.6). The restricted growth of *jazD* roots and leaves was associated with changes in flowering time under long-day growth conditions. *jazD* plants were delayed in their time to flowering compared to *jazQ* but contained a comparable number of leaves at the time of bolting (Figure 2.5).

We next compared the response of *jazQ* and *jazD* mutants to exogenous JA. Root growth assays showed that the extent of JAZ deficiency (*jazD* > *jazQ* > WT) inversely correlated with root length under a range of MeJA concentrations, with growth of *jazD* roots effectively arrested in the presence of 5 μM MeJA (Figure 2.3A and 2.4). Shoot responsiveness to the hormone was assessed by treating intact leaves with coronatine (COR), which is a potent agonist of the JA-Ile receptor (Katsir et al., 2008). WT and *jazQ* leaves showed visible accumulation of anthocyanin pigments at the site of COR application (i.e., midvein) within four days of the treatment with no apparent signs of chlorosis (Figure 2.3B). In contrast, *jazD* leaves exhibited visible chlorosis at the site of COR application within 2 d of treatment and, strikingly, near complete loss of chlorophyll and spreading of necrosis-like symptoms throughout the leaf 4 d after treatment, leading to tissue death (Figure 2.3B). These data indicate that progressive loss of *JAZ* genes in *jazQ* and *jazD* results in both quantitative (e.g., root growth inhibition) and qualitative (e.g., COR-induced tissue necrosis) differences in JA responsiveness, and are consistent with the notion that the hypersensitivity of *jazD* results, at least in part, from loss of JAZ-mediated negative feedback control of JA responses.

Measurements of reproductive output showed that whereas the total seed yield of *jazQ* was only marginally affected, seed production by *jazD* plumented to about one-third of WT levels (Table 2.1). The reduced fecundity of *jazD* resulted from a combination of decreased average mass

per seed and lower total seed number per plant; mutant plants produced fewer seeds per silique, and the size and number of siliques per plant were reduced as well (Table 2.1). The reduced size of *jazD* seeds correlated with a reduction in total fatty acid per seed (Figure 2.3D). Analysis of seed fatty acid profiles showed that *jazQ* and *jazD* seeds contain less oleic acid (18:1) and more linoleic acid (18:2) (Figure 2.7), suggesting alterations in fatty acid metabolism during seed development. The effect of *jazD* on seed size and lipid abundance was associated with reduced rates of seed germination (Figure 2.3E). These findings indicate that constitutive JA responses resulting from JAZ depletion are associated with poor reproductive performance.

Constitutive activation of jasmonate- and ethylene-mediated defense pathways in *jazD* plants

Having established the effects of *jazQ* and *jazD* on growth and reproduction, we next assessed how these mutations impact JA-mediated signaling pathways for defense. Similar to results obtained with long day-grown plants, *jaz*-mediated leaf growth restriction was observed under short-day conditions (Figure 2.8A), which we used to promote leaf biomass and delay flowering in plants used for insect bioassays. In tests performed with the generalist herbivore *Trichoplusia ni* we found that the strength of host resistance to insect feeding positively correlated with the severity of *jaz* mutation (*jazD* > *jazQ* > WT), consistent with a role for JAZs in the negative regulation of defense (Figure 2.8A and 2.8B).

Messenger RNA sequencing (RNA-seq) was used to investigate the molecular basis of the enhanced anti-insect resistance. Global transcript profiles revealed that the total number of differentially expressed genes in *jazD* leaves (relative to WT) was more than 10-fold greater than that in *jazQ* (2,107 and 186 for *jazD* and *jazQ*, respectively) (Figure 2.9). Among the 186 genes whose expression was statistically different in the *jazQ* vs. WT comparison, the majority (59%) of

these were also differentially expressed in *jazD*. Gene Ontology (GO) analysis of 1,290 genes expressed to higher levels in *jazD* than WT showed that "response to JA/wounding", as well as "defense response", were among the biological processes most statistically overrepresented in this comparison (Figure 2.9). These results, together with analysis of metabolic pathways that are differentially activated in *jaz* mutants (see below), indicate that the strength of anti-insect resistance correlates with the extent of JAZ deficiency and concomitant reprogramming of gene expression.

Analysis of the RNA-seq data also revealed that ethylene-response genes were highly expressed in *jazD* but not *jazQ*. In particular, anti-fungal defense genes controlled by the synergistic action of JA and ethylene were modestly repressed in *jazQ* but highly induced in *jazD* (Figure 2.8C). Among these were genes encoding the AP2/ethylene-response factors (ERFs) ERF1 and ORA59, which integrate JA and ethylene signals to promote the expression of antimicrobial compounds, including various defensins (PDFs), pathogenesis-related (PR) proteins, and hydroxycinnamic acid amides (HCAAs) (Figure 2.8C) (Berrocal-Lobo et al., 2002; Pre et al., 2008; Li et al., 2018). Strikingly, several *PDF* transcripts (e.g., *PDF1.2*) were among the most abundant of all mRNAs in *jazD* leaves, with expression levels comparable to that of the most highly expressed photosynthesis transcripts. In agreement with the RNA-seq data, *jazQ* plants were slightly more susceptible than WT to the necrotrophic pathogen *Botrytis cinerea*, whereas *jazD* leaves were more resistant to the spread of disease lesions (Figure 2.8D and 2.8E). To determine whether *jazQ* and *jazD* differentially affect other ethylene responses, we assessed apical hook formation in ethylene-elicited seedlings. Consistent with studies showing that apical hook formation is attenuated by JA signaling (Song et al., 2014), we found that stimulation of hook curvature in response to treatment with the ethylene precursor 1-aminocyclopropane-1-carboxylic

acid (ACC) was reduced in *jazD* but not *jazQ* seedlings (Figure 2.8F). These data indicate that whereas *jazQ* moderately activates JA responses and increases resistance to insect feeding, *jazD* strongly induces both the JA and ethylene branches of immunity to confer robust resistance to insect feeding and infection by *B. cinerea*.

To validate the RNA-seq results and gain additional insight how *jazD* promotes leaf defense, we used quantitative tandem mass spectrometry to quantify global changes in protein abundance in *jazD* vs. WT in leaves. Amongst a total of 4,850 unique proteins identified in both genotypes, 149 and 120 proteins accumulated to higher and lower levels, respectively, in *jazD* (threshold fold change > 1.2, $P < 0.05$). GO analysis of the 120 downregulated proteins revealed enrichment of functional categories related to cytokinin response, cold response, and various functional domains of photosynthesis (Table 2.2). Analysis of proteins that were more abundant in *jazD* showed there was good agreement with the corresponding mRNA levels determined by RNA-seq; transcripts encoding 78% of these 149 proteins were also induced in *jazD* plants. As expected, there was strong enrichment in this protein set of GO categories associated with response to JA, herbivore and fungal attack, among other defense-related processes (Table 2.2). For example, the proteomic analysis revealed that *jazD* coordinately upregulated the abundance of most JA biosynthetic enzymes, as well as canonical JA marker proteins such as VSP1 and VSP2 (Figure 2.10). *jazD* leaves exhibited high expression of an agmatine coumaroyltransferase (At5g61160) and associated transporter (At3g23550) involved in the production of anti-fungal HCAAs (Muroi et al., 2009; Dobritzsch et al., 2016). Transcripts encoding the acyl-CoA N-acyltransferase NATA1 (At2g39030), which catalyzes the formation of the defense compound N(δ)-acetylornithine (Adio et al., 2011), were 50-fold higher in *jazD* leaves compared to WT and *jazQ* and were accompanied by increased NATA1 protein abundance. Perhaps most striking was

the coordinate upregulation in *jazD* leaves, at both the mRNA and protein levels, of most known structural and enzymatic components of the endoplasmic reticulum (ER)-derived ER body (Figure 2.11), which is implicated in induced immunity (Yamada et al., 2011; Nakano et al., 2017). These findings establish a central role for JAZ proteins as negative regulators of diverse leaf defense traits.

Reprogramming of primary and specialized metabolism in *jazD* plants

To investigate how the activation of multiple defense pathways influences primary metabolism, we used the RNA-seq and proteomics data to infer metabolic pathways that are altered in *jazD* leaves. Mapping of differentially expressed genes to KEGG pathway databases showed that the tricarboxylic acid (TCA) cycle, oxidative pentose phosphate pathway (OPP), sulfur assimilation and metabolism, and various amino acid biosynthetic pathways were among the processes most highly induced in *jazD*, whereas photosynthesis components were generally downregulated (Figure 2.12).

One prominent example of a metabolic pathway that was upregulated in *jazD* was the shikimate pathway for the biosynthesis of aromatic amino acids. Trp biosynthetic enzymes involved in the production of indole glucosinolates (IGs) showed particularly high expression at the mRNA and protein levels (Figure 2.12B). Consistent with this finding, genes encoding enzymes in the phosphoserine pathway that supplies Ser for the biosynthesis of Trp and Cys (Benstein et al., 2013) were highly upregulated in *jazD*, as was the abundance of the corresponding enzymes as determined from proteomics data (Figure 2.12B and 2.9). LC-MS analysis of leaf extracts showed that several IGs accumulate to high levels in *jazD* (Figure 2.12C and 2.13), thereby validating the omics data. In agreement with previous studies employing JA elicitation (Sasaki-

Sekimoto et al., 2005; Kruse et al., 2007; Yatusevich et al., 2010), we also found that pathways involved in sulfur assimilation and cysteine biosynthesis, as well as ascorbate and glutathione metabolic pathways that protect against oxidative stress, were strongly upregulated in *jazD* (Figure 2.12B and 2.14). These data indicate that genetic depletion of JAZ proteins recapitulates the transcriptional effects of exogenous JA, and demonstrate that JAZ proteins exert control over pathways that operate at the interface of primary and specialized metabolism.

We next addressed the question of whether *jazD* modulates net carbon assimilation. Despite the downregulation of photosynthetic mRNAs and proteins in *jazD*, modeling of photosynthetic parameters derived from gas exchange data indicated that the leaf area-based photosynthetic rate of *jazD* plants was comparable to WT (Figure 2.12D, 2.15A and 2.15B). This finding was confirmed by 13C isotope discrimination measurements, which showed that the degree of CO_2 resistance through mesophyll cells was similar in WT, *jazQ*, and *jazD* leaves (Figure 2.15C and 2.15D). In contrast to photosynthesis, the net loss of CO_2 from *jazD* leaves in the dark exceeded that of WT by ~50% (Figure 2.12E). Increased cellular respiration in *jazD* was confirmed by experiments showing that the mutant had increased respiration in both the day and night portions of the photoperiod (Figure 15E and 2.15F). These findings are consistent with the notion that increased cellular respiration is associated with high-level production of defense compounds (Bolton, 2009). GO analysis of the 817 downregulated genes in *jazD* leaves showed enrichment for growth-related processes, including ‘response to light stimulus’, ‘cell wall organization’, ‘response to abiotic stimulus’, ‘carbohydrate biosynthetic process’, and ‘lipid biosynthetic process’ (Figure 2.9).

jazD plants exhibit symptoms of carbon starvation

Increased respiration and partitioning of carbon to metabolic defense pathways, in the absence of compensatory changes in photosynthesis, raised the possibility that *jazD* plants have a carbon deficit. Time-course studies showed that the rates of starch accumulation (WT: 0.103 μmol Glc g^{-1} DW h^{-1}; *jazD*: 0.113 μmol Glc g^{-1} DW h^{-1}) and degradation (WT: -0.220 g^{-1} DW h^{-1}; *jazD*: -0.186 μmol Glc g^{-1} DW h^{-1}) were comparable between WT and *jazD* (Figure 2.16A). However, starch levels in *jazD* leaves were slightly lower than WT at all times of the diel cycle except at the end of the night, when starch was mostly depleted but modestly elevated in *jazD* relative to WT. *jazD* leaves also had consistently lower sucrose levels (Figure 2.16B). We also found that genes involved in starch and sucrose metabolism were generally downregulated in *jazD*, including the mRNA and protein abundance of the plastidic starch biosynthetic enzyme phosphoglucomutase (PGM1, At5g51820). To test whether these changes in central metabolism are associated with carbon deficit, we used the RNA-seq data to query the expression of genes that are induced by conditions (e.g., prolonged darkness) leading to carbon starvation. We found that 42 of 278 (15%) sugar starvation marker (SSM) genes defined by (Baena-Gonzalez et al., 2007), including several *DARK INDUCIBLE* (*DIN*) genes that respond to reduced energy status (Fujiki et al., 2001), were expressed to much higher levels in *jazD* than WT and *jazQ* (Figure 2.16C). We also examined the expression of EIN3-regulated glutamate dehydrogenases (GDH) that replenish 2-oxoglutarate for the TCA cycle and are considered metabolic markers of carbon deficiency (Miyashita and Good, 2008; Gibon et al., 2009; Tsai et al., 2016). Both the transcript and protein abundance of GDH1 (At5g181700) and GDH2 (At5g07440) were statistically increased in *jazD* in comparison to WT, consistent with a carbon deficit in this mutant.

To test the hypothesis that carbon limitation contributes to the slow growth of *jaz* mutants, we compared the growth of WT, *jazQ*, and *jazD* seedlings on agar medium supplemented with sucrose. The data showed that although exogenous sucrose promotes increased biomass in all genotypes tested, the stimulatory effect on the growth of *jazD* shoots was statistically greater than that of WT and *jazQ* (Figure 2.16D and 2.16E). Exogenous sucrose also enhanced the root growth of *jazD* in comparison to WT and *jazQ* (Figure 2.16F). Control experiments with sorbitol showed that the growth-promoting effect of sucrose was not attributed to changes in osmotic strength of the growth medium (Figure 2.17). These data provide evidence that the reduced growth of *jazD* but not *jazQ* results in part from a limitation in carbon supply.

A *jaz1/2/3/4/5/6/7/8/9/10/13* undecuple mutant produces few viable seeds

The ability of *jazD* plants to perceive and respond to exogenous JA suggested that the remaining JAZ proteins in the mutant can actively repress JA-responsive genes. We hypothesized that mutation of these remaining *JAZ* loci (i.e., *JAZ8*, *JAZ11*, and *JAZ12*) in the *jazD* background may further enhance the level of growth-defense antagonism. To test this, we focused on *JAZ8* because of its established role in repressing JA responses (Shyu et al., 2012) and the availability of a naturally occurring *jaz8* null allele (Thireault et al., 2015). Moreover, the increased expression of *JAZ8* in *jazD* leaves (> 15-fold relative to WT) (Figure 2.10) was consistent with a role in negative feedback control of JA responses. Screening of progeny derived from genetic crosses between *jazD* and *jaz8* resulted in the identification of an undecuple mutant (*jazU*) homozygous for mutations in *JAZ1/2/3/4/5/6/7/8/9/10/13* (Figure 2.18A). Root growth assays showed that *jazU* roots were even shorter than *jazD* in the presence of very low concentrations (e.g., < 1 μM) of MeJA (Figure 2.19A). When grown on JA-free medium, *jazU* showed an even stronger

constitutive short-root phenotype than *jazD* (Figure 2.19A). Similarly, the rosette morphology of *jazU* confirmed the progressive effect of JAZ depletion on restriction of rosette growth, including reduced biomass, leaf area, and petiole length (Figure 2.19B and 2.18B-D). Most strikingly, *jazU* plants exhibited near complete loss of viable seed production (Figure 2.19C). We estimated that less than 3% of *jazU* flowers set fruit; although *jazU* pollen was viable in crosses, among flowers that produced fruit, most senesced and aborted during silique filling (Figure 2.18E). Among the few *jazU* flowers that did produce seeds, seed set per silique was severely reduced, with recovery of only a few viable seeds per plant (Figure 2.18F-H). The collective seed-yield phenotypes of *jazQ*, *jazD*, and *jazU* strongly support a key role for JAZ proteins in promoting reproductive vigor.

Discussion

A major objective of this study was to employ higher-order *jaz* mutants as novel tools to achieve a deeper understanding of JA responses throughout the plant life cycle. Our data show that moderate and severe JAZ deficiency in *jazQ* and *jazD*, respectively, recapitulates many of the effects of exogenous JA on growth, defense, and metabolism. Comparison of leaf transcriptomes revealed that the degree of JAZ depletion correlated both with the extent of transcriptional reprogramming and the strength of growth-defense antagonism. The complexity of growth- and immune-related phenotypes in higher-order *jaz* mutant is thus consistent with the capacity of JAZ proteins to directly control the activity of diverse TFs (Howe et al., 2018). Based on current annotations of the Arabidopsis TF repertoire (Jin et al., 2017), we identified 218 (147 up- and 71 downregulated) and 20 (11 up and 9 downregulated) TF-encoding genes that are differentially expressed in *jazD* and *jazQ*, respectively. These findings support a general model in which JAZ proteins reside at the apex of a transcriptional hierarchy that promotes defense and simultaneously inhibits growth (Chini et al., 2016; Howe et al., 2018). *jaz* loss-of-function mutations may also indirectly influence gene expression through changes in the expression of TF-encoding genes that promote subsequent waves of transcription or compensatory responses. A future challenge will be to link specific phenotypes of *jaz* mutants to defined JAZ-TF regulatory modules that exert temporal and spatial control over JA responses (Gimenez-Ibanez et al., 2017; Li et al., 2017; Major et al., 2017).

A significant finding of our work was that *jazQ* and *jazD* mutants show not only quantitative variation in JA-related phenotypes but also qualitative differences in select defense traits. This is exemplified by the observation that *jazD* constitutively activates the ethylene branch of immune signaling to increase resistance to *B. cinerea*, whereas *jazQ* moderately inhibits

ethylene-dependent defense responses to this pathogen. The elevated JA/ethylene-dependent resistance of *jazD* is consistent with the ability of some JAZ proteins to repress the activity of two master regulators of ethylene signaling, EIN3 and EIL1, which in turn activate the expression of TFs (e.g., ERF1) that mediate resistance to necrotrophic pathogens (Solano et al., 1998; Berrocal-Lobo et al., 2002; Pre et al., 2008; Zhu et al., 2011; Muller and Munne-Bosch, 2015). Thus, although *jazQ* moderately relieves repression on MYC TFs to enhance resistance to insect feeding, this combination of *jaz* mutations (*jaz1/3/4/9/10*) may be insufficient to derepress EIN3/EIL1. In this scenario, antagonistic interactions between the MYC2 and ERF1 branches of JA signaling (Lorenzo et al., 2004) would explain the increased susceptibility of *jazQ* to *B. cinerea*. By contrast, we propose that the severe JAZ deficiency in *jazD* simultaneously derepresses both the MYC2 and EIN3/EIL1 branches to confer strong resistance to chewing insects and necrotrophic pathogens. Given that EIN3 physically interacts with MYC2 to inhibit JA-regulated defense against insect herbivores (Song et al., 2014), robust activation of insect and fungal pathogen defenses in *jazD* suggests that MYC2-EIN3/EIL1 antagonism may require certain JAZ proteins to control the balance between transcriptional repression and activation (Howe et al., 2018). The distinct biotic stress phenotypes of *jazQ* and *jazD* may reflect a larger pool of JAZs in *jazQ*, or may be attributed specifically to one or more JAZ proteins (i.e., JAZ2/5/6/7/13) present in *jazQ* but absent in *jazD*. Complementation of *jazD* with wild-type *JAZ* genes may help to address this hypothesis. It is noteworthy that many phenotypes of *jazD*, including high expression of *PDF* genes and enhanced resistance to both caterpillar feeding and pathogen infection, are also observed in mutants defective in JA catabolism (Caarls et al., 2017; Smirnova et al., 2017). These findings suggest that changes in JA homeostasis may deplete JAZ abundance to phenocopy the effects of *jaz* mutants.

JAZ depletion in higher-order *jaz* mutants may propagate changes in protein-protein interaction networks that shape the diversity of JA responses and hormone crosstalk (Howe et al., 2018). The strong induction of IG biosynthesis in *jazD* is consistent with the role of MYC-MYB heterodimers in JA-mediated activation of IG biosynthetic genes (Gigolashvili et al., 2007; Schweizer et al., 2013), such that genetic depletion of JAZ favors MYC-MYB interaction. A similar argument applies to the role of JAZ-DELLA interactions in the control of growth-defense balance; JAZ depletion could restrict growth through increased DELLA activity and attenuation of gibberellin-mediated responses (Hou et al., 2010; Yang et al., 2012; Machado et al., 2017). It remains to be determined whether changes in DELLA abundance or other components of the gibberellin pathway contribute to the reduced growth of higher-order *jaz* mutants. In fact, the critical role of MYC2/3/4 in restricting leaf growth and biomass in *jazQ* (Major et al., 2017) suggests that these TFs contribute to the growth phenotype of *jazD*. Other potential factors contributing to the reduced growth rate of *jazD* include downregulation of genes involved in cell wall organization (Bomer et al., 2018), and perturbation in auxin levels resulting from altered Trp metabolism.

Lifetime viable seed production is a reliable measure of the cost of defense. Consistent with studies showing that induced defense responses in the absence of herbivore pressure curtail seed production (Agrawal, 1998; Baldwin, 1998), we found that *jazQ*, *jazD* and *jazU* mutants have weak, moderate, and severe negative effects on seed production, respectively. It therefore appears that either too little (e.g., *coi1* mutation) or too much (e.g., *jazU* mutation) JA response can lead to reproductive failure, albeit for different physiological reasons. Similarly, the reduction in seed size and quality in higher-order *jaz* mutants is consistent with the increased seed size in JA-deficient mutants (Farmer and Dubugnon, 2009). These findings suggest that unrestrained JA responses

give rise to tradeoffs in which increased partitioning of resources to defense in source tissues reduces nutrient availability in sink tissues. It has been shown, for example, that carbon starvation in leaves has direct negative effects on seed development and quality in Arabidopsis (Smith and Stitt, 2007). In demonstrating a critical role for JAZ proteins in promoting reproductive performance, our results provide a fitness-based explanation for the emergence of multi-tiered mechanisms to restrain JA responses, with implications for understanding the evolution of JA signaling systems (Karasov et al., 2017; Howe et al., 2018).

Several features of higher-order *jaz* mutants, including constitutive production of defense compounds, slow growth, and reduced fecundity, are indicative of hyperactive immunity (Bomblies and Weigel, 2007). These effects were exaggerated under conditions designed to further deplete JAZ in the sensitized *jazD* background, either by treatment with exogenous hormone or addition of *jaz8* mutation. The necrosis of COR-treated *jazD* leaves provides strong evidence that JAZ proteins protect against JA-mediated cell death resulting from a runaway immune response. Although the underlying cause of tissue necrosis remains to be determined, we note that JAs have long been known to promote senescence-like symptoms and to elicit the production of ROS (Ueda and Kato, 1980; Orozco-Cardenas et al., 2001; Shan et al., 2011; Qi et al., 2015). Moreover, silencing of the *JAZh* paralog in *Nicotiana attenuata* caused spontaneous necrosis at late stages of leaf development, which was associated with increased ROS production (Oh et al., 2012). It is possible that the growth inhibitory and senescence-like symptoms of *jaz* mutants reflects autotoxicity of defense compounds, as recently proposed for IGs in Arabidopsis (Chen et al., 2017). The emerging link between IG production and ER body formation (Nakano et al., 2017), coupled with our discovery that JAZ proteins suppress the expression of both IGs and ER body components, provides the impetus for future studies aimed at understanding how JA coordinates

the proliferation of specialized organelles with defense metabolism. The striking diversity of chemical defense pathways expressed in *jazD* indicates that *jaz* mutants, potentially from any plant species, may be useful tools for discovery of novel anti-microbial and anti-insect defense compounds.

Our analysis of the effects of chronic JAZ deficiency provides new insights into how vegetative growth rate is coordinated with changes in primary and specialized metabolism. In general, our data support the acclimatory response hypothesis to explain how plant growth rate is modulated in response to changes in the supply and demand for assimilated carbon (Smith and Stitt, 2007; Guo et al., 2018). Several independent lines of evidence indicate that partitioning of resources to a strong defense sink in *jazD* leaves is associated with carbon starvation and downward adjustment of growth rate. First, the expression of genes and protein markers of carbon starvation were upregulated in *jazD* leaves. Consistent with the concept of resource allocation costs, exogenous sucrose partially restored the growth of *jazD* leaves and roots. Second, the area-based respiration rate of *jazD* leaves was increased without a corresponding change in photosynthetic rate, potentially contributing to an energy deficit. Third, the sucrose and starch content in *jazD* leaves was modestly depleted throughout most times of the diel cycle, consistent with studies showing that JA elicitation reduces photoassimilate levels (Machado et al., 2013). Given that the rates of starch synthesis and degradation were similar in *jazD* and WT leaves, it appears that the control mechanisms underlying the precise pacing of starch reserves (Smith and Stitt, 2007; Sulpice et al., 2014) are largely operational under conditions where JA signaling strongly diverts carbon to defense. These findings sugest that JAZ proteins flexibly adjust growth-defense balance to match anticipated changes in resource availability, thereby avoiding the detrimental effects of hyperimmunity.

In summary, our results demonstrate that JA-triggered immunity imposes major metabolic demands which, if not properly restrained, are detrimental to plant fitness. In environments where assimilated carbon, nitrogen, water, and other essential nutrients may be limiting, the bioenergetic and biosynthetic demands associated with increased defense must be tightly coordinated with other physiological tasks. We propose that JAZ proteins assist in balancing the growth-defense continuum not as a binary on-off switch but rather by matching the biotic stress level to available resources. In particular, our results indicate that growth and reproductive penalties of immunity become evident only at high levels of defense; a condition that is buffered by multiple negative feedback mechanisms. The intermediate level of anti-insect defense exhibited by *jazQ* does not appear to impose major allocation costs under laboratory growth conditions (Campos et al., 2016). Rather, the level of growth restriction exhibited by *jazQ* may reflect other adaptive roles of growth-defense antagonism. Downward adjustment of growth may, for example, provide a mechanism to concentrate defense compounds in affected tissues, promote cross resilience to potential future stress by reserving resources, or optimize the timing of vegetative-to-reproductive transition (Havko et al., 2016; Guo et al., 2018; Wang et al., 2018). In contrast to *jazQ*, severe JAZ depletion in *jazD* activates transcriptional programs that dictate much stronger allocation of central metabolites to defense, with significant negative effects on growth and reproduction. A high energetic expense associated with synthesis of defense proteins, provision of amino acid precursors and biosynthetic enzymes, transport, and storage of defense compounds in *jazD* is supported by hallmarks of carbon starvation. The diversion of resources to defense in *jazD* likely extends beyond carbon to other facets of intermediary metabolism. The induced production of defensins and other sulfur-rich defense compounds, for example, provides a plausible explanation for upregulation of enzymes involved sulfate assimilation and the biosynthesis of glutathione cysteine, consistent with

the importance of sulfur metabolism in plant defense (Sasaki-Sekimoto et al., 2005; Kruse et al., 2007; Yatusevich et al., 2010). A challenge for future studies will be to elucidate the mechanisms by which the status of carbon and other nutrients is sensed and adjusted during growth-to-defense transitions.

Methods

Plant material and growth conditions

The Columbia accession (Col-0) of *A. thaliana* was used as wild type for all experiments. *jazD* was constructed by crossing *jazQ* (Campos et al., 2016) to other transfer DNA (T-DNA) or transposon insertion mutants obtained from the *Arabidopsis* Biological Research Center (ABRC; Ohio State University). The following *jaz* single mutants were combined with *jazQ* as described in Figs. S1 and S14 and were named as follows: *jaz2-3* (RIKEN_13-5433-1) (Gimenez-Ibanez et al., 2017), *jaz5-1* (SALK_053775) (Thines et al., 2007), *jaz6-4* (CSHL_ET30) (this study), *jaz7-1* (WiscDsLox7H11) (Thines et al., 2007), *jaz8-V* (Thireault et al., 2015), and *jaz13-1* (GK_193G07) (Thireault et al., 2015). Additional details on *jaz* single mutants and the breeding scheme used to obtain *jazD* are provided in Table 2.3 and Figure 2.1, respectively. Efforts were made to reduce chromosomal contributions from other accessions by testing multiple SSLP polymorphic markers over many generations, so that the majority of *jazD* genome is expected to be derived from Col-0 (1) (Figure 2.1). Following sowing of seeds in soil, potted plants were covered with a transparent plastic dome for 10 days. Soil-grown plants were maintained under a 16-h light (100 μE m^{-2} s^{-1}) and 8-h dark photoperiod at 20 ºC unless otherwise noted. Immediately after seed harvest, small seeds were eliminated by passing bulk seed through a brass sieve with a 250 μm pore size. Seeds retained after sieving (referred to as "sieved seeds") were dried for two weeks in 1.5 mL Eppendorf tubes containing Drierite desiccant.

PCR analysis

PCR-based genotyping of *jazD* and lower-order mutants was performed using primer sets flanking DNA insertion sites and a third primer recognizing the T-DNA border (Table 2.4). PCR reactions

were performed with the following condition: 95 ºC for 5 min, followed by 35 cycles of denaturation (30 s at 95 ºC), annealing (30 s at 56 ºC) and elongation (1.5 min at 72 ºC). Final elongation step was performed at 72 ºC for 10 min and completed reactions were maintained at 12 ºC. *jaz8-V* was distinguished from wild-type *JAZ8* amplicons by digestion with AflII (New England Biolabs). The presence or absence of full-length *JAZ* transcripts in Col-0, *jazQ*, and *jazD* plants was determined by reverse transcription (RT) PCR. RNA was extracted from rosette leaves of soil-grown plants using an RNeasy kit (Qiagen). cDNA was reverse transcribed with a High-Capacity cDNA Reverse Transcription kit (Applied Biosystems, ABI). RT-PCR reactions were performed with primer sets designed to amplify target *JAZ* genes and the internal control *ACTIN1* (At2g37620) by GoTaq Green Master Mix (Promega). Primer sets and additional details of the RT-PCR procedures are provided in Table 2.5.

Growth measurements

For relative growth rate (RGR) analysis, five plants per genotype were harvested every two days beginning and ending 11 and 29 days, respectively, after seed sowing. Excised shoots were lyophilized for determination of dry weight. RGR was calculated from the slope of the log(dry weight) over the duration of the time course (Hummel et al., 2010). Leaf area of 23-day-old plants was determined by photographing rosettes from the top with a Nikon D80 camera. The resulting images were used to measure projected leaf area with GIMP software (http://www.gimp.org).

Root elongation assays

Seeds were surface sterilized with 50% (v/v) bleach for three min, washed 10 times with sterile water and stratified in dark at 4 ºC for two days. Seedlings were grown on 0.7% (w/v) agar media

containing half-strength Linsmaier and Skoog (LS; Caisson Labs) salts supplemented with 0.8% (w/v) sucrose and the indicated concentration of MeJA (Sigma-Aldrich). Each square Petri plate (Fisher; 100 x 100 x 15 mm) contained five seedlings per genotype. Plates were incubated vertically in a growth chamber maintained at 21 ºC for eight days under 16-h-light (80 μE m^{-2} s^{-1})/8-h-dark conditions. The length of primary roots was measured using ImageJ software (https://imagej.nih.gov/ij/).

Coronatine treatment

The eighth true leaf of 40-day-old plants grown under 12-h-light/12-h-dark conditions were spotted with 5 μL of sterile water (mock) or a solution containing 50 μM coronatine (Sigma-Aldrich, C8115) prepared in sterile water. Photographs were taken two and four days after treatment.

Insect and pathogen assays

Insect feeding assays were performed at 20 ºC under a short-day photoperiod of 8-h light and 16-h dark. Neonate *Trichoplusia ni* larvae (Benzon Research) were transferred to fully expanded rosette leaves of 9-week-old plants. Four larvae were reared on each of 12 plants for approximately 12 days, after which larval weights were measured (Herde et al., 2013). *Botrytis cinerea* bioassays were performed as described previously (Rowe and Kliebenstein, 2007), with minor modifications. Detached leaves from 10-week-old short-day-grown (8 h light/16 h dark) plants were placed in Petri dishes containing filter paper moistened with 10 mL sterile water, with petioles submerged in the water. Each leaflet was inoculated with a single 4 μL droplet of *Botrytis cinerea* spore suspension (5,000 spores/mL in 50% organic grape juice). Petri dishes were sealed with Micropore

surgical tape (3M Health Care) and kept under the same conditions used for plant growth. Photographs were taken after five days and lesion area was measured using the ImageJ software (https://imagej.nih.gov/ij/).

Seed yield measurements

Individual plants were grown in 6.5-cm square pots. An inverted plastic cone and plastic tube (Arasystem 360 kit; Arasystem) were fitted to each plant 23 days after seed sowing to collect all seeds from dehiscing siliques. Seeds collected from individual plants were harvested and dried with Drierite desiccant for two weeks, after which total seed mass per plant was measured. Average seed mass was determined by weighing dry seeds in batches of 200 (Jofuku et al., 2005). For each plant, the weights of three sample batches were measured and averaged. The silique length and number of seeds per silique were measured by sampling the fully-elongated seventh, ninth and eleventh siliques on the main stem (Roux et al., 2004).

Germination assays

Germination assays were performed on half-strength LS agar plates without sucrose. Unsieved seeds were surface sterilized and stratified in dark at 4 ºC for two days. Plates were incubated vertically under continuous light at 21 ºC and germination was scored daily for seven days by radicle emergence from the seed coat (Dekkers et al., 2004).

RNA-seq analysis

Global gene expression profiling was performed on the Illumina HiSeq 2000 platform at the Michigan State University Research Technologies Service Facility (https://rtsf.natsci.msu.edu/).

Rosettes of 23-day-old soil-grown Col-0, *jazQ*, and *jazD* plants were harvested for RNA extraction 6 h after the beginning of the light period. Three independent RNA samples (biological replicates) were used for each genotype, with each replicate derived from pooling rosette leaves from 20 plants. Raw sequencing reads were filtered with Illumina quality control tool FASTX-Toolkit (http://hannonlab.cshl.edu/fastx_toolkit/) and then mapped to TAIR10 gene models by RSEM (version 1.2.25) (Li and Dewey, 2011). mRNA abundances for all Arabidopsis genes were expressed as transcripts per million (TPM). DESeq2 (version 3.3) (Anders and Huber, 2010) was used to normalize expected counts from RSEM and to determine differential gene expression by comparing normalized counts in Col-0 to those in mutants. DAVID (version 6.8) (Huang et al., 2009) and MapMan (version 3.6.0) (Thimm et al., 2004) was used to perform gene ontology (GO) analysis of enriched functional categories. Over- and underrepresented GO categories among differentially expressed genes were assessed by hypergeometric test with Benjamini & Hochberg's false discovery rate (FDR) correction at $P < 0.05$. Analysis of the induction or repression of metabolic pathways was performed by Kyoto Encyclopedia of Genes and Genomes (KEGG) Mapper (http://www.genome.jp/kegg/pathway.html) (Kanehisa and Goto, 2000). Data deposition: RNA sequencing data from this study have been deposited in the Gene Expression Omnibus (GEO) database, https://www.ncbi.nlm.nih.gov/geo (accession no. GSE116681).

Quantitative proteomic analysis

Quantitative proteomic analysis was performed with proteins extracted from leaf tissue of 23-day-old soil-grown Col-0 and *jazD* plants. Proteins from three biological replicates (20 plants/replicate) of each genotype were extracted with the following extraction buffer: 100 mM Tris-HCl (pH 6.8), 150 mM NaCl, 10% glycerol (v/v), 4% SDS (w/v), 200 mM DTT, and protease inhibitor (Sigma-

Aldrich, 1 tablet/10 mL buffer). Protein concentrations were determined by Bradford assay. Trypsin-digested peptides derived from these proteins were derivatized with a tandem mass tag (TMT) labeling kit (ThermoFisher) for quantification by mass spectrometry (MS) performed at the Michigan State University Proteomics Core Facility (https://rtsf.natsci.msu.edu/proteomics/). Briefly, protein samples were digested with trypsin using the Filter-Aided Sample Preparation (FASP) protocol according to Wisniewski et al. (Wisniewski et al., 2009). Samples were then labeled with TMTsixple Isobaric Label Reagents (ThermoFisher) according to manufacturer's protocol. After labeling, all six samples were combined and dried by vacuum centrifugation. The combined peptide samples were separated over a pH gradient (pH 3-10) into six fractions using an Agilent OffGel 3100 fractionator (www.agilent.com) according to manufacturer's protocol. Dried fractions were washed and eluted. Eluted peptides were sprayed into a ThermoFisher Q-Exactive mass spectrometer (www.thermo.com) using a FlexSpray nano-spray ion source. Survey scans were taken in the Orbitrap (70,000 resolution, determined at m/z 200) and the top ten ions in each survey scan were then subjected to automatic higher energy collision induced dissociation (HCD) with fragment spectra acquired at 35,000 resolution. Conversion of MS/MS spectra to peak lists and quantitation of TMT reporter ions was done using Proteome Discover, v1.4.1.14. Peptide-to-spectrum matching was performed with the Sequest HT and Mascot search algorithms against the TAIR10 protein sequence database appended with common laboratory contaminants (downloaded from www.arabidopsis.org and www.thegpm.org, respectively). The output from both search algorithms was then combined and analyzed using Scaffold Q+S (version 4.5.3) to probabilistically validate protein identifications and quantification. Assignments validated using the Scaffold 1% FDR confidence filter were considered true.

Gas exchange measurements and ^{13}C discrimination analysis

Plants grown under short-day photoperiod (8 h light/16 h dark) in 'Cone-tainers' (Steuwe and Sons, Tangent, OR, USA) were used for gas exchange analysis. The measurements were performed on LI-6400XT and LI-6800 systems (LI-COR Biosciences, Lincoln, NE, USA) as previously described (Campos et al., 2016). Daytime respiration was determined from slope-intercept regression analysis of the common intersection of five CO_2 response curves (using intercellular CO_2 below 10 Pa) measured at decreasing, sub-saturating irradiances (Walker and Ort, 2015). Leaf tissue was freeze-dried and used for the measurement of the ratio of $^{13}CO_2$ to $^{12}CO_2$ by mass spectrometry at the Stable Isotope Ratio Facility for Environmental Research, University of Utah (Salt Lake City, UT). Isotopic ratios and CO_2 partial pressure at Rubisco were calculated as described (Farquhar et al., 1982; Farquhar et al., 1989; Weraduwagel et al., 2015).

Protein, lipid and cell wall measurements

For protein, lipid and cell wall measurements, leaf tissue was harvested from 23-day-old plants grown under our standard long-day conditions. Excised shoots were lyophilized to determine the dry weight. Total protein was extracted using a Plant Total Protein Extraction Kit (PE0230, Sigma-Aldrich) and quantified by Bradford assay. Lipid extraction, thin-layer chromatography (TLC) of polar and neutral lipids, transesterification, and gas chromatography were performed as described previously (Wang and Benning, 2011; Wang et al., 2018). For polar lipids, lipid separation was performed by activated ammonium sulfate-impregnated silica gel TLC plates (TLC Silica gel 60, EMD Chemical) with a solvent consisting of acetone, toluene, and water (91:30:7.5 by volume). Lipids were visualized by brief exposure to iodine vapor on TLC plates. Acyl groups of the isolated lipids were then converted to methyl esters, which were subsequently quantified by a gas

chromatography. Cell wall was extracted with a solution containing 70% ethanol, chloroform/methanol solution (1:1 v/v) and acetone as described (Foster et al., 2010). Starch was removed from the extracts using amylase and pullulanase (Sigma-Aldrich). Protein, lipid and cell wall content was normalized to leaf dry weight.

Glucosinolate measurements

Plants were grown under long-day conditions (16-h day and 8-h night) for 23 days. Rosette leaves were harvested and frozen in liquid nitrogen immediately. Two plants were pooled for each sample, with three biological replicates collected per sample. Frozen tissue was homogenized with a TissueLyser II (Qiagen) and glucosinolates were extracted following published procedures (Glauser et al., 2012), with minor modifications. Briefly, 80% methanol (v/v) was added to homogenized tissues and the mixture was vortexed for 5 min. Extracts were then centrifuged at 16,000 x g for 5 min and the supernatant was transferred to a 2-mL glass vial (RESTEK). Samples were analyzed in the MSU Mass Spectrometry Facility by ultrahigh pressure liquid chromatography (UPLC) coupled to quadrupole time-of-flight mass spectrometry (QTOFMS) using Waters Xevo G2-XS. Data analysis and processing were performed as described previously (Glauser et al., 2012).

Sucrose rescue assays

The effect of exogenous sucrose on leaf biomass and root growth was determined by growing seedlings on square Petri plates (Greiner Bio-One; 120 x 120 x 17 mm). In order to control for variation in seed quality, seeds were sieved after drying with desiccant for two weeks (see above). After sterilization and washing, seeds were sown without stratification on 0.7% (w/v) agar media

containing half-strength LS salts supplemented with sucrose or sorbitol. Each plate contained ten (for biomass) or five (for root growth) seeds of Col-0 and mutant lines. Plates were placed in dark at 4 ºC for four days and then incubated horizontally (for leaf biomass) or vertically (for root growth) in growth chambers maintained at 21 ºC under 16 h at a light intensity of 80 μE m^{-2} s^{-1} and 8 h dark. ImageJ was used to measure root length after 11 days. Plant biomass and projected leaf area were measured after 16 days.

APPENDIX

Tables and figures

Table 2.1. Seed and fruit production in *jazQ* and *jazD* plants.

Genotype	Seed yield per plant[1] (mg)	Average seed mass[2] (μg)	Silique length[3] (cm)	No. seed per silique[4]	No. silique per plant[5]
Col-0	608.3 ± 103.8	21.6 ± 1.3	1.59 ± 0.07	63 ± 11	451 ± 77
jazQ	524.3 ± 98.5	17.3 ± 0.9*	1.70 ± 0.06	58 ± 6	533 ± 100
jazD	192.7 ± 70.0*	16.6 ± 0.7*	1.45 ± 0.08*	37 ± 4*	329 ± 119*

Data show the mean ± SD of at least ten plants per genotype. Asterisks denote significant difference when compared to Col-0 plants according to Tukey's HSD test ($P < 0.05$).
[1]Seed yield was determined by collecting all seeds from individual plants and drying seeds with Drierite desiccant for two weeks prior to weighing.
[2]Average seed mass was determined by weighing batches of 200 seeds.
[3,4,5]Fully elongated 7th, 9th, and 11th siliques were collected for measurements of silique traits.

Table 2.2. Biological processes in which proteins whose abundance in *jazD* leaves was increased or decreased in comparison to wild-type Col-0 based on gene ontology (GO) analysis.

Upregulated in *jazD*

GO ID	GO description	*P* value
0009695	jasmonic acid biosynthetic process	< 0.0001
0055114	oxidation-reduction process	< 0.0001
0009611	response to wounding	< 0.0001
0009651	response to salt stress	< 0.0001
0009753	response to jasmonic acid	< 0.0001
0008652	cellular amino acid biosynthetic process	< 0.0001
0000162	tryptophan biosynthetic process	< 0.0001
0050832	defense response to fungus	< 0.0001
0006952	defense response	0.0002
0019762	glucosinolate catabolic process	0.0010
0006564	serine biosynthetic process	0.0113
0080027	response to herbivore	0.0226
0009414	response to water deprivation	0.0336

Downregulated in *jazD*

GO ID	GO description	*P* value
0009735	response to cytokinin	< 0.0001
0015979	photosynthesis	< 0.0001
0009409	response to cold	< 0.0001
0010207	photosystem II assembly	0.0001
0019684	photosynthesis, light reaction	0.0079

Table 2.2. (cont'd)

0042549	photosystem II stabilization	0.0239
0042742	defense response to bacterium	0.0257

Enriched functional categories were determined with DAVID (version 6.8) using the hypergeometric test with Benjamini & Hochberg's false discovery rate (FDR) correction.

Table 2.3. Mutants used for construction of *jazD* and *jazU*.

Mutant	Original name	Source	Accession	Mutagen	Resistance[1]
jaz1-2	SM_3.22668	JIC SM	Col-0	dSpm transposon	Basta (confirmed)
jaz2-3	RIKEN_13-5433-1	RIKEN	No-0	Ds transposon	Hygromycin (confirmed)
jaz3-4	GK-097F09	GABI Kat	Col-0	T-DNA (pAC161)	Sulfadiazine (confirmed)
jaz4-1	SALK_141628	SALK	Col-0	T-DNA (pROK2)	Kanamycin (silenced)
jaz5-1	SALK_053775	SALK	Col-0	T-DNA (pROK2)	Kanamycin (confirmed)
jaz6-4	CSHL_ET30	CSHL	Ler	Ds transposon (Enhancer trap GUS)	Kanamycin (confirmed)
jaz7-1	WiscDsLox7H11	Wisconsin	Col-0	T-DNA (pWiscDsLox)	Basta (not tested)
jaz8-V[2]	N/A	ABRC	Vash-1	SNP	N/A
jaz9-4	GK_265H05	GABI Kat	Col-0	T-DNA (pAC161)	Sulfadiazine (confirmed)
jaz10-1	SAIL_92_D08	SAIL	Col-0	T-DNA (pCSA110)	Basta (confirmed) GUS
jaz13-1	GK_193G07	GABI Kat	Col-0	T-DNA (pAC161)	Sulfadiazine (not tested)

[1]Resistance of the mutant line to the indicated selectable marker was tested and confirmed.
[2]The C-to-A nonsense mutation present in *JAZ8* from accession Vash-1 was backcrossed four times to Col-0 to generate a line (#28-6-30) that was used for subsequent genetic crosses (Thireault et al., 2015). N/A, not applicable.

Table 2.4. Primers used for genotyping.

Gene	Locus	Primer	Sequence (5'-3')
JAZ1	AT1G19180	JAZ1_F	ACCGAGACACATTCCCGATT
		JAZ1_R	CATCAGGCTTGCATGCCATT
		JAZ1_border	ACGAATAAGAGCGTCCATTTTAGAG
JAZ2	AT1G74950	JAZ2_F	TCTTCCTCGTGACAAAACGCA
		JAZ2_R	CCAAACACAGAACCATCTCCACA
		JAZ2_border	CCGGATCGTATCGGTTTTCG
JAZ3	AT3G17860	JAZ3_F	ACGGTTCCTCTATGCCTCAAGTC
		JAZ3_R	GTGGAGTGGTCTAAAGCAACCTTC
		JAZ3_border	ATAACGCTGCGGACATCTACATT
JAZ4	AT1G48500	JAZ4_F	TCAGGAAGACAGAGTGTTCCC
		JAZ4_R	TGCGTTTCTCTAAGAACCGAG
		JAZ4_border	TTGGGTGATGGTTCACGTAG
JAZ5	AT1G17380	JAZ5_F	GCTTATACCGAAAACCCGATTCCAG
		JAZ5_R	GGCTCATTGAGATCAGGAAGAACCA
		JAZ5_border	TTGGGTGATGGTTCACGTAG
JAZ6	AT1G72450	JAZ6_F	GACACACATCACTGTCACTTC
		JAZ6_R	AGTTTCTGAGGTCTCTACCTTC
		JAZ6_border	CCGTTTTGTATATCCCGTTTCCGT

Table 2.4. (cont'd)

JAZ7	AT2G34600	JAZ7_F	ATGCGACTTGGAACTTCGCC
		JAZ7_R	GGAGGATCCGAACCGTCTG
		JAZ7_border	ACGTCCGCAATGTGTTATTA
JAZ8	AT1G30135	JAZ8_F	TGTCCTAAGAGTCCGCCGTTGT
		JAZ8_R	TTTGGAGGATCCGACCCGTTTG
JAZ9	AT1G70700	JAZ9_F	TACCGCATAATCATGGTCGTC
		JAZ9_R	TCATGCTCATTGCATTAGTCG
		JAZ9_border	CTTTGAAGACGTGGTTGGAACG
JAZ10	AT5G13220	JAZ10_F	ATTTCTCGATCGCCGTCGTAGT-3
		JAZ10_R	GCCAAAGAGCTTTGGTCTTAGAGTG
		JAZ10_border	GTCTAAGCGTCAATTTGTTTACACC
JAZ13	AT3G22275	JAZ13_F	GCACGTGACCAAATTTGCAGA
		JAZ13_R	TGAAGAGAGGAGGATGATGAGGA
		JAZ13_border	AAACCTCCTCGGATTCCATTGC

Table 2.5. Primers used for RT-PCR.

Gene	Locus	Primer	Sequence (5'-3')	Annealing (ºC)	PCR cycles
JAZ1	AT1G19180	JAZ1_RT_F	ATGTCGAGTTCTATGGAATG	52	30
		JAZ1_RT_R	TCATATTTCAGCTGCTAAAC		
JAZ2	AT1G74950	JAZ2_RT_F	ATGTCGAGTTTTTCTGCCGA	52	30
		JAZ2_RT_R	TTACCGTGAACTGAGCCAAG		
JAZ3	AT3G17860	JAZ3_RT_F	ATGGAGAGAGATTTTCTCGGG	52	30
		JAZ3_RT_R	TTAGGTTGCAGAGCTGAGAGAAG		
JAZ4	AT1G48500	JAZ4_RT_F	ATGGAGAGAGATTTTCTCGGGCTGG	64.7	40
		JAZ4_RT_R	TTAGTGCAGATGATGAGCTGGAGGA		
JAZ5	AT1G17380	JAZ5_RT_F	ATGTCGTCGAGCAATGAAAA	54	35
		JAZ5_RT_R	CTATAGCCTTAGATCGAGAT		
JAZ6	AT1G72450	JAZ6_RT_F	ATGTCAACGGGACAAGCGC	54	35
		JAZ6_RT_R	CTAAAGCTTGAGTTCAAGGT		
JAZ7	AT2G34600	JAZ7_RT_F	ATGATCATCATCATCAAAAACTG	58	40
		JAZ7_RT_R	CTATCGGTAACGGTGGTAAG		
JAZ9	AT1G70700	JAZ9_RT_F	ATGGAAAGAGATTTTCTGGG	52	40
		JAZ9_RT_R	TTATGTAGGAGAAGTAGAAG		

Table 2.5. (cont'd)

JAZ10	AT5G13220	JAZ10_RT_F	ATGTCGAAAGCTACCATAGAAC	52	40
		JAZ10_RT_R	GATAGTAAGGAGATGTTGATACTAATCTCT		
JAZ13	AT3G22275	JAZ13_RT_F	ATGAAGGGTTGCAGCTTAGA	56	35
		JAZ13_RT_R	TTAGAAATTATGAAGAGAGGAGG		
ACTIN1	AT2G37620	Actin1_F	ATGGCTGATGGTGAAGACATTCAA	67.2	40
		Actin1_R	TCAGAAGCACTTCCTGTGAACAAT		

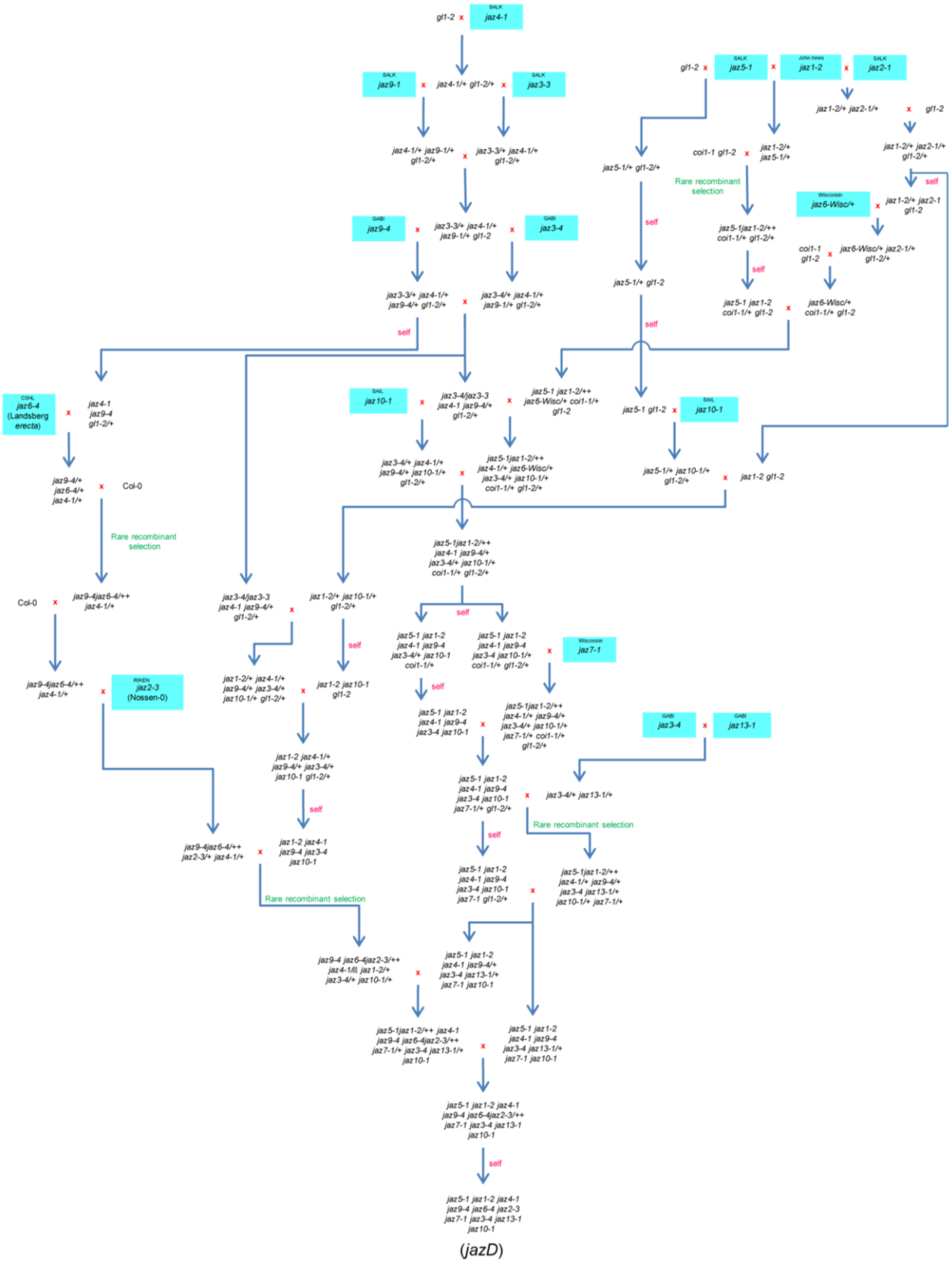

Figure 2.1. *jazD* pedigree.

Figure 2.1. (cont'd) Red 'x' and red 'self' indicate cross-pollination and self-pollination, respectively. *jaz* single mutants in blue shade have been reported previously or are newly characterized in this study (see Table S2 and Methods section). *jaz2-1, jaz3-3*, *jaz9-1* were previously characterized (Chini et al., 2007; Thines et al., 2007) and *jaz6-Wisc* was characterized by the authors, but *jaz2-3*, *jaz3-4*, *jaz6-4* and *jaz9-4* were later selected as alternative alleles for construction of *jazD*. *gl1-2* was included to study trichome development (Yoshida et al., 2009). Male sterility of *coi1-1* mutants was exploited to assist in selection of rare recombination events between closely linked loci (Barth and Jander, 2006).

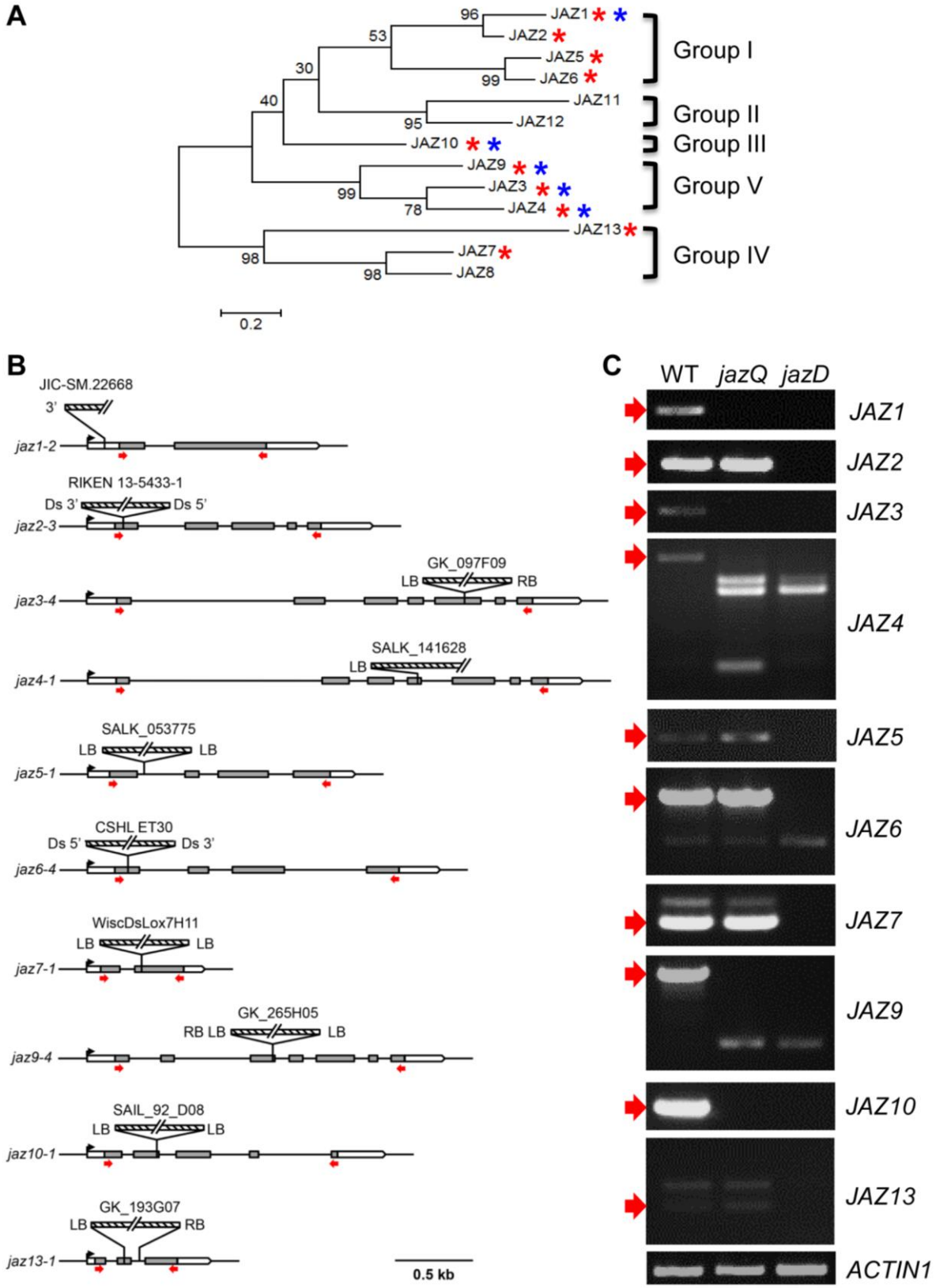

Figure 2.2. Reverse transcription-PCR analysis of mutated *JAZ* genes in *jazD*.

Figure 2.2. (cont'd) (A) Phylogenetic tree of 13 JAZ proteins in Arabidopsis. Blue and red asterisks denote *JAZ* genes that contain insertion mutations in *jazQ* and *jazD*, respectively.
(B) Schematic diagrams of insertion mutations used for construction of *jazQ* and *jazD*. White and grey boxes represent untranslated regions (UTRs) and exons, respectively. The identity and position of each insertion mutation is shown. Red arrows show the position of primers used to assess expression of *JAZ* genes by RT-PCR.
(C) RT-PCR analysis of expression of *JAZ* genes in wild-type Col-0 (WT), *jazQ,* and *jazD*. RNA was extracted from rosette leaves of 23-day-old plants grown under long-day conditions. The *ACTIN1* gene (At2g37620) was used as a positive control. Red arrows denote PCR products that have the predicted size of full-length *JAZ* transcripts.

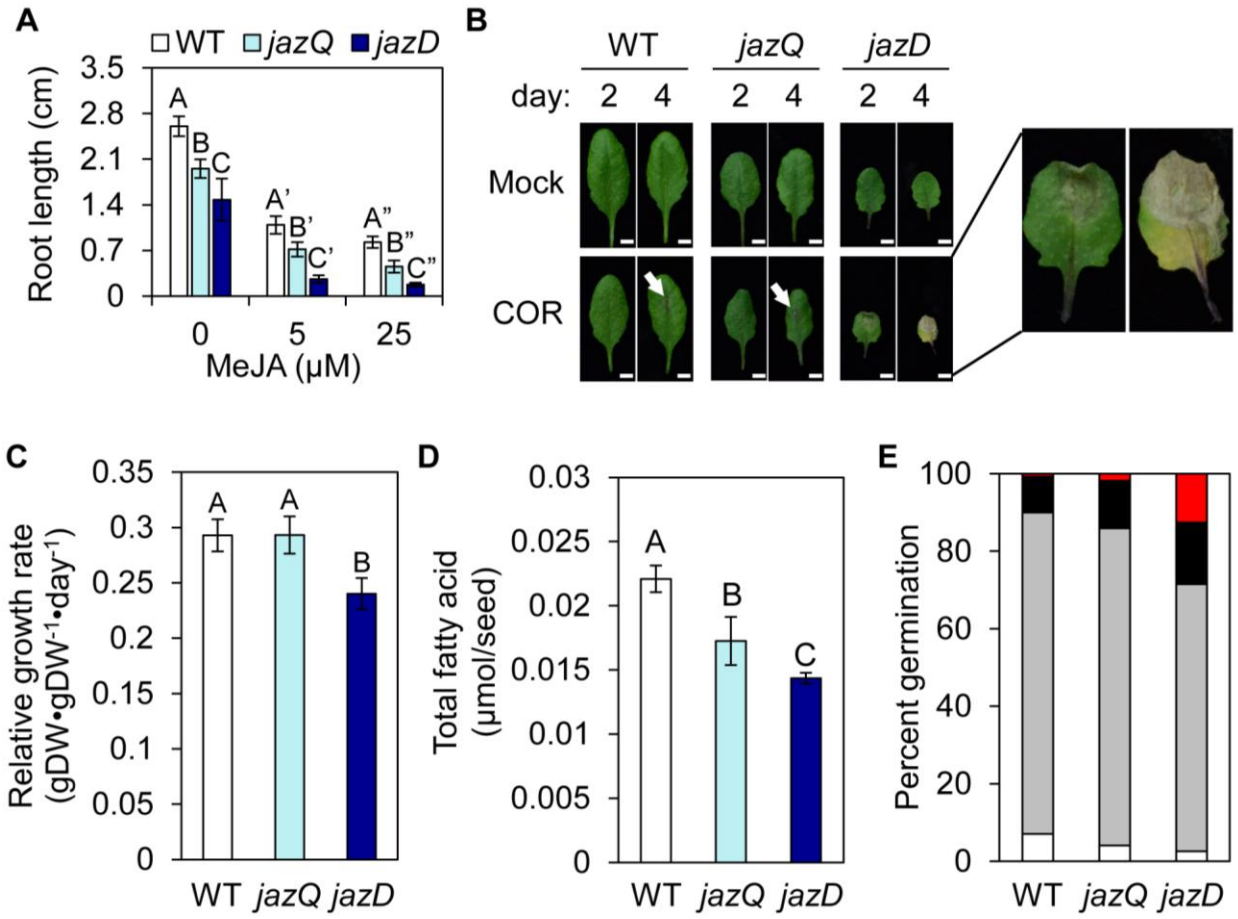

Figure 2.3. A *jaz* decuple mutant (*jazD*) is highly sensitive to jasmonate and exhibits reduced growth and fertility.

(A) Root length of 8-d-old WT Col-0 (WT), *jazQ*, and *jazD* seedlings grown in the presence of 0, 5, or 25 μM MeJA. Data show the mean ± SD of 30 plants per genotype at each concentration. Capital letters denote significant differences according to Tukey's honest significant difference (HSD) test ($P < 0.05$).
(B) *jazD* leaves are hypersensitive to COR. The eighth leaf of 40-d-old plants grown under 12-h light/12-h dark photoperiod was treated with 5 μL water (mock) or 50 μM COR. Leaves were excised and photographed after 2 or 4 d of treatment. Arrows denote location of visible anthocyanin accumulation at the site of COR application. Inset, Right is enlargement of photograph of the COR-treated *jazD*. (Scale bars, 1 cm.)
(C) RGR of soil-grownWT, *jazQ*, and *jazD* plants.
(D) Total fatty acid content in seeds from the indicated genotype. Data show the mean ± SD of seeds obtained from five plants per genotype.
(E) Time course of seed germination. Colored bars indicate the percentage of germinated seeds at various times after sowing on water agar: white, day 1; gray, day 2; black, day 3 and all later times; red, nongerminated seeds.

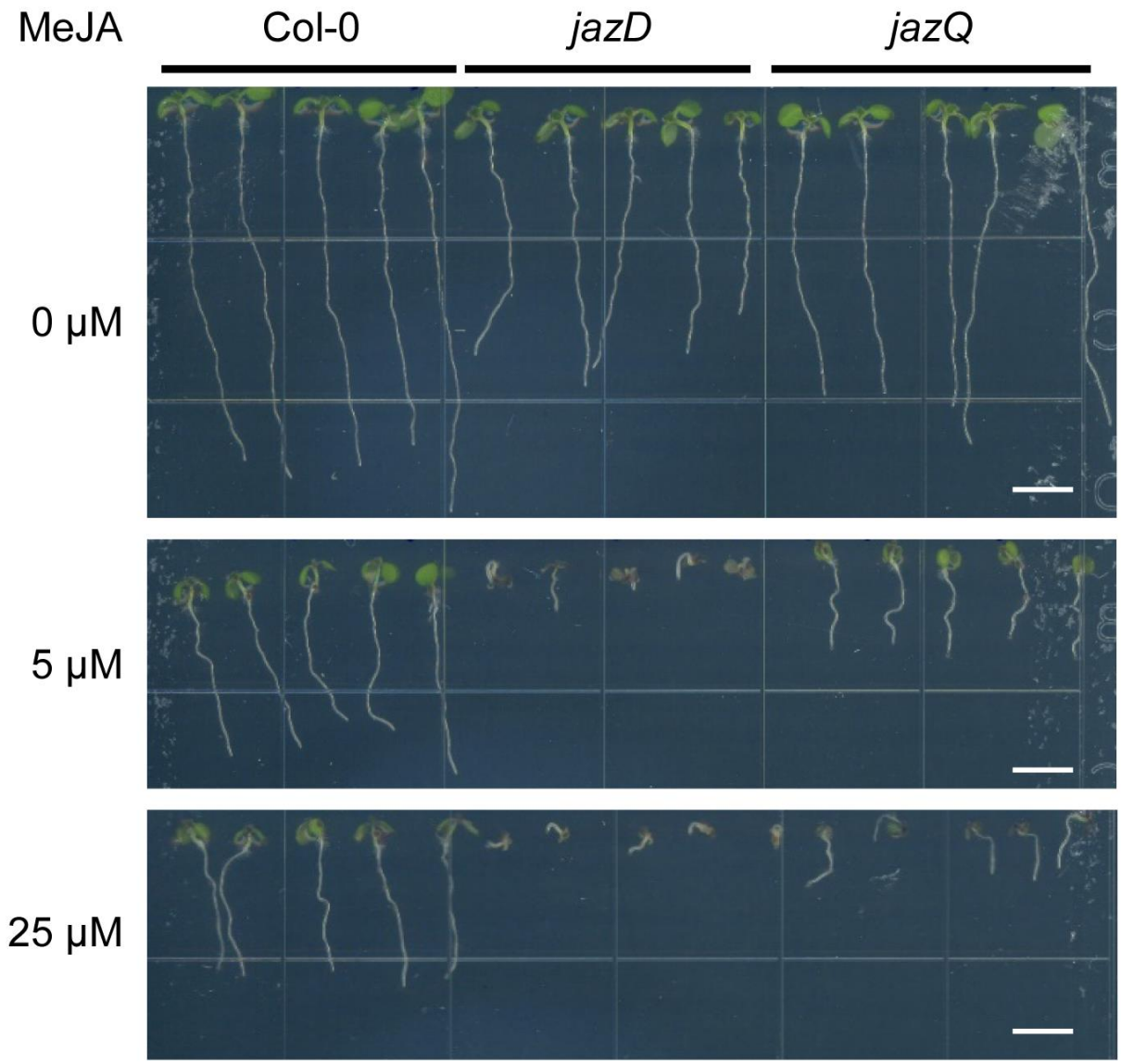

Figure 2.4. Root growth inhibition in response to MeJA treatment.

The photographs show representative 8-day-old seedlings of the indicated genotype grown on 1/2 LS medium supplemented with 0, 5, or 25 µM MeJA.

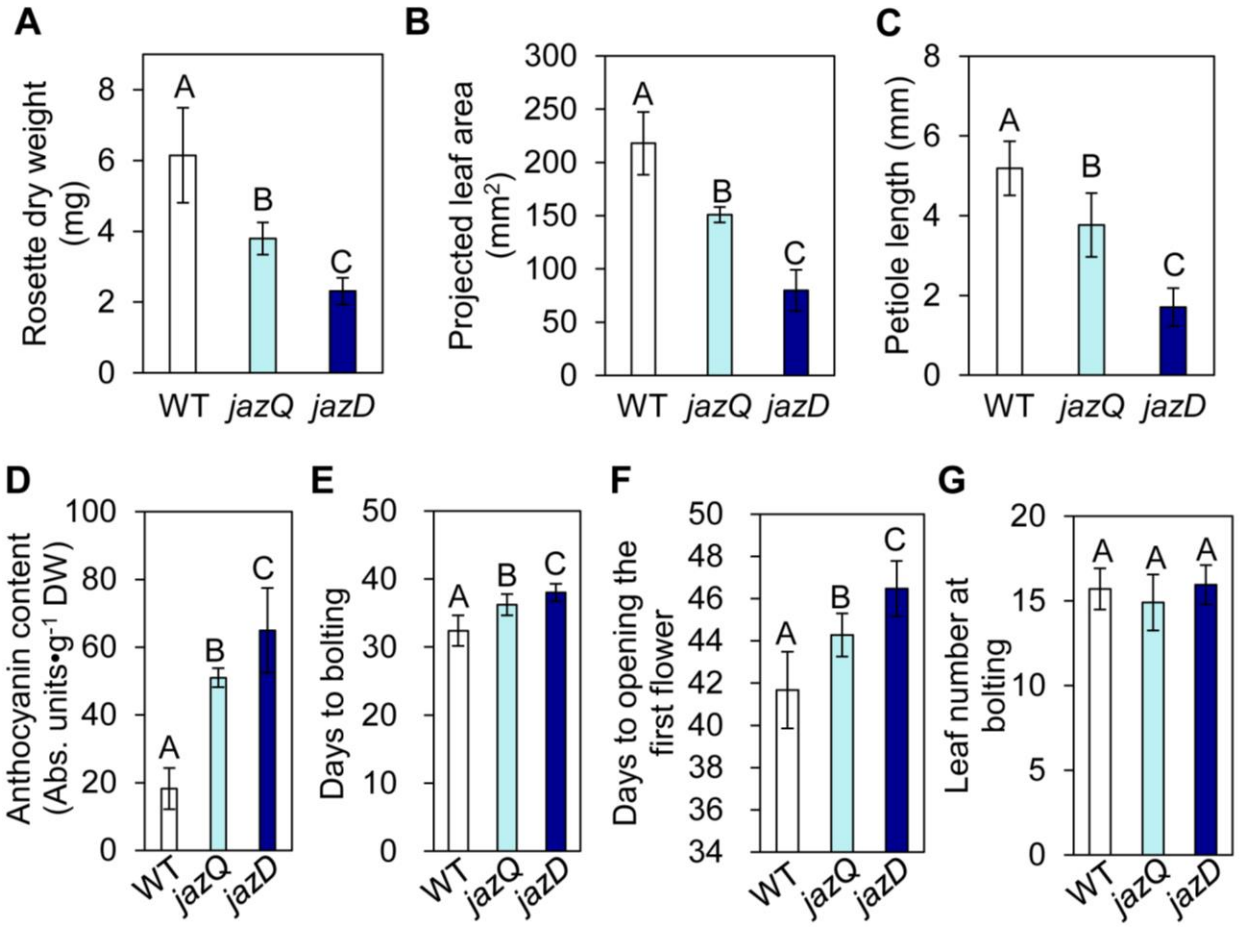

Figure 2.5. Vegetative growth and reproductive phenotypes of *jazD* plants.

(A) and **(B)** Rosette dry weight (A) and projected leaf area (B) was determined for 23-day-old soil-grown plants. Data show the mean ± SD of five plants per genotype. Capitalized letters denote significant differences according to Tukey's HSD test ($P < 0.05$).
(C) Petiole length of the third true leaf of 21-day-old soil-grown plants. Data show the mean ± SD of ten plants per genotype.
(D) Anthocyanin levels in leaves of 23-day-old plants. Data show the mean ± SD of five rosettes per genotype.
(E) and **(F)** The number of days to bolting (E) and opening of the first flower (F). Data show the mean ± SD of at least 18 plants per genotype.
(G) The number of rosette leaves at the time bolting. Data show the mean ± SD of at least 18 plants per genotype.

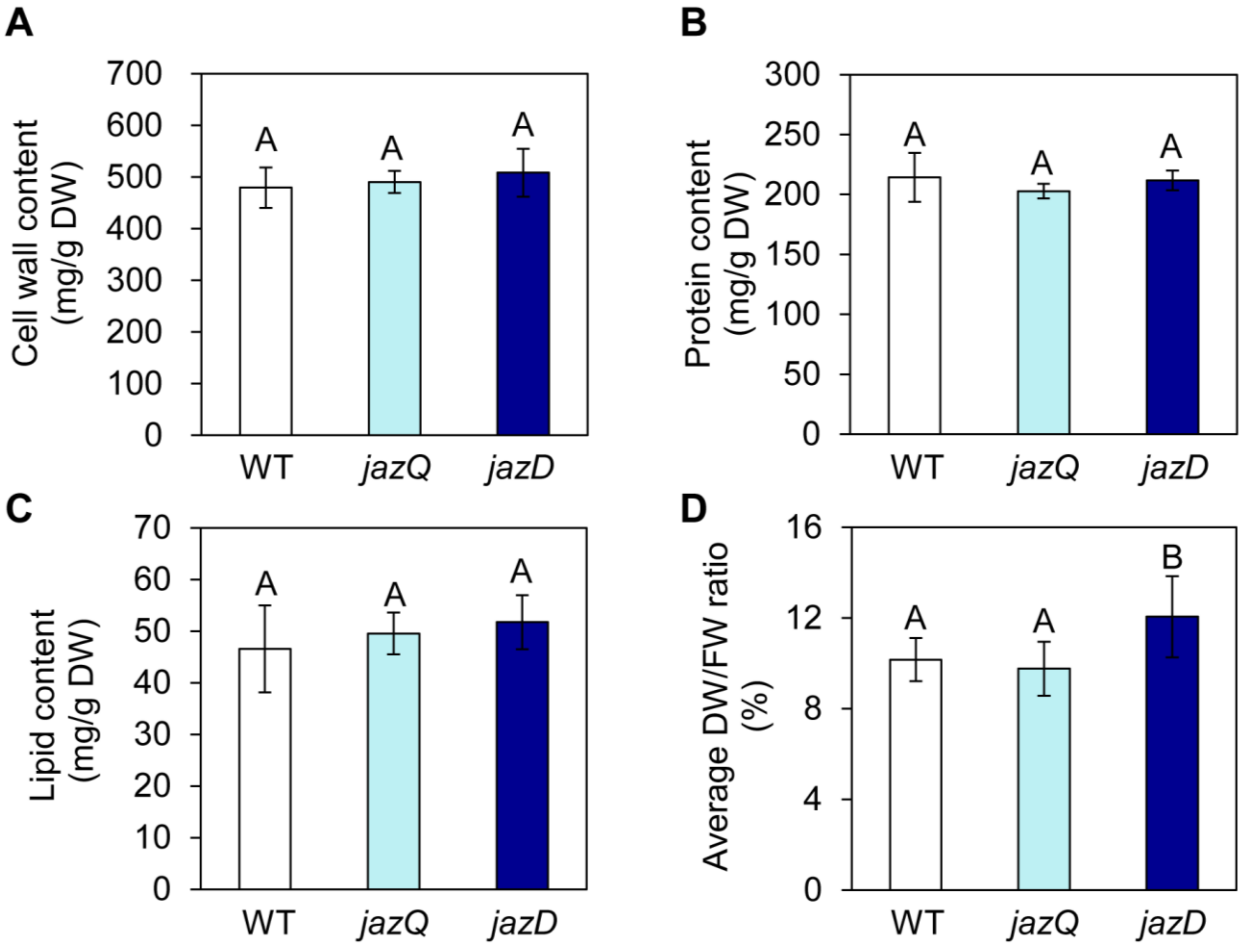

Figure 2.6. Bulk cell wall, protein, lipid, and dry mass content in higher-order *jaz* mutants.

(A-D) Rosette leaf tissue from 23-day-old plants of the indicated genotype was assessed for bulk cell wall (A), protein (B), lipid (C), and dry mass (D, as a ratio of dry weight to fresh weight) content. Data show the mean ± SD of five replicates per genotype. Capital letters denote significant differences according to Tukey's HSD test ($P < 0.05$).

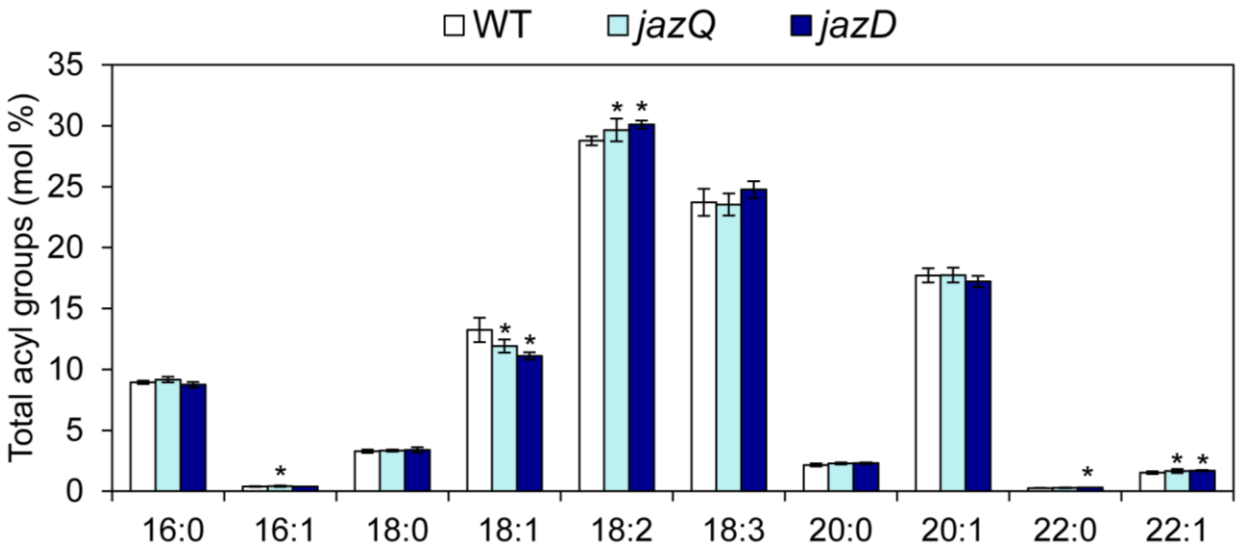

Figure 2.7. Fatty acid composition of seeds.

Values depict the relative abundance of major fatty acids in wild-type Col-0 (WT), *jazQ*, and *jazD* seeds. Asterisks denote significant differences in comparison to Col-0 seeds according to Tukey's HSD test ($P < 0.05$).

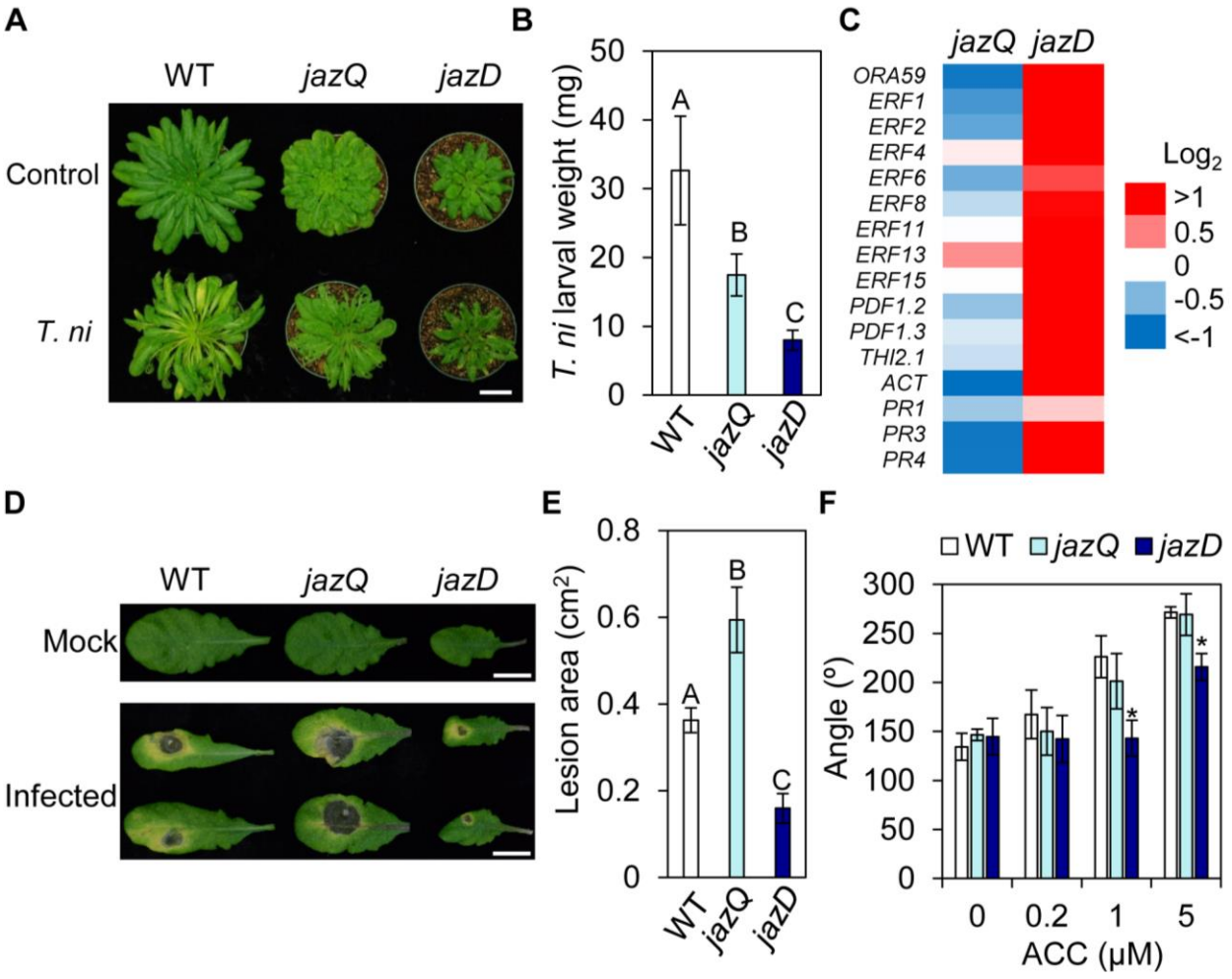

Figure 2.8. *jazD* plants are highly resistant to insect herbivores and necrotrophic pathogens.

(A) Representative short-day grown WT Col-0 (WT), *jazQ*, and *jazD* plants before and after challenge with four *T. ni* larvae for 12 d. (Scale bar: 3 cm.)
(B) Weight gain of *T. ni* larvae reared on plants shown in A. Data show the mean ± SD of at least 30 larvae per genotype. Capital letters denote significant differences according to Tukey's HSD test ($P < 0.05$).
(C) Heat map displaying the expression level of various jasmonate/ethylene-responsive genes in leaves of *jazQ* and *jazD* normalized to WT. ACT, agmatine coumaroyltransferase (At5g61160).
(D) Representative leaf symptoms following 5 d treatment with *B. cinerea* spores or mock solution. (Scale bars: 2 cm.)
(E) Disease lesion size on leaves of the indicated genotype. Data show the mean ± SD of at least 19 leaves per genotype. Capital letters denote significant differences (Tukey's HSD test, $P < 0.05$).
(F) Apical hook angle of seedlings grown in the presence of various concentrations of the ethylene precursor ACC. Data show the mean ± SD of at least 21 seedlings per genotype. Asterisks denote significant difference compared with WT (Tukey's HSD test, $P < 0.05$).

A

Up-regulated genes

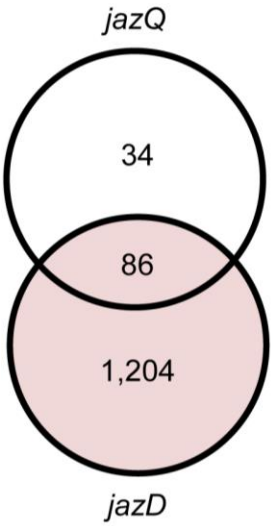

GO ID	GO description	*P* value
0009753	response to jasmonic acid stimulus	< 0.0001
0009611	response to wounding	< 0.0001
0019748	secondary metabolic process	< 0.0001
0042430	indole and derivative metabolic process	< 0.0001
0006790	sulfur metabolic process	< 0.0001
0009743	response to carbohydrate stimulus	< 0.0001
0008652	cellular amino acid biosynthetic process	< 0.0001
0006952	defense response	< 0.0001
0009723	response to ethylene stimulus	< 0.0001
0016053	organic acid biosynthetic process	< 0.0001
0000162	tryptophan biosynthetic process	< 0.0001
0019760	glucosinolate metabolic process	< 0.0001
0006564	serine biosynthetic process	0.0369

B

Down-regulated genes

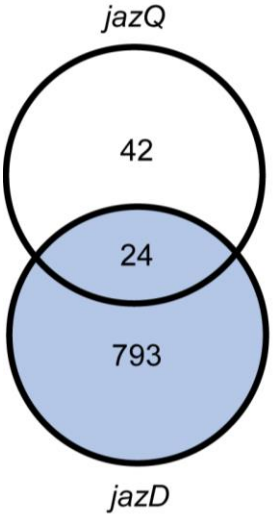

GO ID	GO description	*P* value
0009719	response to endogenous stimulus	< 0.0001
0009725	response to hormone stimulus	< 0.0001
0009416	response to light stimulus	< 0.0001
0009314	response to radiation	< 0.0001
0044042	glucan metabolic process	< 0.0001
0010033	response to organic substance	< 0.0001
0007047	cell wall organization	< 0.0001
0009628	response to abiotic stimulus	0.0016
0016051	carbohydrate biosynthetic process	0.0092
0006073	cellular glucan metabolic process	0.0097
0005976	polysaccharide metabolic process	0.0108
0008610	lipid biosynthetic process	0.0321

Figure 2.9. Differential regulation in *jazD* of genes involved in growth, defense, and metabolism.

Figure 2.9. (cont'd) (A) and **(B)** The Venn diagrams show the numbers of differentially expressed genes in *jazQ* and *jazD* leaves based on analysis of RNA-seq data (threshold > 1.5 fold change and Benjamini-Hochberg corrected *P* value < 0.05). Gene ontology (GO) analysis (biological processes) was performed with genes that were either upregulated (A) and downregulated (B) in *jazD* leaves relative to Col-0. Enriched functional categories were determined with DAVID (version 6.8) using the hypergeometric test with Benjamini & Hochberg's false discovery rate (FDR) correction.

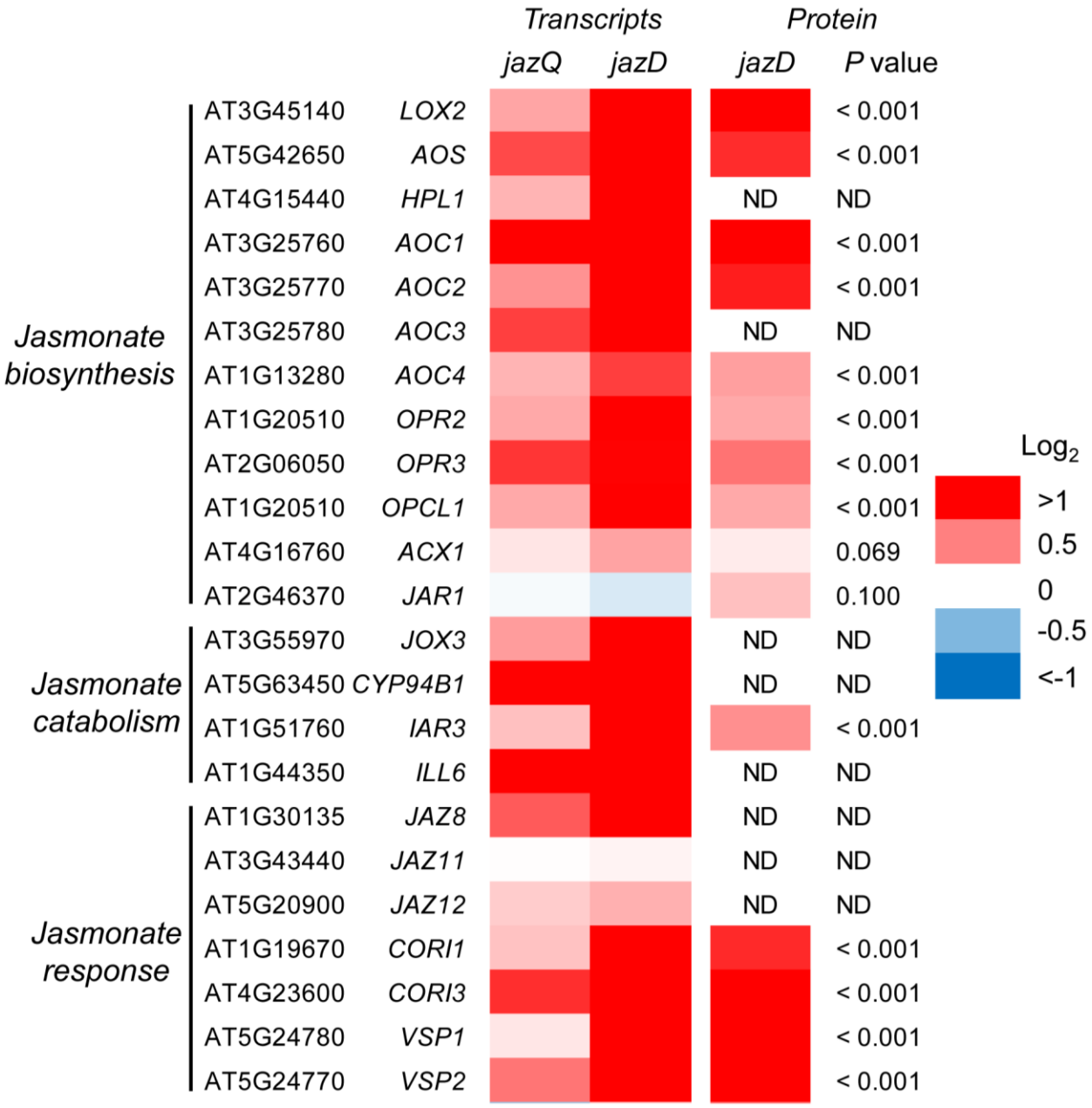

Figure 2.10. Upregulation of jasmonate pathway components in *jazD*.

Heat maps (left and middle) depict the expression level of select transcripts involved in JA biosynthesis, catabolism, and response. Transcript levels in *jazQ* and *jazD* were derived from RNA-seq data and are presented as fold-change (Log_2) over wild-type Col-0 plants. Heat map on right depicts the abundance of the corresponding protein in *jazD*. Protein levels were determined by quantitative proteomic analysis and are presented as fold-change (Log_2) over Col-0 plants. The indicated *P* value shows the statistical significance of the difference in protein levels between *jazD* and Col-0, evaluated using Permutation & Benjamini-Hochberg tests. ND, not detected in proteomic analysis.

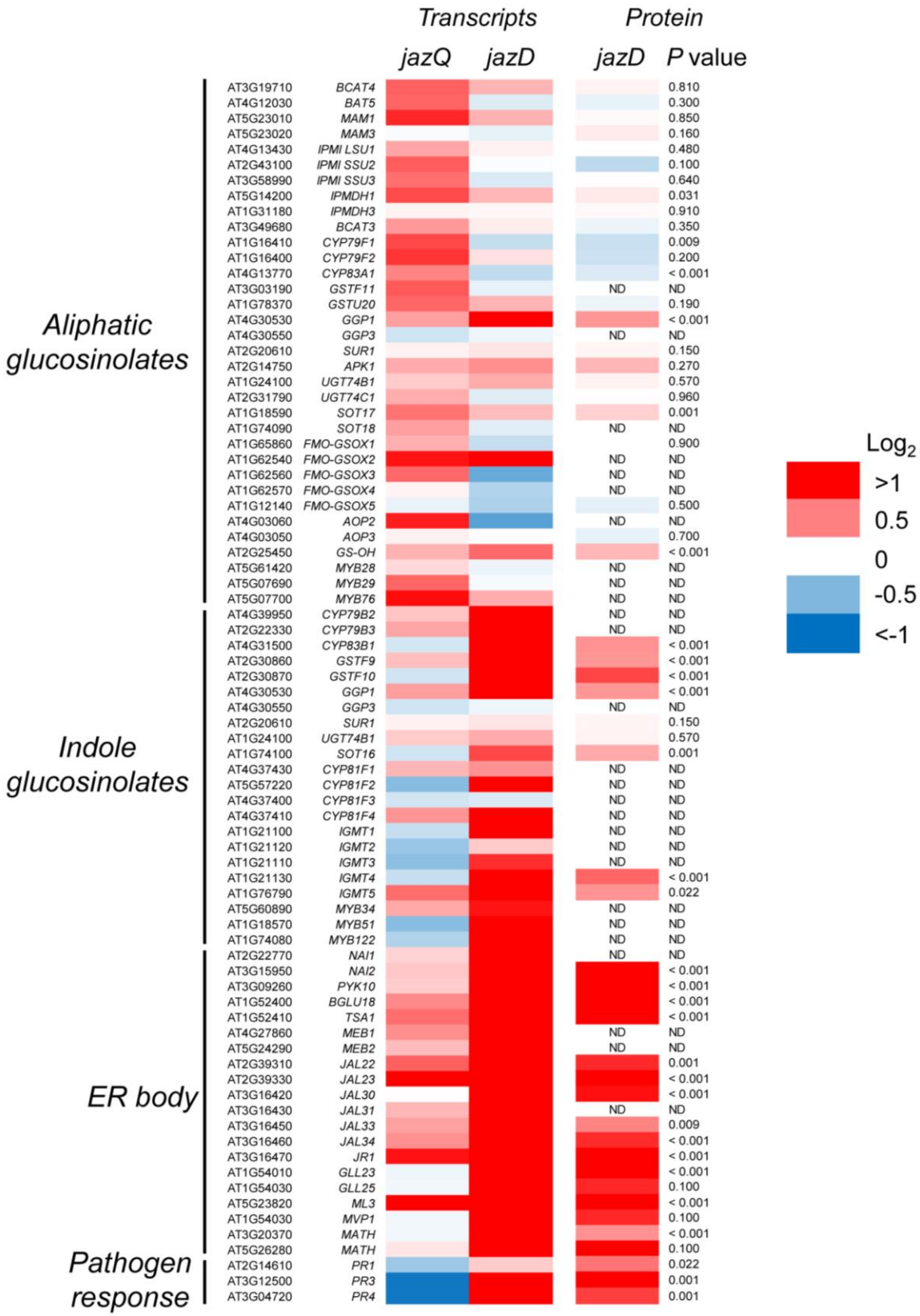

Figure 2.11. Upregulation of ER body and indole glucosinolate defenses in *jazD*.

Figure 2.11. (cont'd) Heat maps (left and middle) depict the expression level of transcripts involved in endoplasmic reticulum (ER) body formation, aliphatic and indole glucosinolate metabolism, and select pathogen defense responses. Transcript levels in *jazQ* and *jazD* were derived from RNA-seq data and are presented as fold-change (Log_2) over Col-0 plants. Heat map on right shows the abundance of the corresponding protein in *jazD*. Protein levels were determined by quantitative proteomic analysis and are presented as fold-change (Log_2) over Col-0. The indicated *P* value shows the statistical significance of the difference in protein levels between *jazD* and Col-0, evaluated using Permutation & Benjamini-Hochberg tests. ND, not detected in proteomic analysis.

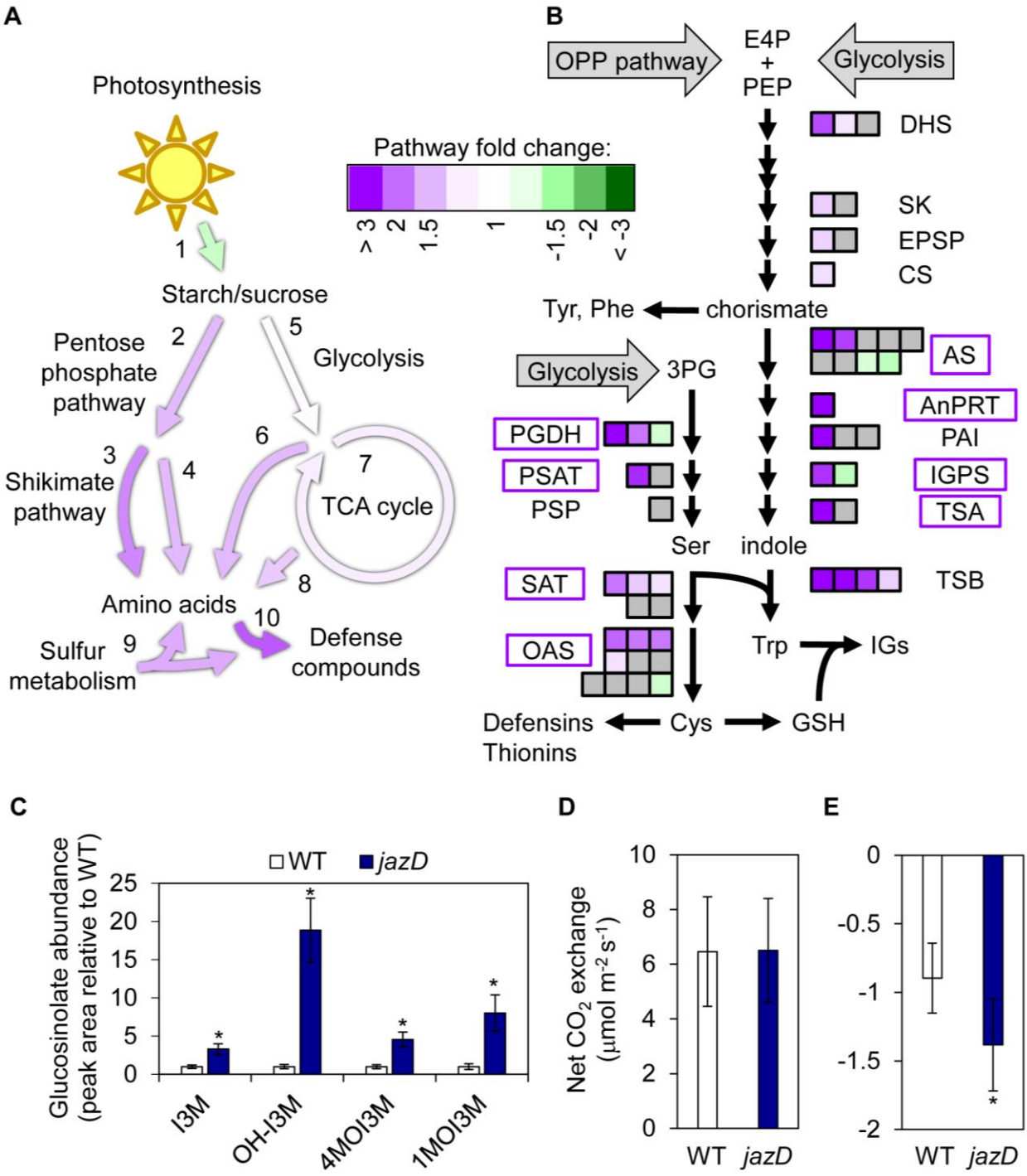

Figure 2.12. Reconfiguration of primary and secondary metabolism in *jazD*.

(A) Mapping of differentially regulated genes in *jazD* to various metabolic pathways implicates elevated production of defense metabolites derived from amino acids. Mapped pathways include photosynthesis (Campos et al., 2016), pentose phosphate pathway (Gimenez-Ibanez et al., 2017), shikimate pathway (Thines et al., 2007), amino acids from pentose phosphate intermediates (Thireault et al., 2015), glycolysis (Hummel et al., 2010), amino acids from glycolysis

Figure 2.12. (cont'd). intermediates (Herde et al., 2013), TCA cycle (Rowe and Kliebenstein, 2007), amino acids from TCA intermediates (Jofuku et al., 2005), sulfur metabolism (Roux et al., 2004), and defense metabolites from amino acids (Dekkers et al., 2004). Colored arrows denote the average foldchange of differentially expressed transcripts mapping to a particular pathway ($P < 0.05$).

(B) Schematic of tryptophan biosynthesis from erythrose 4-phosphate (E4P), phosphoenolpyruvate (PEP), and 3-phosphoglycerate (3PG) illustrates up-regulation of genes and proteins in *jazD*. Each arrow represents an enzymatic reaction in the pathway. Boxes represent individual genes, colored by fold-change of *jazD* relative to WT according to RNA-seq data, whereas gray boxes denote genes with no significant change in expression. Gene names within boxes denote significantly increased protein levels according to proteomics data. Gene abbreviations: AnPRT, anthranilate phosphoribosyltransferase; AS, anthranilate synthase; CS, chorismate synthase; DHQS, 3-dehydroquinate synthase; DHS, 3-deoxy-7-phosphoheptulonate synthase; DQD/SDH, 3-dehydroquinate dehydratase/shikimate dehydrogenase; EPSP, 5-enolpyruvylshikimate-3-phosphate synthase; IGPS, indole-3-glycerol-phosphate synthase; IGs, indole glucosinolates; OAS, O-acetylserine lyase; PAI, phosphoribosylanthranilate isomerase; PGDH, phosphoglycerate dehydrogenase; PSAT, phosphoserine aminotransferase; PSP, phosphoserine phosphatase; SAT, serine acetyltransferase; SK, shikimate kinase; TSA, tryptophan synthase alpha subunit; TSB, tryptophan synthase β-subunit.

(C) Indole glucosinolate levels in *jazD* leaves relative to that in WT leaves. Asterisks denote significant differences in comparison with WT (Student's t test, $P < 0.05$). Abbreviations: 1MOI3M, 1-methoxyindol-3-ylmethyl (neoglucobrassicin); 4MOI3M, 4-methoxyindol-3-ylmethyl (methoxyglucobrassicin); I3M, indol-3-ylmethyl (glucobrassicin); OHI3M, 4-hydroxyindol-3-ylmethyl (hydroxyglucobrassicin).

(D) and **(E)** Net gas exchange rate in WT and *jazD* rosette leaves measured at 400 μmol CO_2 and 20 °C after acclimation in 500 μmol m^{-2} s^{-1} in light (D) or dark (E).

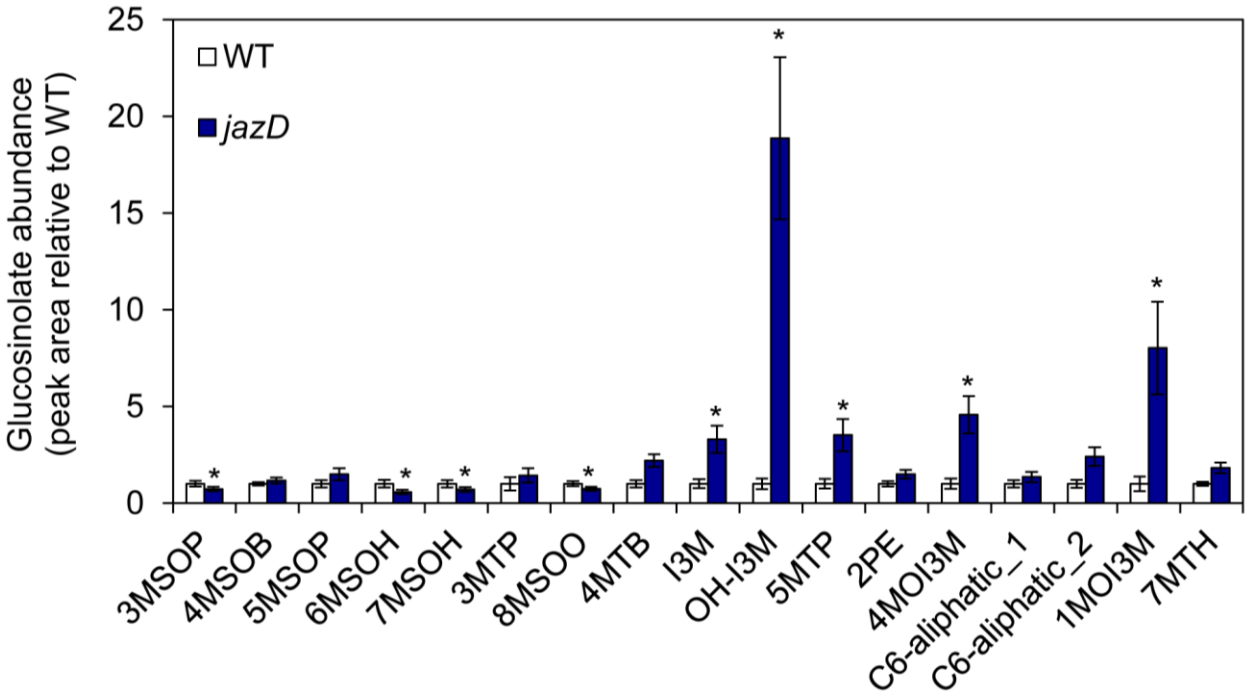

Figure 2.13. Glucosinolate accumulation is elevated in *jazD* leaves.

Glucosinolates were extracted from leaf tissue of 26-day-old *jazD* and Col-0 (WT) plants and measured by LC-MS. Peak area for the indicated glucosinolate compound in the WT sample was set to "1" and the peak area of the same compound in *jazD* was normalized to the WT sample. Asterisks denote significant difference in comparison to WT plants according to the Student's t-test ($P < 0.05$). Abbreviations: 3MSOP, 3-methylsulphinylpropyl (glucoiberin); 4MSOB, 4-methylsulphinylbutyl (glucoraphanin); 5MSOP, 5-methylsulphinylpentyl (glucoalyssin); 6MSOH, 6-methylsulphinylhexyl (glucohesperin); 7MSOH, 7-methylsulphinylheptyl (glucoibarin); 3MTP, 3-methylthiopropyl (glucoiberverin); 8MSOO, 8-methylsulphinyloctyl (glucohirsutin); 4MTB, 4-methylthiobutyl (glucoerucin); I3M, indol-3-ylmethyl (glucobrassicin); OH-I3M, 4-hydroxyindol-3-ylmethyl (hydroxyglucobrassicin); 5MTP, 5-methylthiopentyl (glucoberteroin); 2PE, 2-phenylethyl (gluconasturtiin); 4MOI3M, 4-methoxyindol-3-ylmethyl (methoxyglucobrassicin); 1MOI3M, 1-methoxyindol-3-ylmethyl (neoglucobrassicin); 7MTH, 7-methylthioheptyl.

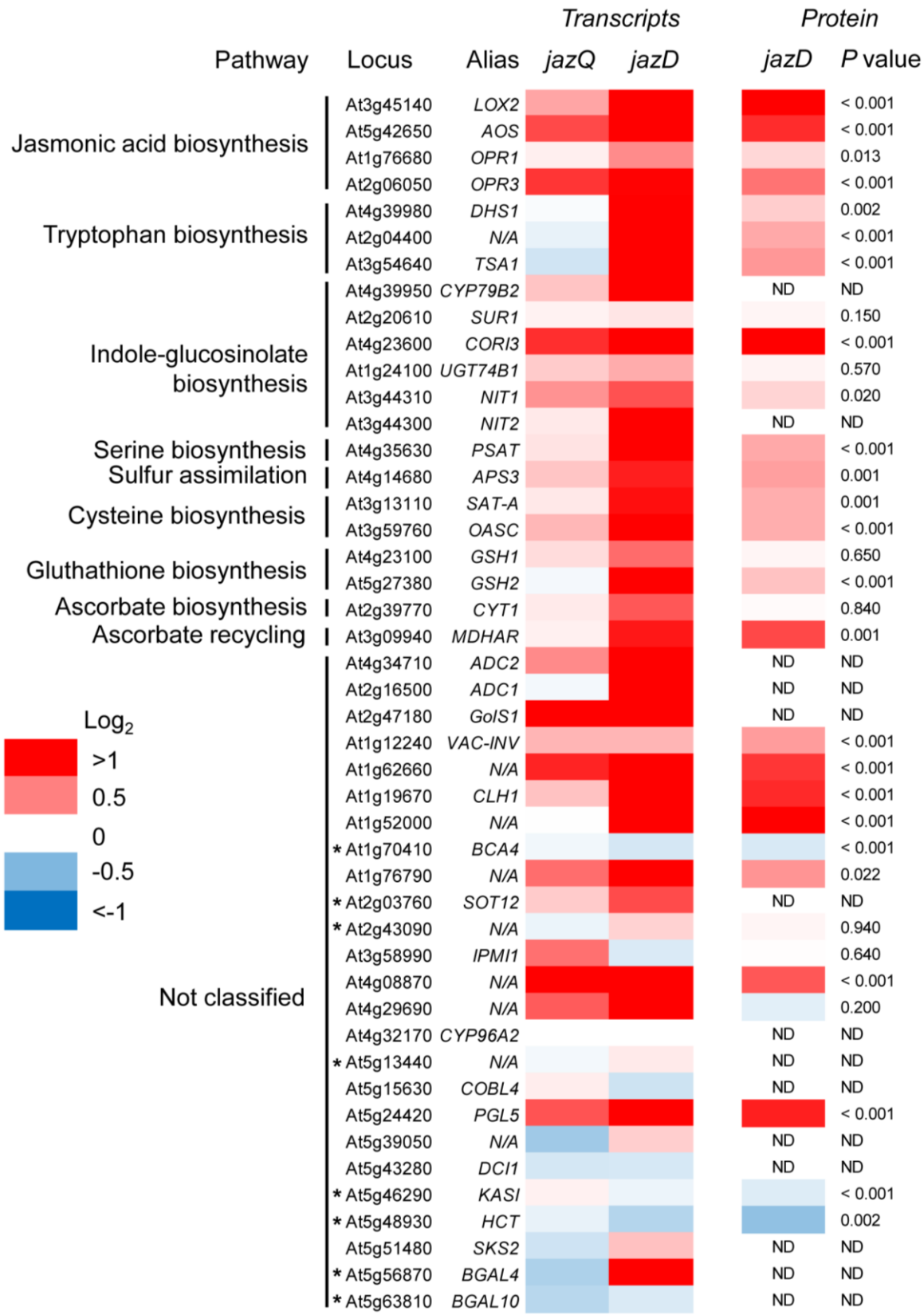

Figure 2.14. Comparison of *jazD* "omics" data to jasmonate-responsive genes (JRGs) described by Sasaki-Sekimoto *et al.* (Sasaki-Sekimoto et al., 2005).

Figure 2.14. (cont'd) Authors of this previous study identified 46 JRGs differentially regulated by exogenous MeJA [38 upregulated genes and 8 downregulated genes (denoted by asterisks)]. These genes (Locus) were classified by Sasaki-Sekimoto *et al*. into the following functional categories using AraCyc as a tool for visualizing Arabidopsis biochemical pathways: I, jasmonic acid biosynthesis; II, tryptophan biosynthesis; III, indole glucosinolate biosynthesis; IV, serine biosynthesis; V, sulfur assimilation; VI, cysteine biosynthesis; VII, gluthathione biosynthesis; VIII, ascorbate biosynthesis; IX, ascorbate recycling; and X, not classified. The depicted heat maps (left and middle) show the expression level of these genes in *jazQ* and *jazD* as determined by our RNA-seq data and are presented as fold-change (Log_2) over Col-0 plants. Heat map on right shows the abundance of the corresponding protein in *jazD*. Protein levels were determined by quantitative proteomic analysis and are presented as fold-change (Log_2) over Col-0 plants. The indicated *P* value shows the statistical significance of the difference in protein levels between *jazD* and Col-0, evaluated using Permutation & Benjamini-Hochberg tests. ND, not detected in proteomic analysis.

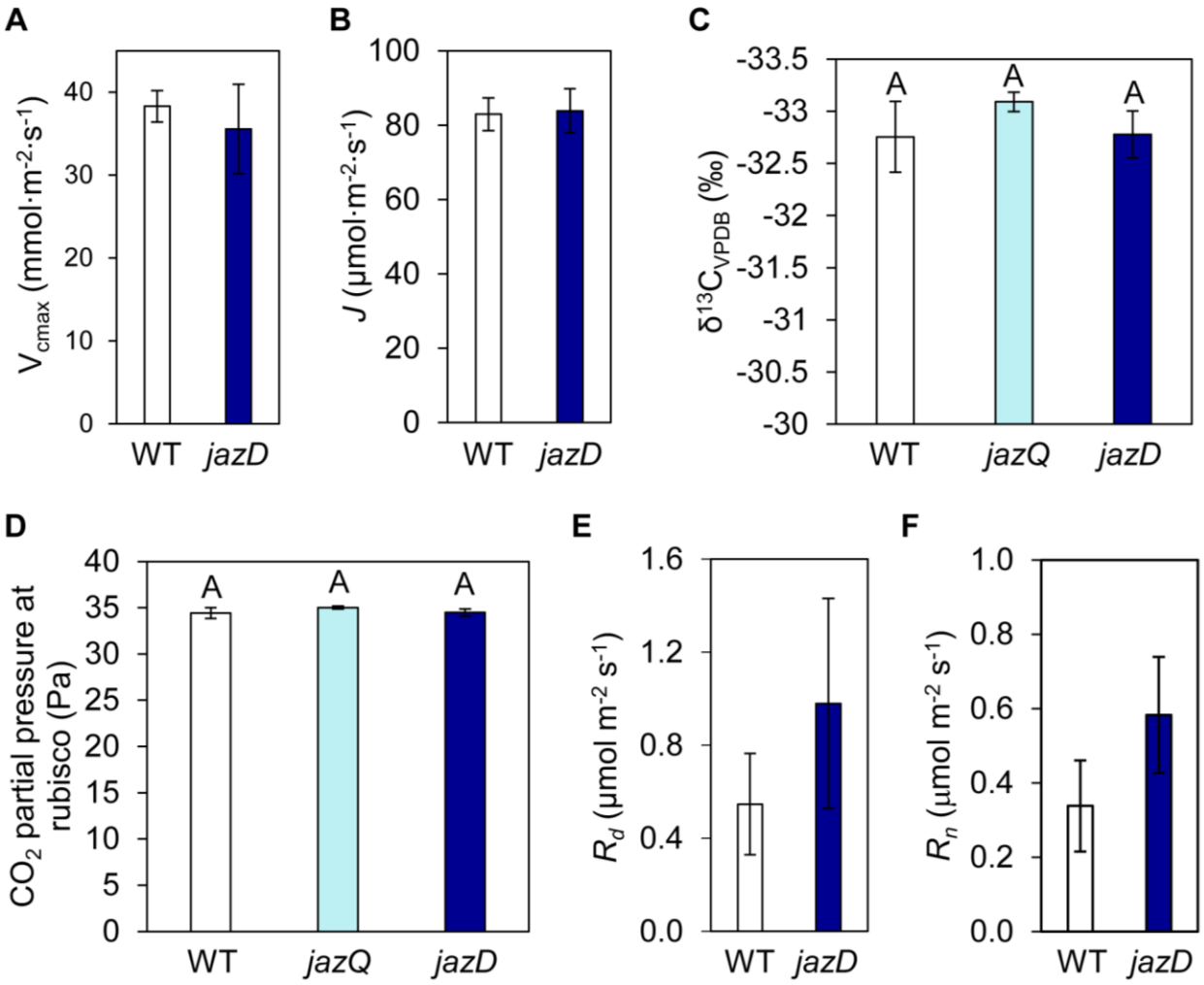

Figure 2.15. *jaz* mutations increase respiration but do not affect resistance to CO_2 diffusion through leaf mesophyll.

(A) and **(B)** Nonlinear curve-fitting to model the maximum velocity of Rubisco (A) and the rate of photosynthetic electron transport (B) from photosynthetic rates in response to increasing CO_2. Data show the mean ± SD of six replicates per genotype.
(C) Comparison of the ^{13}C to ^{12}C isotopic ratio of leaf samples to the ^{13}C to ^{12}C isotopic ratio of the Vienna-Pee-Dee Belemnite (VPDB) standard ($\delta^{13}C_{VPDB}$ (‰)) in wild-type Col-0 (WT), *jazQ*, and *jazD* plants.
(D) Comparison of CO_2 partial pressure at Rubisco in WT, *jazQ*, and *jazD* plants. Data show the mean ± SD of five replicates per genotype. Capital letters denote the lack of significant differences according to Tukey's HSD test ($P < 0.05$).
(E) and **(F)** Daytime respiration (E) and nighttime dark respiration (F) on a leaf area basis. Daytime respiration was determined from the intersection of CO_2 response curves measured at sub-saturating light intensities. Data show the mean ± SD of four replicates per genotype.

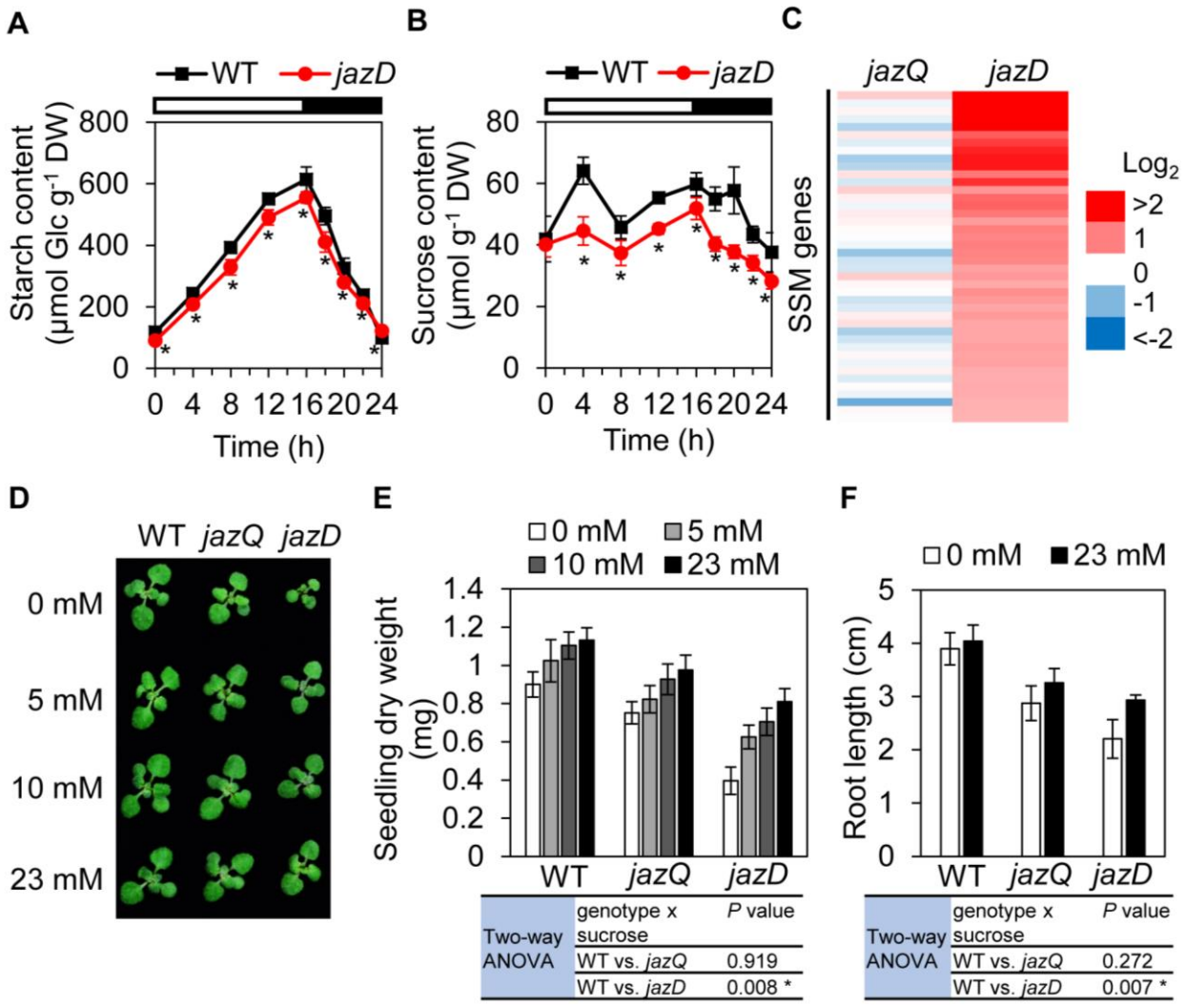

Figure 2.16. *jazD* plants exhibit symptoms of carbon starvation.

(A) and **(B)** Time course of starch (A) and sucrose (B) levels in WT Col-0 (WT) and *jazD* plants during long-day photoperiod (16-h-light/8-h-dark). Leaf tissues of soil-grown plants were harvested after 23 days. Asterisks denote significant differences in comparison with WT (Student's t test, $P < 0.05$).

(C) Heat map showing the expression level of SSM genes in *jazQ* and *jazD* leaves. Gene-expression levels determined by RNA-seq are represented as fold-change ($\log_2$) over WT.

(D) and **(E)** Photograph (D) and DW (E) of 16-d-old WT, *jazQ*, and *jazD* seedlings grown horizontally on MS medium containing the indicated concentration of sucrose. (Scale bar: D, 0.5 cm.)

(F) Root length of 11-d-old WT, *jazQ*, and *jazD* seedlings grown vertically on MS medium lacking sucrose (open bar) or containing 23 mM sucrose (filled bar). Two-way ANOVA was used to test the effect of sucrose on growth (E and F) and showed that, whereas genotype ($P < 0.001$ for both WT vs. *jazQ* and WT vs. *jazD*) and sucrose ($P < 0.001$ for both WT vs. *jazQ* and WT vs. *jazD*)

Figure 2.16. (cont'd) significantly affect shoot and root growth, the genotype × sucrose interaction was significant only for *jazD* comparisons.

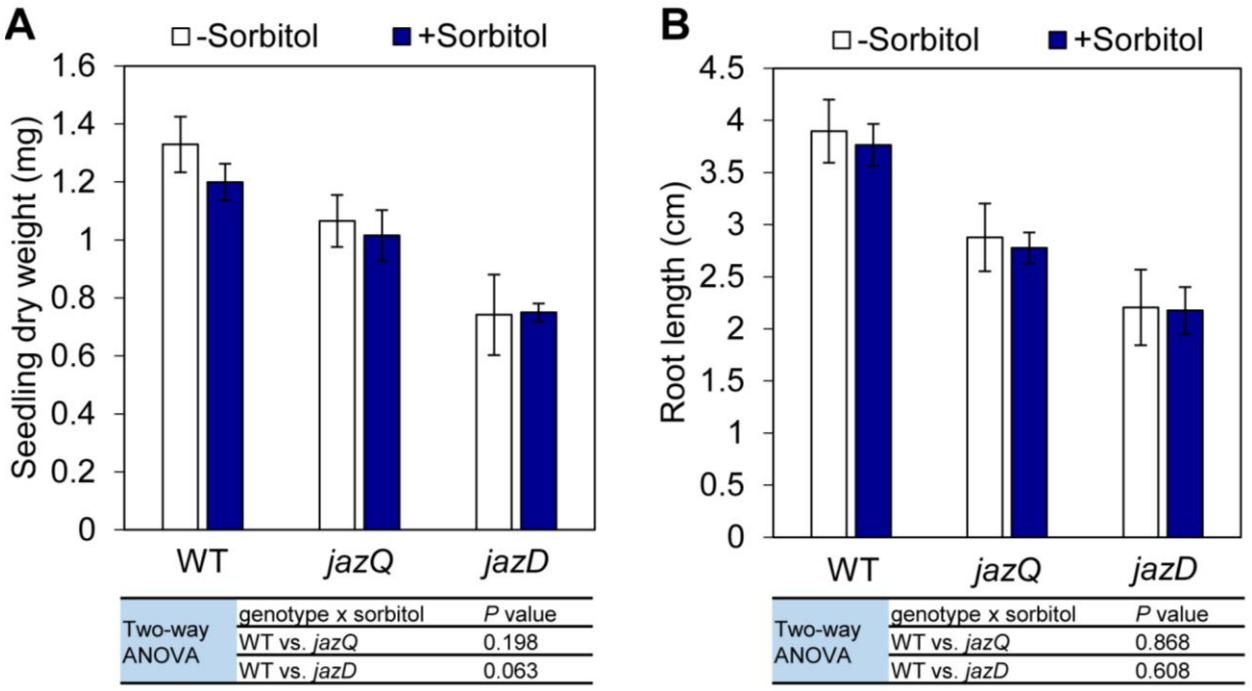

Figure 2.17. Sorbitol does not promote biomass accumulation or root elongation in *jaz* mutants.

(A) Dry weight of 16-day-old wild-type Col-0 (WT), *jazQ*, and *jazD* seedlings grown horizontally on solid MS medium containing or not containing 23 mM sorbitol.
(B) Root length of 11-day-old seedlings grown vertically on solid LS medium containing or not containing 23 mM sorbitol. Data show the mean ± SD of 80 seedlings per genotype.

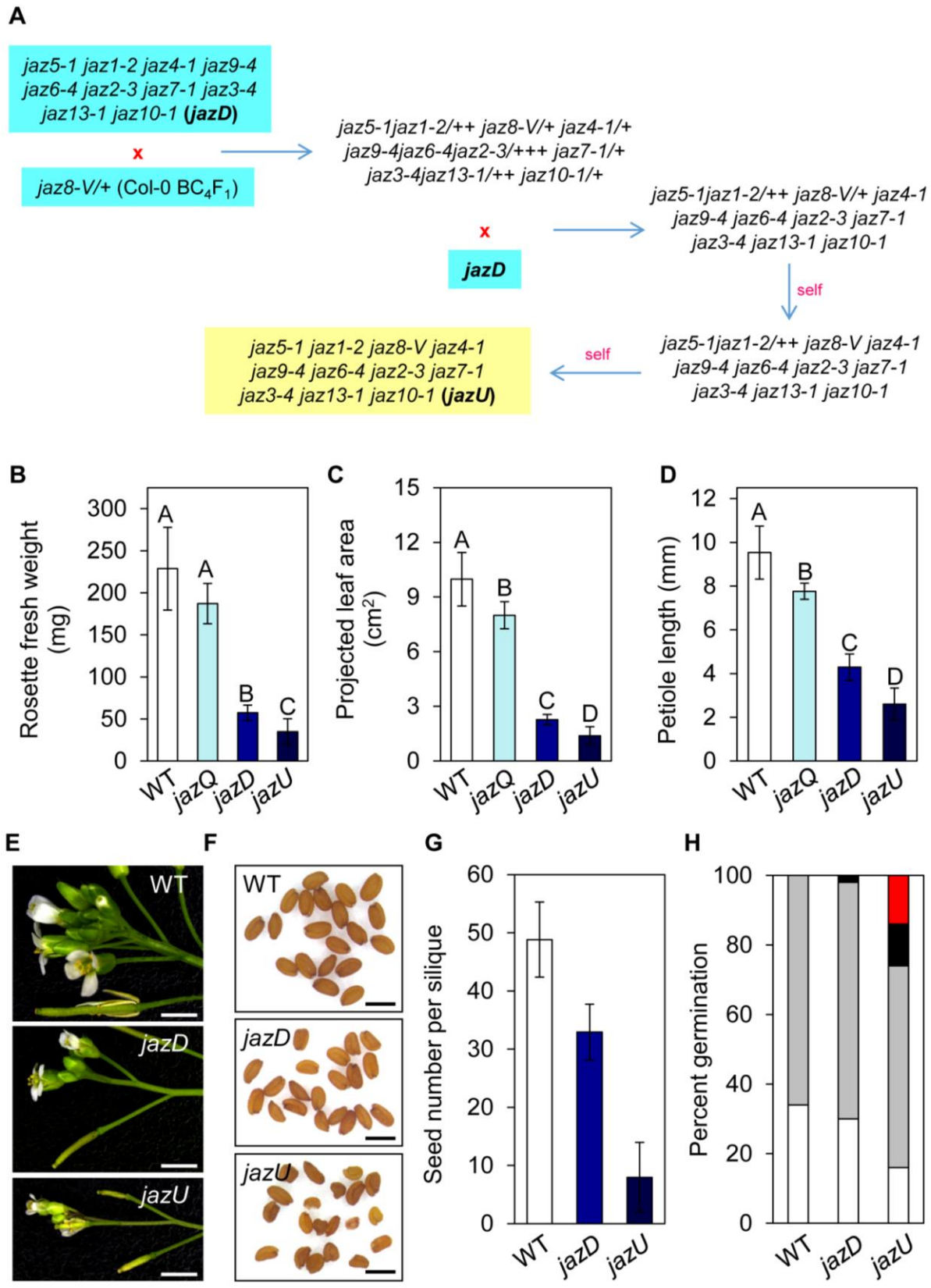

Figure 2.18. Vegetative growth and reproductive phenotypes of *jazU* plants.

Figure 2.18. (cont'd) (A) *jazU* pedigree. Pedigree notations are as described in Fig. S1. Briefly, an introgressed *jaz8-V* mutant was crossed into the *jazD* background. Because the undecuple *jazU* mutant showed near sterility, *jazU* was maintained as a line segregating for the genetically linked *jaz5 jaz1* mutations.
(B-D) Rosette fresh weight (B), projected leaf area (C), and petiole length (third true leaf) (D) were determined for 28-day-old soil-grown plants. Data show the mean ± SD of eight plants per genotype. Capitalized letters denote significant differences according to Tukey's HSD test ($P < 0.05$).
(E) and **(F)** Photograph of inflorescence apices (E) and seeds (F) of wild-type Col-0 (WT), *jazD*, and *jazU*. Flower bud clusters are smaller in *jaz* mutants and after opening, most *jazU* flowers yellow and senesce without setting fruits (E). Many *jazU* seeds are not fully filled, consistent with silique abortion and senescence (F). Bars are 2 mm (E) and 0.5 mm (F).
(G) Number of seeds per silique for WT, *jazD*, and *jazU*. Seeds were counted from each of 100 siliques from 10 plants per genotype.
(H) Time course of seed germination. Colored bars indicate the percentage of germinated seeds at various times after sowing on water agar: white, day 1; grey, day 2; black, day 3 and all later times; red, non-germinated seeds.

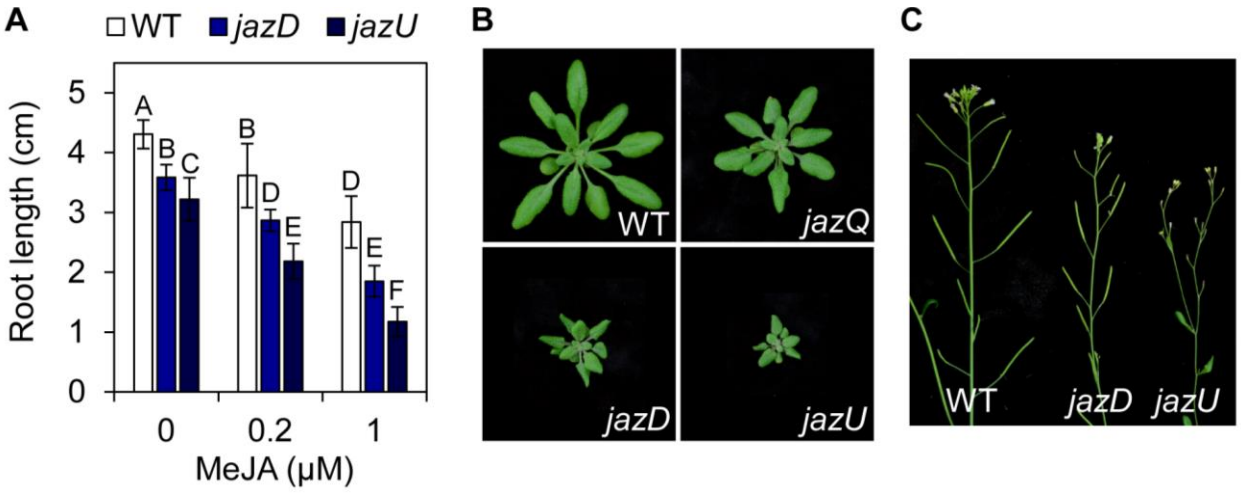

Figure 2.19. Genetic combination of *jaz8* and *jazD* further restricts growth and nearly abolishes seed production in the resulting undecuple mutant.

(A) Root length of 10-d-old WT Col-0 (WT), *jazD*, and *jaz* undecuple (*jazU*) seedlings grown in the presence of 0, 0.2, or 1 μM MeJA. Data show the mean ± SD of 14-20 seedlings per genotype at each concentration. Capital letters denote significant differences according to Tukey's HSD test ($P < 0.05$).
(B) Photograph of WT, *jazQ*, *jazD*, and *jazU* rosettes of 28-d-old plants.
(C) Photograph of WT, *jazD*, and *jazU* inflorescence of 8-wk-old plants.

REFERENCES

REFERENCES

Adio, A.M., Casteel, C.L., De Vos, M., Kim, J.H., Joshi, V., Li, B., Juery, C., Daron, J., Kliebenstein, D.J., and Jander, G. (2011). Biosynthesis and defensive function of Ndelta-acetylornithine, a jasmonate-induced Arabidopsis metabolite. Plant Cell **23,** 3303-3318.

Agrawal, A.A. (1998). Induced responses to herbivory and increased plant performance. Science **279,** 1201-1202.

An, C.P., Li, L., Zhai, Q.Z., You, Y.R., Deng, L., Wu, F.M., Chen, R., Jiang, H.L., Wang, H., Chen, Q., and Li, C.Y. (2017). Mediator subunit MED25 links the jasmonate receptor to transcriptionally active chromatin. Proceedings of the National Academy of Sciences of the United States of America **114,** E8930-E8939.

Anders, S., and Huber, W. (2010). Differential expression analysis for sequence count data. Genome Biol **11,** R106.

Attaran, E., Major, I.T., Cruz, J.A., Rosa, B.A., Koo, A.J.K., Chen, J., Kramer, D.M., He, S.Y., and Howe, G.A. (2014). Temporal Dynamics of Growth and Photosynthesis Suppression in Response to Jasmonate Signaling. Plant Physiol **165,** 1302-1314.

Baena-Gonzalez, E., Rolland, F., Thevelein, J.M., and Sheen, J. (2007). A central integrator of transcription networks in plant stress and energy signalling. Nature **448,** 938-U910.

Baldwin, I.T. (1998). Jasmonate-induced responses are costly but benefit plants under attack in native populations. Proceedings of the National Academy of Sciences of the United States of America **95,** 8113-8118.

Barth, C., and Jander, G. (2006). Arabidopsis myrosinases TGG1 and TGG2 have redundant function in glucosinolate breakdown and insect defense. Plant J **46,** 549-562.

Benstein, R.M., Ludewig, K., Wulfert, S., Wittek, S., Gigolashvili, T., Frerigmann, H., Gierth, M., Flugge, U.I., and Krueger, S. (2013). Arabidopsis Phosphoglycerate Dehydrogenase1 of the Phosphoserine Pathway Is Essential for Development and Required for Ammonium Assimilation and Tryptophan Biosynthesis. Plant Cell **25,** 5011-5029.

Berrocal-Lobo, M., Molina, A., and Solano, R. (2002). Constitutive expression of ETHYLENE-RESPONSE-FACTOR1 in Arabidopsis confers resistance to several necrotrophic fungi. Plant Journal **29,** 23-32.

Bolton, M.D. (2009). Primary Metabolism and Plant Defense-Fuel for the Fire. Molecular Plant-Microbe Interactions **22,** 487-497.

Bomblies, K., and Weigel, D. (2007). Hybrid necrosis: autoimmunity as a potential gene-flow barrier in plant species. Nat Rev Genet **8,** 382-393.

Bomer, M., O'Brien, J.A., Perez-Salamo, I., Krasauskas, J., Finch, P., Briones, A., Daudi, A., Souda, P., Tsui, T.L., Whitelegge, J.P., Paul Bolwell, G., and Devoto, A. (2018). COI1-dependent jasmonate signalling affects growth, metabolite production and cell wall protein composition in arabidopsis. Ann Bot. 10.1093/aob/mcy109.

Browse, J. (2009). Jasmonate Passes Muster: A Receptor and Targets for the Defense Hormone. Annual review of plant biology **60,** 183-205.

Caarls, L., Elberse, J., Awwanah, M., Ludwig, N.R., de Vries, M., Zeilmaker, T., Van Wees, S.C.M., Schuurink, R.C., and Van den Ackerveken, G. (2017). Arabidopsis JASMONATE-INDUCED OXYGENASES down-regulate plant immunity by hydroxylation and inactivation of the hormone jasmonic acid. Proceedings of the National Academy of Sciences of the United States of America **114,** 6388-6393.

Campos, M.L., Kang, J.H., and Howe, G.A. (2014). Jasmonate-Triggered Plant Immunity. J Chem Ecol **40,** 657-675.

Campos, M.L., Yoshida, Y., Major, I.T., de Oliveira Ferreira, D., Weraduwage, S.M., Froehlich, J.E., Johnson, B.F., Kramer, D.M., Jander, G., Sharkey, T.D., and Howe, G.A. (2016). Rewiring of jasmonate and phytochrome B signalling uncouples plant growth-defense tradeoffs. Nat Commun **7,** 12570.

Chen, Y.M., Wang, Y., Huang, J.G., Zheng, C.C., Cai, C.X., Wang, Q.M., and Wu, C.A. (2017). Salt and methyl jasmonate aggravate growth inhibition and senescence in Arabidopsis seedlings via the JA signaling pathway. Plant Sci **261,** 1-9.

Chini, A., Gimenez-Ibanez, S., Goossens, A., and Solano, R. (2016). Redundancy and specificity in jasmonate signalling. Curr Opin Plant Biol **33,** 147-156.

Chini, A., Fonseca, S., Fernandez, G., Adie, B., Chico, J.M., Lorenzo, O., Garcia-Casado, G., Lopez-Vidriero, I., Lozano, F.M., Ponce, M.R., Micol, J.L., and Solano, R. (2007). The JAZ family of repressors is the missing link in jasmonate signalling. Nature **448,** 666-671.

Dekkers, B.J., Schuurmans, J.A., and Smeekens, S.C. (2004). Glucose delays seed germination in Arabidopsis thaliana. Planta **218,** 579-588.

Dobritzsch, M., Lubken, T., Eschen-Lippold, L., Gorzolka, K., Blum, E., Matern, A., Marillonnet, S., Bottcher, C., Drager, B., and Rosahl, S. (2016). MATE Transporter-Dependent Export of Hydroxycinnamic Acid Amides. Plant Cell **28,** 583-596.

Farmer, E.E., and Dubugnon, L. (2009). Detritivorous crustaceans become herbivores on jasmonate-deficient plants. Proceedings of the National Academy of Sciences of the United States of America **106,** 935-940.

Farquhar, G.D., Oleary, M.H., and Berry, J.A. (1982). On the Relationship between Carbon Isotope Discrimination and the Inter-Cellular Carbon-Dioxide Concentration in Leaves. Aust J Plant Physiol **9,** 121-137.

Farquhar, G.D., Ehleringer, J.R., and Hubick, K.T. (1989). Carbon Isotope Discrimination and Photosynthesis. Annu Rev Plant Phys **40,** 503-537.

Fernandez-Calvo, P., Chini, A., Fernandez-Barbero, G., Chico, J.M., Gimenez-Ibanez, S., Geerinck, J., Eeckhout, D., Schweizer, F., Godoy, M., Franco-Zorrilla, J.M., Pauwels, L., Witters, E., Puga, M.I., Paz-Ares, J., Goossens, A., Reymond, P., De Jaeger, G., and Solano, R. (2011). The Arabidopsis bHLH Transcription Factors MYC3 and MYC4 Are Targets of JAZ Repressors and Act Additively with MYC2 in the Activation of Jasmonate Responses. Plant Cell **23,** 701-715.

Figueroa, P., and Browse, J. (2015). Male sterility in Arabidopsis induced by overexpression of a MYC5-SRDX chimeric repressor. Plant Journal **81,** 849-860.

Foster, C.E., Martin, T.M., and Pauly, M. (2010). Comprehensive compositional analysis of plant cell walls (lignocellulosic biomass) part II: carbohydrates. Journal of visualized experiments **37,** 1837.

Fujiki, Y., Yoshikawa, Y., Sato, T., Inada, N., Ito, M., Nishida, I., and Watanabe, A. (2001). Dark-inducible genes from Arabidopsis thaliana are associated with leaf senescence and repressed by sugars. Physiol Plantarum **111,** 345-352.

Gibon, Y., Pyl, E.T., Sulpice, R., Lunn, J.E., Hohne, M., Gunther, M., and Stitt, M. (2009). Adjustment of growth, starch turnover, protein content and central metabolism to a decrease of the carbon supply when Arabidopsis is grown in very short photoperiods. Plant Cell Environ **32,** 859-874.

Gigolashvili, T., Berger, B., Mock, H.P., Muller, C., Weisshaar, B., and Fluegge, U.I. (2007). The transcription factor HIG1/MYB51 regulates indolic glucosinolate biosynthesis in Arabidopsis thaliana. Plant J **50,** 886-901.

Gimenez-Ibanez, S., Boter, M., Ortigosa, A., Garcia-Casado, G., Chini, A., Lewsey, M.G., Ecker, J.R., Ntoukakis, V., and Solano, R. (2017). JAZ2 controls stomata dynamics during bacterial invasion. The New phytologist **213,** 1378-1392.

Glauser, G., Schweizer, F., Turlings, T.C.J., and Reymond, P. (2012). Rapid Profiling of Intact Glucosinolates in Arabidopsis Leaves by UHPLC-QTOFMS Using a Charged Surface Hybrid Column. Phytochem Analysis **23,** 520-528.

Guo, Q., Major, I.T., and Howe, G.A. (2018). Resolution of growth-defense conflict: mechanistic insights from jasmonate signaling. Curr Opin Plant Biol **44,** 72-81.

Havko, N.E., Major, I.T., Jewell, J.B., Attaran, E., Browse, J., and Howe, G.A. (2016). Control of Carbon Assimilation and Partitioning by Jasmonate: An Accounting of Growth-Defense Tradeoffs. Plants (Basel) **5,** E7.

Herde, M., Koo, A.J., and Howe, G.A. (2013). Elicitation of jasmonate-mediated defense responses by mechanical wounding and insect herbivory. Methods Mol Biol **1011,** 51-61.

Hou, X.L., Lee, L.Y.C., Xia, K.F., Yen, Y.Y., and Yu, H. (2010). DELLAs Modulate Jasmonate Signaling via Competitive Binding to JAZs. Dev Cell **19,** 884-894.

Howe, G.A., and Jander, G. (2008). Plant immunity to insect herbivores. Annual review of plant biology **59,** 41-66.

Howe, G.A., Major, I.T., and Koo, A.J. (2018). Modularity in Jasmonate Signaling for Multistress Resilience. Annual Review of Plant Biology **69,** 387-415.

Huang, D.W., Sherman, B.T., and Lempicki, R.A. (2009). Systematic and integrative analysis of large gene lists using DAVID bioinformatics resources. Nat Protoc **4,** 44-57.

Hummel, I., Pantin, F., Sulpice, R., Piques, M., Rolland, G., Dauzat, M., Christophe, A., Pervent, M., Bouteille, M., Stitt, M., Gibon, Y., and Muller, B. (2010). Arabidopsis Plants Acclimate to Water Deficit at Low Cost through Changes of Carbon Usage: An Integrated Perspective Using Growth, Metabolite, Enzyme, and Gene Expression Analysis. Plant Physiol **154,** 357-372.

Jin, J.P., Tian, F., Yang, D.C., Meng, Y.Q., Kong, L., Luo, J.C., and Gao, G. (2017). PlantTFDB 4.0: toward a central hub for transcription factors and regulatory interactions in plants. Nucleic acids research **45,** D1040-D1045.

Jofuku, K.D., Omidyar, P.K., Gee, Z., and Okamuro, J.K. (2005). Control of seed mass and seed yield by the floral homeotic gene APETALA2. Proceedings of the National Academy of Sciences of the United States of America **102,** 3117-3122.

Kanehisa, M., and Goto, S. (2000). KEGG: kyoto encyclopedia of genes and genomes. Nucleic acids research **28,** 27-30.

Karasov, T.L., Chae, E., Herman, J.J., and Bergelson, J. (2017). Mechanisms to Mitigate the Trade-Off between Growth and Defense. Plant Cell **29,** 666-680.

Katsir, L., Schilmiller, A.L., Staswick, P.E., He, S.Y., and Howe, G.A. (2008). COI1 is a critical component of a receptor for jasmonate and the bacterial virulence factor coronatine. Proceedings of the National Academy of Sciences of the United States of America **105,** 7100-7105.

Kazan, K., and Manners, J.M. (2013). MYC2: The Master in Action. Molecular plant **6,** 686-703.

Kruse, C., Jost, R., Lipschis, M., Kopp, B., Hartmann, M., and Hell, R. (2007). Sulfur-enhanced defence: Effects of sulfur metabolism, nitrogen supply, and pathogen lifestyle. Plant Biology **9,** 608-619.

Li, B., and Dewey, C.N. (2011). RSEM: accurate transcript quantification from RNA-Seq data with or without a reference genome. BMC bioinformatics **12,** 323.

Li, J., Zhang, K., Meng, Y., Hu, J., Ding, M., Bian, J., Yan, M., Han, J., and Zhou, M. (2018). Jasmonic acid/ethylene signaling coordinates hydroxycinnamic acid amides biosynthesis through ORA59 transcription factor. The Plant journal : for cell and molecular biology **95,** 444-457.

Li, R., Wang, M., Wang, Y., Schuman, M.C., Weinhold, A., Schafer, M., Jimenez-Aleman, G.H., Barthel, A., and Baldwin, I.T. (2017). Flower-specific jasmonate signaling regulates constitutive floral defenses in wild tobacco. Proceedings of the National Academy of Sciences of the United States of America **114,** E7205-E7214.

Lorenzo, O., Chico, J.M., Sanchez-Serrano, J.J., and Solano, R. (2004). Jasmonate-insensitive1 encodes a MYC transcription factor essential to discriminate between different jasmonate-regulated defense responses in Arabidopsis. Plant Cell **16,** 1938-1950.

Machado, R.A., Ferrieri, A.P., Robert, C.A., Glauser, G., Kallenbach, M., Baldwin, I.T., and Erb, M. (2013). Leaf-herbivore attack reduces carbon reserves and regrowth from the roots via jasmonate and auxin signaling. New Phytol **200,** 1234-1246.

Machado, R.A.R., Baldwin, I.T., and Erb, M. (2017). Herbivory-induced jasmonates constrain plant sugar accumulation and growth by antagonizing gibberellin signaling and not by promoting secondary metabolite production. New Phytol **215,** 803-812.

Major, I.T., Yoshida, Y., Campos, M.L., Kapali, G., Xin, X.F., Sugimoto, K., de Oliveira Ferreira, D., He, S.Y., and Howe, G.A. (2017). Regulation of growth-defense balance by the JASMONATE ZIM-DOMAIN (JAZ)-MYC transcriptional module. New Phytol **215,** 1533-1547.

Miyashita, Y., and Good, A.G. (2008). NAD(H)-dependent glutamate dehydrogenase is essential for the survival of Arabidopsis thaliana during dark-induced carbon starvation. J Exp Bot **59,** 667-680.

Muller, M., and Munne-Bosch, S. (2015). Ethylene Response Factors: A Key Regulatory Hub in Hormone and Stress Signaling. Plant Physiol **169,** 32-41.

Muroi, A., Ishihara, A., Tanaka, C., Ishizuka, A., Takabayashi, J., Miyoshi, H., and Nishioka, T. (2009). Accumulation of hydroxycinnamic acid amides induced by pathogen infection and identification of agmatine coumaroyltransferase in Arabidopsis thaliana. Planta **230,** 517-527.

Nakano, R.T., Pislewska-Bednarek, M., Yamada, K., Edger, P.P., Miyahara, M., Kondo, M., Bottcher, C., Mori, M., Nishimura, M., Schulze-Lefert, P., Hara-Nishimura, I., and Bednarek, P. (2017). PYK10 myrosinase reveals a functional coordination between endoplasmic reticulum bodies and glucosinolates in Arabidopsis thaliana. The Plant journal : for cell and molecular biology **89,** 204-220.

Oh, Y., Baldwin, I.T., and Galis, I. (2012). NaJAZh Regulates a Subset of Defense Responses against Herbivores and Spontaneous Leaf Necrosis in Nicotiana attenuata Plants. Plant Physiol **159,** 769-788.

Orozco-Cardenas, M.L., Narvaez-Vasquez, J., and Ryan, C.A. (2001). Hydrogen peroxide acts as a second messenger for the induction of defense genes in tomato plants in response to wounding, systemin, and methyl jasmonate. Plant Cell **13,** 179-191.

Pauwels, L., Barbero, G.F., Geerinck, J., Tilleman, S., Grunewald, W., Perez, A.C., Chico, J.M., Vanden Bossche, R., Sewell, J., Gil, E., Garcia-Casado, G., Witters, E., Inze, D., Long, J.A., De Jaeger, G., Solano, R., and Goossens, A. (2010). NINJA connects the co-repressor TOPLESS to jasmonate signalling. Nature **464,** 788-U169.

Pieterse, C.M.J., Leon-Reyes, A., Van der Ent, S., and Van Wees, S.C.M. (2009). Networking by small-molecule hormones in plant immunity. Nature chemical biology **5,** 308-316.

Pre, M., Atallah, M., Champion, A., De Vos, M., Pieterse, C.M.J., and Memelink, J. (2008). The AP2/ERF domain transcription factor ORA59 integrates jasmonic acid and ethylene signals in plant defense. Plant Physiol **147,** 1347-1357.

Qi, T., Huang, H., Song, S., and Xie, D. (2015). Regulation of Jasmonate-Mediated Stamen Development and Seed Production by a bHLH-MYB Complex in Arabidopsis. Plant Cell **27,** 1620-1633.

Roux, F., Gasquez, J., and Reboud, X. (2004). The dominance of the herbicide resistance cost in several Arabidopsis thaliana mutant lines. Genetics **166,** 449-460.

Rowe, H.C., and Kliebenstein, D.J. (2007). Elevated genetic variation within virulence-associated Botrytis cinerea polygalacturonase loci. Molecular Plant-Microbe Interactions **20,** 1126-1137.

Santner, A., Calderon-Villalobos, L.I.A., and Estelle, M. (2009). Plant hormones are versatile chemical regulators of plant growth. Nat Chem Biol **5,** 301-307.

Sasaki-Sekimoto, Y., Taki, N., Obayashi, T., Aono, M., Matsumoto, F., Sakurai, N., Suzuki, H., Hirai, M.Y., Noji, M., Saito, K., Masuda, T., Takamiya, K., Shibata, D., and Ohta, H. (2005). Coordinated activation of metabolic pathways for antioxidants and defence compounds by jasmonates and their roles in stress tolerance in Arabidopsis. Plant Journal **44,** 653-668.

Schweizer, F., Fernandez-Calvo, P., Zander, M., Diez-Diaz, M., Fonseca, S., Glauser, G., Lewsey, M.G., Ecker, J.R., Solano, R., and Reymond, P. (2013). Arabidopsis basic helix-loop-helix transcription factors MYC2, MYC3, and MYC4 regulate glucosinolate biosynthesis, insect performance, and feeding behavior. Plant Cell **25,** 3117-3132.

Shan, X.Y., Wang, J.X., Chua, L.L., Jiang, D.A., Peng, W., and Xie, D.X. (2011). The Role of Arabidopsis Rubisco Activase in Jasmonate-Induced Leaf Senescence. Plant Physiol **155,** 751-764.

Shyu, C., Figueroa, P., DePew, C.L., Cooke, T.F., Sheard, L.B., Moreno, J.E., Katsir, L., Zheng, N., Browse, J., and Howe, G.A. (2012). JAZ8 Lacks a Canonical Degron and Has

an EAR Motif That Mediates Transcriptional Repression of Jasmonate Responses in Arabidopsis. Plant Cell **24,** 536-550.

Smirnova, E., Marquis, V., Poirier, L., Aubert, Y., Zumsteg, J., Menard, R., Miesch, L., and Heitz, T. (2017). Jasmonic Acid Oxidase 2 (JAO2) hydroxylates jasmonic acid and represses basal defense and resistance responses against Botrytis cinerea infection. Mol Plant **10,** 1159-1173.

Smith, A.M., and Stitt, M. (2007). Coordination of carbon supply and plant growth. Plant Cell Environ **30,** 1126-1149.

Solano, R., Stepanova, A., Chao, Q.M., and Ecker, J.R. (1998). Nuclear events in ethylene signaling: a transcriptional cascade mediated by ETHYLENE-INSENSITIVE3 and ETHYLENE-RESPONSE-FACTOR1. Gene Dev **12,** 3703-3714.

Song, S.S., Huang, H., Gao, H., Wang, J.J., Wu, D.W., Liu, X.L., Yang, S.H., Zhai, Q.Z., Li, C.Y., Qi, T.C., and Xie, D.X. (2014). Interaction between MYC2 and ETHYLENE INSENSITIVE3 Modulates Antagonism between Jasmonate and Ethylene Signaling in Arabidopsis. Plant Cell **26,** 263-279.

Sulpice, R., Flis, A., Ivakov, A.A., Apelt, F., Krohn, N., Encke, B., Abel, C., Feil, R., Lunn, J.E., and Stitt, M. (2014). Arabidopsis Coordinates the Diurnal Regulation of Carbon Allocation and Growth across a Wide Range of Photoperiods. Molecular plant **7,** 137-155.

Thimm, O., Blasing, O., Gibon, Y., Nagel, A., Meyer, S., Kruger, P., Selbig, J., Muller, L.A., Rhee, S.Y., and Stitt, M. (2004). MAPMAN: a user-driven tool to display genomics data sets onto diagrams of metabolic pathways and other biological processes. The Plant journal : for cell and molecular biology **37,** 914-939.

Thines, B., Katsir, L., Melotto, M., Niu, Y., Mandaokar, A., Liu, G., Nomura, K., He, S.Y., Howe, G.A., and Browse, J. (2007). JAZ repressor proteins are targets of the SCF(COI1) complex during jasmonate signalling. Nature **448,** 661-665.

Thireault, C., Shyu, C., Yoshida, Y., St Aubin, B., Campos, M.L., and Howe, G.A. (2015). Repression of jasmonate signaling by a non-TIFY JAZ protein in Arabidopsis. The Plant journal : for cell and molecular biology **82,** 669-679.

Tsai, K.J., Lin, C.Y., Ting, C.Y., and Shih, M.C. (2016). Ethylene-Regulated Glutamate Dehydrogenase Fine-Tunes Metabolism during Anoxia-Reoxygenation. Plant Physiol **172,** 1548-1562.

Ueda, J., and Kato, J. (1980). Isolation and Identification of a Senescence-Promoting Substance from Wormwood (Artemisia-Absinthium L). Plant Physiol **66,** 246-249.

Walker, B.J., and Ort, D.R. (2015). Improved method for measuring the apparent CO2 photocompensation point resolves the impact of multiple internal conductances to CO2 to net gas exchange. Plant Cell Environ **38,** 2462-2474.

Wang, K., Guo, Q., Froehlich, J.E., Hersh, H.L., Zienkiewicz, A., Howe, G.A., and Benning, C. (2018). Two Abscisic Acid-Responsive Plastid Lipase Genes Involved in Jasmonic Acid Biosynthesis in Arabidopsis thaliana. Plant Cell **30,** 1006-1022.

Wang, Z., and Benning, C. (2011). Arabidopsis thaliana Polar Glycerolipid Profiling by Thin Layer Chromatography (TLC) Coupled with Gas-Liquid Chromatography (GLC). Journal of visualized experiments **37,** 2518.

Wasternack, C., and Hause, B. (2013). Jasmonates: biosynthesis, perception, signal transduction and action in plant stress response, growth and development. An update to the 2007 review in Annals of Botany. Ann Bot-London **111,** 1021-1058.

Weraduwagel, S.M., Chen, J., Anozie, F.C., Morales, A., Weise, S.E., and Sharkey, T.D. (2015). The relationship between leaf area growth and biomass accumulation in Arabidopsis thaliana. Frontiers in plant science **6**.

Wisniewski, J.R., Zougman, A., Nagaraj, N., and Mann, M. (2009). Universal sample preparation method for proteome analysis. Nat Methods **6,** 359-362.

Wu, J.Q., and Baldwin, I.T. (2010). New Insights into Plant Responses to the Attack from Insect Herbivores. Annu Rev Genet **44,** 1-24.

Yamada, K., Hara-Nishimura, I., and Nishimura, M. (2011). Unique Defense Strategy by the Endoplasmic Reticulum Body in Plants. Plant Cell Physiol **52,** 2039-2049.

Yan, J.B., Yao, R.F., Chen, L., Li, S.H., Gu, M., Nan, F.J., and Xie, D.X. (2018). Dynamic Perception of Jasmonates by the F-Box Protein COI1. Molecular plant **11,** 1237-1247.

Yan, Y.X., Stolz, S., Chetelat, A., Reymond, P., Pagni, M., Dubugnon, L., and Farmer, E.E. (2007). A downstream mediator in the growth repression limb of the jasmonate pathway. Plant Cell **19,** 2470-2483.

Yang, D.L., Yao, J., Mei, C.S., Tong, X.H., Zeng, L.J., Li, Q., Xiao, L.T., Sun, T.P., Li, J.G., Deng, X.W., Lee, C.M., Thomashow, M.F., Yang, Y.N., He, Z.H., and He, S.Y. (2012). Plant hormone jasmonate prioritizes defense over growth by interfering with gibberellin signaling cascade. Proceedings of the National Academy of Sciences of the United States of America **109,** E1192-E1200.

Yatusevich, R., Mugford, S.G., Matthewman, C., Gigolashvili, T., Frerigmann, H., Delaney, S., Koprivova, A., Flugge, U.I., and Kopriva, S. (2010). Genes of primary sulfate assimilation are part of the glucosinolate biosynthetic network in Arabidopsis thaliana. Plant J **62,** 1-11.

Yoshida, Y., Sano, R., Wada, T., Takabayashi, J., and Okada, K. (2009). Jasmonic acid control of GLABRA3 links inducible defense and trichome patterning in Arabidopsis. Development **136,** 1039-1048.

Zhang, F., Yao, J., Ke, J., Zhang, L., Lam, V.Q., Xin, X.F., Zhou, X.E., Chen, J., Brunzelle, J., Griffin, P.R., Zhou, M., Xu, H.E., Melcher, K., and He, S.Y. (2015). Structural basis of JAZ repression of MYC transcription factors in jasmonate signalling. Nature **525,** 269-273.

Zhang, Y., and Turner, J.G. (2008). Wound-Induced Endogenous Jasmonates Stunt Plant Growth by Inhibiting Mitosis. Plos One **3,** e3699.

Zhu, Z.Q., An, F.Y., Feng, Y., Li, P.P., Xue, L., Mu, A., Jiang, Z.Q., Kim, J.M., To, T.K., Li, W., Zhang, X.Y., Yu, Q., Dong, Z., Chen, W.Q., Seki, M., Zhou, J.M., and Guo, H.W. (2011). Derepression of ethylene-stabilized transcription factors (EIN3/EIL1) mediates jasmonate and ethylene signaling synergy in Arabidopsis. Proceedings of the National Academy of Sciences of the United States of America **108,** 12539-12544.

Zust, T., and Agrawal, A.A. (2017). Trade-Offs Between Plant Growth and Defense Against Insect Herbivory: An Emerging Mechanistic Synthesis. Annual review of plant biology **68,** 10.11-10.22.

CHAPTER THREE - MYC TRANSCRIPTION FACTORS PLAY OVERLAPPING AND DISTINCT ROLES IN REGULATING GROWTH-DEFENSE TRADEOFFS IN ARABIDOPSIS

Contributions:

The *jazD myc* mutants (*jazD myc2*, *jazD myc3*, *jazD myc4*, *jazD myc23*, *jazD myc24*, *jazD myc34*, and *jazD myc234*) utilized in this chapter were developed by Dr. Ian T. Major and George Kapali. Dr. Ian T. Major performed respiration measurements.

Abstract

Innate immune responses triggered by the plant hormone jasmonate (JA) are often accompanied by constrained growth. MYC2 and two closely related proteins, MYC3 and MYC4, are among the best characterized transcription factors (TFs) involved in executing JA-mediated growth and defense responses. However, an understanding of the specific contributions of MYC2/3/4 in growth and defense processes remains unclear. Here, we combined a *jaz* decuple mutant (*jaz1 jaz2 jaz3 jaz4 jaz5 jaz6 jaz7 jaz9 jaz10 jaz13*; *jazD*) with *myc* single (*myc2*, *myc3*, and *myc4*), double (*myc23*, *myc24*, and *myc34*) and triple (*myc234*) mutants to investigate the overlapping and distinct impacts of MYC2/3/4 on plant growth, defense, and metabolism. We demonstrate that simultaneous loss of MYC2/3/4 completely or partially abolishes constitutive JA signaling phenotypes of *jazD*, including hypersensitivity to JA, growth stunting, and decreased fecundity. Among the three MYCs, MYC2 was the most prominent regulator of *jazD* sensitivity to JA, whereas MYC2 and MYC3 played essential roles in restricting biomass accumulation. Comparison of *jazD* and *jazD myc* mutants showed that the enhanced resistance of *jazD* to insect herbivores and necrotrophic pathogens require MYC TFs, and MYC3 was primarily responsible for the resistance of *jazD* to necrotrophic pathogens. The heightened defense of *jazD* was associated with overaccumulation of an endoplasmic reticulum (ER)-derived structure called the ER body, which contains a myriad of β-glucosidases that exhibit myrosinase activity. Further analysis showed that the biogenesis of ER bodies is dependent on MYC TFs, with MYC2 and MYC3 having a main role. In demonstrating that MYC TFs are a major target of the JAZ-repressible transcriptional hierarchy, our study establishes a central role for MYC TFs in the control of growth-defense balance.

Introduction

Plants continuously integrate stress and other environmental cues to tailor their growth, development and metabolism. Coordination of plant responses to stress signals is largely dependent on the biosynthesis and action of various hormones (Pieterse et al., 2009; Santner et al., 2009). Among the hormones that control plant protection against biotic challengers is jasmonate (JA), a member of the larger group of oxylipin compounds derived from oxygenated lipids (Wasternack and Hause, 2013; Howe et al., 2018). The bioactive form JA, jasmonoyl-L-isoleucine (JA-Ile), controls transcriptional programs that modulate diverse chemical and morphological defense traits (Howe and Jander, 2008; Wu and Baldwin, 2010; Campos et al., 2014). JA-Ile-induced transcriptional reprogramming also retards plant growth and impairs reproduction (Yan et al., 2007; Zhang and Turner, 2008; Guo et al., 2018b). In the past decade, tremendous progress has been made in identifying the key components that connect JA-Ile perception with transcriptional outputs (Howe et al., 2018), as well as the multiple roles of JA in growth, development, and immunity (Campos et al., 2014; Huot et al., 2014; Havko et al., 2016; Guo et al., 2018a). However, little is known about the mechanisms by which JA signaling integrates growth and defense responses to optimize fitness in changing environmental conditions.

The core JA signaling pathway involves JAZ transcriptional repressor proteins that block JA responses by inhibiting the activity of JA-responsive transcription factors (TFs) (Figure 3.2A) (Chini et al., 2007; Thines et al., 2007; Yan et al., 2007). When endogenous JA-Ile levels are below a certain threshold concentration, JAZ proteins interact with various TFs, the most thoroughly studied of which are MYC2 and its homologs MYC3 and MYC4 (Figure 3.2A) (Dombrecht et al., 2007; Fernandez-Calvo et al., 2011; Figueroa and Browse, 2015; Qi et al., 2015a). JAZ proteins inhibit MYC activity by recruiting the co-repressor TOPLESS (TPL), either through direct JAZ-

TPL interaction or indirectly via the NOVEL INTERACTOR OF JAZ (NINJA) adaptor protein (Pauwels et al., 2010; Shyu et al., 2012). In addition, binding of JAZ to MYC TFs prevents the association of MYC with the coactivator MED25 (Zhang et al., 2015; An et al., 2017; Howe et al., 2018). Upon the accumulation of JA-Ile, JAZ proteins associate with the CORONATINE INSENSITIVE 1 (COI1)-containing Skp1/Cullin/F-box (SCF^{COI1}) E3 ubiquitin ligase complex in a hormone-dependent manner, leading to JAZ ubiquitylation and degradation by the 26S proteasome (Figure 3.2A) (Xie et al., 1998; Chini et al., 2007; Thines et al., 2007; Katsir et al., 2008). Destruction of JAZ proteins in response to the JA-Ile signal thereby relieves the transcriptional repression on MYC and other TFs, such as EIN3 (Zhu et al., 2011), MYB (Qi et al., 2011; Song et al., 2011), and WRKY (Jiang et al., 2014) family TFs. JAZ proteins belong to the TIFY protein family. The C terminus of all JAZ proteins contains a Jas motif, which can be used to distinguish JAZ from other TIFY family members (Bai et al., 2011). Although there are 13 *JAZ* genes in the Arabidopsis genome, the number of *JAZ* genes in land plants is highly variable. The liverwort *Marchantia polymorpha* contains a single *JAZ* gene, whereas many higher plant species have more than 20 *JAZ* genes (Bai et al., 2011; Howe et al., 2018).

Many JA-induced defense responses depend on MYC2, MYC3, and MYC4, which belong to subclade IIIe of the basic helix-loop-helix (bHLH) superfamily of TFs (Heim et al., 2003) and exhibit overlapping and conserved functions (Figure 3.2A). These three TFs promote the expression of chemical defense traits that confer resistance to insect herbivores. For example, *myc2/3/4* triple mutants of Arabidopsis that lack these three TFs are deficient in the production of glucosinolates (Schweizer et al., 2013; Major et al., 2017), which are a prominent class of anti-insect compounds in the *Brassicales* order (Howe and Jander, 2008; Bednarek et al., 2009; Hopkins et al., 2009). Chromatin-immuno precipitation (ChIP) experiments have established that

at least some glucosinolate biosynthetic genes are direct targets of MYC2 (Schweizer et al., 2013). Consistent with their roles in promoting metabolic defense pathways, feeding assays performed with *myc* single (*myc2*, *myc3*, and *myc4*), double (*myc23*, *myc24* and *myc34*) and triple (*myc234*) mutants showed that all three MYCs participate in resistance to non-adapted insect herbivores (e.g., *Spodoptera littoralis*), although MYC3 and MYC4 display stronger roles than MYC2 (Fernandez-Calvo et al., 2011). In addition to insect herbivores, MYC2, MYC3, and MYC4 are also involved in JA-dependent defense against necrotrophic pathogens, such as *Botrytis cinerea* (*B. cinerea*). Unlike anti-insect resistance, MYC2/3/4 perform distinct roles in regulating anti-fungal resistance. *myc2* is more resistant to *B. cinerea* (Lorenzo et al., 2004), whereas *myc234* is more susceptible to this pathogen (Chico et al., 2014). Thus, it is a question that which MYC plays a positive role in defending this fungal pathogen. In addition to their role as positive regulators of defense responses, MYC TFs exert negative control over growth. For example, *mycT* plants (defective in MYC2, MYC3, and MYC4) accumulate more biomass than WT plants, suggesting that one or more of these three JA-inducible TFs negatively regulate leaf growth (Major et al., 2017). However, the specific role of MYC2/3/4 in mediating growth traits remains unclear.

Glucosinolates are spatially sequestered from activating myrosinase enzymes, which belong to the larger family of β-glucosidases (Wittstock and Burow, 2010). Disruption of plant tissues during insect chewing and other forms of biotic challenge allow myrosinases to mix with their glucosinolate substrates, thereby producing toxic thiocyanates, isothiocyanates, and nitriles (Bones and Rossiter, 2006). Recently, Nakano *et al.* reported that a β-glucosidase called PYK10/BGLU23, which is the major component of the endoplasmic reticulum (ER) body (Matsushima et al 2003), possesses myrosinase activity (Nakano et al., 2017). ER bodies are constitutively formed in epidermal cells of cotyledons, hypocotyls, and roots of Arabidopsis

seedlings, but are absent in rosette leaves under normal growth conditions (Matsushima et al., 2002; Ogasawara et al., 2009). In response to stress signals such as wounding and JA treatment, however, inducible-type ER bodies proliferate in mature leaves (Matsushima et al., 2002), suggesting that ER bodies are a component of the plant's induced defense responses. However, the signal transduction pathway that links wound-induced JA biosynthesis to ER body formation remains unknown.

Here, we employed a genetic approach to interrogate how JA-inducible MYC2/3/4 impact growth-defense balance. Our study took advantage of a *jaz* decuple (*jazD*) mutant that harbors mutations in ten *JAZ* genes (*JAZ1/2/3/4/5/6/7/9/10/13*), and exhibits strong constitutive JA responses and various JA-induced growth and defense phenotypes (Guo et al., 2018b). We introduced *myc* single (*myc2*, *myc3*, and *myc4*), double (*myc23*, *myc24* and *myc34*) and triple (*myc234* or *mycT*) mutations into *jazD*. Detailed comparison between *jazD* and the *jazD myc* mutants showed that the increased sensitivity of *jazD* to JA is mainly mediated by MYC2, whereas MYC2 and MYC3 but not MYC4 partially accounted for stunted leaf growth of *jazD*. Further analyses suggest that the growth restriction of *jazD* does not involve the antagonistic interaction between JAZ and DELLA proteins, but rather is directly linked to the activity of MYC TFs. MYCs stimulate defense responses by promoting secondary metabolism, including the biosynthesis of secondary metabolites, as well as the production of ER bodies. Among the three MYCs, MYC3 appears to play a main role in governing *jazD* resistance to *B. cinerea*. Comparison of the transcript and protein levels of ER body components in *jazD* and *jazD myc* mutants indicate that MYC2 and MYC3 play stronger roles than MYC4 in inducing ER body components. In addition to leaf growth, the increased production of defense compounds triggered by MYC TFs is also associated with curtailed reproduction of *jazD* plants. Our collective data suggest that MYC TFs restrain leaf

growth and reproduction by reprograming of plant metabolism to defense pathways, and that MYC2, MYC3, and MYC4 perform overlapping and distinct roles in mediating growth-defense tradeoffs.

Results

JA hypersensitivity of *jazD* roots mainly depends on MYC2

To dissect the biological roles of individual MYC TFs in mediating JA-inducible responses in Arabidopsis, we constructed a series of *jazD myc* mutants using T-DNA and transposon insertion mutations (Table 3.1 and 3.2; Figure 3.1).The previously described *jazD* mutant carries mutations in ten members (*JAZ1/2/3/4/5/6/7/9/10/13*) of the *JAZ* gene family (Guo et al., 2018b). Various combinations of *myc2*, *myc3*, and *myc4* were introduced into *jazD* by genetic crosses between *jazD* and a previously constructed *jaz myc* octuple mutant (*jazQ mycT*) (Major et al., 2017) harboring mutations in five *JAZ* (*JAZ1/3/4/9/10*) and three *MYC* (*MYC2/3/4*) genes (Figure 3.2A) (see Methods). The resulting undecuple (*jazD myc2*, *jazD myc3*, and *jazD myc4*), duodecuple (*jazD myc23*, *jazD myc24*, and *jazD myc34*), and treducuple (*jazD myc234*; referred to as *jazD mycT*) mutants were initially used to assess the role of MYC2/3/4 in the extreme sensitivity of *jazD* to exogenous JA. Root growth assays performed on JA-free medium showed that *jazD* roots were constitutively shorter than WT Col-0 (WT), whereas the root length of *mycT* seedlings was indistinguishable from WT seedlings (Figure 3.2B; Table 3.3). All *jazD myc* mutant combinations retained the constitutive short root of *jazD* (Figure 3.2B; Table 3.3), consistent with the idea that this trait is expressed independently of the canonical JA signaling pathway (Major et al., 2017). Assays performed on media supplemented with JA showed that *mycT* seedlings have reduced sensitivity to JA in comparison to WT (Figure 3.2B; Table 3.3). The JA sensitivity of *jazD myc3*, *jazD myc4* and *jazD myc34* was similar to *jazD*, indicating that MYC3 and MYC4 do not promote root growth sensitivity to the hormone in the presence of MYC2. The *myc2* mutation alone significantly reduced the heightened sensitivity of *jazD* to JA, which was further reduced in mutant combinations that combined *myc3* and/or *myc4* with *myc2* (Figure 3.2B; Table 3.3). These results

suggest that MYC2 plays a major role in mediating the JA hypersensitivity of *jazD* roots but that MYC3 and MYC4 can also contribute to the phenotype in the absence of MYC2.

Shoot responses to JA were evaluated by treatment of fully-expanded leaves with coronatine (COR), which is a structural and functional mimic of JA-Ile. As previously reported (Guo et al., 2018b), anthocyanin accumulation was observed in WT leaves within four days of COR treatment (Figure 3.3A). Compared to WT, COR-treated *mycT* leaves showed little if any symptoms of anthocyanin accumulation (Figure 3.3A). *jazD* leaves displayed chlorosis within two days (Figure 3.4A), and within four days of COR application necrosis-like symptoms spread throughout the treated leaves in a manner that was largely dependent on light (Figure 3.3A, 3.4A and 3.4B). Consistent with a critical role for MYC2/3/4 in mediating JA-induced chlorosis, COR-treated *jazD mycT* leaves did not exhibit chlorosis or necrosis-like symptoms (Figure 3.3A). To further investigate the distinct roles of MYC2/3/4 in mediating the hypersensitivity of *jazD* leaves to COR, we applied COR to *jazD myc2*, *jazD myc3*, and *jazD myc4* undecuple mutants as well as *jazD myc23*, *jazD myc24*, and *jazD myc34* duodecuple mutants. The results showed that COR-induced chlorosis of *jazD* leaves is greatly alleviated by *myc2* and partially relieved by *myc3*, whereas *myc4* appeared to have little or no effect on COR-triggered chlorosis (Figure 3.3A). Similar to *jazD mycT*, *jazD myc23* leaves did not display visible signs of chlorosis (Figure 3.3A). COR-induced chlorosis was observed on *jazD myc24* leaves, and was further intensified on *jazD myc34* leaves (Figure 3.3A). These findings suggest that MYC2 makes the major contribution to COR-induced leaf chlorosis and that MYC3 also plays a discernable role, with little if any role attributed to MYC4. These conclusions based on qualitative analysis of visible symptoms were validated by quantitative measurements of leaf chlorophyll in mock- and COR-treated plants (Figure 3.3B; Table 3.4).

MYC2 and MYC3 partially contribute to restricted growth of *jazD*

We next determined whether MYC2/3/4 are involved in suppressing shoot growth of *jazD* by comparing soil-grown WT Col-0 (WT), *mycT*, *jazD*, and *jazD mycT* plants with respect to various leaf growth traits, including shoot biomass, projected leaf area, and rosette diameter. Loss of MYC2/3/4 in *mycT* resulted in moderate (but not statistically significant) increases in leaf growth parameters relative to WT (Figure 3.5), as previously reported (Major et al., 2017). *mycT* partially restored the growth phenotype of *jazD* rosettes, such that the size and weight of *jazD mycT* leaves were intermediate between WT and *jazD* (Figure 3.5). To assess the relative contribution of MYC2/3/4 to growth inhibition, we measured the biomass and projected leaf area of WT, *mycT*, *jazD*, *jazD myc* undecuple mutants, and *jazD mycT*. *jazD myc2* and *jazD myc3* showed increased growth compared to *jazD*, whereas *jazD myc4* plants were indistinguishable from *jazD* (Figure 3.6). Furthermore, the biomass of *jazD myc2* was slightly greater than *jazD myc3* (Figure 3.6A). These data provide evidence that MYC2 and MYC3 both contribute to leaf growth restriction of *jazD*, whereas MYC4 does not.

In addition to MYC TFs (Zhang and Turner, 2008; Major et al., 2017), among the regulatory factors implicated in JA-mediated growth repression are DELLA repressors in the GA response pathway (Yang et al., 2012; Huot et al., 2014). It has been reported that JAZ proteins antagonistically interact with DELLA proteins (Figure 3.7A), and that treatment of Arabidopsis seedlings with MeJA increases the level of a DELLA protein RGA (Yang et al., 2012). Thus, removal of JAZ proteins in higher-order *jaz* mutants may increase the level of DELLA proteins, which suppress elongation growth by restraining the activity of PHYTOCHROME-INTERACTING FACTOR (PIF) TFs (Figure 3.7A). To test this hypothesis, WT, *jazQ*, and *jazD* seedlings were grown on medium supplemented with different concentrations of GA, which

triggers the degradation of DELLAs. The results showed that GA promoted hypocotyl elongation of all three genotypes to a similar extent (Figure 3.7B; two-way ANOVA analysis). Western blot analysis of RGA protein levels showed that WT, *jazQ*, and *jazD* leaves accumulated comparable levels of RGA protein (Figure 3.7C). These findings suggest that growth restriction of *jazD* is unlikely ascribed to increased DELLA protein levels.

MYC2/3/4 are required for the overaccumulation of defense compounds in *jazD*

To assess whether the elevation of Trp flux mediated by MYC TFs gives rise to increased production of IGs, we compared the level of glucosinolates in leaves of 23-day-old WT, *mycT*, *jazD*, and *jazD mycT* plants. Our data showed that the levels of most aliphatic glucosinolates did not differ between WT and *jazD* leaves (Figure 3.8A). However, *jazD* leaves accumulated much higher levels of indole glucosinolates, including I3M, OH-I3M, 4MOI3M, and 1MOI3M (Figure 3.8A). *mycT* mutation clearly compromised IGs production in *jazD*, such that the levels of these compounds in *jazD mycT* were similar to WT (Figure 3.8A). In addition to glucosinolates, the *mycT* mutation weakly but consistently reduced the basal level of anthocyanin accumulation in WT leaves, although this difference was not statistically significant ($P = 0.78$, Figure 3.8B). The anthocyanin content in *jazD mycT* leaves was intermediate between WT and *jazD* (Figure 3.8B), consistent with the notion that TFs in addition to MYC2/3/4 promote anthocyanin production in response to JA (Qi et al., 2011; Major et al., 2017). These collective data demonstrate a key role for MYC2/3/4 in activation of specialized metabolism in response to depletion of JAZ repressors.

Constitutive formation of ER bodies in *jazD* is dependent on MYC TFs

ER bodies are repositories for several myrosinase enzymes involved in the breakdown of glucosinolates into toxic defense compounds (Nakano et al., 2014). The elevated expression of ER

body-associated mRNAs and proteins in *jazD* (Guo et al., 2018b) suggested that ER body structures, which in WT leaves are induced in response to wounding and JA treatment (Matsushima et al., 2002), might constitutively proliferate in *jazD* leaves. To address this question, we used Agrobacterium-mediated transformation to express an ER-localized yellow fluorescent protein (ER-YFP) (Nelson et al., 2007) in either a WT or *jazD* genetic background. Confocal imaging of *jazD* leaves expressing the ER-YFP marker revealed the constitutive presence of rod-shaped structures having size dimensions of typical ER bodies (Figure 3.9A and 3.9B) (Matsushima et al., 2003b; Nakano et al., 2014). That these structures were not observed in ER-YFP-expressing WT leaves (Figure 3.9A) indicate that JAZ proteins negatively regulate the wound- and JA-induced formation of ER bodies.

We next used *jaz myc* polymutants to determine whether the induction of the ER body genes in *jazD* leaves is mediated by MYC TFs. Quantitative real-time PCR (qRT-PCR) was used to measure the accumulation of *BGLU18* and *TSA1* transcripts that encode proteins residing in inducible ER bodies (Ogasawara et al., 2009; Yamada et al., 2009; Nakano et al., 2014; Geem et al., 2018), as well as *NAI1*, *NAI2* and *PYK10* mRNAs that encode components associated with constitutive ER bodies (Matsushima et al., 2003a; Matsushima et al., 2004; Yamada et al., 2008; Nakano et al., 2014). The results showed that *mycT* had only a modest negative effect on *BGLU18* and *TSA1* transcript levels in comparison WT (Figure 3.9C). Strikingly, however, the *mycT* mutation eliminated the elevated expression of these genes in the *jazD* genetic background (Figure 3.9C). In contrast to the strong dependence in *jazD* of *BGLU18* and *TSA1* expression on MYC2/3/4, the basal expression of *NAI1*, *NAI2* and *PYK10* in WT leaves was not affected by *mycT* (Figure 3.9C). Moreover, *mycT* only partially reduced the accumulation of these marker genes in the *jazD* background (Figure 3.9C).

The results obtained from qRT-PCR experiments were validated by SDS-PAGE analyses showing that *jazD* leaves hyperaccumulate myrosinases known to reside in ER bodies. Specifically, we found that *jazD* accumulates a ~60-kD polypeptide that is largely absent in leaf protein from WT, *mycT*, and *jazD mycT* plants (Figure 3.9D). Mass-spectrometry (MS) analysis identified the BGLU18 myrosinase as the major protein component of the ~60 kD band, with lower levels (based on spectral counts) of the PKY10 myrosinase also detected (Table 3.5). BGLU18 and PYK10 have previously been identified as abundant resident proteins in inducible and constitutive ER bodies, respectively (Matsushima et al., 2003a; Ogasawara et al., 2009). Using SDS-PAGE as a semi-quantitative measure of protein abundance, we tested *jaz myc* polymutants for the presence of these ER body myrosinases. The results showed that the 60-kD protein accumulated in *jazD* but not in WT, *mycT*, or *jazD mycT* leaves (Figure 3.9D). In support of these data, confocal microscopy of *jazD mycT* plants stably expressing the ER-YFP marker showed that the proliferation of ER bodies in *jazD* is largely dependent on MYC2/3/4 (Figure 3.9A). Collectively, these data indicate that MYC2/3/4 positively regulate the induction of ER body genes and proteins, as well as the formation of ER body structures.

We then assessed the contribution of MYC2, MYC3, and MYC4 to the expression of ER body genes. The relative transcript levels of *BGLU18, TSA1*, *NAI1*, *NAI2*, and *PYK10* in rosette leaves of *jazD myc* undecuple and duodecuple mutants were quantified by qRT-PCR. As shown in Figure 3.10A, the expression of ER body genes in these mutants was either similar to *jazD* or intermediate between *jazD* and *jazD mycT* (Figure 3.10A). Among the *jaz myc* polymutants tested, *jazD myc23* displayed the greatest reduction of ER body transcripts compared to *jazD* (Figure 3.10A). SDS-PAGE analysis of leaf protein extracts confirmed that the *jazD myc23* mutant combination had the greatest effect on reducing the abundance of the 60-kD band corresponding

to the BGLU18/PYK10 myrosinases (Figure 3.10B). Taken together, our results indicate that MYC2/3/4 additively activate ER body genes, and that MYC2 and MYC3 appear to exert a stronger positive control on ER body components.

Control of cellular respiration by the JAZ-MYC transcriptional module

The increased production of plant defense compounds is often associated with elevated cellular respiration, which is required to generate the metabolic precursors of defense compounds (Bolton, 2009). Consistent with this notion, both day and night respiration rates in *jazD* leaves were significantly increased compared to WT (Figure 3.11), in agreement with previous results (Guo et al., 2018b). Analysis of the *jazD mycT* polymutant showed that the stimulatory effect of *jazD* on day and night respiration rates was largely reduced in the absence of MYC2/3/4 (Figure 3.11). Moreover, control experiments showed that *mycT* mutant alone had little or no effect on respiration (Figure 3.11). These findings demonstrate that metabolic defenses controlled by the JAZ-MYC transcriptional module are linked to changes in cellular respiration.

MYC TFs are required for resistance of *jazD* to chewing insects and necrotrophic pathogens

The ability of the *mycT* triple mutation to eliminate the accumulation of defense-related glucosinolates and associated ER body structures in *jazD* suggests that MYC2/3/4 TFs are also important for the previously reported resistance of *jazD* plants to chewing insects and necrotrophic pathogens (Guo et al., 2018b). To test this hypothesis, we compared the resistance of WT, *mycT*, *jazD*, and *jazD mycT* plants to insect challenge. Bioassays performed with neonate cabbage looper (*Trichoplusia ni*) larvae showed that the hyper-resistance of *jazD* to this generalist insect was strictly dependent on MYC2/3/4 (Figure 3.12A and 3.12B). The larval weight gain on both *mycT* and *jazD mycT* plants was significantly greater than that on WT plants (Figure 3.12A and 3.12B),

highlighting the importance of MYC TFs in anti-insect resistance. These results also indicate that MYC2/3/4 activity is epistatic to JAZ, consistent with current models of JA signaling in which JAZ proteins repress the activity of MYC TFs.

We also investigated the response of *jaz myc* polymutants to infection by the necrotrophic fungal pathogen *Botrytis cinerea* (*B. cinerea*). Consistent with previous reports, *mycT* leaves were more susceptible to *B. cinerea* than WT (Figure 3.12C and 3.12D) (Chico et al., 2014), whereas *jazD* leaves were highly resistant to the pathogen (Figure 3.12C and 3.12D) (Guo et al., 2018b). Lesion area on *jazD myc2* and *jazD myc4* leaves was comparable to that on *jazD* leaves (Figure 3.12C and 3.12D). However, the robust resistance of *jazD* leaves was partially compromised in *jazD myc3* and *jazD mycT* leaves (Figure 3.12C and 3.12D). These data suggest that MYC3 performs a more important function than MYC2 and MYC4 in promoting the high level of resistance of *jazD* to *B. cinerea*.

Derepression of MYC TFs in *jazD* compromises reproductive fitness

Induced defense responses are often associated with decreased seed quality and yield (Agrawal, 1998; Baldwin, 1998). We previously reported that seed production in *jazD* plants is less than half of that in WT on a per plant basis, and that the size and quality of *jazD* seeds is reduced as well (Guo et al., 2018b). To test whether MYC TFs contribute to this apparent tradeoff between defense and reproductive output, we compared the fecundity of WT and *jazD* plants to that of *mycT* and *jazD mycT* plants. Whereas *jazD* plants produced far fewer seeds than WT as previously observed (Guo et al., 2018b), the seed yield of *mycT* and *jazD mycT* plants grown under identical conditions was comparable to WT (Figure 3.13A). We also found that *mycT* was epistatic to *jazD* with respect

to seed size, silique length, and seed number per fruit (Figure 3.13B-D). Thus, the decreased fertility of *jazD* can be largely attributed to the activity of MYC2/3/4 TFs.

Discussion

A key innovation of our study was the development of a series of *jazD myc* mutants, including *jazD myc2*, *jazD myc3*, and *jazD myc4* undecuple, *jazD myc23*, *jazD myc24*, and *jazD myc34* duodecuple, as well as the *jazD mycT* tredecuple mutants, which allowed us to dissect specific functions of MYC2/3/4. Our results suggest that MYC2 is the major MYC TF that determines root sensitivity of *jazD* to exogenous JA, which is consistent with previous findings showing that MYC2 performs a dominant role in root responses to JA (Fernandez-Calvo et al., 2011; Niu et al., 2011). Sub-functionalization of MYC isoforms may reflect differences in the spatiotemporal accumulation pattern of MYC2/3/4 (Chini et al., 2016). For example, *MYC2* is expressed in most cell types of the root, whereas the expression of *MYC3* (elongation and maturation zones) and *MYC4* (root cap) is limited to certain regions of the root (Gasperini et al., 2015). In contrast to roots, it is unclear why MYC2 is the principle regulator of *jazD* shoot sensitivity to COR. It has been reported that JA-mediated leaf senescence and chlorophyll degradation is attenuated by *myc2* but not by *myc3* or *myc4* (Qi et al., 2015b), suggesting that MYC2 plays a critical role in regulating JA-induced senescence. It is thus plausible that MYC2 promotes the expression of genes involved in senescence and chlorophyll depletion in COR-treated *jazD* leaves. Another possible explanation for the necrosis-like symptoms of COR-treated *jazD* is that overaccumulation of indole glucosinolates or other defense compounds exerts autotoxic effects in the leaf (Chen et al., 2017). Results from the current and previous studies (Schweizer et al., 2013) have shown that MYC TFs perform essential roles in indole glucosinolate biosynthesis. However, whether MYC2 is the major activator of the biosynthesis of indole glcuosinolates or other defense compounds in *jazD* remains to be assessed. The unique role of MYC3 in controlling *jazD* resistance to *B. cinerea* agrees with previous studies showing that MYC3 promotes the expression of *PDF* genes (Niu et al., 2011),

which encode anti-fungal peptides (Penninckx et al., 1996). This interpretation is also consistent with previous studies showing that MYC2 and MYC4 negatively regulate *PDF* expression (Boter et al., 2004; Lorenzo et al., 2004; Niu et al., 2011). MYC3 may also confer fungal resistance by specifically inducing the biosynthesis of other anti-fungal compounds, such as hydroxycinnamic acid amides (HCAAs) (Muroi et al., 2009) and camalexin (Khare et al., 2017). Additional work, however, is needed to address this hypothesis.

Our previous studies suggested that the strong defense sink in *jazD* is associated with changes in carbon sensing and metabolism, which may link to restricted leaf growth of *jazD* (Guo et al., 2018b). In this study, we show that *myc* mutations concomitantly reduce resource allocation to metabolic defense and partially restore the slow growth of *jazD*. These data support the conclusion that the growth inhibitory effect of JA is obligately linked through MYC TFs to increase investment of resources in defense, as previously observed in a study of the relationship between MYC TFs and *jazQ* (Major et al., 2017). Recent studies suggest that MYCs may also inhibit growth directly by blocking the expression of genes involved in cell division or cell expansion (Pauwels et al., 2008; Zhang and Turner, 2008; Noir et al., 2013). In roots, MYC2 binds directly to and inhibits the promoter activity of genes encoding PLETHORA (PLT) TFs, which regulate auxin-induced root stem cell niche maintenance (Chen et al., 2011). It is thus conceivable that MYCs perform similar roles in leaf tissues as well. MYC2 has also been shown to hamper the activity of PIFs (Zhang et al., 2018), which are positive regulators of elongation growth (de Lucas and Prat, 2014; Leivar and Monte, 2014) and auxin responses (Nozue et al., 2011; Hornitschek et al., 2012). In addition to leaf growth, our data also demonstrate that activation of MYC TFs in response to JAZ depletion by *jazD* curtails reproductive output (Figure 3.13). Many studies have shown that induction of defense responses impedes reproductive fitness (Agrawal, 1998; Baldwin,

1998) but the underlying reasons remain largely unknown. It is conceivable that MYC TF-regulated production of defense metabolites reduces the amount assimilated carbon and other nutrients available for seed production. Alternatively, MYC TFs may impede fertility directly by targeting genes involved in seed development. Seed storage proteins and triacylglycerols (TAGs) account for approximate 40% of the seed weight (Baud et al., 2002). It has been reported that MYC2/3/4 redundantly inhibit Arabidopsis seed mass by constraining the production of seed storage proteins (Gao et al., 2016). It was proposed that MYC TFs adjust the content of seed storage proteins by modulating the expression seed storage protein biosynthetic genes (Gao et al., 2016). Whether MYC TFs directly control the expression of genes involved in TAG biosynthesis remains to be determined.

The stunted growth of *jazQ* was completely recovered upon disruption of MYC2/3/4 activity in a *jazQ mycT* mutant (Major et al., 2017). In contrast, we report here that *mycT* mutation does not fully restore the slow growth phenotype of *jazD* (Figure 3.5 and 3.6). Given that GA treatment failed to recover *jazD* growth and that the level of the RGA DELLA protein was not elevated in *jazD* leaves (Figure 3.7), the incomplete growth recovery of *jazD mycT* mutant cannot likely be ascribed to increased activity of DELLA proteins. The incomplete recovery of *jazD mycT* may also be attributed to MYC5, which belongs to the same subfamily of bHLH TFs as MYC2, MYC3, and MYC4 (Figueroa and Browse, 2015; Qi et al., 2015a). It has been reported that *mycT* (*myc2 myc3 myc4*) and a *myc2 myc3 myc4 myc5* quadruple (*mycQ*) mutant showed no difference in petiole length and leaf number (Major et al., 2017), indicating that MYC5 performs negligible roles in leaf growth in an otherwise wild-type genetic background. Additional studies are needed to test the possibility that MYC5 participates in restricting leaf biomass in the *jazD* genetic background.

Another interpretation for partial growth recovery of *jazD mycT* mutants is that other regulators in addition to MYCs contribute to the production of defense compounds in *jazD*. Although it is well established that MYC TFs promote the accumulation of anthocyanin (Niu et al., 2011), it is increasingly recognized that the biosynthesis of these compounds is controlled by a complex network of TFs. For instance, the WD-repeat/bHLH/MYB transcriptional complex, consisting of the WD-repeat protein TRANSPARENT TESTA GLABRA 1 (TTG1), bHLH TFs TRANSPARENT TESTA 8 (TT8), GLABRA 3 (GL3) or ENHANCER OF GLABRA 3 (EGL3), and R2R3 MYB transcription factors MYB75, MYB90, MYB113, or MYB114 (Qi et al., 2011), is a positive regulator of anthocyanin production. JAZ proteins interact with several components of this complex, including all three bHLH TFs (TT8, GL3 and EGL3) and one MYB TF (MYB75) to suppress anthocyanin accumulation (Qi et al., 2011). In addition, JAZ3 indirectly inhibits *MYB75* expression by targeting a YAB family TF called FILAMENTOUS FLOWER (FIL), which binds to the promoter of *MYB75* to stimulate anthocyanin biosynthesis (Boter et al., 2015). Thus, incomplete elimination of anthocyanin in *jazD* by *mycT* likely reflects the involvement of additional JAZ-regulated TFs in promoting anthocyanin biosynthesis. Consistent with the idea that JAZ proteins regulate the activity of diverse TFs involved in specialized metabolism, a recent study provided evidence that the expression of spatially clustered triterpenoid biosynthetic genes in Arabidopsis are repressed by JAZ independently of MYC2/3/4 (Major et al., 2017). Gene ontology (GO) analysis performed with upregulated genes in *jazD* showed that triterpenoid metabolic process (GO ID: 0006722) is also induced in *jazD* (Guo et al., 2018b). Based on the results of Major *et al.* (Major et al., 2017), it is likely that MYC TFs do not promote the induction of triterpenoid biosynthetic genes in *jazD* as well. In future studies it may be informative to measure triterpene levels in *jazD* and *jazD myc* mutants, particularly in root tissues where these

genes are most highly expressed. Given the complex genetic background of *jazD* (Guo et al., 2018) and the partial growth recovery by *mycT*, we cannot exclude the possibility that unknown genetic changes contribute to the growth phenotype of this mutant line. Reconstruction of the *jaz* decuple mutant using CRISPR technology may help to test this hypothesis.

ER bodies were first discovered in epidermal and cortical cells of radish roots (Bonnett and Newcomb, 1965). Currently, it is generally recognized that these ER membrane-derived compartments are restricted to the order of *Brassicales* in which glucosinolates are found (Iversen, 1970; Behnke and Eschlbeck, 1978; Jorgensen, 1981). ER bodies are increasingly recognized as a repository for a large variety of β-glucosidases (Matsushima et al., 2003a; Ogasawara et al., 2009). That at least some of these enzymes (i.e. PYK10/BGLU23) display myrosinase activity suggests that ER bodies serve to physically separate myrosinases from their glucosinolate substrates until the tissue is disrupted by an appropriate biotic stress (Nakano et al., 2014; Nakano et al., 2017). Although there is evidence showing that JA treatment induces the formation of ER bodies (Matsushima et al., 2002), the mechanism by which JA triggers ER body accumulation has remained unclear. Our results significantly advance insight into this question by demonstrating that ER body biogenesis is positively regulated by the JAZ-MYC transcriptional module (Figure 3.9 and 3.10). Consistent with the emerging link between ER body formation and indole glucosinolates production, the extent of ER body formation in *jazD* and *jazD mycT* positively correlates with their indole glucosinolate levels (Figure 3.8A and 3.9A). Direct measurements of total myrosinase activity in *jaz myc* polymutants may be useful to identify specific JAZ and MYC proteins that control ER body function (Nakano et al., 2017). Interestingly, ER bodies are repositories not only for β-glucosidases but also for anti-fungal defensins such as PDF1.2 (Watanabe et al., 2013). That these low-molecular weight, cysteine-rich peptides deter a wide

variety of fungal pathogens is consistent with a role for ER bodies in anti-fungal defense (Penninckx et al., 1996; Campos et al., 2018). Recent studies indicate that PDFs are localized to ER bodies before fungal attack but that during pathogen invasion the peptides are secreted to apoplastic space (Watanabe et al., 2013). Given that *PDF* expression is highly elevated in *jazD* (Guo et al., 2018b), it will be interesting to determine whether ER bodies in *jazD* leaves serve as sites for PDF storage.

We found that the expression of genes associated with both constitutive and inducible ER bodies are positively regulated by MYC2/3/4 (Figure 3.9C and 3.10A). However, our results also indicate MYC TFs exert differential control over the expression of these two types of ER body genes. The expression of inducible ER body genes (*BGLU18* and *TSA1*) was strictly dependent on MYCs, whereas the expression of constitutive ER body genes (*NAI1*, *NAI2*, and *PYK10*) was only partially controlled by MYCs (Figure 3.9C and 3.10A). These results are consistent with previous studies showing that the biogenesis of constitutive ER bodies requires another bHLH TF called NAI1; among the constitutive ER body genes directly regulated by NAI1 are *PYK10*, *NAI2*, *MEB1*, *MEB2*, and several *JACALIN-RELATED LECTINs* (*JALs*) (Nakano et al., 2014). Loss of NAI1 completely disrupts ER body formation in seedlings (Matsushima et al., 2004). Thus, it is plausible that NAI1 is targeted by JAZ proteins and depressed in *jazD* to induce the expression of constitutive ER body genes, as well as the biogenesis of these structures. To test this hypothesis, we performed a yeast-two-hybrid (Y2H) analysis to determine whether NAI1 interacts with members of the Arabidopsis JAZ protein family. With the possible exception of a very weak interaction between NAI1 and JAZ8, robust interaction between NAI1 and other JAZs was not observed (Figure 3.14). This finding does not support the hypothesis that JAZ proteins inhibit ER body formation through physical interaction with NAI1. The mechanisms by which the biogenesis

of constitutive and inducible ER bodies is controlled in a different manner remain to be elucidated. In this context, it is interesting to note that MYC and MYB TFs co-activate the expression of glucosinolate biosynthetic genes via direct binding to their promoters, and that these two types of TFs physically interact with each other (Schweizer et al., 2013; Frerigmann et al., 2014; Frerigmann, 2016). We found that the induction of *BGLU18* and *PYK10* is dependent on MYC2/3/4 (Figure 3.9C and 3.10A). Examination of the *BGLU18* promoter showed that it contains putative binding sites for both MYC and MYB TFs. Based on the increasing evidence for a link between glucosinolates and ER bodies (Nakano et al., 2017; Wang et al., 2017), we speculate that MYC and MYB TFs act synergistically to promote the formation of inducible ER bodies. Additional studies are needed to test whether and how MYC and MYB TFs directly target the promoters of ER body genes.

Methods

Plant material and growth conditions

Arabidopsis thaliana ecotype Columbia-0 (Col-0) was the wild-type (WT) genetic background for all experiments. Soil-grown plants were maintained at 20 ºC (± 1 ºC) in a growth chamber with a 16-h day (100 µE m^{-2} s^{-1}) and 8-h night unless otherwise noted. For experiments involving growth of seedlings on agar plates, seeds were surface-sterilized in 50% bleach (v/v) for 3 min, washed 8 times with sterile water and then stratified in dark at 4 ºC for two days. Seeds were then sown on 0.7% (w/v) phytoblend agar (Caisson Labs) media containing half-strength Linsmaier and Skoog (LS; Caisson Labs) salts supplemented with 0.8% (w/v) sucrose. Construction of the *jazD* decuple and the *jazQ mycT* octuple mutants has been described previously (Major et al., 2017; Guo et al., 2018b). The *jazD mycT* tredecuple mutant was generated by combining *jazD* and *jazQ myT*. PCR-based genotyping of mutants was performed using primer sets flanking T-DNA insertion sites, together with a third primer specific for the T-DNA border (Campos et al., 2016; Major et al., 2017).

Root and shoot growth measurements

Root growth inhibition assays were performed by growing seedlings on square Petri plates (Thermo Fisher Scientific) containing half-strength LS salts, 0.8% (w/v) sucrose and 0.7% (w/v) phytoblend agar supplemented with the indicated concentration of methyl-JA (MeJA; Sigma-Aldrich) (Shyu et al., 2012). Plates were incubated vertically in a growth chamber maintained at 20 ºC with an 16 h : 8 h, day (80 µE m^{-2} s^{-1}) : night photoperiod for 7 days. Primary root length was determined using the ImageJ software (https://imagej.nih.gov/ij/). WT and mutant lines were grown the same plate to avoid plate-to-plate variation. Measurement of growth parameters,

including leaf fresh weight, projected leaf area and rosette diameter, was performed as described previously (Campos et al., 2016).

Coronatine treatment and chlorophyll quantification

The fifth true leaves of 26-day-old soil-grown plants were spotted with 5 µL of sterile water (mock) or 50 µM coronatine (prepared in sterile water). Treated leaves were scanned 2 and 4 days after treatment. For whole-rosette treatment, similar plants were sprayed with sterile water or 5 µM coronatine, as described previously (Attaran et al., 2014). Rosettes were scanned after 3 and 4 days of coronatine treatment. For chlorophyll measurement, leaves of 25-day-old plants were sprayed with 5 µM coronatine or water (mock), and harvested three days after spray. Chlorophyll was extracted by 80% acetone buffered by 2.5 mM sodium phosphate solution (pH 7.8), and absorbance at 646 nm, 663 nm, and 750 nm was determined by spectrophotometer (Beckman Coulter DU-800) (Porra et al., 1989). The following equation was used for estimation of chlorophyll concentration (µg/mL): Chlorophyll a + b = (17.76 x (A_{646} - A_{750})) + (7.34 x (A_{663} - A_{750})) (Porra et al., 1989).

Seed yield measurements

Inspection of seed yield was performed as described previously (Guo et al., 2018b). An inverted plastic cone and plastic tube (Arasystem 360 kit; Arasystem) were fitted to each plant 23 days after seed sowing to collect all seeds from dehiscing siliques. Seeds collected from individual plants were dried with Drierite desiccant for two weeks, after which total seed mass per plant was measured. Average seed mass was determined by weighing dry seeds in batches of 100 (Jofuku et al., 2005). For each plant, the weights of five sample batches were measured and averaged. The

silique length and number of seeds per silique were determined by sampling the fully-elongated seventh, ninth and eleventh siliques on the main stem (Roux et al., 2004).

Glucosinolate analysis

Plants were grown under long-day conditions (16-h day and 8-h night) for 23 days. Rosette leaves were harvested and frozen in liquid nitrogen immediately. Two plants were pooled for each sample, with three biological replicates were collected per sample. Glucosinolates were extracted with 80% methanol as described previously (Glauser et al., 2012; Guo et al., 2018b). Samples were analyzed by Waters Xevo G2-XS ultrahigh pressure liquid chromatography (UPLC) coupled to quadrupole time-of-flight mass spectrometry (QTOFMS) in the MSU Mass Spectrometry Facility. Data analysis and processing were performed as described before (Glauser et al., 2012).

Insect and pathogen assays

Insect-feeding assays were performed with soil-grown plants maintained at 20 ºC in a growth chamber with a photoperiod of 8 h light (100 µE m^{-2} s^{-1}) and 16 h dark. Four neonate *Trichoplusia ni* larvae (Benzon Research) were reared on each of 8 plants (10-week-old) for nine days, after which larval weights were measured (Herde et al., 2013). *Botrytis cinerea* inoculation assays were performed as described previously (Rowe and Kliebenstein, 2007), with minor modifications. Detached leaves from 10-week-old short-day-grown (8 h light/16 h dark) plants were placed in Petri dishes containing filter papers moistened with 10 mL of sterile H_2O, with petioles embedded in the H_2O. Each leaflet was inoculated with a single 4 µL droplet of *B. cinerea* spore suspension (5,000 spores/mL in 50% organic grape juice). Petri dishes were sealed with microspore surgical tapes (3M Health Care) and kept under the same conditions used for plant growth. Photographs

were taken after five days and lesion area was measured using the ImageJ software (https://imagej.nih.gov/ij/).

Confocal laser scanning microscopy

To express the ER luminal marker protein ER-YFP in plants, the coding sequence of *ER-YFP*, which includes the signal peptide of WALL-ASSOCIATED KINASE 2 (WAK2), YFP and HDEL ER retention signal (Nelson et al., 2007), was subcloned into the pYL436 binary vector which contains the 35S promoter sequence (Rubio et al., 2005). Transformation of WT and *jazD* plants with *Agrobacterium tumefaciens* (strain GV3101) was performed using the floral dip method (Clough and Bent, 1998). Seedlings (T1 generation) of transformed lines were screened on LS plates containing gentamycin (100 µg/mL) and transferred into soil. Homozygous lines were selected by testing the T3 progeny for resistance to gentamycin. *jazD mycT* plants overexpressing *ER-YFP* was obtained by crossing *jazD mycT* to *jazD* plants harboring *35S:ER-YFP*. The fifth rosette leaves of 30-day-old homozygous lines were inspected by confocal laser scanning microscopy with a Nikon A1Rsi microscope. NIS-Elements Advanced Research (Nikon) and Photoshop (Adobe) software were used for image processing.

SDS-polyacrylamide gel electrophoresis and mass-spectrometry analysis

Crude proteins were extracted from leaves of 23-day-old soil-grown Arabidopsis plants with an extraction buffer consisting of 100 mM Tris-HCl pH 6.8, 150 mM NaCl, 10% glycerol, 4% SDS, 200 mM DTT, and one tablet of Complete Mini EDTA-free proteinase inhibitors (one tablet per 10 mL; Roche) (Schilmiller et al., 2010). Lipophilic contaminants that would interfere with electrophoresis were removed by chloroform-methanol extraction of the solubilized protein.

Protein pellets from the chloroform-methanol extraction were resuspended in the buffer containing 100 mM Tris-HCl pH 6.8, 150 mM NaCl, 10% glycerol, 1% SDS, and 200 mM DTT, and protein concentrations were determined by the Bradford assay (Bio-Rad). The isolated proteins were then separated by SDS-polyacrylamide gel electrophoresis (SDS-PAGE) and stained with Coomassie Brilliant Blue R-250. The *jazD*-specific band, which was in the 70-kd region of the gel, was cut out and subjected to mass-spectrometry analysis at the Michigan State University Proteomics Core Facility (https://rtsf.natsci.msu.edu/proteomics/).

Quantitative PCR

For quantitative PCR (qPCR) analysis, rosette leaves of two 23-day-old soil-grown plants were pooled together for each sample, with three biological replicates collected per sample. Harvested tissues were immediately frozen in liquid nitrogen and stored at -80 ºC until processing. Frozen tissues were homogenized with a TissueLyser II (Qiagen) and RNA was extracted using an RNA extraction kit (Macherey-Nagel), as per the manufacturer's instructions. RNA quality was assessed by A_{260}/A_{280} ratios using an ND-1000 UV Nanodrop spectrophotometer (Thermo Scientific). Complementary DNA (cDNA) was reverse transcribed using the High Capacity cDNA Reverse Transcription kit (Applied Biosystems, ABI) as per the manufacturer's protocols, and cDNA was diluted to 15 ng/µL with nuclease-free water. Quantitative real-time PCR reactions consisted of 2 µL of diluted cDNA template (30 ng in total), 5 µL of 2 x Power SYBR Green Master Mix (ABI), 1 µL of 5 µM forward and reverse primers, and 2 µL of nuclease-free water for a final reaction volume of 10 µL. The forward and reverse primers used were as follows: *PP2A*, 5'-AAGCAGCGTAATCGGTAGG-3' and 5'- GCACAGCAATCGGGTATAAAG-3'; *BGLU18*, 5'-CGACAACGGAAAGAAAGCTC-3' and 5'-GCAGTTTCTGAATGCGTCAA-3'; *TSA1*, 5'-

AATGCTCTTCAAGGCAAGGA-3’ and 5’-TGATCCAACAGACTCGAACG-3’; *PYK10*, 5’-CAATGAGCCATGGGTTTTCT-3’ and 5’-CAACTGCTTCTGCGTGAGAG-3’; *NAI2*, 5’-CCGAATTTCGATGCGATTAT-3’ and 5’-CCGAGTCTACGGTTCTCTGC-3’; and *NAI1*, 5’-GGTTCTCGCACGTCACAAGT-3’ and 5’-CTTCCTCCATTGTTAACACAATCTT-3’. Reactions were run on an ABI 7500 Fast qPCR instrument with the following conditions: 50 ºC for 2 min, 95 ºC for 10 min, then 40 cycles of 15 s at 95 ºC for denaturation and 60 s at 60 ºC for annealing and polymerization. A dissociation curve was performed at the end of each reaction using default parameters (15 s at 95 ºC, 60 s at 60 ºC-95 ºC in 1 ºC increments, and 15 s at 95 ºC), which confirmed a single peak for each set of primers. All reactions were run with three technical replicates, which typically did not differ by more than 0.2 to 0.5 cycle threshold. Target gene expression was normalized to the expression of *PROTEIN PHOSPHATASE 2A* (*PP2A*), which is stable under JA-inducing conditions (Attaran et al., 2014). The efficiencies for each primer set were determined by LinRegPCR.

Yeast two-hybrid assays

Yeast two-hybrid (Y2H) assays were performed with the Matchmaker LexA system (Clontech) as previously described (Melotto et al., 2008; Chung and Howe, 2009). Full-length *JAZ* cDNAs were subcloned into the pGILDA vector to generate fusions of the bait protein with the LexA DNA binding domain. Full-length cDNAs encoding MYC2 and NAI1 were subcloned into the pB42AD vector to generate fusions of the prey protein with the B42 activation domain. Bait and prey vectors were cotransformed into yeast (*Saccharomyces cerevisiae*) strain EGY48 using the frozen-EZ yeast transformation II kit (Zymo Research). Transformants were selected for colorimetric

detection (β-galactosidase) of protein-protein interaction as described by Chung and Howe (Chung and Howe, 2009). Y2H plates were scanned after six days of incubation at 30 ºC.

APPENDIX

Tables and figures

Table 3.1. Mutants used for construction of *jazD myc* mutants.

Mutant	Original name	Source	Accession	Mutagen	Resistance[1]
jaz1-2	SM_3.22668	JIC SM	Col-0	dSpm transposon	Basta (confirmed)
jaz2-3	RIKEN_13-5433-1	RIKEN	No-0	Ds transposon	Hygromycin (confirmed)
jaz3-4	GK-097F09	GABI Kat	Col-0	T-DNA (pAC161)	Sulfadiazine (confirmed)
jaz4-1	SALK_141628	SALK	Col-0	T-DNA (pROK2)	Kanamycin (silenced)
jaz5-1	SALK_053775	SALK	Col-0	T-DNA (pROK2)	Kanamycin (confirmed)
jaz6-4	CSHL_ET30	CSHL	Ler	Ds transposon (Enhancer trap GUS)	Kanamycin (confirmed)
jaz7-1	WiscDsLox7H11	Wisconsin	Col-0	T-DNA (pWiscDsLox)	Basta (not tested)
jaz9-4	GK_265H05	GABI Kat	Col-0	T-DNA (pAC161)	Sulfadiazine (confirmed)
jaz10-1	SAIL_92_D08	SAIL	Col-0	T-DNA (pCSA110)	Basta (confirmed) GUS
jaz13-1	GK_193G07	GABI Kat	Col-0	T-DNA (pAC161)	Sulfadiazine (not tested)
myc2-1	SALK_040500	SALK	Col-0	T-DNA (pROK2)	Kanamycin (silenced)
myc3-1	GK-445B11	GABI Kat	Col-0	T-DNA (pAC161)	Sulfadiazine (confirmed)
myc4-1	GK-491E10	GABI Kat	Col-0	T-DNA (pAC161)	Sulfadiazine (confirmed)

[1]Resistance of the mutant line to the indicated selectable marker was tested and confirmed.

Table 3.2. Primers used for genotyping *jaz* and *myc* mutants.

Gene	Locus	Primer	Sequence (5'-3')
JAZ1	AT1G19180	JAZ1_F	ACCGAGACACATTCCCGATT
		JAZ1_R	CATCAGGCTTGCATGCCATT
		JAZ1_border	ACGAATAAGAGCGTCCATTTTAGAG
JAZ2	AT1G74950	JAZ2_F	TCTTCCTCGTGACAAAACGCA
		JAZ2_R	CCAAACACAGAACCATCTCCACA
		JAZ2_border	CCGGATCGTATCGGTTTTCG
JAZ3	AT3G17860	JAZ3_F	ACGGTTCCTCTATGCCTCAAGTC
		JAZ3_R	GTGGAGTGGTCTAAAGCAACCTTC
		JAZ3_border	ATAACGCTGCGGACATCTACATT
JAZ4	AT1G48500	JAZ4_F	TCAGGAAGACAGAGTGTTCCC
		JAZ4_R	TGCGTTTCTCTAAGAACCGAG
		JAZ4_border	TTGGGTGATGGTTCACGTAG
JAZ5	AT1G17380	JAZ5_F	GCTTATACCGAAAACCCGATTCCAG
		JAZ5_R	GGCTCATTGAGATCAGGAAGAACCA
		JAZ5_border	TTGGGTGATGGTTCACGTAG
JAZ6	AT1G72450	JAZ6_F	GACACACATCACTGTCACTTC
		JAZ6_R	AGTTTCTGAGGTCTCTACCTTC
		JAZ6_border	CCGTTTTGTATATCCCGTTTCCGT
JAZ7	AT2G34600	JAZ7_F	ATGCGACTTGGAACTTCGCC
		JAZ7_R	GGAGGATCCGAACCGTCTG
		JAZ7_border	ACGTCCGCAATGTGTTATTA
JAZ9	AT1G70700	JAZ9_F	TACCGCATAATCATGGTCGTC
		JAZ9_R	TCATGCTCATTGCATTAGTCG
		JAZ9_border	CTTTGAAGACGTGGTTGGAACG

Table 3.2 (cont'd)

JAZ10	AT5G13220	JAZ10_F	ATTTCTCGATCGCCGTCGTAGT-3
		JAZ10_R	GCCAAAGAGCTTTGGTCTTAGAGTG
		JAZ10_border	GTCTAAGCGTCAATTTGTTTACACC
JAZ13	AT3G22275	JAZ13_F	GCACGTGACCAAATTTGCAGA
		JAZ13_R	TGAAGAGAGGAGGATGATGAGGA
		JAZ13_border	AAACCTCCTCGGATTCCATTGC
MYC2	AT1G32640	MYC2_F	GCTACAACCAACGATGAATC
		MYC2_R	TCATCAACAGCGTCATCCGA
		MYC2_border	TTGGGTGATGGTTCACGTAG
MYC3	AT5G46760	MYC3_F	GTTAGATCAGCTGCGAATGATTCGG
		MYC3_R	CTCCGACTTTCGTCATCAAAGCAAC
		MYC3_border	ATAACGCTGCGGACATCTACATT
MYC4	AT4G17880	MYC4_F	GGATCCATGTCTCCGACGAATGTTC AAGTA
		MYC4_R	TCTCTCACAACTTGATCCAGCTAA
		MYC4_border	ATAACGCTGCGGACATCTACATT

Table 3.3. Letters that denote significant differences according to Tukey's HSD test ($P < 0.05$) for Figure 3.2B.

Genotype	MeJA			
	0 μM	1 μM	5 μM	25 μM
WT	A	FG	IJ	LMN
mycT	A	EF	FG	GH
jazD	BCD	JKLM	O	O
jazD myc2	BCD	FG	IJK	N
jazD myc3	D	IJKL	O	O
jazD myc4	CD	JKLM	O	O
jazD myc23	AB	F	GH	KLMN
jazD myc24	DE	FGH	HI	MN
jazD myc34	DE	KLM	O	O
jazD mycT	ABC	EF	GH	IJKL

Table 3.4. Letters that denote significant differences according to Tukey's HSD test ($P < 0.05$) for Figure 3.3B.

Genotype	Treatment	Chlorophyll a	Chlorophyll b	Chlorophyll a + b
Col-0	Mock	ABC	A	A
Col-0	COR	ABC	AB	A
mycT	Mock	B	AB	A
mycT	COR	ABC	AB	A
jazD	Mock	ABC	B	A
jazD	COR	D	C	B
jazD myc2	Mock	C	AB	A
jazD myc2	COR	E	D	C
jazD myc3	Mock	ABC	AB	A
jazD myc3	COR	F	E	D
jazD myc4	Mock	ABC	B	A
jazD myc4	COR	D	C	B
jazD mycT	Mock	C	AB	A
jazD mycT	COR	ABC	B	A

Table 3.5. Summary of proteins that were identified in the *jazD*-specific protein band in SDS-PAGE analyses.

Protein ID	GeneBank accession no.	M^r	Spectral counts, percent amino acid coverage	
			WT	*jazD*
Beta glucosidase 18	AT1G52400	60	ND	25, 37.5
NADP-malic enzyme 2	AT5G11670	64	ND	8, 18.4
Beta glucosidase 23	AT3G09260	60	ND	4, 0
Succinate dehydrogenase 1-1	AT5G66760	70	ND	2, 1.6
FtsH extracellular protease family	AT2G30950	74	ND	2, 3.7
Sulfite reductase	AT5G04590	72	ND	2, 3.1
10-formyltetrahydrofolate synthetase	AT1G50480	68	ND	2, 1.6
Glucoside glucohydrolase 2	AT5G25980	63	3, 4.2	1, 1.8
Leucine-rich repeat protein kinase family protein	AT2G01210	78	1, 1.1	1, 1.1
Lipoxygenase 2	AT3G45140	102	ND	1, 1.6
26S proteasome regulatory subunit (putative)	AT5G57950	24	1, 3.5	1, 3.5
Phosphoglycerate mutase (2,3-bisphosphoglycerate-independent)	AT1G09780	61	ND	1, 2.0
Vacuolar ATP synthase subunit A	AT1G78900	69	ND	1, 1.9
Transducin family protein/WD-40 repeat family protein	AT2G19520	56	ND	1, 3.4
AICARFT/IMPCHase bienzyme family protein	AT2G35040	65	ND	1, 1.7
Nuclear transport factor 2 family protein with RNA binding domain	AT3G25150	53	ND	1, 2.1
P-loop containing nucleoside triphosphate hydrolases superfamily protein	AT3G53110	55	ND	1, 2.4
RNAse l inhibitor protein 2	AT4G19210	68	ND	1, 1.5
Winged-helix DNA-binding transcription factor family protein	AT4G35890	56	ND	1, 2.5
Nuclear transport factor 2 family protein with RNA binding domain	AT5G60980	49	ND	1, 2.4
Apoptosis inhibitory protein 5	AT2G34040	62	ND	1, 2.0
Translation elongation factor EF1A/initiation factor IF2gamma family protein	AT1G18070	59	ND	1, 1.7
Ribulose-bisphosphate carboxylases	ATCG00490	53	5, 11.1	ND
Transducin/WD40 repeat-like superfamily protein	AT3G05090	82	2, 3.1	ND
U5 small nuclear ribonucleoprotein helicase (putative)	AT1G20960	247	1, 0.4	ND

Table 3.5. (cont'd) LC-MS/MS was used to identify proteins in the 60-kD region of the WT and *jazD* SDS-PAGE gel. The number of spectral counts (i.e., the number of times the mass spectrometer detected a peptide corresponding to a particular protein) and the percent of the full-length protein sequence that was covered by the peptides (percent amino acid coverage) are shown. ND, not detected.

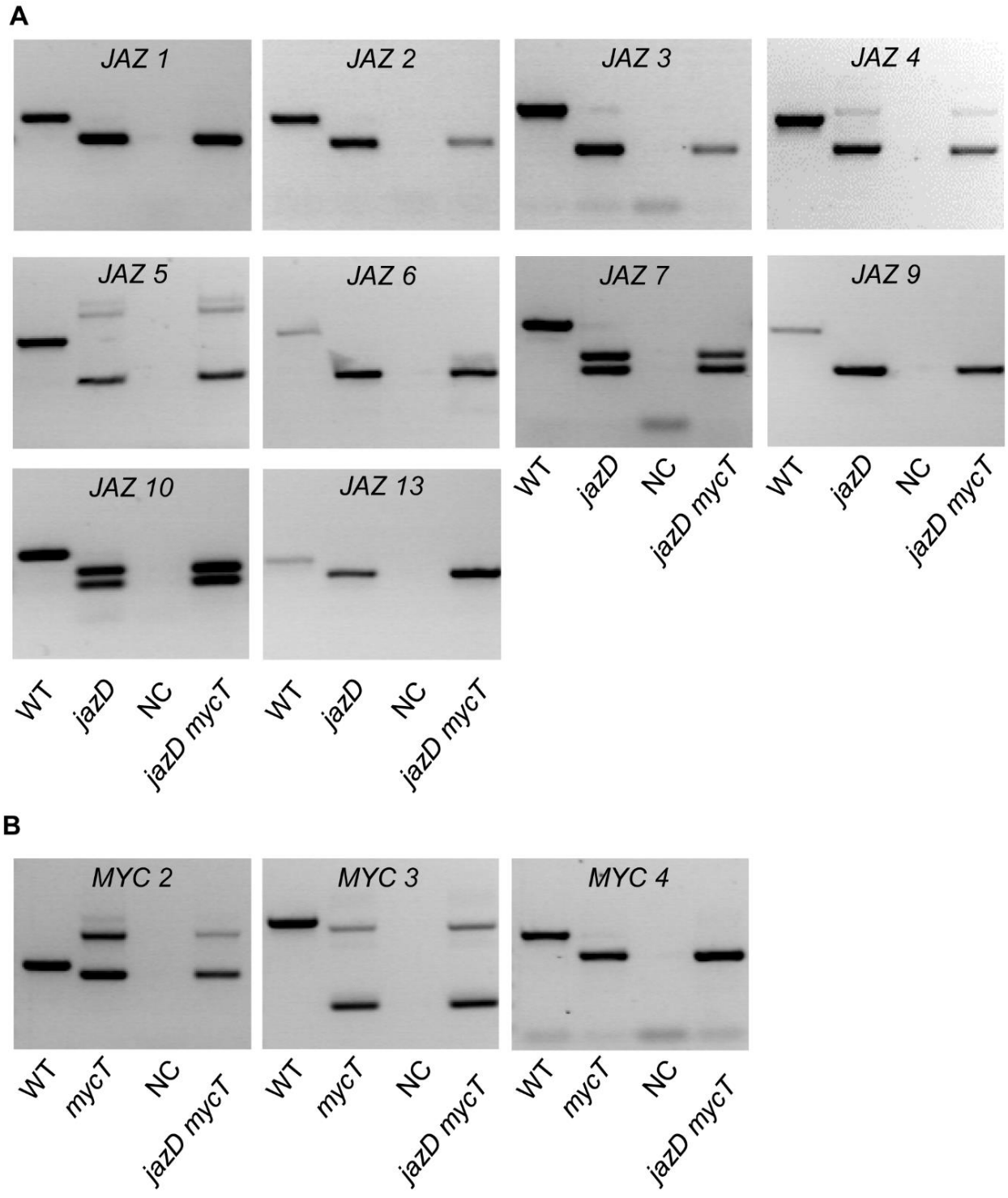

Figure 3.1. PCR-based genotyping of *jazD mycT*.

Figure 3.1. (cont'd) (A) and **(B)** Genotyping of *jazD mycT* for *JAZ1/2/3/4/5/6/7/9/10/13* (A) and *MYC2/3/4* (B) was performed using primer sets flanking DNA insertion sites and a third primer recognizing the T-DNA border (Table 3.1 and 3.2). NC, negative control.

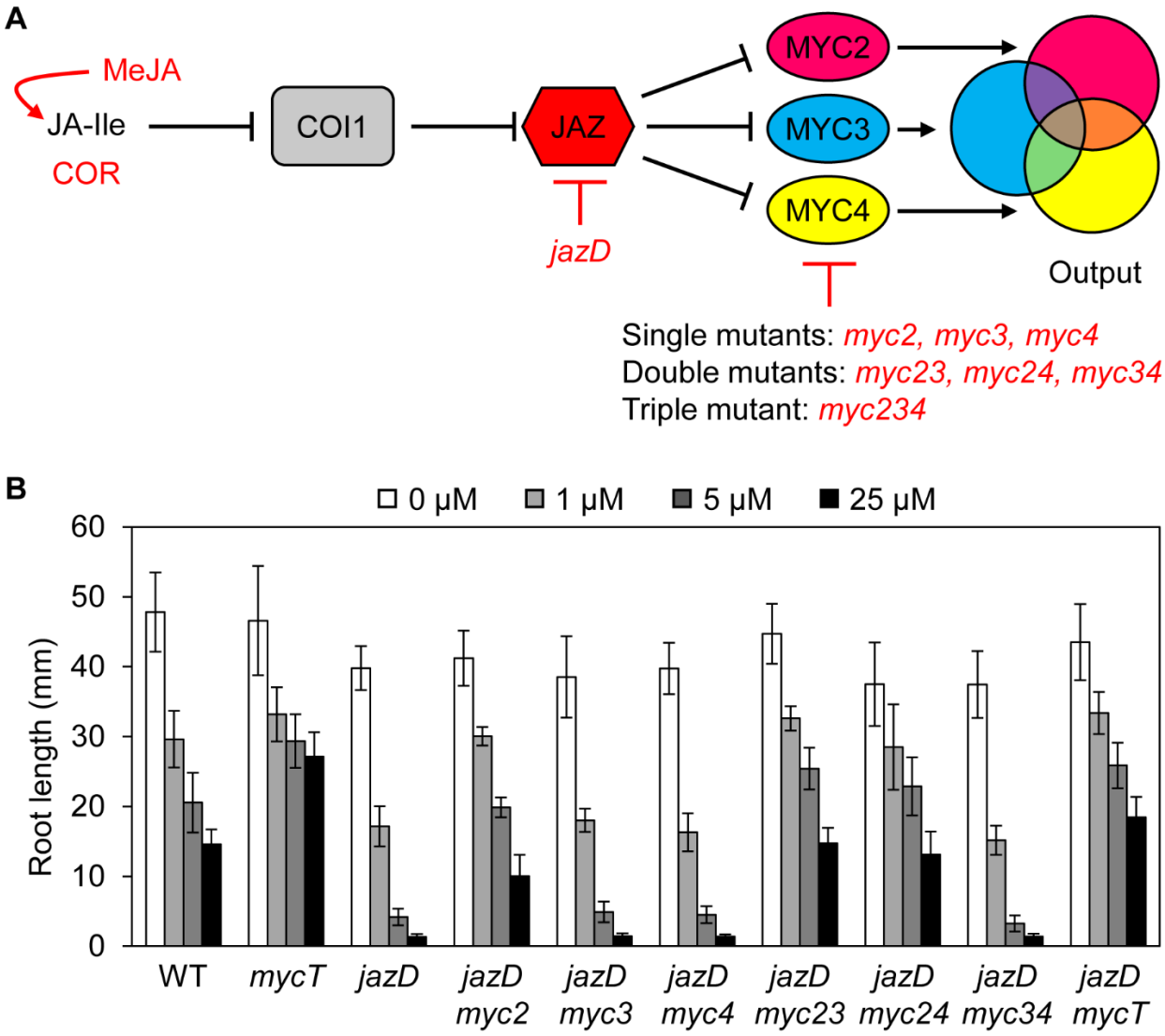

Figure 3.2. Sensitivity of *jazD* roots to JA is driven mainly by MYC2.

(A) Perturbations (shown in red) used in this study to manipulate JA responses involve treatment with exogenous methyl-JA (MeJA) or coronatine (COR), as well as loss-of-function mutations of ten JASMONATE ZIM-DOMAIN (JAZ) repressors (*jazD*) or MYC transcription factors (*myc2*, *myc3*, *myc4*, *myc23*, *myc24, myc34*, and *myc234*). The Venn diagram at right depicts that three MYC TFs (pink: MYC2, blue: MYC3, and yellow: MYC4) may play independent or overlapping roles in mediating JA outputs.
(B) Root length of 10-day-old WT Col-0 (WT), *mycT*, *jazD*, *jazD myc2*, *jazD myc3*, *jazD myc4*, *jazD myc23*, *jazD myc24*, *jazD myc34,* and *jazD mycT* seedlings grown in the presence of 0, 1, 5 or 25 µM MeJA. Data show the mean ± SD of 13-20 seedlings per genotype. Letters that denote significant differences according to Tukey's HSD test ($P < 0.05$) are shown in Table 3.3.

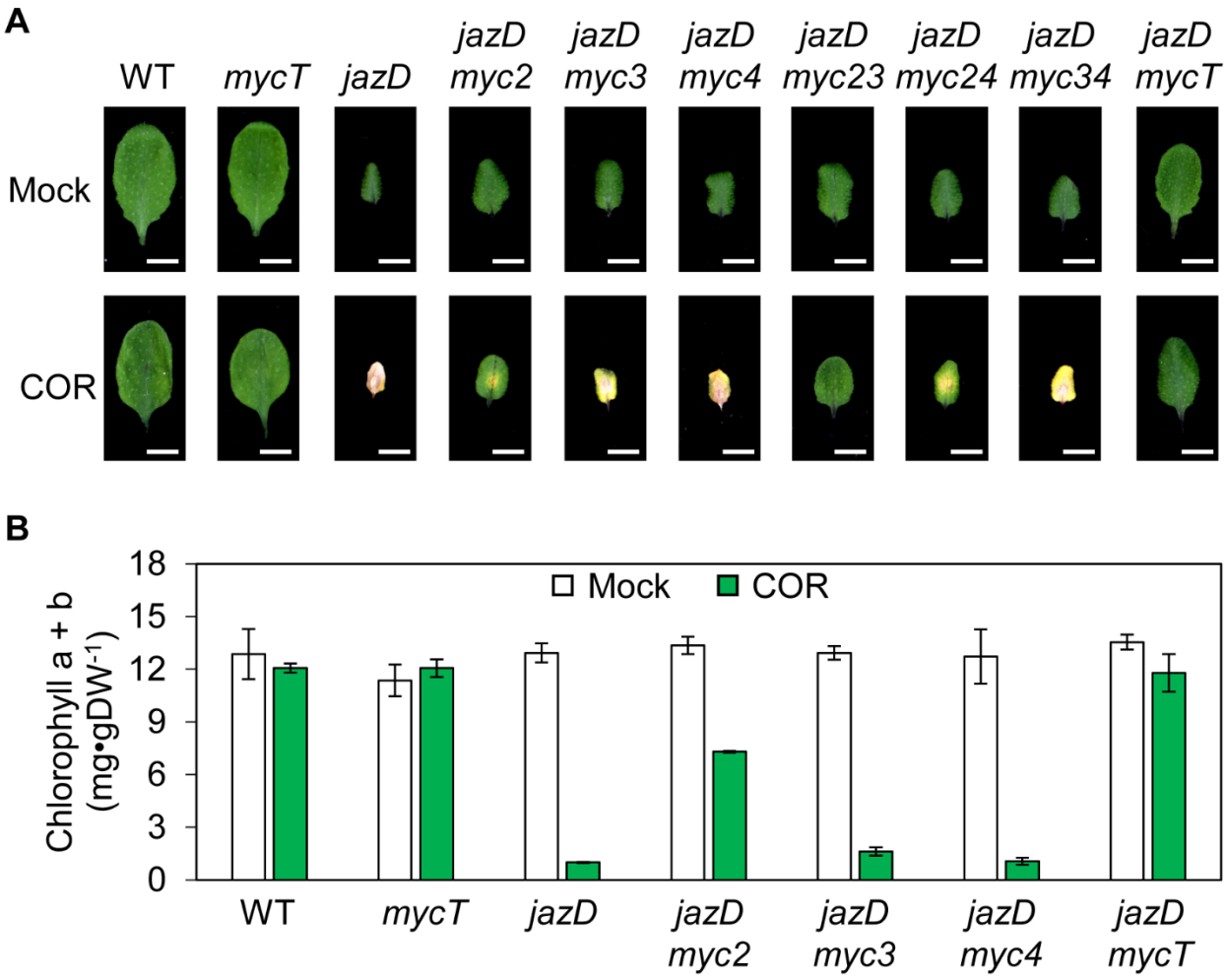

Figure 3.3. MYC2 is the major regulator of *jazD* sensitivity to coronatine.

(A) Photographs of leaves after coronatine (COR) treatment. The 5th rosette leaves of 24-day-old plants grown under 16-h-light/8-h-dark photoperiod were spotted with 5 µL of water (mock) or 50 µM COR. Leaves were excised and photographed after four days of COR treatment. Scale bars, 0.5 cm.
(B) Chlorophyll content (chlorophyll a + b) in COR-sprayed leaves. Soil-grown plants (25-day-old) were sprayed with either water (mock) or 5 µM COR. Leaves were harvested three days after spray and subjected to chlorophyll extraction. Data show the mean ± SD of three samples per genotype. Chlorophyll content was $\log_2$ transformed according to Box-Cox Normality Plot for statistical tests. Letters that denote significant differences according to Tukey's HSD test ($P < 0.05$) are shown in Table 3.4.

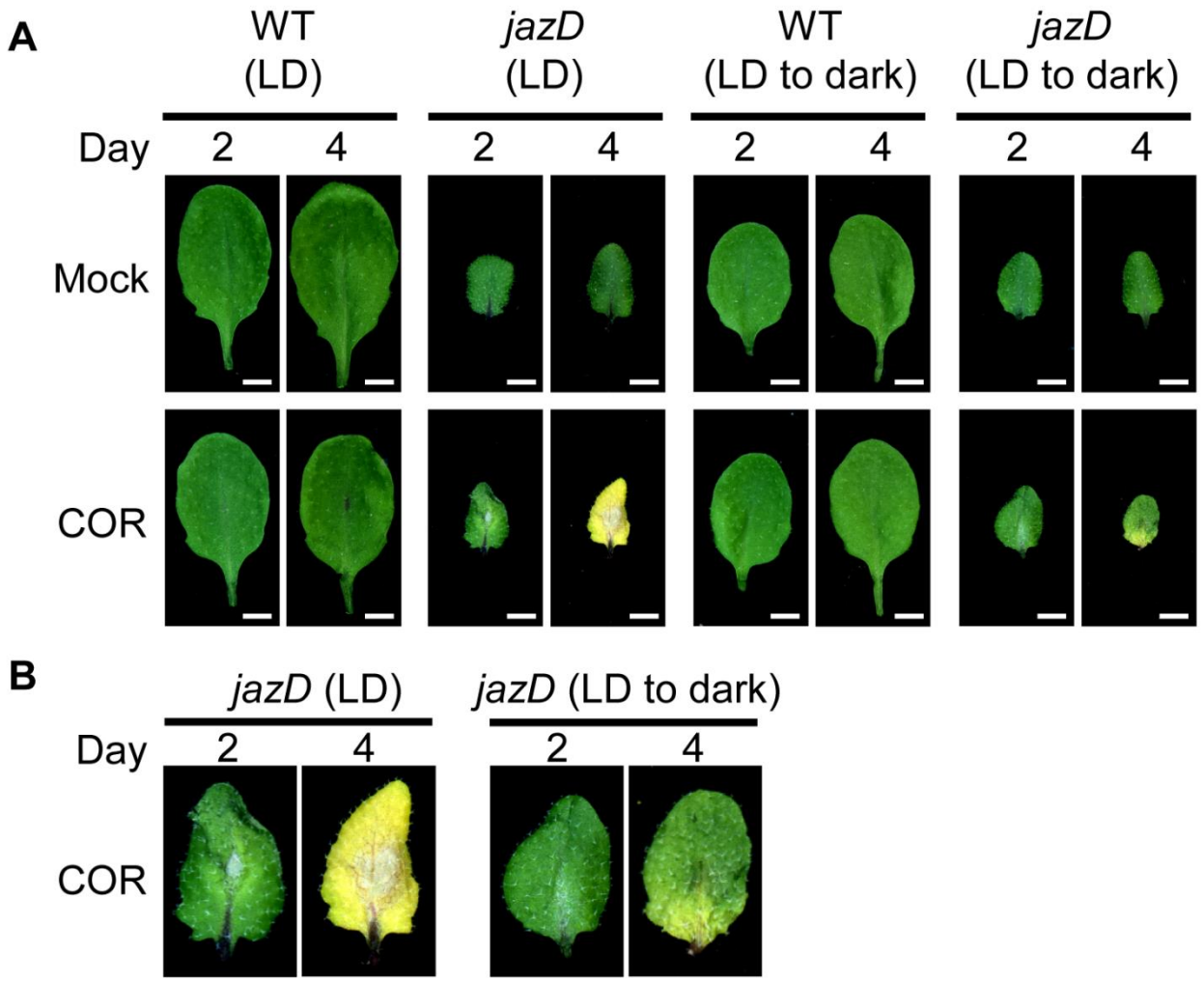

Figure 3.4. Coronatine (COR)-induced chlorosis in *jazD* is partially dependent on light.

(A) Photographs of leaves after COR or COR/dark treatment. The 5th rosette leaves of 25-day-old plants grown under LD conditions were spotted with 5 µL of water (mock) or 50 µM COR. Plants were either maintained under LD conditions or transferred into dark conditions (LD to dark) after COR treatment. Leaves were excised and photographed after two or four days of COR treatment. Scale bars, 0.3 cm.
(B) Enlarged photographs of COR- or COR/dark-treated *jazD* leaves in Panel A.

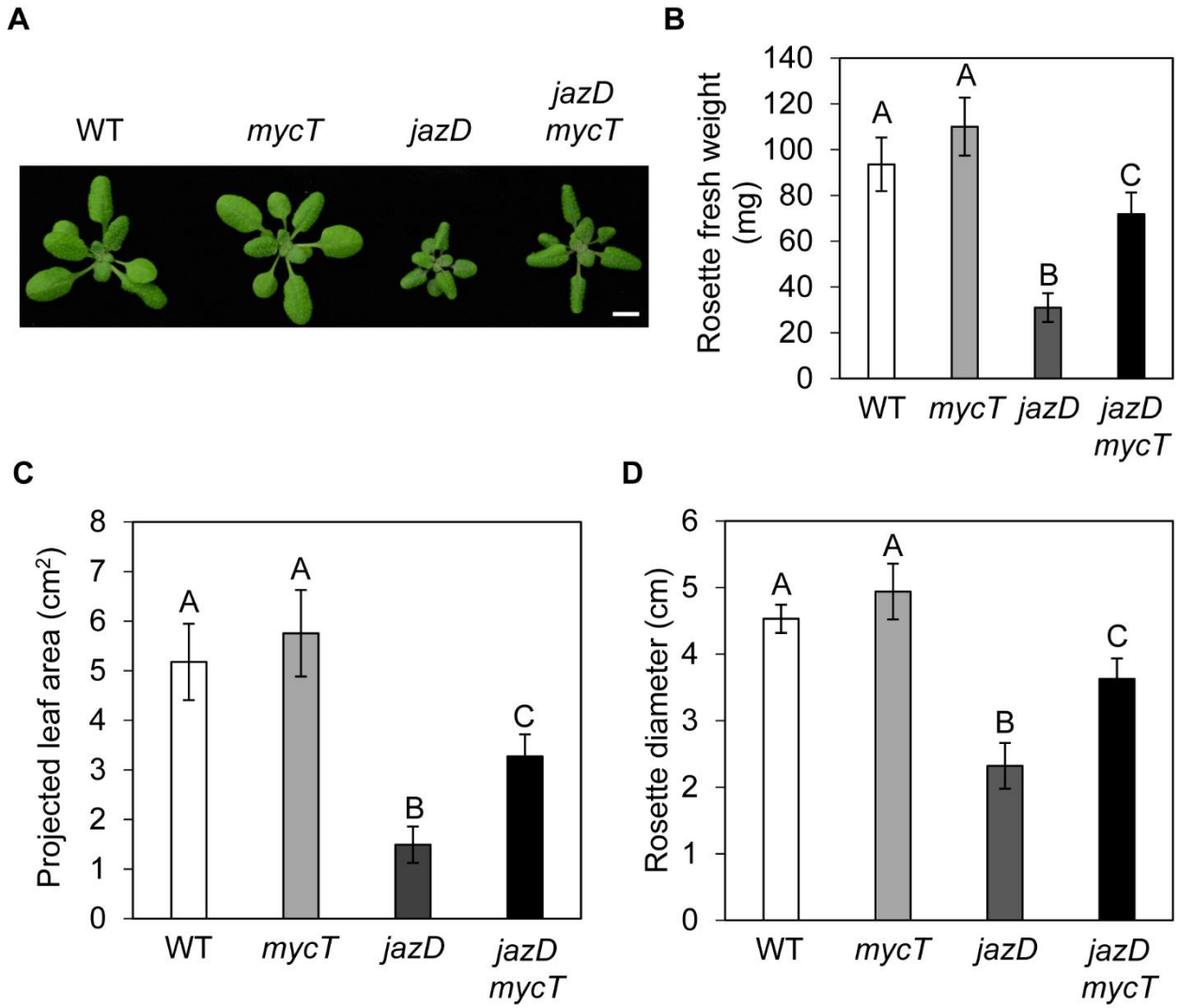

Figure 3.5. The growth deficiency of *jazD* is partially recovered by *mycT*.

(A) Photograph of WT Col-0 (WT), *mycT*, *jazD*, and *jazD mycT* rosettes of 23-day-old plants grown under 16-h-light/8-h-dark photoperiod. Scale bars, 0.5 cm.
(B-D) Rosette fresh weight (B), projected leaf area (C) and rosette diameter (D) of WT, *mycT*, *jazD*, and *jazD mycT* plants shown in Panel A. Data show the mean ± SD of five plants per genotype. Capital letters denote significant differences according to Tukey's HSD test ($P < 0.05$).

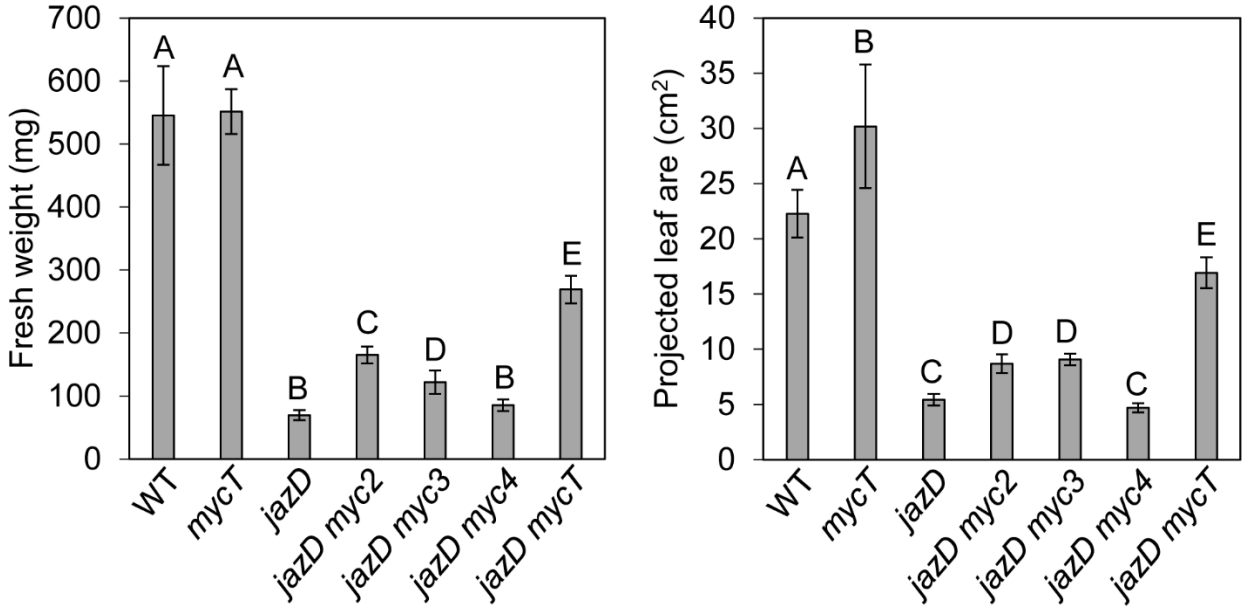

Figure 3.6. MYC2 and MYC3 play stronger roles in growth promotion compared to MYC4.

(A) Fresh weight of 28-day-old WT Col-0 (WT), *mycT*, *jazD*, *jazD myc2*, *jazD myc3*, *jazD myc4* and *jazD mycT* plants grown under long-day conditions (16-h-light/8-h-dark). Data show the mean ± SD of five plants per genotype. Fresh weight was $\log_2$-transformed according to Box-Cox Normality Plot for statistical tests. Capital letters denote significant differences according to Tukey's HSD test ($P < 0.05$).
(B) Projected leaf area of 53-day-old WT, *mycT*, *jazD*, *jazD myc2*, *jazD myc3*, *jazD myc4* and *jazD mycT* plants grown under short-day conditions (8-h-light/16-h-dark). Data show the mean ± SD of five plants per genotype. Projected leaf area was $\log_2$-transformed according to Box-Cox Normality Plot for statistical tests. Capital letters denote significant differences according to Tukey's HSD test ($P < 0.05$).

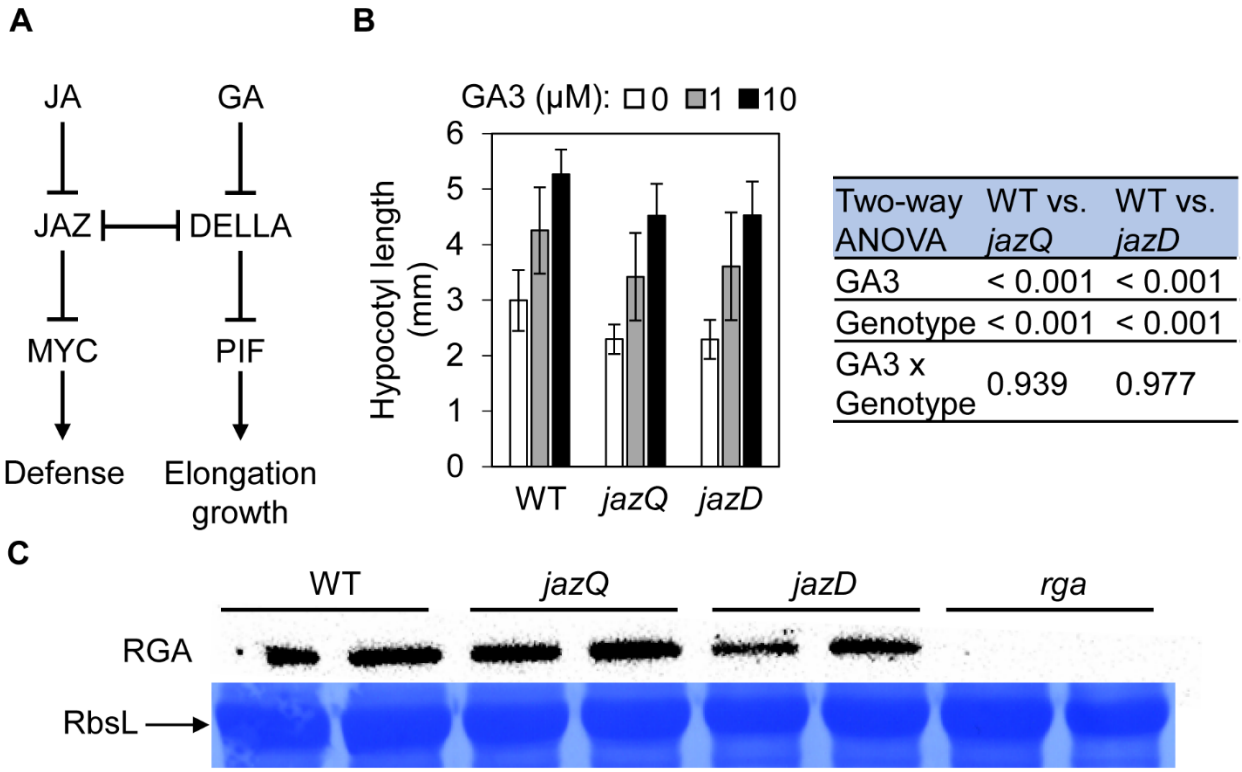

Two-way ANOVA	WT vs. *jazQ*	WT vs. *jazD*
GA3	< 0.001	< 0.001
Genotype	< 0.001	< 0.001
GA3 x Genotype	0.939	0.977

Figure 3.7. The restricted growth of *jazD* cannot be restored by exogenous gibberellic acid (GA3) treatment.

(A) Schematic diagram illustrating the interaction between JA and GA signaling pathways.
(B) Hypocotyl length of WT Col-0 (WT), *jazQ* and *jazD* seedlings grown on half-strength LS medium supplemented with different concentrations (0, 1 or 10 μM) of GA3. Seedlings were grown under 16-h-light (10 μE m^{-2} s^{-1})/8-h-dark photoperiod at 20 ºC for seven days. Data show the mean ± SD of ten seedlings per genotype. Two-way ANOVA was performed to test the effect of GA3 on hypocotyl elongation (*E* and *F*) and showed that the GA3 x genotype interaction was insignificant for WT vs. *jazQ* or WT vs. *jazD* comparisons ($P < 0.05$).
(C) Detection of RGA protein in WT, *jazQ*, *jazD* and *rga* seedlings by western blot. Seedlings were grown on half-strength LS medium containing 0.8% (w/v) sucrose under long-day conditions for 16 days. Western blot was performed with anti-RGA antibody. Coomassie brilliant blue staining of the PVDF membrane was used as loading control. The region of the gel corresponding to the large subunit of Rubisco (RbsL) is shown. Duplicate samples (biological replicates) were loaded for each genotype.

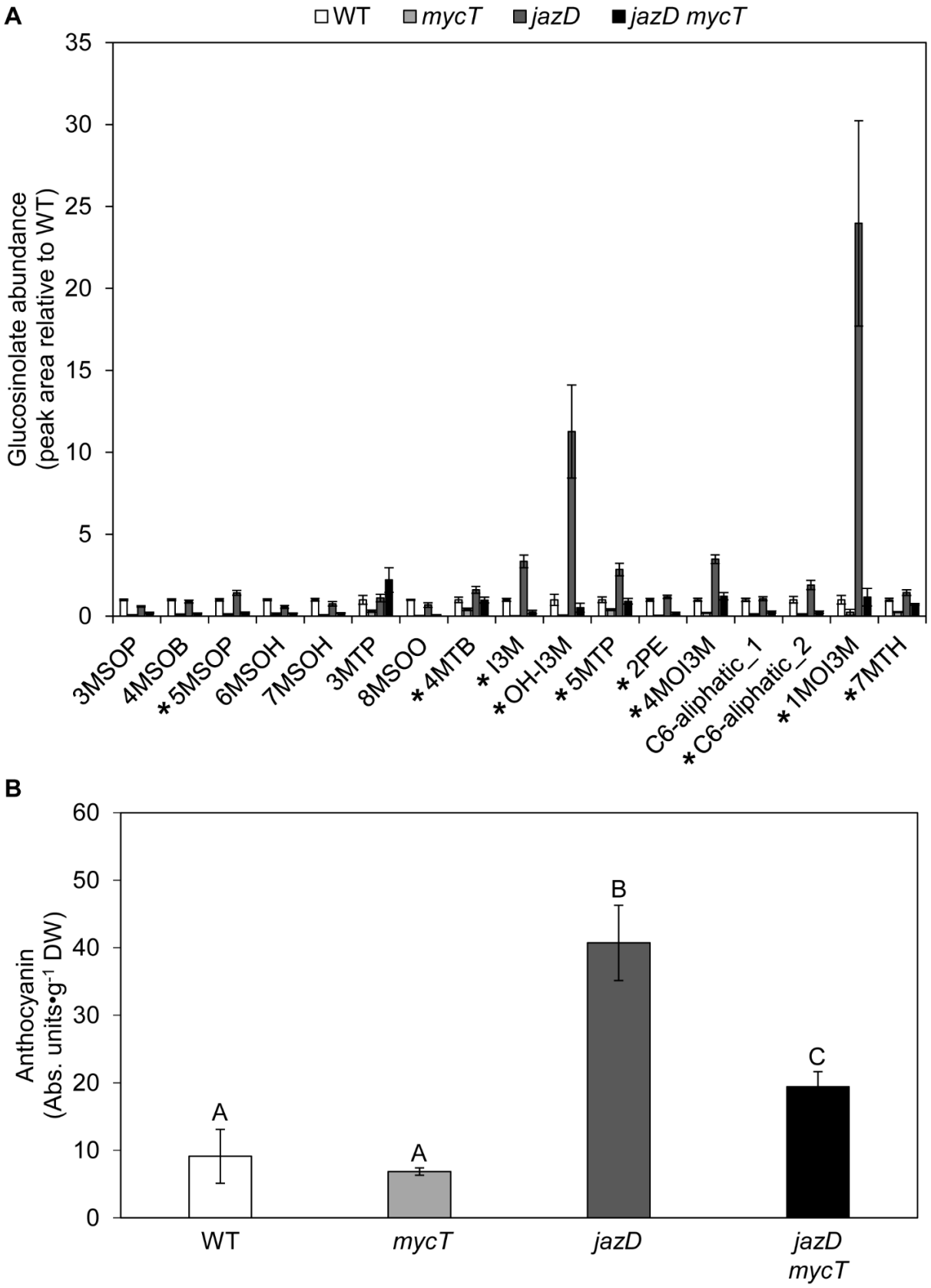

Figure 3.8. Elevated accumulation of defense compounds in *jazD* is dependent on MYC TFs.

Figure 3.8 (cont'd) (A) Comparison of glucosinolate levels in leaves of WT Col-0 (WT), *mycT*, *jazD* and *jazD mycT* plants. Glucosinolates were extracted from leaf tissues of 26-day-old plants and quantified by LC-MS. Peak area for the indicated glucosinolate compound in the WT sample was set to "1" and the peak area of the same compound in other genotypes was normalized to the WT sample. Abbreviations: 3MSOP: 3-methylsulphinylpropyl, glucoiberin; 4MSOB: 4-methylsulphinylbutyl, glucoraphanin; 5MSOP: 5-methylsulphinylpentyl, glucoalyssin; 6MSOH: 6-methylsulphinylhexyl, glucohesperin; 7MSOH: 7-methylsulphinylheptyl, glucoibarin; 3MTP: 3-methylthiopropyl, glucoiberverin; 8MSOO: 8-methylsulphinyloctyl, glucohirsutin; 4MTB: 4-methylthiobutyl, glucoerucin; I3M: indol-3-ylmethyl, glucobrassicin; OH-I3M: 4-hydroxyindol-3-ylmethyl, hydroxyglucobrassicin; 5MTP: 5-methylthiopentyl, glucoberteroin; 2PE: 2-phenylethyl, gluconasturtiin; 4MOI3M: 4-methoxyindol-3-ylmethyl, methoxyglucobrassicin; 1MOI3M: 1-methoxyindol-3-ylmethyl, neoglucobrassicin; 7MTH: 7-methylthioheptyl. Asterisks denote glucosinolates that were upregulated in *jazD* but not in *jazD mycT* compared to WT according to Tukey's HSD test ($P < 0.05$).
(B) Anthocyanin levels in 23-day-old WT, *mycT*, *jazD* and *jazD mycT* leaves. Data show the mean ± SD of five rosettes per genotype. Capital letters denote significant differences according to Tukey's HSD test ($P < 0.05$).

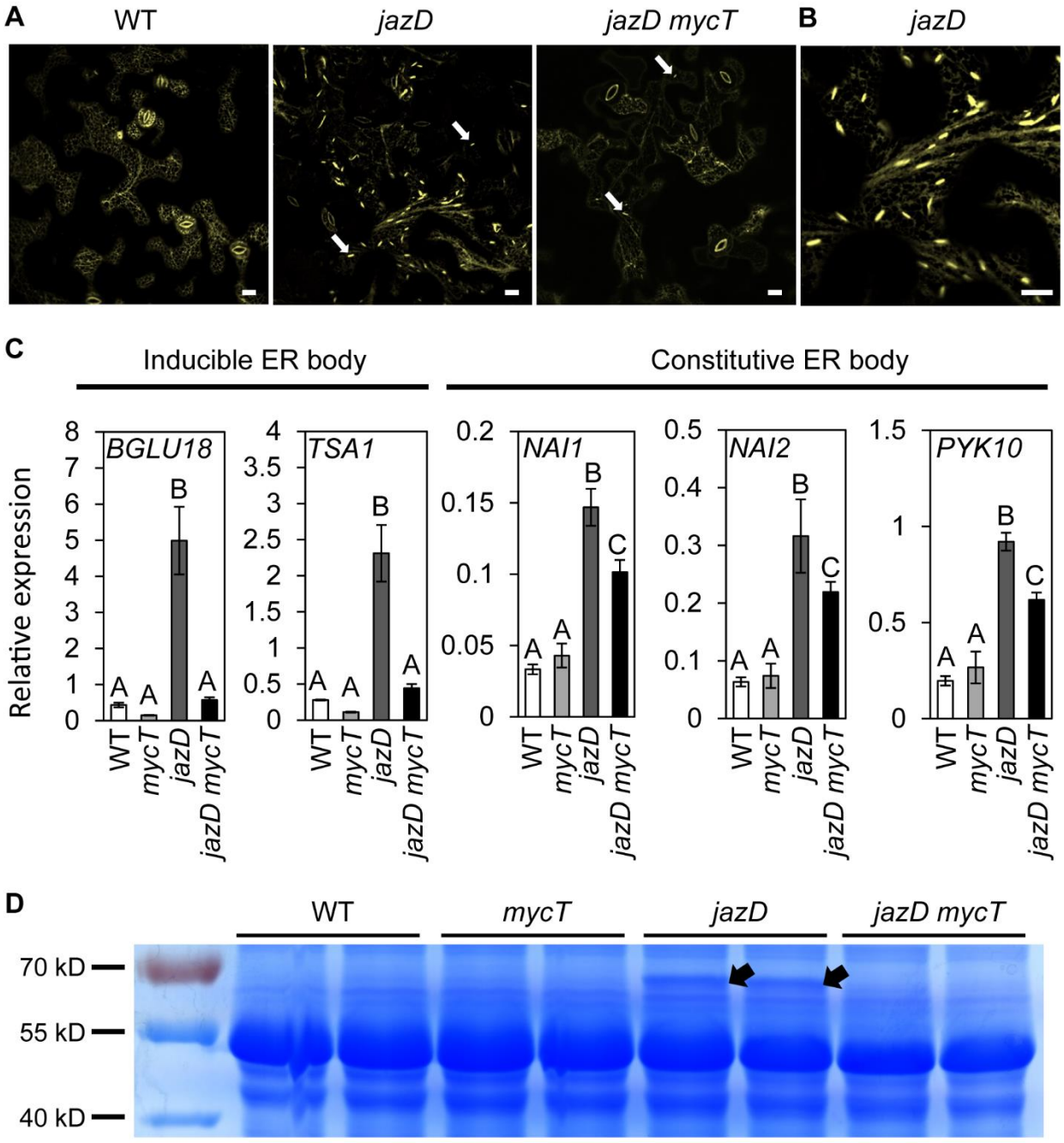

Figure 3.9. Induction of ER body genes is mediated by MYC2/3/4.

(A) Confocal images of the fifth rosette leaves of 30-day-old plants grown under long-day conditions (16-h-light/8-h-dark). The endoplasmic reticulum (ER) luminal marker protein ER-YFP, which includes the signal peptide of WALL-ASSOCIATED KINASE 2 (WAK2), YFP and HDEL ER retention signal, was overexpressed in WT Col-0 (WT), *jazD* and *jazD mycT* plants. White arrows depict ER body structures. Scale bars, 10 µm.
(B) Enlargement of ER bodies at the surface of ER network in *jazD*. Scale bars, 10 µm.

Figure 3.9. (cont'd) (C) Relative expression levels of ER body genes regulated by stress signals (*BGLU18* and *TSA1*) or developmental cues (*NAI1*, *NAI2* and *PYK10*) in WT, *mycT*, *jazD* and *jazD mycT* leaves. *PP2A* (At1g13320) was used for qPCR normalization. Data show the mean ± SD of three biological replicates per genotype. Capital letters denote significant differences according to Tukey's HSD test ($P < 0.05$).
(D) SDS-PAGE analyses of total rosette proteins show that a band in the 60-kD region (black arrows) appears in *jazD* but not in WT, *mycT* or *jazD mycT*. Duplicate samples (biological replicates) were loaded for each genotype.

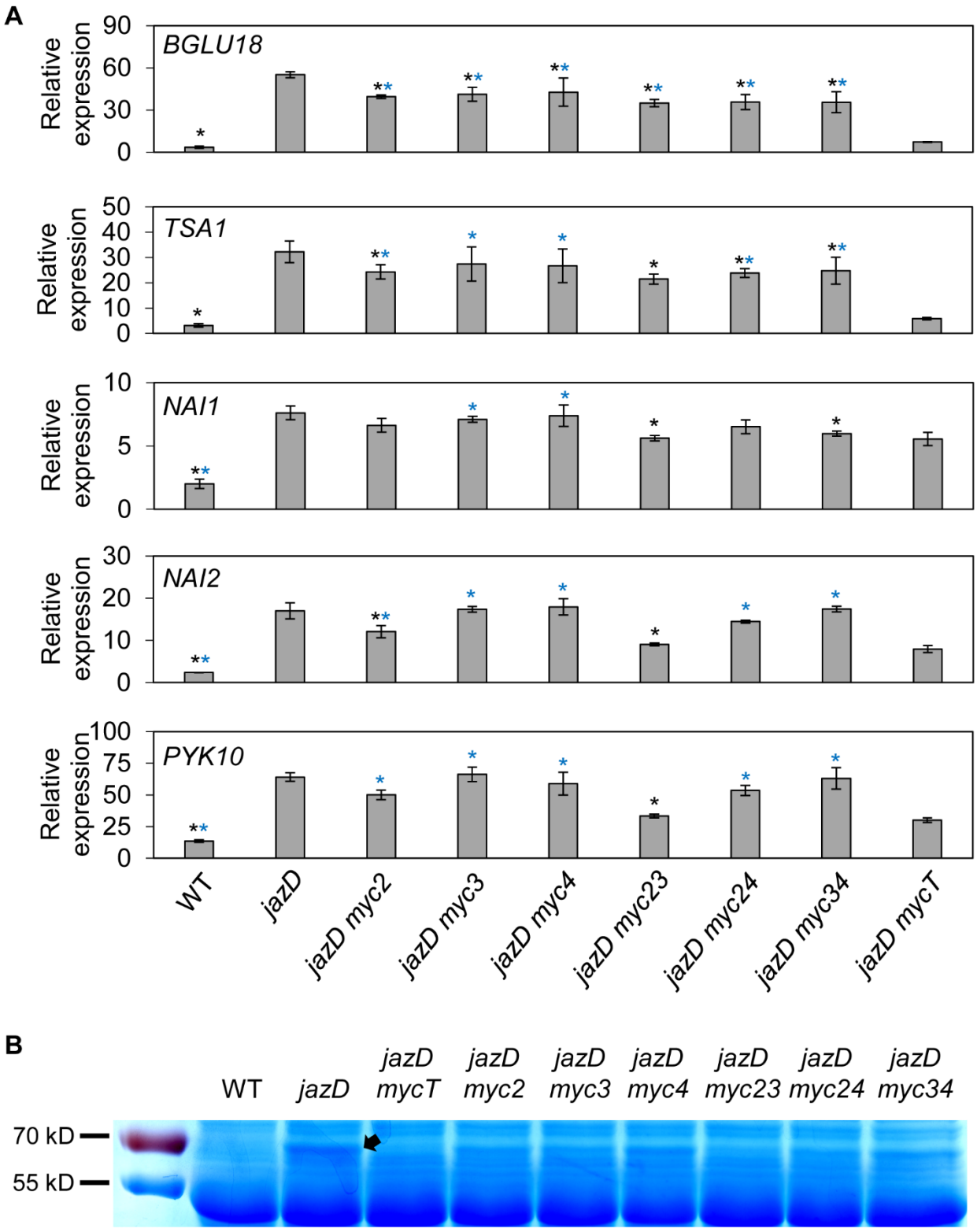

Figure 3.10. MYC2/3/4 display additive effects on inducing the expression of ER body genes.

Figure 3.10. (cont'd) (A) Relative expression levels of ER body genes in WT Col-0 (WT), *jazD* and *jazD myc* leaves. Plants were grown under long-day (16-h-light/8-h-dark) conditions for 25 days. *PP2A* (At1g13320) was used for qPCR normalization. Data show the mean ± SD of three biological replicates per genotype. Black and blue asterisks denote significant differences when comparing indicated genotypes to *jazD* or *jazD mycT* respectively according to Tukey's HSD test ($P < 0.05$).
(B) Removal of one or two MYC TFs in the *jazD* background fails to deplete the 60-kD protein band.

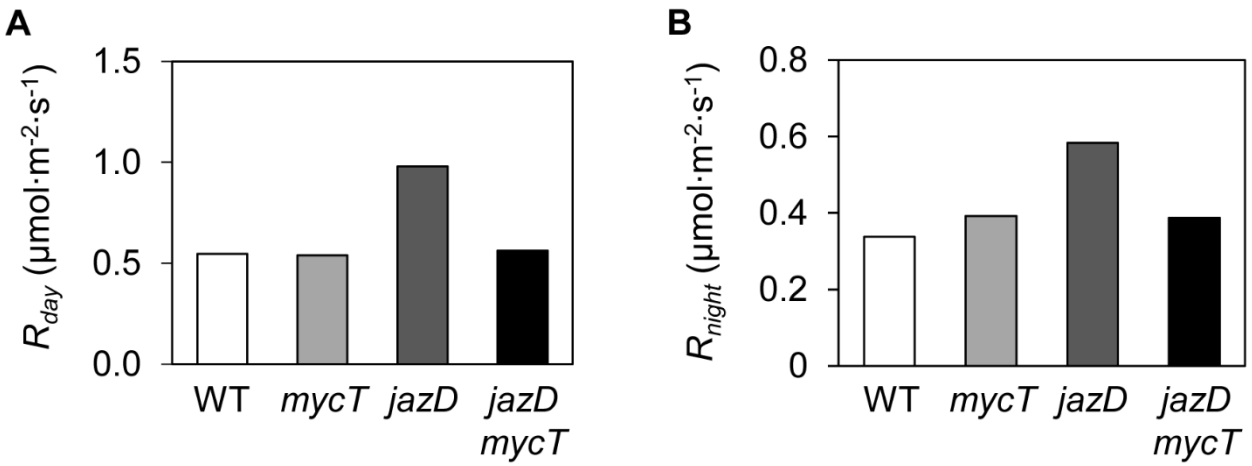

Figure 3.11. Increased respiration rates of *jazD* is dependent on MYC TFs.

(A) and **(B)** Respiration rates of WT, *mycT*, *jazD*, and *jazD mycT* plants measured at 400 µmol CO_2 in light (A) or dark (B). Plants were grown under short-day (8-h-light/16-h-dark) conditions for eight weeks. Data show the mean ± SD of three plants per genotype except for *mycT* in Panel A, which represents one plant.

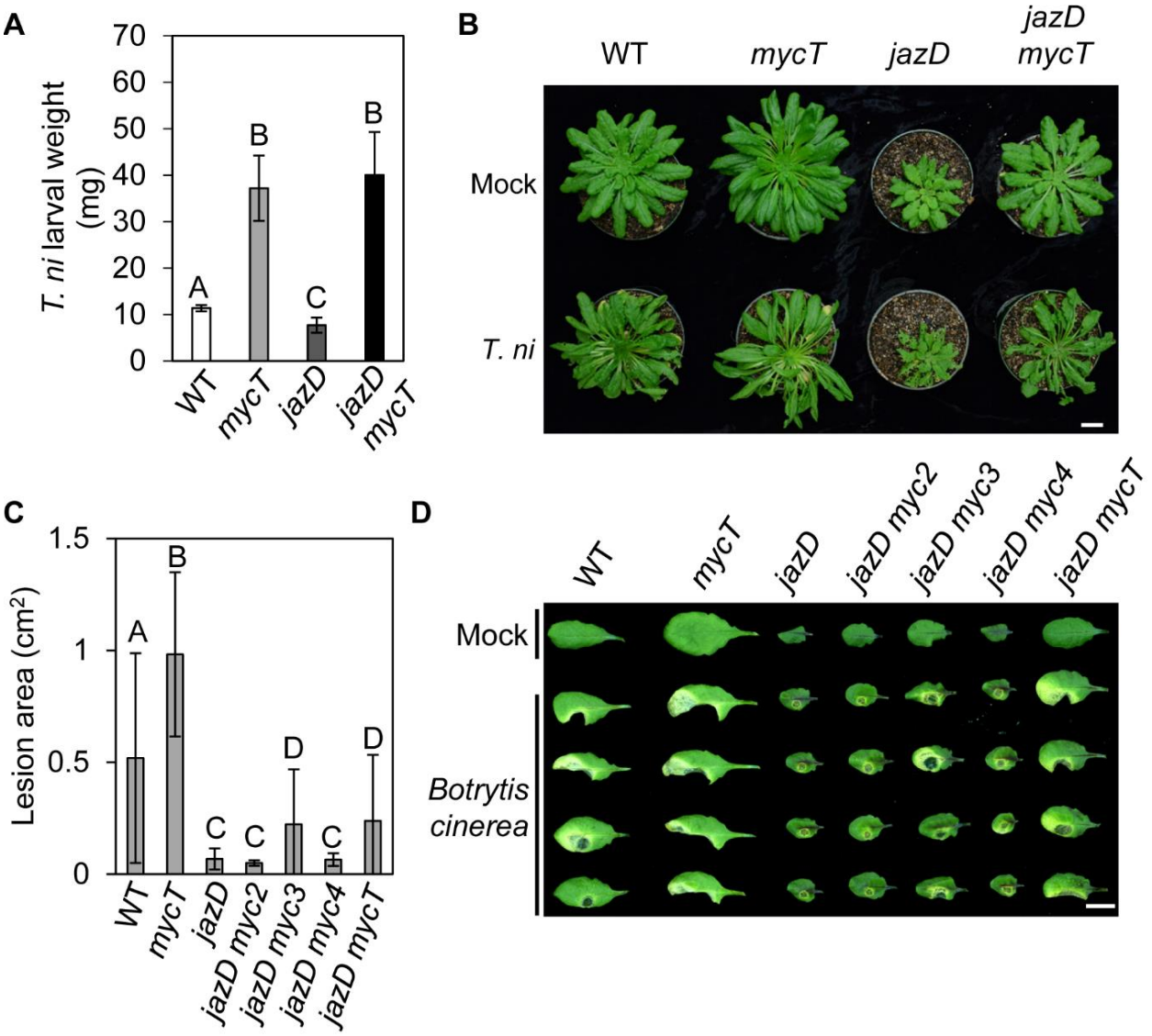

Figure 3.12. MYC TFs account for increased resistance of *jazD* to insect herbivores and necrotrophic pathogens.

(A) Average weight of *T. ni* larvae after nine days of feeding on WT Col-0 (WT), *mycT*, *jazD* and *jazD mycT* leaves. Plants were grown under short-day conditions (8-h-dark/16-h-light). Data show the mean ± SD of at least 26 larvae per genotype. Larval weight were $\log_2$ transformed according to Box-Cox Normality Plot for statistical tests. Capital letters denote significant differences according to Tukey's HSD test ($P < 0.05$).
(B) Representative short-day grown plants before and after challenged with *T. ni* larvae. Scale bars, 2 cm.
(C) Necrotic lesion area measured after six days of *Botrytis cinerea* (*B. cinerea*) infection of WT, *mycT, jazD, jazD myc2, jazD myc3, jazD myc4*, and *jazD mycT* leaves. Data show the mean ± SD of 13-15 leaves per genotype. Lesion area was $\log_2$ transformed according to Box-Cox Normality

Figure 3.12. (cont'd) Plot for statistical tests. Capital letters denote significant differences according to Tukey's HSD test ($P < 0.05$).
(D) Representative Arabidopsis leaves after infection with *B. cinerea* for six days. Scale bars, 1 cm.

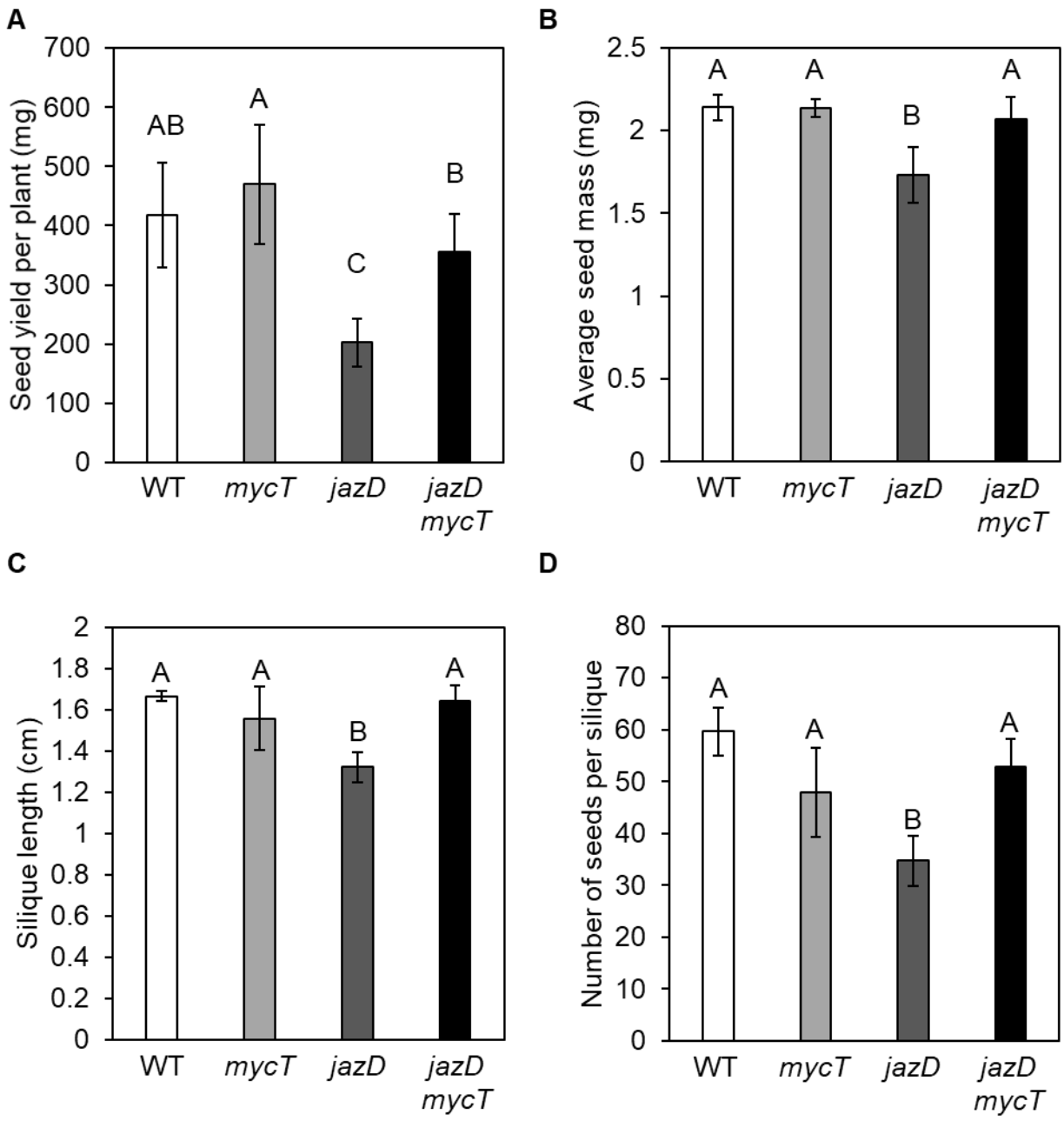

Figure 3.13. Compromised fertility of *jazD* is recovered by the *myc2 myc3 myc4* triple mutation.

(A) and **(B)** Seed yield (A) and seed mass (B) of WT Col-0 (WT), *mycT*, *jazD*, and *jazD mycT* plants. Plants were grown under long-day conditions (16-h-light/8-h-dark) until they stop generating new flowers. Seed yield was determined by collecting all seeds from individual plants and drying seeds with Drierite desiccant for two weeks prior to weighing. Average seed mass was determined by weighing batches of 100 seeds. Data show the mean ± SD of at least five plants per genotype. Capital letters denote significant differences according to Tukey's HSD test ($P < 0.05$).

Figure 3.13. (cont'd) (C) and **(D)** Silique length and number of seeds per silique of WT, *mycT*, *jazD* and *jazD mycT* plants. Fully elongated 7^{th}, 9^{th} and 11^{th} siliques were collected for examination of silique traits. Data show the mean ± SD of at least four plants per genotype. Capital letters denote significant differences according to Tukey's HSD test ($P < 0.05$).

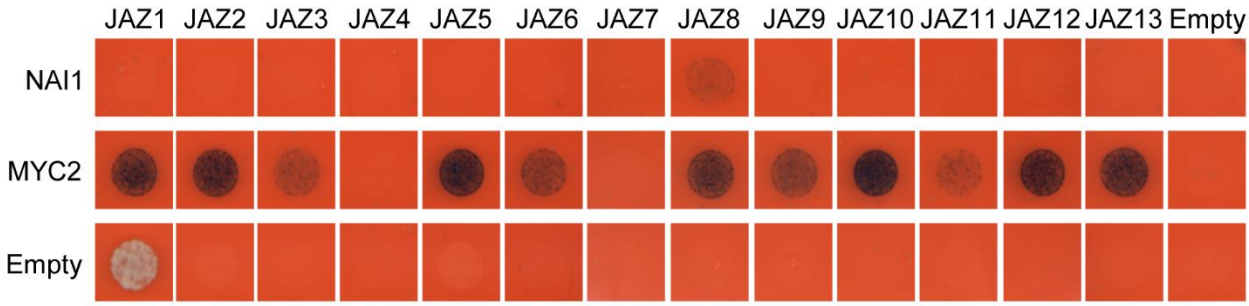

Figure 3.14. Yeast two-hybrid analysis of NAI1-JAZ interactions.

Yeast strains expressing both the bait (JAZs) and prey (NAI1 and MYC2) proteins were plated on media containing X-gal. Blue colony color indicates interaction while white colony color indicates no interaction. Images of yeast cells were taken after six days of incubation at 30 ºC. Empty bait (pGILDA) and prey (pB42AD) vectors were used as negative controls.

REFERENCES

REFERENCES

Agrawal, A.A. (1998). Induced responses to herbivory and increased plant performance. Science **279,** 1201-1202.

An, C.P., Li, L., Zhai, Q.Z., You, Y.R., Deng, L., Wu, F.M., Chen, R., Jiang, H.L., Wang, H., Chen, Q., and Li, C.Y. (2017). Mediator subunit MED25 links the jasmonate receptor to transcriptionally active chromatin. Proceedings of the National Academy of Sciences of the United States of America **114,** E8930-E8939.

Attaran, E., Major, I.T., Cruz, J.A., Rosa, B.A., Koo, A.J.K., Chen, J., Kramer, D.M., He, S.Y., and Howe, G.A. (2014). Temporal Dynamics of Growth and Photosynthesis Suppression in Response to Jasmonate Signaling. Plant Physiol **165,** 1302-1314.

Baldwin, I.T. (1998). Jasmonate-induced responses are costly but benefit plants under attack in native populations. Proceedings of the National Academy of Sciences of the United States of America **95,** 8113-8118.

Baud, S., Boutin, J.P., Miquel, M., Lepiniec, L., and Rochat, C. (2002). An integrated overview of seed development in Arabidopsis thaliana ecotype WS. Plant Physiol Bioch **40,** 151-160.

Bednarek, P., Pislewska-Bednarek, M., Svatos, A., Schneider, B., Doubsky, J., Mansurova, M., Humphry, M., Consonni, C., Panstruga, R., Sanchez-Vallet, A., Molina, A., and Schulze-Lefert, P. (2009). A Glucosinolate Metabolism Pathway in Living Plant Cells Mediates Broad-Spectrum Antifungal Defense. Science **323,** 101-106.

Behnke, H.D., and Eschlbeck, G. (1978). Dilated Cisternae in Capparales - Attempt Towards the Characterization of a Specific Endoplasmic-Reticulum. Protoplasma **97,** 351-363.

Bolton, M.D. (2009). Primary metabolism and plant defense--fuel for the fire. Mol Plant Microbe Interact **22,** 487-497.

Bones, A.M., and Rossiter, J.T. (2006). The enzymic and chemically induced decomposition of glucosinolates. Phytochemistry **67,** 1053-1067.

Bonnett, H.T., and Newcomb, E.H. (1965). Polyribosomes and Cisternal Accumulations in Root Cells of Radish. J Cell Biol **27,** 423-432.

Boter, M., Ruiz-Rivero, O., Abdeen, A., and Prat, S. (2004). Conserved MYC transcription factors play a key role in jasmonate signaling both in tomato and Arabidopsis. Gene Dev **18,** 1577-1591.

Boter, M., Golz, J.F., Gimenez-Ibanez, S., Fernandez-Barbero, G., Franco-Zorrilla, J.M., and Solano, R. (2015). FILAMENTOUS FLOWER Is a Direct Target of JAZ3 and Modulates Responses to Jasmonate. Plant Cell **27,** 3160-3174.

Campos, M.L., Kang, J.H., and Howe, G.A. (2014). Jasmonate-Triggered Plant Immunity. J Chem Ecol **40,** 657-675.

Campos, M.L., de Souza, C.M., de Oliveira, K.B.S., Dias, S.C., and Franco, O.L. (2018). The role of antimicrobial peptides in plant immunity. Journal of experimental botany **69,** 4997-5011.

Campos, M.L., Yoshida, Y., Major, I.T., de Oliveira Ferreira, D., Weraduwage, S.M., Froehlich, J.E., Johnson, B.F., Kramer, D.M., Jander, G., Sharkey, T.D., and Howe, G.A. (2016). Rewiring of jasmonate and phytochrome B signalling uncouples plant growth-defense tradeoffs. Nature communications **7,** 12570.

Chen, Q., Sun, J., Zhai, Q., Zhou, W., Qi, L., Xu, L., Wang, B., Chen, R., Jiang, H., Qi, J., Li, X., Palme, K., and Li, C. (2011). The basic helix-loop-helix transcription factor MYC2 directly represses PLETHORA expression during jasmonate-mediated modulation of the root stem cell niche in Arabidopsis. Plant Cell **23,** 3335-3352.

Chen, Y.M., Wang, Y., Huang, J.G., Zheng, C.C., Cai, C.X., Wang, Q.M., and Wu, C.A. (2017). Salt and methyl jasmonate aggravate growth inhibition and senescence in Arabidopsis seedlings via the JA signaling pathway. Plant Sci **261,** 1-9.

Chico, J.M., Fernandez-Barbero, G., Chini, A., Fernandez-Calvo, P., Diez-Diaz, M., and Solano, R. (2014). Repression of Jasmonate-Dependent Defenses by Shade Involves Differential Regulation of Protein Stability of MYC Transcription Factors and Their JAZ Repressors in Arabidopsis. Plant Cell **26,** 1967-1980.

Chini, A., Gimenez-Ibanez, S., Goossens, A., and Solano, R. (2016). Redundancy and specificity in jasmonate signalling. Current Opinion in Plant Biology **33,** 147-156.

Chini, A., Fonseca, S., Fernandez, G., Adie, B., Chico, J.M., Lorenzo, O., Garcia-Casado, G., Lopez-Vidriero, I., Lozano, F.M., Ponce, M.R., Micol, J.L., and Solano, R. (2007). The JAZ family of repressors is the missing link in jasmonate signalling. Nature **448,** 666-671.

Chung, H.S., and Howe, G.A. (2009). A critical role for the TIFY motif in repression of jasmonate signaling by a stabilized splice variant of the JASMONATE ZIM-domain protein JAZ10 in Arabidopsis. Plant Cell **21,** 131-145.

Clough, S.J., and Bent, A.F. (1998). Floral dip: a simplified method for Agrobacterium-mediated transformation of Arabidopsis thaliana. Plant J **16,** 735-743.

de Lucas, M., and Prat, S. (2014). PIFs get BRright: PHYTOCHROME INTERACTING FACTORs as integrators of light and hormonal signals. New Phytol **202,** 1126-1141.

Dombrecht, B., Xue, G.P., Sprague, S.J., Kirkegaard, J.A., Ross, J.J., Reid, J.B., Fitt, G.P., Sewelam, N., Schenk, P.M., Manners, J.M., and Kazan, K. (2007). MYC2 differentially modulates diverse jasmonate-dependent functions in Arabidopsis. Plant Cell **19,** 2225-2245.

Fernandez-Calvo, P., Chini, A., Fernandez-Barbero, G., Chico, J.M., Gimenez-Ibanez, S., Geerinck, J., Eeckhout, D., Schweizer, F., Godoy, M., Franco-Zorrilla, J.M., Pauwels, L., Witters, E., Puga, M.I., Paz-Ares, J., Goossens, A., Reymond, P., De Jaeger, G., and Solano, R. (2011). The Arabidopsis bHLH Transcription Factors MYC3 and MYC4 Are Targets of JAZ Repressors and Act Additively with MYC2 in the Activation of Jasmonate Responses. Plant Cell **23,** 701-715.

Figueroa, P., and Browse, J. (2015). Male sterility in Arabidopsis induced by overexpression of a MYC5-SRDX chimeric repressor. Plant J **81,** 849-860.

Frerigmann, H. (2016). Glucosinolate Regulation in a Complex Relationship - MYC and MYB - No One Can Act Without Each Other. Advances in Botanical Research **80,** 57-97.

Frerigmann, H., Berger, B., and Gigolashvili, T. (2014). bHLH05 Is an Interaction Partner of MYB51 and a Novel Regulator of Glucosinolate Biosynthesis in Arabidopsis. Plant Physiol **166,** 349-369.

Gao, C.H., Qi, S.H., Liu, K.G., Li, D., Jin, C.Y., Li, Z.W., Huang, G.Q., Hai, J.B., Zhang, M., and Chen, M.X. (2016). MYC2, MYC3, and MYC4 function redundantly in seed storage protein accumulation in Arabidopsis. Plant Physiol Bioch **108,** 63-70.

Gasperini, D., Chetelat, A., Acosta, I.F., Goossens, J., Pauwels, L., Goossens, A., Dreos, R., Alfonso, E., and Farmer, E.E. (2015). Multilayered Organization of Jasmonate Signalling in the Regulation of Root Growth. Plos Genet **11**.

Geem, K.R., Kim, D.H., Lee, D.W., Kwon, Y., Lee, J., Kim, J.H., and Hwang, I. (2018). Jasmonic acid-inducible TSA1 facilitates ER body formation. Plant J 10.1111/tpj.14112.

Glauser, G., Schweizer, F., Turlings, T.C.J., and Reymond, P. (2012). Rapid Profiling of Intact Glucosinolates in Arabidopsis Leaves by UHPLC-QTOFMS Using a Charged Surface Hybrid Column. Phytochem Analysis **23,** 520-528.

Guo, Q., Major, I.T., and Howe, G.A. (2018a). Resolution of growth-defense conflict: mechanistic insights from jasmonate signaling. Curr Opin Plant Biol **44,** 72-81.

Guo, Q., Yoshida, Y., Major, I.T., Wang, K., Sugimoto, K., Kapali, G., Havko, N.E., Benning, C., and Howe, G.A. (2018b). JAZ repressors of metabolic defense promote growth and reproductive fitness in Arabidopsis. Proceedings of the National Academy of Sciences of the United States of America **115,** E10768-E10777.

Havko, N.E., Major, I.T., Jewell, J.B., Attaran, E., Browse, J., and Howe, G.A. (2016). Control of Carbon Assimilation and Partitioning by Jasmonate: An Accounting of Growth-Defense Tradeoffs. Plants (Basel) **5**.

Heim, M.A., Jakoby, M., Werber, M., Martin, C., Weisshaar, B., and Bailey, P.C. (2003). The basic helix-loop-helix transcription factor family in plants: A genome-wide study of protein structure and functional diversity. Mol Biol Evol **20,** 735-747.

Herde, M., Koo, A.J., and Howe, G.A. (2013). Elicitation of jasmonate-mediated defense responses by mechanical wounding and insect herbivory. Methods Mol Biol **1011,** 51-61.

Hopkins, R.J., van Dam, N.M., and van Loon, J.J. (2009). Role of glucosinolates in insect-plant relationships and multitrophic interactions. Annual review of entomology **54,** 57-83.

Hornitschek, P., Kohnen, M.V., Lorrain, S., Rougemont, J., Ljung, K., Lopez-Vidriero, I., Franco-Zorrilla, J.M., Solano, R., Trevisan, M., Pradervand, S., Xenarios, I., and Fankhauser, C. (2012). Phytochrome interacting factors 4 and 5 control seedling growth in changing light conditions by directly controlling auxin signaling. Plant J **71,** 699-711.

Howe, G.A., and Jander, G. (2008). Plant immunity to insect herbivores. Annual Review of Plant Biology **59,** 41-66.

Howe, G.A., Major, I.T., and Koo, A.J. (2018). Modularity in Jasmonate Signaling for Multistress Resilience. Annual Review of Plant Biology **69,** 387-415.

Huot, B., Yao, J., Montgomery, B.L., and He, S.Y. (2014). Growth-defense tradeoffs in plants: a balancing act to optimize fitness. Mol Plant **7,** 1267-1287.

Iversen, T.H. (1970). Morphology, Occurrence, and Distribution of Dilated Cisternae of Endoplasmic Reticulum in Tissues of Plants of Cruciferae. Protoplasma **71,** 467-&.

Jiang, Y.J., Liang, G., Yang, S.Z., and Yu, D.Q. (2014). Arabidopsis WRKY57 Functions as a Node of Convergence for Jasmonic Acid- and Auxin-Mediated Signaling in Jasmonic Acid-Induced Leaf Senescence. Plant Cell **26,** 230-245.

Jofuku, K.D., Omidyar, P.K., Gee, Z., and Okamuro, J.K. (2005). Control of seed mass and seed yield by the floral homeotic gene APETALA2. Proceedings of the National Academy of Sciences of the United States of America **102,** 3117-3122.

Jorgensen, L.B. (1981). Myrosin cells and dilated cisternae of the endoplasmic reticulum in the order Capparales. Nordic J. Bot.

Katsir, L., Schilmiller, A.L., Staswick, P.E., He, S.Y., and Howe, G.A. (2008). COI1 is a critical component of a receptor for jasmonate and the bacterial virulence factor coronatine. Proceedings of the National Academy of Sciences of the United States of America **105,** 7100-7105.

Khare, D., Choi, H., Huh, S.U., Bassin, B., Kim, J., Martinoia, E., Sohn, K.H., Paek, K.H., and Lee, Y. (2017). Arabidopsis ABCG34 contributes to defense against necrotrophic pathogens by mediating the secretion of camalexin. Proceedings of the National Academy of Sciences of the United States of America **114,** E5712-E5720.

Leivar, P., and Monte, E. (2014). PIFs: Systems Integrators in Plant Development. Plant Cell **26,** 56-78.

Lorenzo, O., Chico, J.M., Sanchez-Serrano, J.J., and Solano, R. (2004). Jasmonate-insensitive1 encodes a MYC transcription factor essential to discriminate between different jasmonate-regulated defense responses in Arabidopsis. Plant Cell **16,** 1938-1950.

Major, I.T., Yoshida, Y., Campos, M.L., Kapali, G., Xin, X.F., Sugimoto, K., de Oliveira Ferreira, D., He, S.Y., and Howe, G.A. (2017). Regulation of growth-defense balance by the JASMONATE ZIM-DOMAIN (JAZ)-MYC transcriptional module. New Phytol **215,** 1533-1547.

Matsushima, R., Kondo, M., Nishimura, M., and Hara-Nishimura, I. (2003a). A novel ER-derived compartment, the ER body, selectively accumulates a beta-glucosidase with an ER-retention signal in Arabidopsis. Plant J **33,** 493-502.

Matsushima, R., Fukao, Y., Nishimura, M., and Hara-Nishimura, I. (2004). NAI1 gene encodes a basic-helix-loop-helix-type putative transcription factor that regulates the formation of an endoplasmic reticulum-derived structure, the ER body. Plant Cell **16,** 1536-1549.

Matsushima, R., Hayashi, Y., Kondo, M., Shimada, T., Nishimura, M., and Hara-Nishimura, I. (2002). An endoplasmic reticulum-derived structure that is induced under stress conditions in Arabidopsis. Plant Physiol **130,** 1807-1814.

Matsushima, R., Hayashi, Y., Yamada, K., Shimada, T., Nishimura, M., and Hara-Nishimura, I. (2003b). The ER body, a novel endoplasmic reticulum-derived structure in Arabidopsis. Plant and Cell Physiology **44,** 661-666.

Melotto, M., Mecey, C., Niu, Y., Chung, H.S., Katsir, L., Yao, J., Zeng, W., Thines, B., Staswick, P., Browse, J., Howe, G.A., and He, S.Y. (2008). A critical role of two positively charged amino acids in the Jas motif of Arabidopsis JAZ proteins in mediating coronatine- and jasmonoyl isoleucine-dependent interactions with the COI1 F-box protein. Plant J **55,** 979-988.

Muroi, A., Ishihara, A., Tanaka, C., Ishizuka, A., Takabayashi, J., Miyoshi, H., and Nishioka, T. (2009). Accumulation of hydroxycinnamic acid amides induced by pathogen infection and identification of agmatine coumaroyltransferase in Arabidopsis thaliana. Planta **230,** 517-527.

Nakano, R.T., Yamada, K., Bednarek, P., Nishimura, M., and Hara-Nishimura, I. (2014). ER bodies in plants of the Brassicales order: biogenesis and association with innate immunity. Front Plant Sci **5,** 73.

Nakano, R.T., Pislewska-Bednarek, M., Yamada, K., Edger, P.P., Miyahara, M., Kondo, M., Bottcher, C., Mori, M., Nishimura, M., Schulze-Lefert, P., Hara-Nishimura, I., and Bednarek, P. (2017). PYK10 myrosinase reveals a functional coordination between endoplasmic reticulum bodies and glucosinolates in Arabidopsis thaliana. Plant J **89,** 204-220.

Nelson, B.K., Cai, X., and Nebenfuhr, A. (2007). A multicolored set of in vivo organelle markers for co-localization studies in Arabidopsis and other plants. Plant J **51,** 1126-1136.

Niu, Y.J., Figueroa, P., and Browse, J. (2011). Characterization of JAZ-interacting bHLH transcription factors that regulate jasmonate responses in Arabidopsis. J Exp Bot **62,** 2143-2154.

Noir, S., Bomer, M., Takahashi, N., Ishida, T., Tsui, T.L., Balbi, V., Shanahan, H., Sugimoto, K., and Devoto, A. (2013). Jasmonate Controls Leaf Growth by Repressing Cell Proliferation and the Onset of Endoreduplication while Maintaining a Potential Stand-By Mode. Plant Physiol **161,** 1930-1951.

Nozue, K., Harmer, S.L., and Maloof, J.N. (2011). Genomic analysis of circadian clock-, light-, and growth-correlated genes reveals PHYTOCHROME-INTERACTING FACTOR5 as a modulator of auxin signaling in Arabidopsis. Plant Physiol **156,** 357-372.

Ogasawara, K., Yamada, K., Christeller, J.T., Kondo, M., Hatsugai, N., Hara-Nishimura, I., and Nishimura, M. (2009). Constitutive and inducible ER bodies of Arabidopsis thaliana accumulate distinct beta-glucosidases. Plant Cell Physiol **50,** 480-488.

Pauwels, L., Morreel, K., De Witte, E., Lammertyn, F., Van Montagu, M., Boerjan, W., Inze, D., and Goossens, A. (2008). Mapping methyl jasmonate-mediated transcriptional reprogramming of metabolism and cell cycle progression in cultured Arabidopsis cells. Proceedings of the National Academy of Sciences of the United States of America **105,** 1380-1385.

Pauwels, L., Barbero, G.F., Geerinck, J., Tilleman, S., Grunewald, W., Perez, A.C., Chico, J.M., Vanden Bossche, R., Sewell, J., Gil, E., Garcia-Casado, G., Witters, E., Inze, D., Long, J.A., De Jaeger, G., Solano, R., and Goossens, A. (2010). NINJA connects the co-repressor TOPLESS to jasmonate signalling. Nature **464,** 788-U169.

Penninckx, I.A., Eggermont, K., Terras, F.R., Thomma, B.P., De Samblanx, G.W., Buchala, A., Metraux, J.P., Manners, J.M., and Broekaert, W.F. (1996). Pathogen-induced systemic activation of a plant defensin gene in Arabidopsis follows a salicylic acid-independent pathway. Plant Cell **8,** 2309-2323.

Pieterse, C.M.J., Leon-Reyes, A., Van der Ent, S., and Van Wees, S.C.M. (2009). Networking by small-molecule hormones in plant immunity. Nature chemical biology **5,** 308-316.

Porra, R.J., Thompson, W.A., and Kriedemann, P.E. (1989). Determination of Accurate Extinction Coefficients and Simultaneous-Equations for Assaying Chlorophyll-a and Chlorophyll-B Extracted with 4 Different Solvents - Verification of the Concentration of Chlorophyll Standards by Atomic-Absorption Spectroscopy. Biochim Biophys Acta **975,** 384-394.

Qi, T., Huang, H., Song, S., and Xie, D. (2015a). Regulation of Jasmonate-Mediated Stamen Development and Seed Production by a bHLH-MYB Complex in Arabidopsis. Plant Cell **27,** 1620-1633.

Qi, T.C., Wang, J.J., Huang, H., Liu, B., Gao, H., Liu, Y.L., Song, S.S., and Xie, D.X. (2015b). Regulation of Jasmonate-Induced Leaf Senescence by Antagonism between bHLH Subgroup IIIe and IIId Factors in Arabidopsis. Plant Cell **27,** 1634-1649.

Qi, T.C., Song, S.S., Ren, Q.C., Wu, D.W., Huang, H., Chen, Y., Fan, M., Peng, W., Ren, C.M., and Xie, D.X. (2011). The Jasmonate-ZIM-Domain Proteins Interact with the WD-Repeat/bHLH/MYB Complexes to Regulate Jasmonate-Mediated Anthocyanin Accumulation and Trichome Initiation in Arabidopsis thaliana. Plant Cell **23,** 1795-1814.

Roux, F., Gasquez, J., and Reboud, X. (2004). The dominance of the herbicide resistance cost in several Arabidopsis thaliana mutant lines. Genetics **166,** 449-460.

Rowe, H.C., and Kliebenstein, D.J. (2007). Elevated genetic variation within virulence-associated Botrytis cinerea polygalacturonase loci. Mol Plant Microbe In **20,** 1126-1137.

Rubio, V., Shen, Y.P., Saijo, Y., Liu, Y.L., Gusmaroli, G., Dinesh-Kumar, S.P., and Deng, X.W. (2005). An alternative tandem affinity purification strategy applied to Arabidopsis protein complex isolation. Plant J **41,** 767-778.

Santner, A., Calderon-Villalobos, L.I.A., and Estelle, M. (2009). Plant hormones are versatile chemical regulators of plant growth. Nat Chem Biol **5,** 301-307.

Schilmiller, A.L., Miner, D.P., Larson, M., McDowell, E., Gang, D.R., Wilkerson, C., and Last, R.L. (2010). Studies of a Biochemical Factory: Tomato Trichome Deep Expressed Sequence Tag Sequencing and Proteomics. Plant Physiol **153,** 1212-1223.

Schweizer, F., Fernandez-Calvo, P., Zander, M., Diez-Diaz, M., Fonseca, S., Glauser, G., Lewsey, M.G., Ecker, J.R., Solano, R., and Reymond, P. (2013). Arabidopsis Basic Helix-Loop-Helix Transcription Factors MYC2, MYC3, and MYC4 Regulate Glucosinolate Biosynthesis, Insect Performance, and Feeding Behavior. Plant Cell **25,** 3117-3132.

Shyu, C., Figueroa, P., DePew, C.L., Cooke, T.F., Sheard, L.B., Moreno, J.E., Katsir, L., Zheng, N., Browse, J., and Howe, G.A. (2012). JAZ8 Lacks a Canonical Degron and Has an EAR Motif That Mediates Transcriptional Repression of Jasmonate Responses in Arabidopsis. Plant Cell **24,** 536-550.

Song, S.S., Qi, T.C., Huang, H., Ren, Q.C., Wu, D.W., Chang, C.Q., Peng, W., Liu, Y.L., Peng, J.R., and Xie, D.X. (2011). The Jasmonate-ZIM Domain Proteins Interact with the R2R3-MYB Transcription Factors MYB21 and MYB24 to Affect Jasmonate-Regulated Stamen Development in Arabidopsis. Plant Cell **23,** 1000-1013.

Thines, B., Katsir, L., Melotto, M., Niu, Y., Mandaokar, A., Liu, G., Nomura, K., He, S.Y., Howe, G.A., and Browse, J. (2007). JAZ repressor proteins are targets of the SCF(COI1) complex during jasmonate signalling. Nature **448,** 661-665.

Wang, J.Z., Li, B., Xiao, Y., Ni, Y., Ke, H., Yang, P., de Souza, A., Bjornson, M., He, X., Shen, Z., Balcke, G.U., Briggs, S.P., Tissier, A., Kliebenstein, D.J., and Dehesh, K. (2017).

Initiation of ER Body Formation and Indole Glucosinolate Metabolism by the Plastidial Retrograde Signaling Metabolite, MEcPP. Mol Plant **10,** 1400-1416.

Wasternack, C., and Hause, B. (2013). Jasmonates: biosynthesis, perception, signal transduction and action in plant stress response, growth and development. An update to the 2007 review in Annals of Botany. Ann Bot-London **111,** 1021-1058.

Watanabe, S., Shimada, T.L., Hiruma, K., and Takano, Y. (2013). Pathogen infection trial increases the secretion of proteins localized in the endoplasmic reticulum body of Arabidopsis. Plant Physiol **163,** 659-664.

Wittstock, U., and Burow, M. (2010). Glucosinolate breakdown in Arabidopsis: mechanism, regulation and biological significance. Arabidopsis Book **8,** e0134.

Wu, J.Q., and Baldwin, I.T. (2010). New Insights into Plant Responses to the Attack from Insect Herbivores. Annu Rev Genet **44,** 1-24.

Xie, D.X., Feys, B.F., James, S., Nieto-Rostro, M., and Turner, J.G. (1998). COI1: an Arabidopsis gene required for jasmonate-regulated defense and fertility. Science **280,** 1091-1094.

Yamada, K., Nagano, A.J., Nishina, M., Hara-Nishimura, I., and Nishimura, M. (2008). NAI2 Is an Endoplasmic Reticulum Body Component That Enables ER Body Formation in Arabidopsis thaliana. Plant Cell **20,** 2529-2540.

Yamada, K., Nagano, A.J., Ogasawara, K., Hara-Nishimura, I., and Nishimura, M. (2009). The ER body, a new organelle in Arabidopsis thaliana, requires NAI2 for its formation and accumulates specific beta-glucosidases. Plant signaling & behavior **4,** 849-852.

Yan, Y.X., Stolz, S., Chetelat, A., Reymond, P., Pagni, M., Dubugnon, L., and Farmer, E.E. (2007). A downstream mediator in the growth repression limb of the jasmonate pathway. Plant Cell **19,** 2470-2483.

Yang, D.L., Yao, J., Mei, C.S., Tong, X.H., Zeng, L.J., Li, Q., Xiao, L.T., Sun, T.P., Li, J.G., Deng, X.W., Lee, C.M., Thomashow, M.F., Yang, Y.N., He, Z.H., and He, S.Y. (2012). Plant hormone jasmonate prioritizes defense over growth by interfering with gibberellin signaling cascade. Proceedings of the National Academy of Sciences of the United States of America **109,** E1192-E1200.

Zhang, F., Yao, J., Ke, J., Zhang, L., Lam, V.Q., Xin, X.F., Zhou, X.E., Chen, J., Brunzelle, J., Griffin, P.R., Zhou, M., Xu, H.E., Melcher, K., and He, S.Y. (2015). Structural basis of JAZ repression of MYC transcription factors in jasmonate signalling. Nature **525,** 269-273.

Zhang, X., Ji, Y.S., Xue, C., Ma, H.H., Xi, Y.L., Huang, P.X., Wang, H., An, F.Y., Li, B.S., Wang, Y.C., and Guo, H.W. (2018). Integrated Regulation of Apical Hook Development by Transcriptional Coupling of EIN3/EIL1 and PIFs in Arabidopsis. Plant Cell **30,** 1971-1988.

Zhang, Y., and Turner, J.G. (2008). Wound-Induced Endogenous Jasmonates Stunt Plant Growth by Inhibiting Mitosis. Plos One **3,** e3699.

Zhu, Z.Q., An, F.Y., Feng, Y., Li, P.P., Xue, L., Mu, A., Jiang, Z.Q., Kim, J.M., To, T.K., Li, W., Zhang, X.Y., Yu, Q., Dong, Z., Chen, W.Q., Seki, M., Zhou, J.M., and Guo, H.W. (2011). Derepression of ethylene-stabilized transcription factors (EIN3/EIL1) mediates jasmonate and ethylene signaling synergy in Arabidopsis. Proceedings of the National Academy of Sciences of the United States of America **108,** 12539-12544.

CHAPTER FOUR - USE OF GENETIC SUPPRESSOR SCREENS TO UNCOUPLE GROWTH-DEFENSE ANTAGONISM

Abstract

Plants deter biotic aggressors with innate immune responses that are energetically demanding and that are often accompanied by growth restriction. Despite the impact of growth-defense tradeoffs on many aspects of plant development and productivity, the molecular mechanisms connecting defense with growth are not well understood. Here, we used a genetic suppressor screen to identify EMS-induced mutants in which the slow-growth phenotype of a *jaz* decuple mutant (*jazD*) is rescued without apparent disruption of defense traits. Hypocotyl elongation assays performed with monochromatic light showed that ten of 13 *suppressors of jazD* (*sjd*) were insensitive to red light, suggesting that the underlying causal mutations are associated with red light signaling, such as *PHYTOCHROME B* (*PHYB*). Assessment of apical hook formation of the 13 *sjd* lines revealed that the hook curvature of *sjd10* was attenuated. Comparison between *jazD* and two non-red-light-insensitive suppressors (*sjd56* and *sjd78*) showed that whereas both mutants exhibited increased growth, only *sjd56* retained the defense phenotypes of *jazD*. Subsequent characterization of these suppressors promises to identify mechanisms that uncouple growth-defense tradeoffs in plants.

Introduction

As a consequence of their sessile nature, plant growth and development are subject to restraint by resource limitations in the microenvironment. In response to attack by biotic aggressors that consume plant tissues as a food source, plants mount various defense responses that require acquisition of photoassimilates and other nutrients (Havko et al., 2016; Guo et al., 2018a). Considerable resources are required for the biosynthesis, modification, transport and storage of defense compounds, which are largely derived from precursors in primary metabolism (Gershenzon, 1994). Therefore, defense induction is presumed to generate allocation costs that reflect partitioning to defense pathways at the expense of growth and other physiological processes (Zust and Agrawal, 2017). In addition to allocation costs, immune responses can also incur ecological costs (Simms, 1992; Karasov et al., 2017; Zust and Agrawal, 2017). For instance, high defense levels may unintentionally repel mutualists (e.g., pollinators) required for seed production (Strauss et al., 1999). Owing to the tradeoffs between growth and immunity, efforts to improve crop productivity through breeding may select against robust expression of defense traits (Chen et al., 2015). Thus, advances in understanding the molecular mechanisms that govern the antagonistic relationships between growth and defense may help to boost the development of crop varieties having both high yield and resilience to biotic stresses.

Jasmonic acid and its derivatives (JAs) constitute a class of lipid-derived compounds that regulate plant immunity against insect herbivores and necrotrophic pathogens, and also play important roles in growth and reproduction (Wasternack and Hause, 2013; Guo et al., 2018a; Guo et al., 2018b; Howe et al., 2018). The bioactive form of JA, JA-Ile, is perceived by the receptor protein CORONATINE INSENSITIVE 1 (COI1) (Xie et al., 1998; Katsir et al., 2008), which is part of the Skp1/Cullin/F-box (SCF^{COI1}) E3 ubiquitin ligase complex that ubiquitinates

JASMONATE ZIM DOMAIN (JAZ) transcriptional repressors upon JA perception (Thines et al., 2007; Chini et al., 2016). Ubiquitinated JAZs are degraded by the 26S proteasome, followed by the release of JA-responsive transcription factors (TFs), the best examples of which are bHLH MYC TFs (Major et al., 2017; Howe et al., 2018).

Although the mechanisms by which JA deploys immune responses against insect herbivores and pathogens have been intensively studied, it is still poorly understood how JA restricts growth. In a previous study, Campos *et al.* combined mutations in five *JAZ* genes to construct a *jaz* quintuple (*jazQ*) mutant that displays constitutive activation of JA signaling and growth-defense antagonism (Campos et al., 2016). Visual screening of *jazQ* mutagenized with ethyl methanesulfonate (EMS) identified suppressors that restored the slow growth of *jazQ* without impairing defense (Campos et al., 2016). Among these suppressors was *suppressor of jazQ 11* (*sjq11*), which carries a null mutation in *PHYTOCHROME B* (*PHYB*), a red light receptor that inhibits the activity of growth-promoting PHYTOCHROME-INTERACTING FACTORS (PIFs) (Campos et al., 2016). Genetic reconstruction of *jazQ phyB* confirmed that removal of phyB in the *jazQ* background is sufficient to recover the growth phenotype of *jazQ* without compromising defense, and suggested that rewiring of JA and red light signaling pathways can allow simultaneous growth and defense (Campos et al., 2016). Despite this progress, much remains to be learned about how plant growth is impacted by various levels of defense; the constitutive defense responses exhibited by *jazQ* are relatively modest and do not appear to have allocation costs under the growth conditions employed (Campos et al., 2016; Guo et al., 2018b). It thus remains to be determined whether growth-defense antagonism can also be uncoupled when higher levels of defense traits generate allocation costs.

In this study, we exploited a recently developed *jaz* decuple (*jazD*) mutant in which growth-defense tradeoffs are much stronger than those observed in *jazQ* plants as a consequence of more severe depletion of JAZ repressors (Guo et al., 2018b). Screening of an EMS-mutagenized population of *jazD* plants identified 13 *suppressors of jazD* (*sjd*) that partially recovered the stunted growth of *jazD* while retaining high levels of anthocyanin accumulation as a proxy for defense traits. Most of the *sjd* mutants were insensitive to red light, suggesting defects in red light signaling like loss of phyB function. Among the three (*sjd10*, *sjd56* and *sjd78*) non-red-light-insensitive *sjd* mutants, one (*sjd10*) displayed an attenuated apical hook phenotype. Examination of growth and defense traits revealed partial uncoupling of growth-defense antagonism in *sjd56*. These collective findings highlight the effectiveness of using genetic suppressor screens to uncouple growth-defense tradeoffs.

Results

Identification of *suppressors of jazD*

To better understand the mechanisms by which activation of plant defense pathways antagonize vegetative growth, we devised a genetic screen to identify plants that exhibit enhanced defense responses without growth penalties. We previously showed that a *jaz* decuple (*jazD*) mutant defective in ten *JAZ* genes (*JAZ1/2/3/4/5/6/7/9/10/13*) displays not only robust resistance to insect herbivores and necrotrophic pathogens, but also stunted vegetative growth and development (Guo et al., 2018b). We exploited these phenotypes of *jazD* as a tool to dissect the molecular components involved in growth-defense antagonism. To this end, we mutagenized *jazD* seeds with EMS and visually screened approximately 30,000 M2 plants for individuals that showed recovery of the slow-growth phenotype but retention of anthocyanin accumulation, a marker of JA-regulated defense (Figure 4.1A). A total of 13 *suppressor of jazD* (*sjd*) lines were identified (Table 4.1 and Figure 4.1B-G).

One class of *sjd* mutants are insensitive to monochromatic red light

Among the 13 *sjd* mutants identified, 11 (*sjd1*, *sjd2*, *sjd4*, *sjd40*, *sjd56*, *sjd83*, *sjd93*, *sjd109*, *sjd110*, *sjd111* and *sjd113*) of them displayed similar phenotypes, including long petioles and elongated hypocotyls under white light. These phenotypes were confirmed in the M3 generation and were reminiscent of phenotypes displayed by photomorphogenic mutants. It has been shown that a null mutation of the photoreceptor gene *PHYB* in the *jazQ* background recovers the growth of *jazQ* without altering its defense traits (Campos et al., 2016). Thus, we hypothesized that this group of morphologically similar *sjd* mutants may be impaired in light signaling. To test this possibility, the hypocotyl elongation response of *sjd* seedlings (M3 generation) to monochromatic light was

compared to well-characterized photoreceptor mutants. We found that ten *sjd* mutants (*sjd1*, *sjd2*, *sjd4*, *sjd40*, *sjd83*, *sjd93*, *sjd109*, *sjd110*, *sjd111* and *sjd113*) were insensitive to red light like *phyB*, but responded normally to both far red and blue light (Figure 4.2 and 4.3), suggesting that these suppressors carry mutations in components of red light signaling. One mutant (*sjd56*) responded normally to red and far red light but was insensitive to blue light like the blue light receptor mutant *cry1* (Figure 4.3). The identification of multiple suppressor mutants insensitive to light perception suggests a potentially important role of light signaling pathways in JA-driven growth-defense decisions.

Apical hook formation of *sjd10* is attenuated

The growth inhibitory properties of ethylene (Dubois et al., 2018), together with constitutive activation of ethylene responses in *jazD* (Guo et al., 2018b), raised the possibility that *sjd* mutants are impaired in ethylene signaling. To test this, we compared the apical hook curvature of dark-grown wild-type and *sjd* seedlings, which is a well characterized ethylene response (De Paepe and Van Der Straeten, 2005; Li and Guo, 2007). One mutant, *sjd10*, displayed a clearly attenuated apical hook (Figure 4.4A and 4.4B), suggesting that *sjd10* may be defective in ethylene signaling.

In addition to the attenuated apical hook formation, *sjd10* also produced leaves that were broader than those of the *jazD* parental line (Table 4.1 and Figure 4.1C). However, analysis of a segregating F2 population from a *sjd10* to *jazD* backcross showed that the broad-leaf phenotype did not co-segregate with the increased size of *sjd10* rosettes (Figure 4.4C).

Growth-defense antagonism is partially uncoupled in *sjd56*

We next examined the growth and defense phenotypes of the *sjd56* and *sjd78* mutants, which had normal light sensitivities. Measurements of leaf biomass and projected leaf area showed that the slow-growth phenotype of *jazD* was partially rescued in *sjd56* and *sjd78* (Figure 4.5). These two suppressor mutants also accumulated leaf anthocyanins to a similar level as parental *jazD* (Figure 4.6A). To assess whether *sjd56* and *sjd78* retained resistance to necrotrophic pathogens, we inoculated leaves with *Botrytis cinerea* spores. Whereas *sjd56* was as resistant to this pathogen as *jazD*, the disease lesion area on *sjd78* was much larger, comparable to that of WT leaves (Figure 4.6B). Feeding assays performed with *Trichoplusia ni* larvae showed that *sjd56*, but not *sjd78*, maintained elevated resistance to this generalist insect herbivore (Figure 4.6C and 4.6D). These results demonstrate that *sjd56* partially suppressed the growth-restriction phenotype of *jazD* without impairing several defense traits. In contrast to *sjd56*, the partial growth restoration of *sjd78* was associated with loss of defense.

Genetic analysis of *sjd56* and *sjd78*

As an initial step toward identification of causal mutations in *sjd56* and *sjd78*, *sjd56* and *sjd78* were each backcrossed to *jazD* (using *jazD* as the female parent), and the resulting BC1F2 populations showed segregation of rosette size for both mutants (Figure 4.7). The segregation ratios for *sjd56* and *sjd78* were approximately 1:7 and 1:3, respectively, and generally consistent with Mendelian inheritance (Table 4.2), suggesting that the increased growth of each mutant was caused by a single recessive mutation in each suppressor line. A second backcross used to generate BC2F2 populations validated the conclusion that increased rosette size in each mutant was likely caused by a single recessive mutation (Table 4.2 and Figure 4.8).

To determine whether the blue light-insensitive phenotype of *sjd56* was linked to the growth phenotype, BC1F3 seeds from 15 independent BC1F2 plants exhibiting increased growth were used for hypocotyl elongation assays under blue light. The results revealed a wide range of hypocotyl lengths in these lines (Figure 4.9), indicating that blue light insensitivity of *sjd56* does not appear to be linked to the increased rosette growth phenotype.

Discussion

JA is a key modulator of plant defense responses (Wasternack, 2015). In contrast to its positive role in fending off herbivorous insects and pathogens, this hormone often negatively affects growth and reproductive fitness (Baldwin, 1998; Yan et al., 2007; Zhang and Turner, 2008; Gao et al., 2016; Guo et al., 2018a; Guo et al., 2018b), giving rise to growth-defense antagonism in plants. Elucidation of the mechanisms that mitigate JA-mediated growth inhibition may benefit agricultural practices to develop crop species with desirable growth and defense traits. A previous study using *jazQ* as a tool to screen for suppressors that uncouple growth-defense tradeoffs showed that rewiring of the JA and phyB signaling pathways allows plants to maintain robust growth and defense at the same time (Campos et al., 2016). However, the JA responses in *jazQ* are moderate, and thus the expression of defense traits in *jazQ* does not represent situations when defense traits are activated to an extreme extent. Here, we performed a genetic suppressor screen using *jazD*, in which defense responses are highly activated in comparison to *jazQ* (Guo et al., 2018b). Our study showed that mutations in components of the red light signaling pathway reduced the intensity of growth restriction by *jazD*. Comparison of growth and defense traits in *jazD* and *sjd56* demonstrated that mutations in *sjd56* partially recovered the growth traits of *jazD* while retaining its enhanced defense. Our findings build on previous studies (Campos et al., 2016) showing that genetic suppressor screens provide a powerful approach to better understand the antagonistic relationship between growth and JA-mediated defense. Further characterization of the *sjd* mutants described here should provide insight into the molecular mechanisms by which resource allocation to growth and defense pathways is regulated.

Among the 13 *sjd* mutants identified in this study, ten were insensitive to red light (Figure 4.2A). The ratio of red (R) light to far red (FR) light is detected by the phytochrome photoreceptors,

including phyB (Ballare, 2014). When the ratio of R:FR is high, phyB is in its active form and inhibits the activity of PIF TFs (Bae and Choi, 2008; Fiorucci and Fankhauser, 2017), which promote cell elongation (de Lucas and Prat, 2014; Leivar and Monte, 2014). Under shading conditions when the R:FR ratio is low, phyB is inactivated and increased PIF activity enhances growth (Bae and Choi, 2008; Fiorucci and Fankhauser, 2017). Thus, simultaneous removal of phyB and JAZ may promote growth and defense at the same time by relieving repression of growth (i.e. PIFs)- and defense (i.e. MYCs)-promoting TFs. Given the previous identification of *phyB* as a mutation that uncouples growth-defense tradeoffs in *jazQ* (Campos et al., 2016), it seems likely that *phyB* mutations are also responsible for reverting the growth phenotype of some red light-insensitive *sjd* mutants described here. Genetic complementation tests and sequencing of *PHYB* in these mutants are needed to test this hypothesis. It will also be important to genetically reconstruct *jazD phyB* with a null *phyB* allele to exclude the possibility that spurious mutations resulting from EMS mutagenesis contribute to the phenotypes of these *sjd* mutations.

Blue light is perceived by the cryptochrome photoreceptors (CRY1 and CRY2) (Chaves et al., 2011). Recent studies demonstrate that CRY1 and CRY2 physically interact with PIF4 and PIF5, suggesting that CRYs suppress elongation growth (Pedmale et al., 2016). However, although *sjd56* was insensitive to blue light, subsequent analyses demonstrated that *cry1* or *cry2* (data not shown) were unlikely to be the causal mutations in this suppressor mutant. Reoccurrence of red light insensitivity but no other monochromatic light insensitivity suggests that red light signaling may perform special roles in regulating plant growth. Further studies are needed to reveal the underlining mechanisms and to verify the causal mutations in *sjd56*.

Inspection of the apical hook revealed attenuated apical hook curvature for *sjd10* (Figure 4.4A and 4.4B). The apical hook protects cotyledons and meristem tissues during seedling

emergence from the soil, and is mediated by a number of plant hormones, including auxin, ethylene, gibberellins, and brassinosteroids (Bleecker et al., 1988; Guzman and Ecker, 1990; Lehman et al., 1996; Achard et al., 2003; Li et al., 2004; Vriezen et al., 2004; De Grauwe et al., 2005; Vandenbussche et al., 2010). Among these hormones, previous studies have shown that JA antagonizes ethylene signaling to inhibit apical hook formation (Turner et al., 2002). MYC2 physically interacts with ETHYLENE-INSENSITIVE3 (EIN3) to attenuate its transcriptional activity in promoting apical hook curvature (Song et al., 2014). Consistent with these studies, hook curvature of *jazD* in response to treatment with the ethylene precursor 1-aminocyclopropane-1-carboxylic acid (ACC) is reduced (Guo et al., 2018b). The ethylene signaling cascade is activated when ethylene is recognized by members of the cognate receptor family, which in Arabidopsis consists of ETHYLENE RESPONSE 1 (ETR1), ETR2, ETHYLENE RESPONSE SENSOR 1 (ERS1), ERS2 and ETHYLENE INSENSITIVE 4 (EIN4) (Merchante et al., 2013). Perception of ethylene activates EIN2 and subsequently stabilizes EIN3 and EIN3-LIKE 1 (EIL1) TFs to induce various ethylene responses (Merchante et al., 2013). Mutants deficient in the ethylene signaling pathway (i.e. *ein2-1* and *ein3-1 eil1-3*) exhibit reduced hook curvature in the absence of ACC (Song et al., 2014). Thus, altered apical hook formation in *sjd10* raises the possibility that the ethylene signaling pathway is disrupted in this mutant. However, we cannot exclude the possibility that the attenuated hook curvature of *sjd10* results from mutations of components in other hormone signaling pathways. For example, the establishment of an auxin gradient in the hypocotyl is essential for proper hook development (Schwark and Schierle, 1992). A recent study showed that a mutant defective in the auxin influx carrier LAX3 displayed reduced hook curvature without ACC treatment (Vandenbussche et al., 2010). Therefore, *sjd10* could also harbor a mutation in auxin-related genes. In an F2 population derived from a cross between *sjd10* and *jazD*, we

observed that rosette size and morphology did not segregate in a manner consistent with a single recessive mutation (Figure 4.4C). In future studies, it will be necessary to determine whether the attenuated apical hook formation co-segregates with the large-rosette phenotype.

In addition to altered apical hook formation, ethylene retards leaf growth by suppressing cell division and cell elongation (Dubois et al., 2018). For example, one of the ethylene response factors (ERFs) BOLITA activates type II *TEOSINTE BRANCHED 1*/*CYCLOIDEA*/*PCF* (*TCP*) genes, which in turn induce *RETINOBLASTOMA RELATED 1* (*RBR1*) (Marsch-Martinez et al., 2006). *RBR1* encodes a protein that represses E2Fa by phosphorylation, and consequently inhibits progression of cell cycle into the S-phase (Marsch-Martinez et al., 2006). Another ethylene response factor ERF6 induces the gibberellin-degrading enzyme GIBBERELLIN 2-OXIDASE 6, leading to the stabilization of DELLA repressors (Dubois et al., 2013), which are associated with the inhibition of cell expansion (Claeys et al., 2014). Therefore, it is conceivable that mutations of ethylene signaling components in *jazD* may result in growth recovery. If the causal mutation in *sjd10* is related to ethylene signaling, this mutant may be a good candidate to dissect how JA and ethylene signaling pathways act together to control growth and defense.

Methods

jazD suppressor screen

Approximately 30,000 *jazD* seeds were mutagenized by immersion in a solution of 0.1% or 0.2% (v/v) EMS (Sigma-Aldrich) for 16 h at room temperature, with constant agitation (Campos et al., 2016). Seeds (M1 generation) were thoroughly washed with H_2O, stratified in the dark at 4 ºC for two days and then immediately sowed on soil. M2 seed was collected from 24 pools of self-pollinated M1 plants (approximately 1,000 M1 plants/pool). Soil-grown M2 plants were visually screened for individuals with a larger rosette size than *jazD* and accumulation of anthocyanin. Putative *sjd* (*suppressor of jazD*) mutants were rescreened in the M3 generation to confirm heritability of phenotypes.

Genetic analysis of *sjd* mutants

sjd mutants (M3 generation) were used as the recurring male parent for backcrossing to the *jazD* parental line. For segregation analysis of BC1F2 and BC2F2 populations, seeds were sowed on half-strength Linsmaier and Skoog (LS; Caisson Labs) plates supplemented with 0.8% (w/v) sucrose and stratified at 4 ºC in dark for four days. Plates were then transferred to a growth chamber maintained at 20 ºC and incubated for eight days under 16-h-light/8-h-dark conditions (80 μmol m^{-2} s^{-1}). Seedlings were transferred to soil, in square pots containing four seedlings per pot. Potted plants were covered with a transparent plastic dome for two days and were maintained under a 16-h light (100 μmol m^{-2} s^{-1}) and 8-h dark photoperiod at 20 ºC until photographed.

Hypocotyl elongation assays under monochromatic light

WT (Col-0), *jazD* and *sjd* (M3 generation) seeds were sowed on half-strength LS plates supplemented with 0.8% (w/v) sucrose and stratified at 4 ºC in dark for four days. Plates were then transferred to monochromatic LED chambers outfitted to emit blue (470 ± 20 nm, 25 μmol m^{-2} s^{-1}), red (670 ± 20 nm, 50 μmol m^{-2} s^{-1}) or far-red (740 ± 20 nm, 5 μmol m^{-2} s^{-1}) light. As controls, the light-sensing mutants *cry1-400*, *phyA-75* and *phyB-9* and were included (Reed et al., 1993; Reed et al., 1994; Ruckle et al., 2007). WT and mutant lines were grown on the same plate to control for plate-to-plate variation. Following seven days of growth under the specified monochromatic light conditions, seedling hypocotyls were placed between transparent films and scanned for length measurement using the ImageJ software (https://imagej.nih.gov/ij/).

Measurement of apical hook curvature

Seedlings were grown on 0.7% (w/v) agar media containing half-strength LS salts supplemented with 0.8% (w/v) sucrose. After stratification at 4 ºC in the dark for three days, plates were incubated horizontally in the dark at 20 ºC for four days. Images of apical hook were photographed. The angle of apical hook curvature was measured by ImageJ software (https://imagej.nih.gov/ij/). The angle of apical hook curvature is defined as 180° minus (when the hook is not exaggerated) or plus (in the case of hook exaggeration) the angle between the apical part and the lower part of the hypocotyl (Vandenbussche et al., 2010).

APPENDIX

Tables and figures

Table 4.1. List of *sjd* mutants identified in a suppressor screen.

Name	Suppressed *jazD* phenotypes	Elevated defense	Additional phenotypes
sjd1	Small rosette, short petiole	ND[1]	Elongated hypocotyl
sjd2	Small rosette, short petiole	ND	Elongated hypocotyl
sjd4	Small rosette, short petiole	ND	Elongated hypocotyl
sjd10	Small rosette	ND	Broad leaf
sjd40	Small rosette, short petiole	ND	Elongated hypocotyl
sjd56	Small rosette, short petiole	Yes	Elongated hypocotyl
sjd78	Small rosette	No	ND
sjd83	Small rosette, short petiole	ND	Elongated hypocotyl
sjd93	Small rosette, short petiole	ND	Elongated hypocotyl
sjd109	Small rosette, short petiole	ND	Elongated hypocotyl
sjd110	Small rosette, short petiole	ND	Elongated hypocotyl
sjd111	Small rosette, short petiole	ND	Elongated hypocotyl
sjd113	Small rosette, short petiole	ND	Elongated hypocotyl

[1] ND, not detected.

Table 4.2. Segregation of rosette size in backcross populations of *sjd56* and *sjd78*.

Mutant	Backcross population[1]	*sjd*-like	*jazD*-like	Segregation ratio (*sjd*-like : *jazD*-like)	*P* value (Chi-squared test)
sjd56	BC1F2	95	657	1:7	< 0.001
sjd78	BC1F2	125	370	1:3	0.897
sjd56	BC2F2	120	579	1:5	< 0.001
sjd78	BC2F2	114	348	1:3	0.872

[1] Segregating F2 populations derived from crossing the indicated *sjd* mutants to *jazD* were visually scored for rosette size (small *jazD*-like rosettes or larger *sjd*-like rosettes).

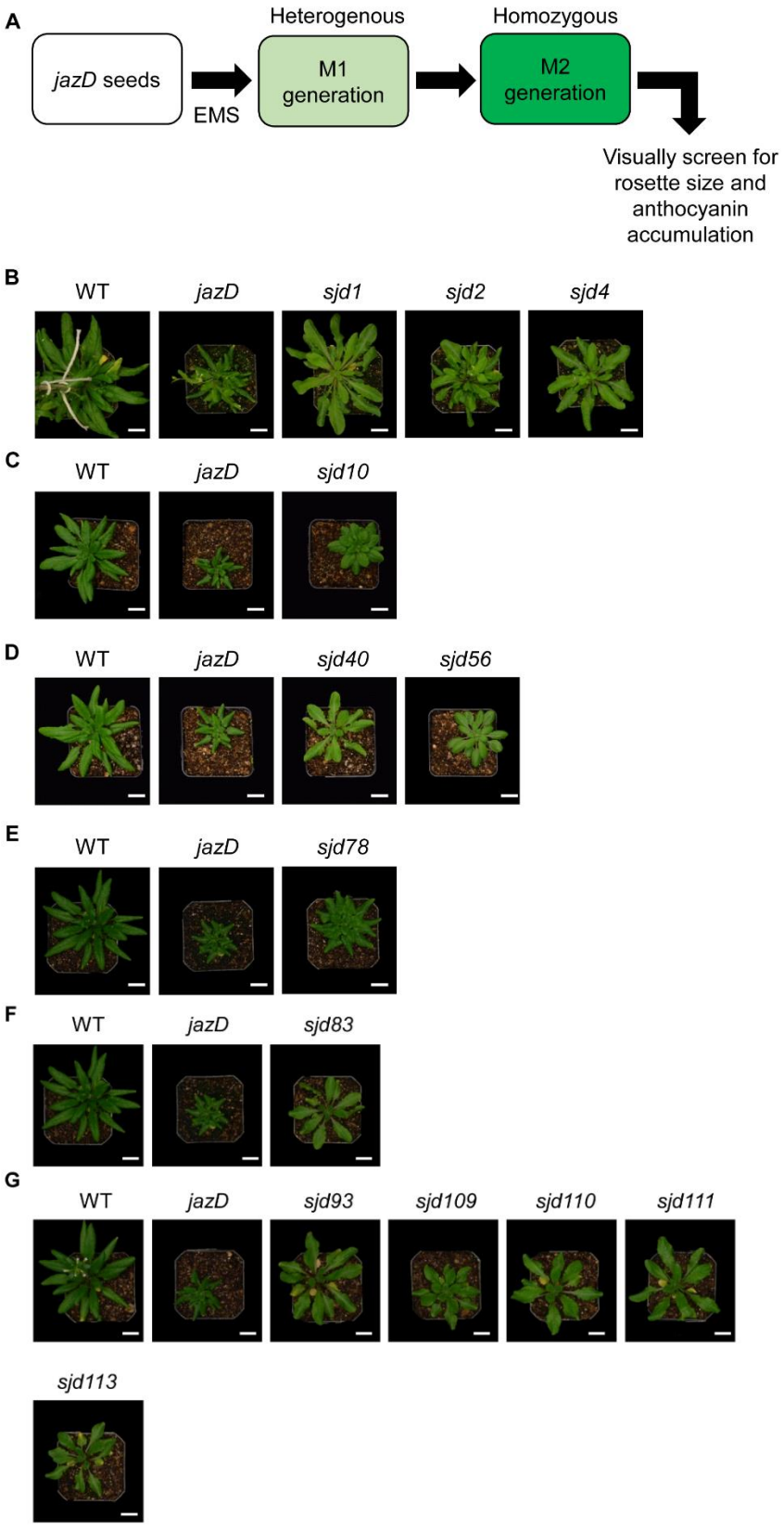

Figure 4.1. Identification of *suppressor of jazD* (*sjd*) mutants.

Figure 4.1. (cont'd) (A) Schematic diagram of suppressor screens of *jazD*. *jazD* seeds were mutagenized by EMS and visually screened for mutants (M2 generation) that partially recovered the slow-growth phenotype of *jazD* while retaining elevated anthocyanin levels.
(B-G) Photographs of WT, *jazD* and *sjd* plants (M3 generation) grown under long-day (16-h-light/8-h-dark) conditions. Sets of plants were photographed at different ages: (A) 34-day-old; (B-C) 30-day-old; (D-E) 34-day-old; and (F) 36-day-old. Scale bars, 1 cm.

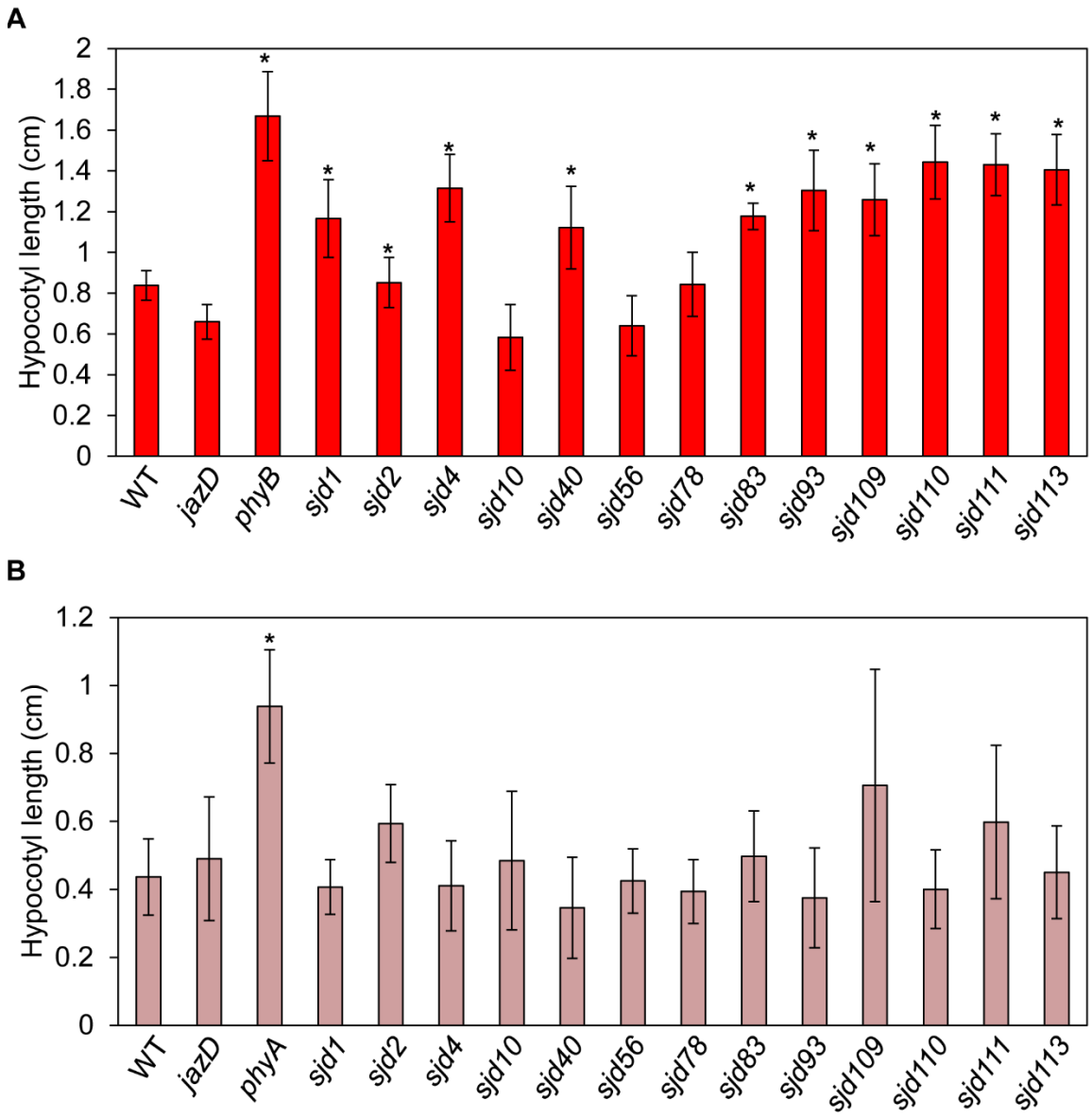

Figure 4.2. Sensitivity of *sjd* mutants to red and far red light.

(A) and **(B)** Hypocotyl lengths of *sjd* mutants grown under red (A; 50 µmol m^{-2} s^{-1}) and far-red (B; 5 µmol m^{-2} s^{-1}) light. Seedlings were grown for seven days on half-strength LS agar plates supplemented with 0.8% (w/v) sucrose. Data show the mean ± SD of at least ten seedlings per genotype. Asterisks denote significant differences compared to *jazD* according to Student's t-test ($P < 0.05$).

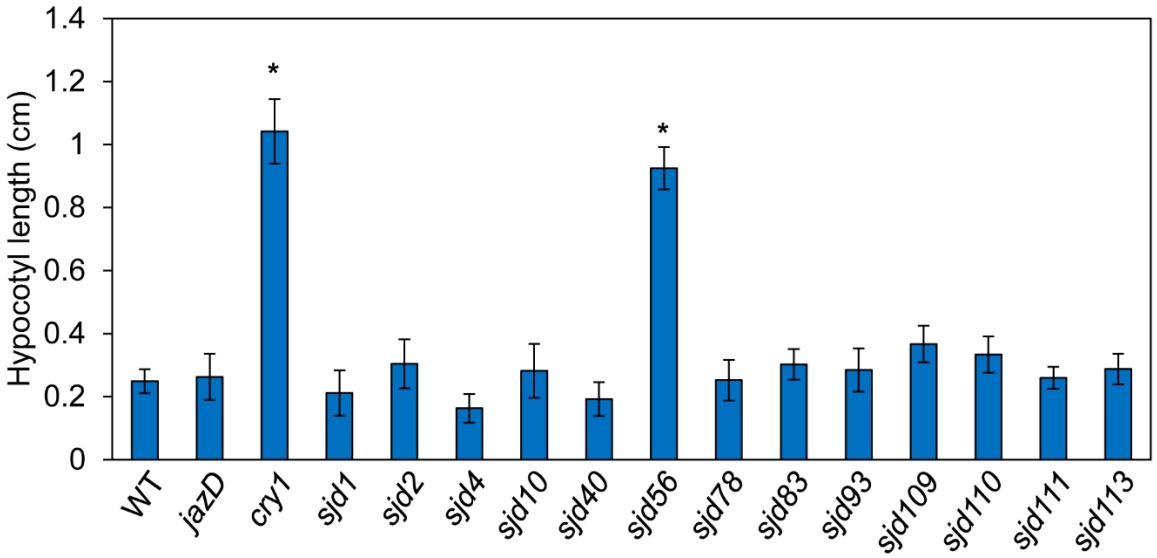

Figure 4.3. *sjd56* is insensitive to blue light.

Hypocotyl lengths of *sjd* mutants grown under blue (25 µmol m^{-2} s^{-1}) light. Seedlings were grown for seven days on half-strength LS agar plates supplemented with 0.8% (w/v) sucrose. Data show the mean ± SD of at least ten seedlings per genotype. Asterisks denote significant differences compared to *jazD* according to Student's t-test ($P < 0.05$).

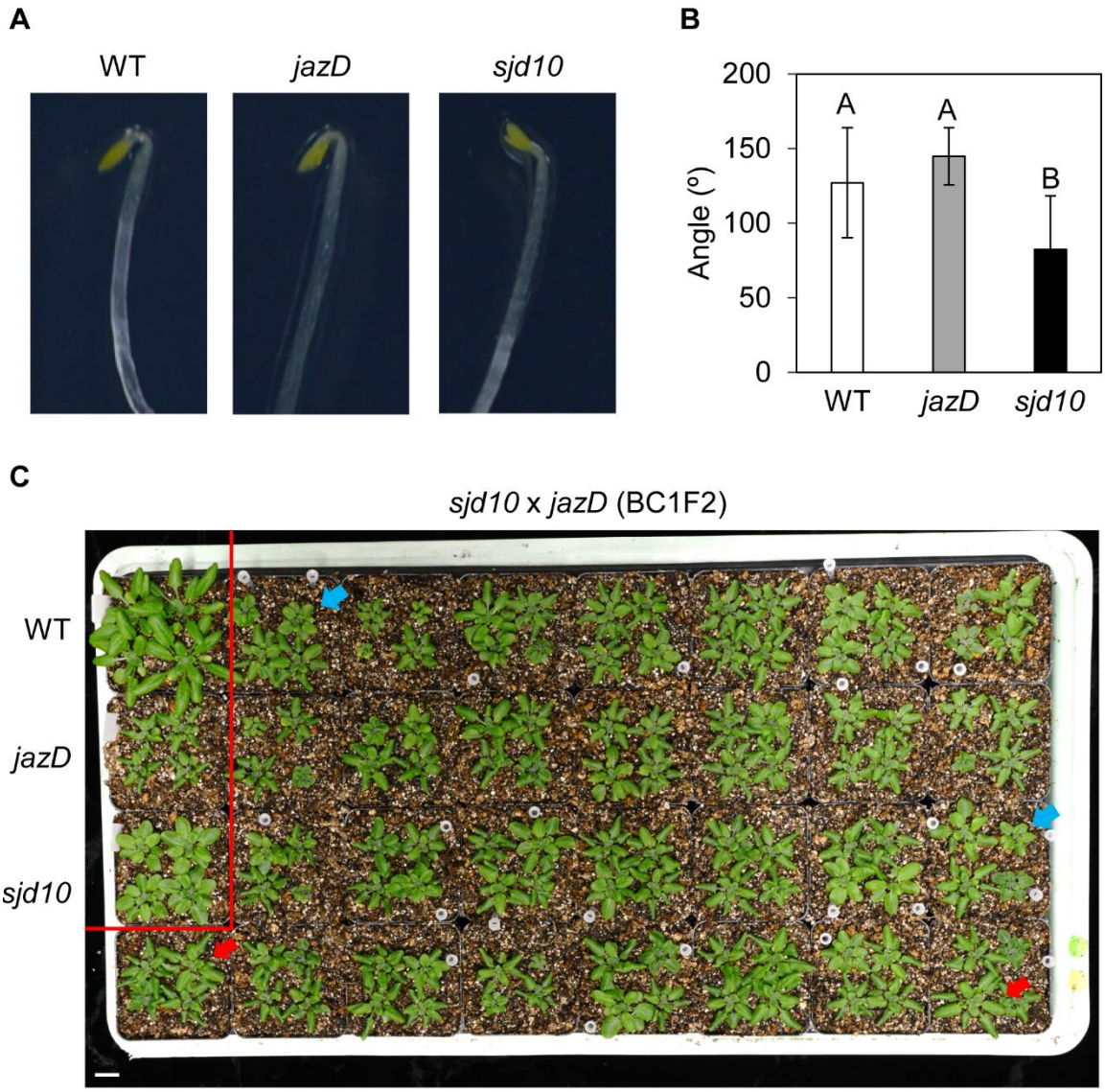

Figure 4.4. Apical hook curvature of *sjd10* is attenuated.

(A) Representative apical hooks of WT, *jazD* and *sjd10* seedlings grown for four days in dark on half-strength LS agar plates supplemented with 0.8% (w/v) sucrose.
(B) Angles of WT, *jazD* and *sjd10* apical hooks measured by ImageJ. Data show the mean ± SD of at least ten seedlings per genotype. Capital letters denote significant differences according to Tukey's HSD test ($P < 0.05$).
(C) Photograph of *sjd10* (M3 generation), *jazD* and a BC1F2 population of *sjd10*. Seedlings were started on half-strength LS agar plates supplemented with 0.8% (w/v) sucrose for eight days followed by 14 d growth under a 16 h light/8 h dark photoperiod after transferring to soil. The blue arrows denote F2 plants that show the broad-leaf phenotype without recovery of rosette size. The red arrows denote F2 plants that display the large-rosette phenotype without changes in leaf morphology. Scale bars, 1 cm.

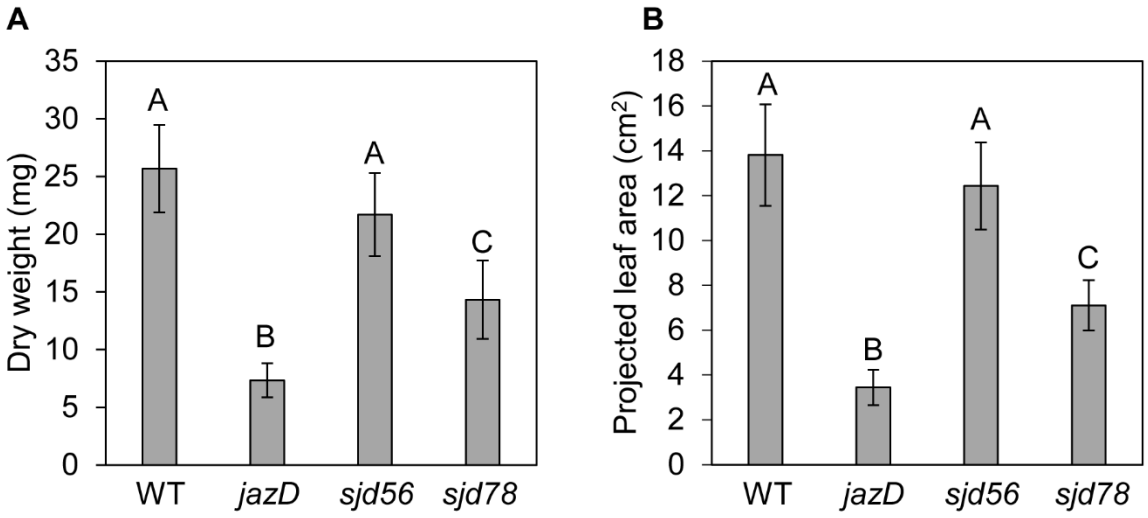

Figure 4.5. *sjd56* and *sjd78* partially recover the slow growth of *jazD*.

(A) and **(B)** Dry weight (A) and projected leaf area (B) were determined for 30-day-old plants grown under long-day conditions. Data show the mean ± SD of at least eight plants per genotype. Capital letters denote significant differences according to Tukey's HSD test ($P < 0.05$).

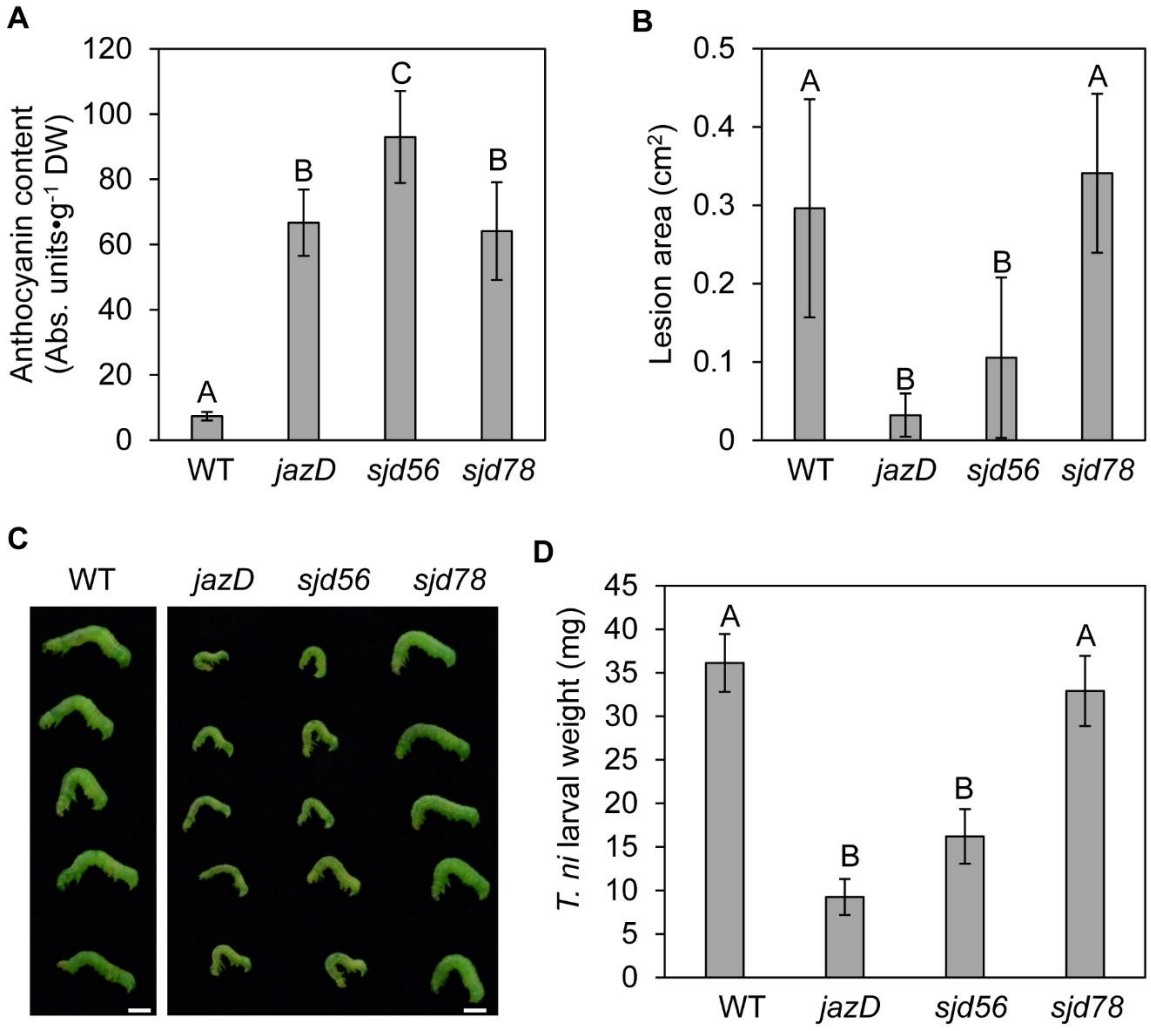

Figure 4.6. *sjd56* maintains the elevated defense of *jazD*.

(A) Anthocyanin levels of 23-day-old WT, *jazD*, *sjd56* and *sjd78* plants. Data show the mean ± SD of five plants per genotype. Capital letters denote significant differences according to Tukey's HSD test ($P < 0.05$).
(B) Necrotic lesion area measured five days after infection with *Botrytis cinerea*. Data show the mean ± SD of at least eight leaves per genotype.
(C) Photograph of representative *T. ni* larvae after ten days of feeding on WT, *jazD*, *sjd56* and *sjd78* plants. Scale bars, 0.5 cm.
(D) Weights of *T. ni* larvae reared on WT, *jazD*, *sjd56* and *sjd78* plants. Data show the mean ± SD of at least 30 larvae per genotype.

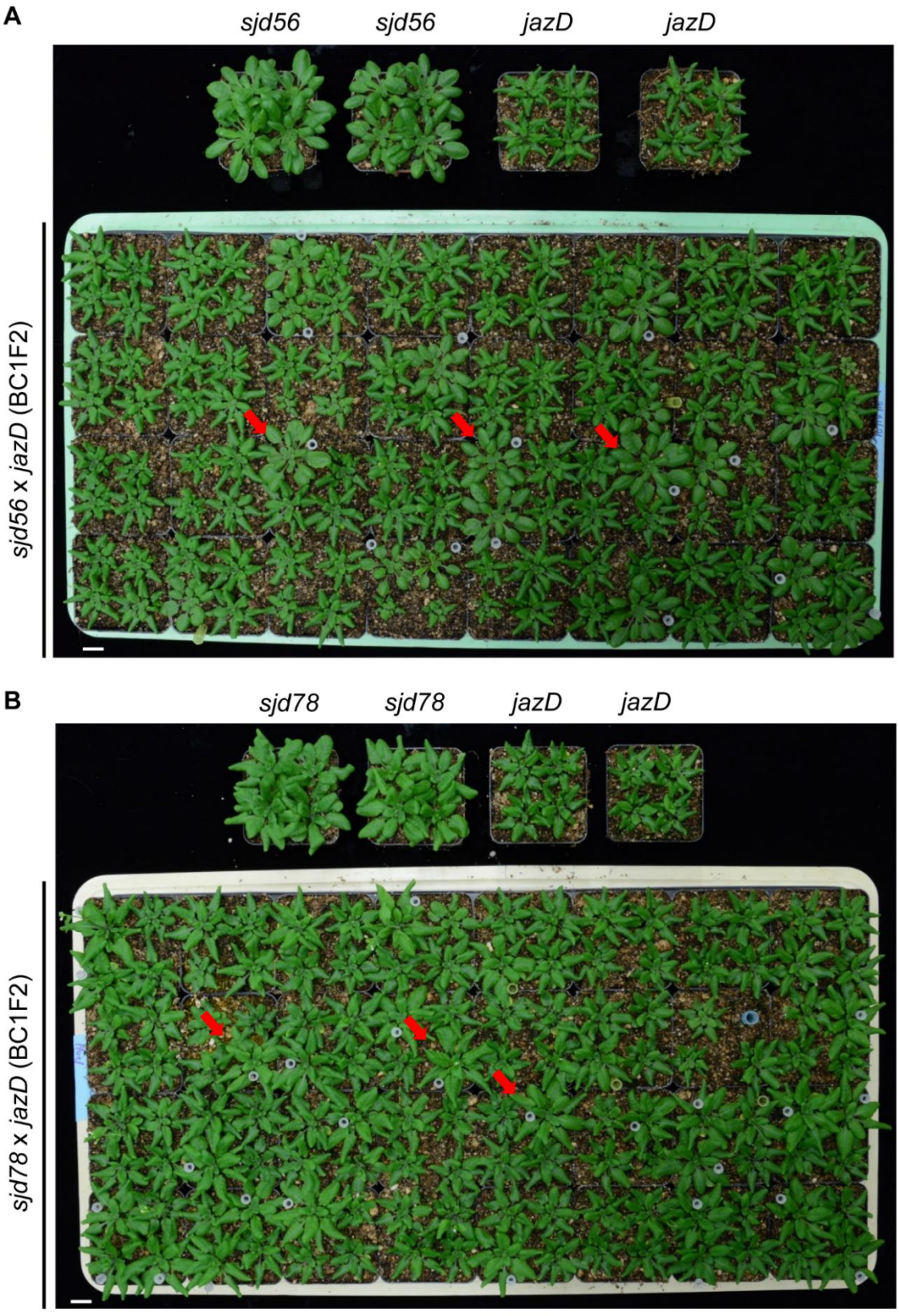

Figure 4.7. BC1F2 populations of *sjd56* and *sjd78*.

Figure 4.7. (cont'd) (A) and **(B)** Photographs of *sjd56* (A) and *sjd78* (B) mutants (M3 generation), *jazD* and their BC1F2 populations. Seedlings were started on half-strength LS agar plates supplemented with 0.8% (w/v) sucrose for eight days followed by 28 d growth under a 16 h light/8 h dark photoperiod. Scale bars, 1 cm.

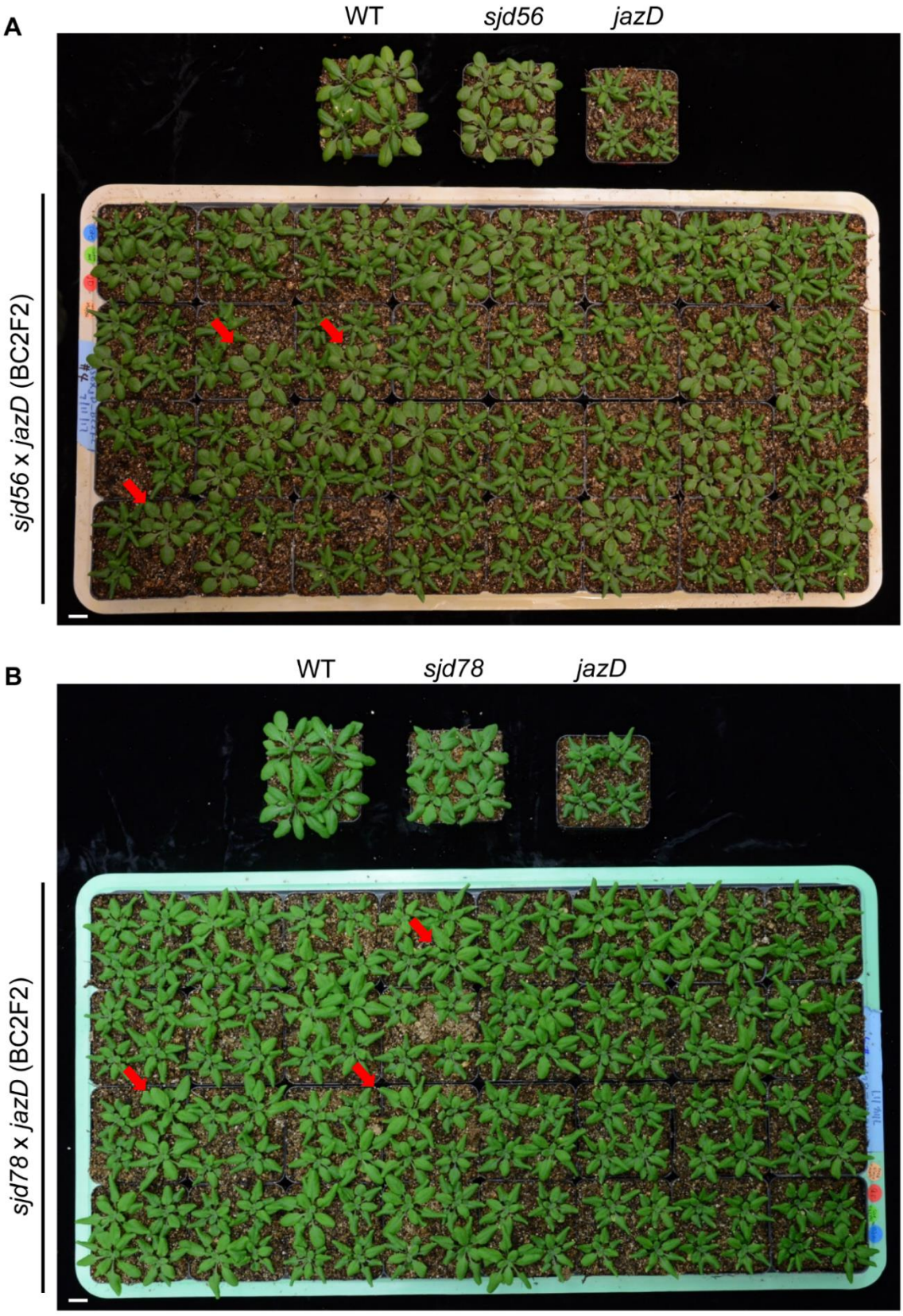

Figure 4.8. BC2F2 populations of *sjd56* and *sjd78*.

Figure 4.8. (cont'd) (A) and **(B)** Photographs of wildtype Col-0 (WT) with *sjd56* (A) and *sjd78* (B) mutants (M3 generation), *jazD* and their BC2F2 populations. Seedlings were started on half-strength LS agar plates supplemented with 0.8% (w/v) sucrose for eight days followed by 22 d growth under a 16 h light/8 h dark photoperiod. Scale bars, 1 cm.

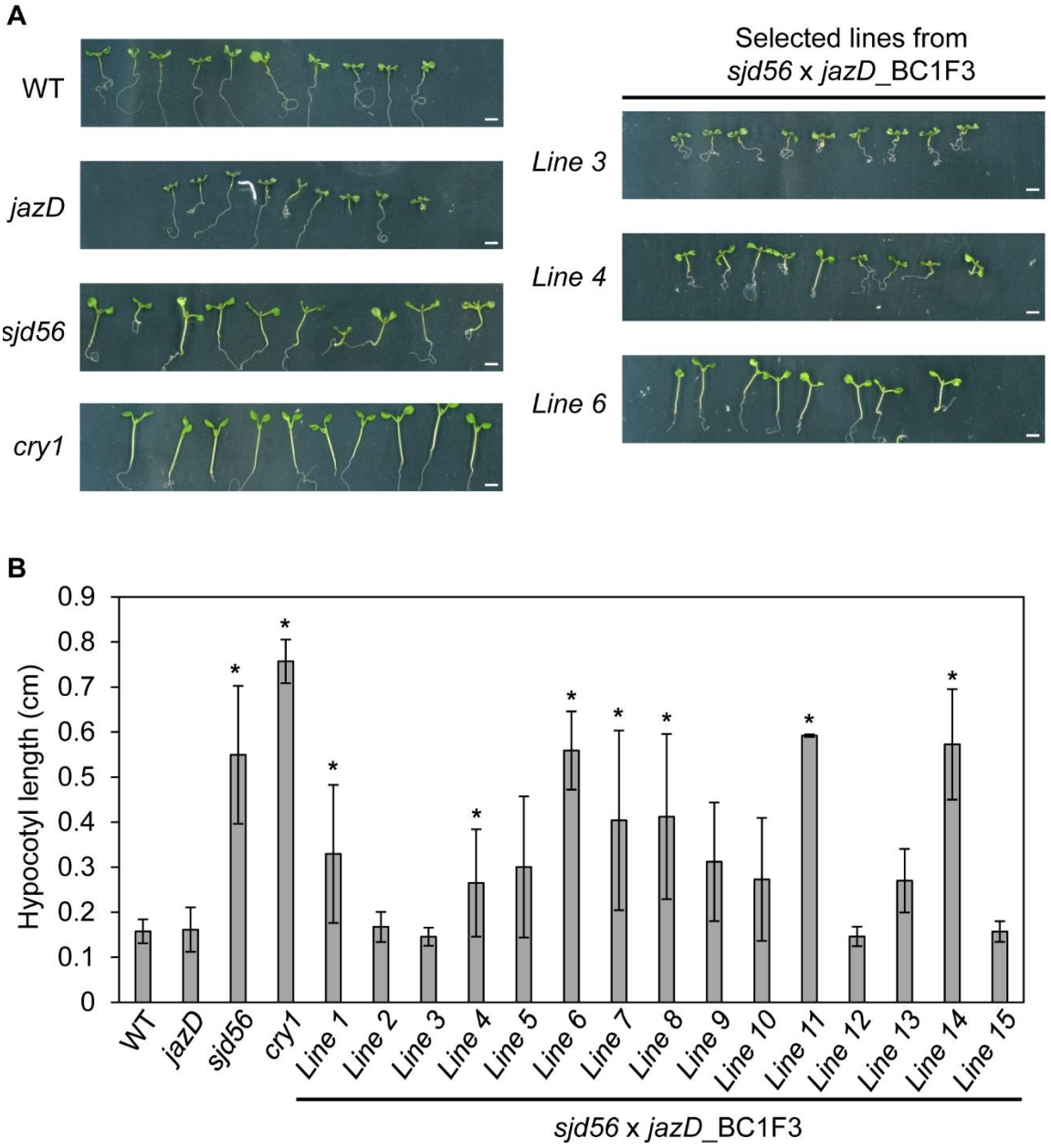

Figure 4.9. The blue light-insensitive phenotype of *sjd56* is not associated with its growth phenotype.

(A) Photographs of representative seedlings of WT, *jazD*, *sjd56* (M3 generation), *cry1* and three selected *sjd56* BC1F3 lines (Line #3, 4 and 6) grown under blue light (25 μmol m^{-2} s^{-1}). Scale bars, 0.2 cm.
(B) Hypocotyl lengths of WT, *jazD*, *sjd56*, *cry1* and *sjd56* BC1F3 seedlings grown under blue light. Seedlings were grown on half-strength LS agar plates supplemented with 0.8% (w/v) sucrose for seven days. Data show the mean ± SD of at least ten seedlings per genotype. Asterisks denote significant differences compared to *jazD* according to Student's t-test ($P < 0.05$).

REFERENCES

REFERENCES

Achard, P., Vriezen, W.H., Van Der Straeten, D., and Harberd, N.P. (2003). Ethylene regulates Arabidopsis development via the modulation of DELLA protein growth repressor function. Plant Cell **15,** 2816-2825.

Bae, G., and Choi, G. (2008). Decoding of light signals by plant phytochromes and their interacting proteins. Annu Rev Plant Biol **59,** 281-311.

Baldwin, I.T. (1998). Jasmonate-induced responses are costly but benefit plants under attack in native populations. Proc Natl Acad Sci USA **95,** 8113-8118.

Ballare, C.L. (2014). Light regulation of plant defense. Annu Rev Plant Biol **65,** 335-363.

Bleecker, A.B., Estelle, M.A., Somerville, C., and Kende, H. (1988). Insensitivity to ethylene conferred by a dominant mutation in *Arabidopsis thaliana*. Science **241,** 1086-1089.

Campos, M.L., Yoshida, Y., Major, I.T., de Oliveira Ferreira, D., Weraduwage, S.M., Froehlich, J.E., Johnson, B.F., Kramer, D.M., Jander, G., Sharkey, T.D., and Howe, G.A. (2016). Rewiring of jasmonate and phytochrome B signalling uncouples plant growth-defense tradeoffs. Nat Commun **7,** 12570.

Chaves, I., Pokorny, R., Byrdin, M., Hoang, N., Ritz, T., Brettel, K., Essen, L.O., van der Horst, G.T.J., Batschauer, A., and Ahmad, M. (2011). The cryptochromes: blue light photoreceptors in plants and animals. Annu Rev Plant Biol **62,** 335-364.

Chen, Y.H., Gols, R., and Benrey, B. (2015). Crop domestication and its impact on naturally selected trophic interactions. Annu Rev Entomol **60,** 35-58.

Chini, A., Gimenez-Ibanez, S., Goossens, A., and Solano, R. (2016). Redundancy and specificity in jasmonate signalling. Curr Opin Plant Biol **33,** 147-156.

Claeys, H., De Bodt, S., and Inze, D. (2014). Gibberellins and DELLAs: central nodes in growth regulatory networks. Trends Plant Sci **19,** 231-239.

De Grauwe, L., Vandenbussche, F., Tietz, O., Palme, K., and Van Der Straeten, D. (2005). Auxin, ethylene and brassinosteroids: tripartite control of growth in the Arabidopsis hypocotyl. Plant Cell Physiol **46,** 827-836.

de Lucas, M., and Prat, S. (2014). PIFs get bright: PHYTOCHROME INTERACTING FACTORs as integrators of light and hormonal signals. New Phytol **202,** 1126-1141.

De Paepe, A., and Van Der Straeten, D. (2005). Ethylene biosynthesis and signaling: an overview. Vitam Horm **72,** 399-430.

Dubois, M., Van den Broeck, L., and Inze, D. (2018). The pivotal role of ethylene in plant growth. Trends Plant Sci **23,** 311-323.

Dubois, M., Skirycz, A., Claeys, H., Maleux, K., Dhondt, S., De Bodt, S., Vanden Bossche, R., De Milde, L., Yoshizumi, T., Matsui, M., and Inze, D. (2013). ETHYLENE RESPONSE FACTOR 6 acts as a central regulator of leaf growth under water-limiting conditions in Arabidopsis. Plant Physiol **162,** 319-332.

Fiorucci, A.S., and Fankhauser, C. (2017). Plant strategies for enhancing access to sunlight. Curr Biol **27,** R931-R940.

Gao, C.H., Qi, S.H., Liu, K.G., Li, D., Jin, C.Y., Li, Z.W., Huang, G.Q., Hai, J.B., Zhang, M., and Chen, M.X. (2016). MYC2, MYC3, and MYC4 function redundantly in seed storage protein accumulation in Arabidopsis. Plant Physiol Bioch **108,** 63-70.

Gershenzon, J. (1994). The cost of plant chemical defense against herbivory: a biochemical perspective. Insect-plant interactions, ed. EA Bernays, pp. 105-73. CRC Press.

Guo, Q., Major, I.T., and Howe, G.A. (2018a). Resolution of growth-defense conflict: mechanistic insights from jasmonate signaling. Curr Opin Plant Biol **44,** 72-81.

Guo, Q., Yoshida, Y., Major, I.T., Wang, K., Sugimoto, K., Kapali, G., Havko, N.E., Benning, C., and Howe, G.A. (2018b). JAZ repressors of metabolic defense promote growth and reproductive fitness in Arabidopsis. Proc Natl Acad Sci USA **115,** E10768-E10777.

Guzman, P., and Ecker, J.R. (1990). Exploiting the triple response of Arabidopsis to identify ethylene-related mutants. Plant Cell **2,** 513-523.

Havko, N.E., Major, I.T., Jewell, J.B., Attaran, E., Browse, J., and Howe, G.A. (2016). Control of carbon assimilation and partitioning by jasmonate: an accounting of growth-defense tradeoffs. Plants **5,** E7.

Howe, G.A., Major, I.T., and Koo, A.J. (2018). Modularity in jasmonate signaling for multistress resilience. Annu. Rev. Plant Biol **69,** 387-415.

Karasov, T.L., Chae, E., Herman, J.J., and Bergelson, J. (2017). Mechanisms to mitigate the trade-off between growth and defense. Plant Cell **29,** 666-680.

Katsir, L., Schilmiller, A.L., Staswick, P.E., He, S.Y., and Howe, G.A. (2008). COI1 is a critical component of a receptor for jasmonate and the bacterial virulence factor coronatine. Proc Natl Acad Sci USA **105,** 7100-7105.

Lehman, A., Black, R., and Ecker, J.R. (1996). HOOKLESS1, an ethylene response gene, is required for differential cell elongation in the Arabidopsis hypocotyl. Cell **85,** 183-194.

Leivar, P., and Monte, E. (2014). PIFs: systems integrators in plant development. Plant Cell **26,** 56-78.

Li, H., Johnson, P., Stepanova, A., Alonso, J.M., and Ecker, J.R. (2004). Convergence of signaling of differential cell growth pathways in the control in Arabidopsis. Dev Cell **7,** 193-204.

Li, H.J., and Guo, H.W. (2007). Molecular basis of the ethylene signaling and response pathway in Arabidopsis. J Plant Growth Regul **26,** 106-117.

Major, I.T., Yoshida, Y., Campos, M.L., Kapali, G., Xin, X.F., Sugimoto, K., de Oliveira Ferreira, D., He, S.Y., and Howe, G.A. (2017). Regulation of growth-defense balance by the JASMONATE ZIM-DOMAIN (JAZ)-MYC transcriptional module. New Phytol **215,** 1533-1547.

Marsch-Martinez, N., Greco, R., Becker, J.D., Dixit, S., Bergervoet, J.H.W., Karaba, A., de Folter, S., and Pereira, A. (2006). BOLITA, an Arabidopsis AP2/ERF-like transcription factor that affects cell expansion and proliferation/differentiation pathways. Plant Mol Biol **62,** 825-843.

Merchante, C., Alonso, J.M., and Stepanova, A.N. (2013). Ethylene signaling: simple ligand, complex regulation. Curr Opin Plant Biol **16,** 554-560.

Pedmale, U.V., Huang, S.C., Zander, M., Cole, B.J., Hetzel, J., Ljung, K., Reis, P.A.B., Sridevi, P., Nito, K., Nery, J.R., Ecker, J.R., and Chory, J. (2016). Cryptochromes interact directly with PIFs to control plant growth in limiting blue light. Cell **164,** 233-245.

Reed, J.W., Nagpal, P., Poole, D.S., Furuya, M., and Chory, J. (1993). Mutations in the gene for the red far-red light receptor phytochrome B alter cell elongation and physiological-responses throughout Arabidopsis development. Plant Cell **5,** 147-157.

Reed, J.W., Nagatani, A., Elich, T.D., Fagan, M., and Chory, J. (1994). Phytochrome A and phytochrome B have overlapping but distinct functions in Arabidopsis development. Plant Physiol **104,** 1139-1149.

Ruckle, M.E., DeMarco, S.M., and Larkin, R.M. (2007). Plastid signals remodel light signaling networks and are essential for efficient chloroplast biogenesis in Arabidopsis. Plant Cell **19,** 3944-3960.

Schwark, A., and Schierle, J. (1992). Interaction of ethylene and auxin in the regulation of hook growth 1 the role of auxin in different growing regions of the hypocotyl hook of *Phaseolus vulgaris*. J Plant Physiol **140,** 562-570.

Simms, E.L. (1992). Costs of plant resistance to herbivory. Plant resistance to herbivores and pathogens: ecology, evolution and genetics, ed. RS Fritz, EL Simms, pp. 392-425. Univ. Chicago Press.

Song, S.S., Huang, H., Gao, H., Wang, J.J., Wu, D.W., Liu, X.L., Yang, S.H., Zhai, Q.Z., Li, C.Y., Qi, T.C., and Xie, D.X. (2014). Interaction between MYC2 and ETHYLENE INSENSITIVE 3 modulates antagonism between jasmonate and ethylene signaling in Arabidopsis. Plant Cell **26,** 263-279.

Strauss, S.Y., Siemens, D.H., Decher, M.B., and Mitchell-Olds, T. (1999). Ecological costs of plant resistance to herbivores in the currency of pollination. Evolution **53,** 1105-1113.

Thines, B., Katsir, L., Melotto, M., Niu, Y., Mandaokar, A., Liu, G., Nomura, K., He, S.Y., Howe, G.A., and Browse, J. (2007). JAZ repressor proteins are targets of the $SCF^{(COI1)}$ complex during jasmonate signalling. Nature **448,** 661-665.

Turner, J.G., Ellis, C., and Devoto, A. (2002). The jasmonate signal pathway. Plant Cell **14,** S153-S164.

Vandenbussche, F., Petrasek, J., Zadnikova, P., Hoyerova, K., Pesek, B., Raz, V., Swarup, R., Bennett, M., Zazimalova, E., Benkova, E., and Van Der Straeten, D. (2010). The auxin influx carriers AUX1 and LAX3 are involved in auxin-ethylene interactions during apical hook development in *Arabidopsis thaliana* seedlings. Development **137,** 597-606.

Vriezen, W.H., Achard, P., Harberd, N.P., and Van Der Straeten, D. (2004). Ethylene-mediated enhancement of apical hook formation in etiolated *Arabidopsis thaliana* seedlings is gibberellin dependent. Plant J **37,** 505-516.

Wasternack, C. (2015). How jasmonates earned their laurels: past and present. J Plant Growth Regul **34,** 761-794.

Wasternack, C., and Hause, B. (2013). Jasmonates: biosynthesis, perception, signal transduction and action in plant stress response, growth and development. Ann Bot **111,** 1021-1058.

Xie, D.X., Feys, B.F., James, S., Nieto-Rostro, M., and Turner, J.G. (1998). COI1: An Arabidopsis gene required for jasmonate-regulated defense and fertility. Science **280,** 1091-1094.

Yan, Y.X., Stolz, S., Chetelat, A., Reymond, P., Pagni, M., Dubugnon, L., and Farmer, E.E. (2007). A downstream mediator in the growth repression limb of the jasmonate pathway. Plant Cell **19,** 2470-2483.

Zhang, Y., and Turner, J.G. (2008). Wound-induced endogenous jasmonates stunt plant growth by inhibiting mitosis. Plos One **3,** e3699.

Zust, T., and Agrawal, A.A. (2017). Trade-offs between plant growth and defense against insect herbivory: an emerging mechanistic synthesis. Annu Rev Plant Biol **68,** 10.11-10.22.

CHAPTER FIVE - SUMMARY AND FUTURE PERSPECTIVES

Summary of dissertation

Since its first isolation from jasmine flowers in the 1960's (Demole et al., 1962), numerous studies have been carried out to understand how jasmonate (JA) exerts control over a myriad of physiological processes in plants. Identification of JA signaling components, including the receptor CORONATINE INSENSITIVE 1 (COI1) (Xie et al., 1998), the transcriptional repressor JASMONATE ZIM-DOMAIN (JAZ) proteins (Thines et al., 2007; Yan et al., 2007; Chini et al., 2018), and the bHLH MYC and other JA-responsive transcription factors (TFs) (Chini et al., 2007; Thines et al., 2007; Howe et al., 2018), marked key steps to reveal the mechanisms by which JA reprograms gene expression. Among the major tasks performed by JA is activation of defense gene expression in response to challenge by biotic aggressors (Farmer and Ryan, 1990; Howe et al., 1996). Interestingly, JA-induced expression of defense traits is often accompanied by growth restriction (Havko et al., 2016). One theory to explain the growth inhibition imposed by JA is that transcriptional networks are hardwired to restrict growth upon activation of JA signaling cascade (Campos et al., 2016). This notion is supported by the successful unlocking of growth-defense tradeoffs through relief of transcriptional repression of the JA and phyB signaling pathways (Campos et al., 2016). Detailed characterization of the *jaz* quintuple (*jazQ*) mutant has shown that the strength of growth-defense antagonism in the mutant is relatively weak, which may explain the ability of a *phyB* mutation to completely rescue the growth defect of *jazQ* without compromising defense (Campos et al., 2016). It was therefore of interest to develop higher-order *jaz* mutants in which severe JAZ depletion strongly activates defense responses. Towards this goal, a major focus of this dissertation was detailed physiological, and biochemical characterization of higher-order *jaz* mutants.

Another interpretation of JA-mediated growth-defense tradeoffs is that investment of metabolic resources in defense restricts the allocation of resources to vegetative and reproductive growth (Zust and Agrawal, 2017). At the time this dissertation research was initiated, there was little direct evidence to support this "metabolic tradeoff" hypothesis (Coley et al., 1985; Herms and Mattson, 1992; Heil and Baldwin, 2002; Stamp, 2003; Havko et al., 2016; Kliebenstein, 2016). The investigation of how JA affects resource allocation has been hindered by functional redundancy within the JAZ protein family (Chini et al., 2016). To help resolve the question, we constructed a *jaz* decuple (*jazD*) mutant defective in ten *JAZ* genes (*JAZ1/2/3/4/5/6/7/9/10/13*), as described in Chapter Two of this dissertation. Characterization of this higher-order *jaz* mutant showed that the JA signaling pathway is constitutively activated upon JAZ depletion. Correspondingly, *jazD* exhibits increased resistance to insect herbivores and necrotrophic pathogens compared to WT and *jazQ*. Global transcript and protein profiling suggested that resource allocation to defense-related metabolic pathways is highly elevated in *jazD*. Results obtained from these omics analyses were supported by direct measurements of defense compounds (e.g., indole glucosinolates) and increased rates of cellular respiration. The enhanced expression of defense traits in *jazD* leaves appeared to be linked to depletion in carbon reserves, as determined by a modest reduction in starch and sucrose levels. The slow growth of *jazD* leaves and roots was also associated with symptoms of sugar starvation and defects in reproductive fitness.

My findings suggest that JAZ proteins function to fine-tune the expression level of defense traits. In the absence of biotic attack, JAZ proteins repress the JA signaling cascade to limit resource allocation to defense pathways. Under these conditions, the plant appears

to prioritize the use of photoassimilates and other resources for growth and seed production. When plants experience mild attack from insects or microbes, elevated JA levels lead to JAZ degradation, which in turn triggers immune responses. The rapid induction of *JAZ* genes in JA-elicited cells likely leads to *de novo* synthesis of JAZ repressors that exert negative feedback control on the pathway. In this way, JAZ proteins play an important role in mitigating the high cost of induced defense responses, and growth restriction mainly comes from rewiring of signaling networks connected with JA, which is similar to the situation in *jazQ*. However, as the biotic stress escalates past a threshold level, more JAZs are depleted and defense traits are expressed to an extreme extent that starves plants for carbon and other nutrients. It is conceivable that this signal is sensed by unknown mechanisms, and that plants adjust their growth rates accordingly.

JAZ proteins execute JA outputs by targeting various JA-responsive TFs, the most intensively studied of which are the basic helix-loop-helix (bHLH) MYC TFs, including MYC2, MYC3 and MYC4 (Chini et al., 2007; Thines et al., 2007; Fernandez-Calvo et al., 2011). To determine whether MYC TFs are required for defense responses observed in *jazD*, we introduced T-DNA insertion mutations that disrupt one, two or three members among *MYC2*, *MYC3* and *MYC4* in the *jazD* genetic background. Comparison of the resulting *jazD myc* mutants to WT, *jazD*, and *mycT* lines showed that the defense traits of *jazD*, including elevated resistance to insect and pathogen attack, are dependent on MYC2/3/4. Among the three MYCs, MYC3 plays dominant roles in driving tryptophan flux and plant resistance to necrotrophic pathogens. Interestingly, we discovered that the formation of endoplasmic reticulum (ER)-derived structures called ER bodies, which are repositories for defense-related β-glucosidases, is constitutively activated in *jazD* leaves.

Further analyses showed that the induction of ER body genes in *jazD* is mediated by MYC TFs, especially MYC2 and MYC3. These results indicate that MYC TFs largely account for the allocation of resources to defense-related processes in *jazD*, and that MYC2/3/4 perform overlapping and distinct functions in metabolic reprogramming. However, we found that loss of MYC2/3/4 does not fully restore the slow-growth phenotype of *jazD*. It is possible that additional JAZ-interacting factors contribute to the growth phenotype of *jazD*.

Given the fact that defense responses are strongly and constitutively activated in *jazD*, this mutant provides a tool to investigate the antagonistic relationship between growth and defense without having to impose actual biotic stress. Chapter Four of this dissertation describes an ethyl methanesulfonate (EMS)-based genetic screen to identify suppressors of *jazD* in which growth is partially recovered without impeding defense. The screen identified 13 *suppressors of jazD* (*sjd*) that display increased growth while accumulating similar levels of anthocyanin compared to *jazD*. Hypocotyl elongation assays performed under monochromatic light showed that ten *sjd* mutants are insensitive to red light, suggesting that they carry mutations in components of the red light signaling pathway. Evaluation of apical hook formation of *sjd* mutants showed that one red light-sensitive mutant (*sjd10*) exhibits attenuated formation of apical hook. Therefore, we speculate that *sjd10* may harbor mutations in genes involved in regulating hook formation (i.e. genes in auxin- and ethylene-signaling pathways). Finally, measurement of growth and defense parameters showed that the red light-sensitive *sjd56* mutant partially recovers the stunted growth of *jazD* while maintaining enhanced resistance to insect herbivores and necrotrophic pathogens. Thus, our screen of EMS-mutagenized *jazD* successfully

identified mutants that uncouple growth-defense tradeoffs. Characterization of theses mutants in the future may shed light on the molecular mechanisms that govern plant growth and immunity.

To summarize, research in this dissertation demonstrates that JAZ proteins promote growth and fertility by preventing detrimental metabolic processes triggered by unrestrained JA responses. The bHLH MYC TFs play a key role in mediating resource allocation to defense pathways, and also appear to mediate growth restriction. The use of suppressor screens further showed that growth-defense tradeoffs observed in *jazD* can be uncoupled.

Future perspectives

In the past five years, many discoveries have advanced our understanding of JA biology and how this hormone impacts plant performance. The crystal structure has been resolved for JAZ proteins interacting with MYC TFs, revealing how JAZ proteins switch between the repressor function and the co-receptor function (Zhang et al., 2015). MED25 was found to physically interact with COI1 and facilitate COI1-dependent degradation of JAZ repressors (An et al., 2017). Uncoupling of growth and defense antagonism was achieved through genetic removal of JAZ and phyB proteins (Campos et al., 2016). The role of MYC TFs in modulating growth-defense balance was also elucidated (Major et al., 2017). Furthermore, a number of novel interactions between JAZ proteins and TFs were identified (Hu et al., 2013b; Zhao et al., 2013; Jiang et al., 2014; Boter et al., 2015; Zhai et al., 2015), and these findings greatly expanded the scope of physiological processes regulated by JA. Collectively, these findings establish JAZ proteins as an integrative hub of JA signaling that exerts master control over growth, defense and various other physiological processes. However, many interesting questions remain to be answered.

Although it is known that JA signaling switches on the production of defense compounds, the quantitative analyses showing how JA reconfigures carbon distribution among diverse metabolic pathways remain an open question. Isotopic labelling is one way to directly measure the incorporation of carbon into different metabolites. For example, $^{14}CO_2$ labeling was employed to track assimilated carbon in both source and sink tissues of Arabidopsis (Kolling et al., 2015). In another study, Hanik *et al.* used $^{11}CO_2$ labeling to track carbon partitioning into several metabolite pools in *Nicotiana tabacum* upon MeJA treatment (Hanik et al., 2010). They revealed that MeJA increased carbon partitioning into

aromatic amino acids (i.e. tryptophan) in the shikimate acid pathway (Hanik et al., 2010). In Chapter Two of this dissertation, changes of carbon allocation to growth and defense pathways in higher-order *jaz* mutants were discerned from global transcript and protein profiling. These mutants are good candidates for isotopic carbon labeling to better understand how JA remobilizes carbon during the growth to defense transition.

Much of the research aimed at understanding JA-mediated resource tradeoffs has concerned tradeoffs imposed by biotic stresses. However, increasing evidence has implicated JA in the control of abiotic stress responses, including those triggered by low temperature, drought and high salinity. A subgroup of JAZ proteins physically interact with INDUCER OF CBF EXPRESSION (ICE) TFs that regulate plant resilience to cold stress (Hu et al., 2013b). This study showed that exogenous JA enhances plant tolerance to cold (Hu et al., 2013b). In addition, several lines of evidence suggest that the JA-responsive TF MYC2 is involved in abscisic acid (ABA) signaling (Kazan and Manners, 2013), which is triggered by water deficiency and high salinity (Osakabe et al., 2014). The expression of *MYC2* can be induced by ABA and drought stress, and *MYC2* overexpressing plants displayed increased ABA sensitivity (Abe et al., 2003). However, the role of MYC2 in drought tolerance is not conclusive. Transgenic plants overexpressing both *MYC2* and *MYB2*, another drought-inducible MYB TF, exhibited decreased electrolyte leakage upon mannitol treatment, suggesting that MYC2 positively regulates plant resilience to drought (Abe et al., 2003). By contrast, the *myc2* mutant has been reported to be more tolerant to drought (Harb et al., 2010). Our preliminary data showed that *jazD* exhibited increased sensitivity to exogenous ABA treatment with respect to seed germination, and this hypersensitivity was not observed in *jazD mycT* (data now shown). Therefore, the higher-

order *jaz* mutants may be valuable tools to study how JA contributes to drought tolerance. Further studies are needed to provide more information about how these mutants perform under abiotic stresses and how JA remodels resource allocation to growth and resilience under abiotic stresses.

ER bodies are ER-derived structures that contain several defense proteins, including β-glucosidases and plant defensins (Watanabe et al., 2013; Nakano et al., 2014). Although the induction of ER body formation by exogenous MeJA was demonstrated more than 15 years ago (Matsushima et al., 2002), the mechanisms by which JA triggers the proliferation of this specialized structure remain unclear. We provide evidence in Chapter Three that the JAZ-MYC transcriptional module regulates the expression of ER body genes. However, molecular and biochemical analyses (e.g. chromatin immunoprecipitation sequencing) are required to determine whether MYC TFs induce ER body genes through direct binding to their promoters. It also remains to be determined how ER bodies are disrupted upon insect attack to release stored defense proteins.

Advances in understanding growth-defense tradeoffs raise the possibility that these two physiological processes can be uncoupled. Suppressor screens starting with *jazQ* identified a mutant exhibiting heightened growth and defense traits as a result of *phyB* mutation (Campos et al., 2016). Likewise, screens for suppressors of *jazD* (Chapter Four) are expected to reveal new mechanisms that unlock growth-defense tradeoffs. Future studies will search for the causal mutations in *sjd* mutants and explore the molecular mechanisms that disconnect growth and defense. In addition to rewiring distinct signaling pathways, an alternative to uncouple JA-mediated growth-defense antagonism is to manipulate components of JA metabolism or signaling pathways. Loss-of-function

mutations that impair enzymes (e.g. JAO2/JOX) involved in JA catabolism were shown to promote plant resistance against fungal pathogens while retaining normal growth rates (Caarls et al., 2017; Smirnova et al., 2017). In another study, RNAi lines of JASMONATE-ASSOCIATED VQ MOTIF GENE 1 (JAV1), which also functions to repress JA signaling, displayed increased resistance to insect attack without obvious changes in growth traits (Hu et al., 2013a). Application of this collective knowledge to develop agricultural crops that maintain optimal growth and defense is an important direction for future research. The development of CRISPR technology to modify genomes in a timely manner will facilitate this process.

Taken together, characterization of the physiological roles of JAZ proteins have ushered in a new era of understanding how plants manage their resource balance in harsh environments. Large-scale omics analyses, mathematical modeling and novel genetic modification tools will assist the quest to uncover how JA exerts control over various physiological traits to maximize plant fitness in response to dynamic environmental cues.

REFERENCES

REFERENCES

Abe, H., Urao, T., Ito, T., Seki, M., Shinozaki, K., and Yamaguchi-Shinozaki, K. (2003). Arabidopsis AtMYC2 (bHLH) and AtMYB2 (MYB) function as transcriptional activators in abscisic acid signaling. Plant Cell **15,** 63-78.

An, C., Li, L., Zhai, Q., You, Y., Deng, L., Wu, F., Chen, R., Jiang, H., Wang, H., Chen, Q., and Li, C. (2017). Mediator subunit MED25 links the jasmonate receptor to transcriptionally active chromatin. Proceedings of the National Academy of Sciences of the United States of America **114,** E8930-E8939.

Boter, M., Golz, J.F., Gimenez-Ibanez, S., Fernandez-Barbero, G., Franco-Zorrilla, J.M., and Solano, R. (2015). FILAMENTOUS FLOWER Is a Direct Target of JAZ3 and Modulates Responses to Jasmonate. Plant Cell **27,** 3160-3174.

Caarls, L., Elberse, J., Awwanah, M., Ludwig, N.R., de Vries, M., Zeilmaker, T., Van Wees, S.C.M., Schuurink, R.C., and Van den Ackerveken, G. (2017). Arabidopsis JASMONATE-INDUCED OXYGENASES down-regulate plant immunity by hydroxylation and inactivation of the hormone jasmonic acid. Proceedings of the National Academy of Sciences of the United States of America **114,** 6388-6393.

Campos, M.L., Yoshida, Y., Major, I.T., de Oliveira Ferreira, D., Weraduwage, S.M., Froehlich, J.E., Johnson, B.F., Kramer, D.M., Jander, G., Sharkey, T.D., and Howe, G.A. (2016). Rewiring of jasmonate and phytochrome B signalling uncouples plant growth-defense tradeoffs. Nature communications **7,** 12570.

Chini, A., Gimenez-Ibanez, S., Goossens, A., and Solano, R. (2016). Redundancy and specificity in jasmonate signalling. Current Opinion in Plant Biology **33,** 147-156.

Chini, A., Fonseca, S., Fernandez, G., Adie, B., Chico, J.M., Lorenzo, O., Garcia-Casado, G., Lopez-Vidriero, I., Lozano, F.M., Ponce, M.R., Micol, J.L., and Solano, R. (2007). The JAZ family of repressors is the missing link in jasmonate signalling. Nature **448,** 666-671.

Chini, A., Monte, I., Zamarreno, A.M., Hamberg, M., Lassueur, S., Reymond, P., Weiss, S., Stintzi, A., Schaller, A., Porzel, A., Garcia-Mina, J.M., and Solano, R. (2018). An OPR3-independent pathway uses 4,5-didehydrojasmonate for jasmonate synthesis. Nat Chem Biol **14,** 171-178.

Coley, P.D., Bryant, J.P., and Chapin, F.S. (1985). Resource Availability and Plant Antiherbivore Defense. Science **230,** 895-899.

Demole, E., Lederer, E., and Mercier, D. (1962). Isolement Et Determination De La Structure Du Jasmonate De Methyle, Constituant Odorant Caracteristique De Lessence De Jasmin. Helv Chim Acta **45,** 675-685.

Farmer, E.E., and Ryan, C.A. (1990). Interplant communication: airborne methyl jasmonate induces synthesis of proteinase inhibitors in plant leaves. Proceedings of the National Academy of Sciences of the United States of America **87,** 7713-7716.

Fernandez-Calvo, P., Chini, A., Fernandez-Barbero, G., Chico, J.M., Gimenez-Ibanez, S., Geerinck, J., Eeckhout, D., Schweizer, F., Godoy, M., Franco-Zorrilla, J.M., Pauwels, L., Witters, E., Puga, M.I., Paz-Ares, J., Goossens, A., Reymond, P., De Jaeger, G., and Solano, R. (2011). The Arabidopsis bHLH Transcription Factors MYC3 and MYC4 Are Targets of JAZ Repressors and Act Additively with MYC2 in the Activation of Jasmonate Responses. Plant Cell **23,** 701-715.

Hanik, N., Gomez, S., Best, M., Schueller, M., Orians, C.M., and Ferrieri, R.A. (2010). Partitioning of New Carbon as C-11 in Nicotiana tabacum Reveals Insight into Methyl Jasmonate Induced Changes in Metabolism. J Chem Ecol **36,** 1058-1067.

Harb, A., Krishnan, A., Ambavaram, M.M.R., and Pereira, A. (2010). Molecular and Physiological Analysis of Drought Stress in Arabidopsis Reveals Early Responses Leading to Acclimation in Plant Growth. Plant Physiol **154,** 1254-1271.

Havko, N.E., Major, I.T., Jewell, J.B., Attaran, E., Browse, J., and Howe, G.A. (2016). Control of Carbon Assimilation and Partitioning by Jasmonate: An Accounting of Growth-Defense Tradeoffs. Plants (Basel) **5,** E7.

Heil, M., and Baldwin, I.T. (2002). Fitness costs of induced resistance: emerging experimental support for a slippery concept. Trends Plant Sci **7,** 61-67.

Herms, D.A., and Mattson, W.J. (1992). The Dilemma of Plants - to Grow or Defend. Q Rev Biol **67,** 283-335.

Howe, G.A., Major, I.T., and Koo, A.J. (2018). Modularity in Jasmonate Signaling for Multistress Resilience. Annual Review of Plant Biology, **69,** 387-415.

Howe, G.A., Lightner, J., Browse, J., and Ryan, C.A. (1996). An octadecanoid pathway mutant (JL5) of tomato is compromised in signaling for defense against insect attack. Plant Cell **8,** 2067-2077.

Hu, P., Zhou, W., Cheng, Z.W., Fan, M., Wang, L., and Xie, D.X. (2013a). JAV1 Controls Jasmonate-Regulated Plant Defense. Mol Cell **50,** 504-515.

Hu, Y.R., Jiang, L.Q., Wang, F., and Yu, D.Q. (2013b). Jasmonate Regulates the INDUCER OF CBF EXPRESSION-C-REPEAT BINDING FACTOR/DRE BINDING FACTOR1 Cascade and Freezing Tolerance in Arabidopsis. Plant Cell **25,** 2907-2924.

Jiang, Y.J., Liang, G., Yang, S.Z., and Yu, D.Q. (2014). Arabidopsis WRKY57 Functions as a Node of Convergence for Jasmonic Acid- and Auxin-Mediated Signaling in Jasmonic Acid-Induced Leaf Senescence. Plant Cell **26,** 230-245.

Kazan, K., and Manners, J.M. (2013). MYC2: The Master in Action. Molecular Plant **6,** 686-703.

Kliebenstein, D.J. (2016). False idolatry of the mythical growth versus immunity tradeoff in molecular systems plant pathology. Physiol Mol Plant P **95,** 55-59.

Kolling, K., Thalmann, M., Muller, A., Jenny, C., and Zeeman, S.C. (2015). Carbon partitioning in Arabidopsis thaliana is a dynamic process controlled by the plants metabolic status and its circadian clock. Plant Cell Environ **38,** 1965-1979.

Major, I.T., Yoshida, Y., Campos, M.L., Kapali, G., Xin, X.F., Sugimoto, K., de Oliveira Ferreira, D., He, S.Y., and Howe, G.A. (2017). Regulation of growth-defense balance by the JASMONATE ZIM-DOMAIN (JAZ)-MYC transcriptional module. New Phytol **215,** 1533-1547.

Matsushima, R., Hayashi, Y., Kondo, M., Shimada, T., Nishimura, M., and Hara-Nishimura, I. (2002). An endoplasmic reticulum-derived structure that is induced under stress conditions in Arabidopsis. Plant Physiol **130,** 1807-1814.

Nakano, R.T., Yamada, K., Bednarek, P., Nishimura, M., and Hara-Nishimura, I. (2014). ER bodies in plants of the Brassicales order: biogenesis and association with innate immunity. Front Plant Sci **5,** 73.

Osakabe, Y., Yamaguchi-Shinozaki, K., Shinozaki, K., and Tran, L.S.P. (2014). ABA control of plant macroelement membrane transport systems in response to water deficit and high salinity. New Phytol **202,** 35-49.

Smirnova, E., Marquis, V., Poirier, L., Aubert, Y., Zumsteg, J., Menard, R., Miesch, L., and Heitz, T. (2017). Jasmonic Acid Oxidase 2 Hydroxylates Jasmonic Acid and Represses Basal Defense and Resistance Responses against Botrytis cinerea Infection. Mol Plant **10,** 1159-1173.

Stamp, N. (2003). Out of the quagmire of plant defense hypotheses. Q Rev Biol **78,** 23-55.

Thines, B., Katsir, L., Melotto, M., Niu, Y., Mandaokar, A., Liu, G., Nomura, K., He, S.Y., Howe, G.A., and Browse, J. (2007). JAZ repressor proteins are targets of the SCF(COI1) complex during jasmonate signalling. Nature **448,** 661-665.

Watanabe, S., Shimada, T.L., Hiruma, K., and Takano, Y. (2013). Pathogen Infection Trial Increases the Secretion of Proteins Localized in the Endoplasmic Reticulum Body of Arabidopsis. Plant Physiol **163,** 659-664.

Xie, D.X., Feys, B.F., James, S., Nieto-Rostro, M., and Turner, J.G. (1998). COI1: An Arabidopsis gene required for jasmonate-regulated defense and fertility. Science **280,** 1091-1094.

Yan, Y.X., Stolz, S., Chetelat, A., Reymond, P., Pagni, M., Dubugnon, L., and Farmer, E.E. (2007). A downstream mediator in the growth repression limb of the jasmonate pathway. Plant Cell **19,** 2470-2483.

Zhai, Q.Z., Zhang, X., Wu, F.M., Feng, H.L., Deng, L., Xu, L., Zhang, M., Wang, Q.M., and Li, C.Y. (2015). Transcriptional Mechanism of Jasmonate Receptor COI1-Mediated Delay of Flowering Time in Arabidopsis. Plant Cell **27,** 2814-2828.

Zhang, F., Yao, J., Ke, J., Zhang, L., Lam, V.Q., Xin, X.F., Zhou, X.E., Chen, J., Brunzelle, J., Griffin, P.R., Zhou, M., Xu, H.E., Melcher, K., and He, S.Y. (2015). Structural basis of JAZ repression of MYC transcription factors in jasmonate signalling. Nature **525,** 269-273.

Zhao, M.L., Wang, J.N., Shan, W., Fan, J.G., Kuang, J.F., Wu, K.Q., Li, X.P., Chen, W.X., He, F.Y., Chen, J.Y., and Lu, W.J. (2013). Induction of jasmonate signalling regulators MaMYC2s and their physical interactions with MaICE1 in methyl jasmonate-induced chilling tolerance in banana fruit. Plant Cell Environ **36,** 30-51.

Zust, T., and Agrawal, A.A. (2017). Trade-Offs Between Plant Growth and Defense Against Insect Herbivory: An Emerging Mechanistic Synthesis. Annual Review of Plant Biology **68,** 10.11-10.22.